University of Miami
Scholarly Repository

Open Access Dissertations | Electronic Theses and Dissertations

2013-05-08

Concrete Durability and Environmental Performance of Mixtures Containing Recycled Hazardous Waste Aggregates

Diego F. Romero
University of Miami, diego86@gmail.com

Follow this and additional works at: https://scholarlyrepository.miami.edu/oa_dissertations

Recommended Citation
Romero, Diego F., "Concrete Durability and Environmental Performance of Mixtures Containing Recycled Hazardous Waste Aggregates" (2013). *Open Access Dissertations*. 1020.
https://scholarlyrepository.miami.edu/oa_dissertations/1020

This Open access is brought to you for free and open access by the Electronic Theses and Dissertations at Scholarly Repository. It has been accepted for inclusion in Open Access Dissertations by an authorized administrator of Scholarly Repository. For more information, please contact repository.library@miami.edu.

UNIVERSITY OF MIAMI

CONCRETE DURABILITY AND ENVIRONMENTAL PERFORMANCE OF MIXTURES CONTAINING RECYCLED HAZARDOUS WASTE AGGREGATES

By

Diego F. Romero

A DISSERTATION

Submitted to the Faculty
of the University of Miami
in partial fulfillment of the requirements for
the degree of Doctor of Philosophy

Coral Gables, Florida

May 2013

©2013
Diego F. Romero
All Rights Reserved

UNIVERSITY OF MIAMI

A dissertation submitted in partial fulfillment of
the requirements for the degree of
Doctor of Philosophy

CONCRETE DURABILITY AND ENVIRONMENTAL PERFORMANCE OF MIXTURES CONTAINING RECYCLED HAZARDOUS WASTE AGGREGATES

Diego F. Romero

Approved:

_____
Carol D. Hays, Ph.D.
Associate Professor of Civil, Architectural,
and Environmental Engineering

_____
M. Brian Blake, Ph.D.
Dean of the Graduate School

_____
Helena Solo-Gabriele, Ph.D.
Professor of Civil, Architectural,
and Environmental Engineering

_____
James Englehardt, Ph.D.
Professor of Civil, Architectural
and Environmental Engineering

_____
Jacqueline James, Ph.D.
President
Imara Architectural Engineering
Miami, Florida

_____
Rodrigo Mora, Ph.D.
Faculty
British Columbia Institute of
Technology

_____
Cesar Constantino, Ph.D.
Senior Director of Process and Quality
Titan America
Miami, Florida

ROMERO, DIEGO FERNANDO (Ph.D., Civil Engineering)

Concrete Durability and Environmental Performance of Mixtures Containing Recycled Hazardous Waste Aggregates (May 2013)

Abstract of a dissertation at the University of Miami.

Dissertation supervised by Professor Carol Hays.
No. of pages in text. (207)

Cathode ray tube (CRT) glass, when disposed, is considered a hazardous material due to its lead toxicity. Currently available disposal methods for this material are being phased out due to their adverse environmental impacts. A study of the durability, material mechanical properties, and the potential for adverse environmental impact of the use of hazardous waste materials as a component in portland cement concrete is presented. This dissertation uses CRT glass as a test bed material to promote sustainable construction materials and hazardous waste recycling. An important goal of this dissertation is to fill an existing knowledge gap between the research methodology applied to assessing concrete durability and methods of evaluating environmentally detrimental leachates such as lead that is found in CRT waste materials.

CRT glass was used to substitute up to 30% of the fine-aggregate component of a typical South Florida non-structural concrete mixture. An organic biopolymer admixture solution of guar gum and boric acid was used in the concrete mixture to bind and encapsulate the lead ions to the cementitious matrix. Additionally, modifications to accelerated aging, diffusion, and durability tests were developed and combined to innovatively simulate the service life of CRT-concrete and to evaluate the effects that

concrete deterioration (i.e. micro-crack formation from alkali-silica reaction expansions, micro-structure changes due to accelerated aging, and surface spalling from freeze-thaw testing) have on contaminant leaching.

The biopolymer solution was shown to be effective by encapsulating lead leachate to concentrations that are below US government-regulated drinking water limits. Additionally, the compressive strength of CRT-concrete was comparable to the control mixture. The results of the modified deterioration and leaching tests show that microcracks, surface spalling, and loss of modulus of elasticity had an adverse impact on the durability and strength of the composite material. A relationship between alkali-silica reaction expansions and the gradient in contaminant leaching could not be observed due to the rapid rate of saturation of the leachate solution with the constituent of concern. The results from combined accelerated aging and diffusion tests revealed that lead leaching behavior for specimens that were exposed to an elevated temperature and a neutral pH environment deviate slightly from the behavior typically found in purely diffusion-controlled specimens. However, Crank's numerical solution to Fick's 2nd Law of Diffusion was still able to conservatively predict the contaminant release. Finally, the combined freeze-thaw/diffusion tests showed that surface deterioration of CRT-concrete results in a statistically significant increase in lead leaching.

Overall, the use of CRT glass as a component of concrete was shown not to be detrimental to the structural and durability performance when compared to control mixtures. Furthermore, a framework was developed to guide researchers, regulatory agencies and environmental engineers through a number of structural, environmental, and management-related issues that need to be addressed during each phase of the life cycle

of a concrete material that contains recycled waste aggregates. A maximum use of 10% CRT glass is recommended to meet the durability (alkali-silica reactions) and environmental requirements. Lastly, the observed relationship between the combined durability and leaching tests demonstrates the importance of encouraging researchers and regulatory agencies to consider durability as a contributing factor in the assessment of a material containing hazardous wastes for possible adverse environmental impact.

To God, for always protecting me,

keeping my family safe,

and guiding us through difficult times.

To my Mom, Dad, and Sister

who always provided me with

unconditional love, support, and guidance.

Lo hicimos!

ACKNOWLEDGMENTS

My Ph.D. years at the University of Miami had mentorship from numerous outstanding individuals from both within the university and outside of it. It is to these individuals who contributed so much of their time and effort to help me in my study that my heartfelt gratitude goes out to. Without them, none of this would be possible.

I would like to thank Dr. Carol Hays, who without hesitation, became my advisor in the middle of my career and aided me in completing this dissertation. Without her help, guidance, and support, this dissertation would not be possible.

I would also like to thank Dr. Rodrigo Mora and Dr. Jacqueline James, who proposed the idea of recycling CRT glass into concrete and approached me to work on this project. Without them, the foundation for this dissertation would never have happened. Thank you for your support.

Many thanks go to Dr. Helena Solo-Gabriele, Dr. James Englehardt, and Dr. Cesar Constantino for your participation in my committee and for taking your time to help me with any concerns that I had throughout this experience.

I am grateful to the Hinkley Center for Solid and Hazardous Waste Management and specifically to Tim Vinson, for believing in my work and for funding two different studies of this dissertation. Also to SuperMix for providing all of the concrete aggregates used in this dissertation, and Mr. Nader Nejad from Recycletronics for providing technical knowledge and the CRT glass used in this dissertation.

To my research colleagues, faculty members, administration staff and friends; I would not have done this without your company. Special thanks to Dr, Antonio Nanni for giving me the opportunity to seek this degree, as well as Maria Aldana, Lizett Bowen,

Dr. Francisco De Caso y Basalo, Sean October, Gerald Sanders, Keith Holmes, Dr. David Kosson, and Dr. Andrew Garrabrants. Also thanks to my graduate and undergraduate friends and colleagues who helped me with this research and through my Ph.D. years; Joseph Fanara, Sarah Fiol, Ali Haji, Maria Ronderos, Luis Torres Chavez, Vanessa Benzecry, Allison Korth, Omar de Leon, Sabina Rakhimbekova, Matteo di Benedetti, Kevin Schwartz, Gavin Good, Andrew Maxwell, Maggie Giraldo, Felipe Gheiman, Vanessa Benzecry, Bernardo Benzecry, Matteo Di Benedetti, Giovanni Loreto, Derek Schesser, Steven Verbovszky, Lauren Millman, Diana Arboleda, Navid Nemati, Tala Shokri, Felipe Mejia, Adane Abegaz, Alessandra Laricchia, and Carmen Pineda. Lastly, the Graduate Student Association for allowing me to be your Treasurer and help fight for the rights of graduate students, GAFAC for financial support for my conference presentation, and SalsaCraze because you were always there when I needed to let go of the books and just dance.

To my best friends Juan, Jeffrey, Luis, Stephan, Richard, and Jorge who are always by my side, no matter what, no matter when, no matter where, no matter how.

Last, but not least, to my parents, Walter and Vivian, for sacrificing everything to give me an education and putting me in the first place, for teaching me about the ups and downs of life and for introducing me to the wonderful world of construction. Thanks to my sister, Selene, for your company and help and for being an amazing individual with such drive to succeed and be a good person. And finally, to the rest of my family in Argentina who are thousands of miles away but I can still feel their support and encouragement.

There may be more supporting people that I might have forgotten, but keep in mind that your role in my life and in this dissertation will be forever engraved in me.

Thank you everyone!!!

Table of Contents

List of Figures

List of Tables

Chapter 1

Introduction

1.1 Background

The twentieth century has witnessed an extraordinary population growth with an increase of almost 4 billion people and the largest annual population growth of 86 million people each year since the late 1980s [1]. With the increase in population comes an increase in consumption of both man-made and natural resources which ultimately becomes an environmental concern. Concrete, the cornerstone of our infrastructure, is universally known for its structural capabilities and ease of use. By proportioning and mixing readily available materials such as cement, natural aggregates, and water, one can easily form concrete into virtually any shape imaginable for a variety of applications. Every year, 10 billion tons of sand and rock, and 1 billion tons of mixing water are used annually in cement or aggregate manufacturing [2]. Similarly, billions of tons of CO_2 are produced due to transportation, mining, and production of these materials. For every ton of portland cement that is manufactured, one ton of CO_2 is produced. It is estimated that in 2010 3.3 billion tons of cement were produced, an increase of 51.5% over the previous ten years [3]. Increased awareness is now focused on the detrimental impacts that unchecked consumption has on the environment for generations to come. The concrete industry is now one of many industries concentrating on more sustainable alternatives for concrete production.

The waste industry is another source of pollution that results in adverse effects on the environment. Industrial waste is rapidly increasing as the demand and consumption of both raw and processed materials increases. Approximately 243 million tons of solid

waste were produced in 2009, out of which only 82 million tons (33.8%) were recycled [4]. With regard to construction and demolition (C&D) waste, one study found the United States recycles approximately 82% of its waste [5], while Canada recycles approximately 42% of its waste [6]. Non-biodegradable and hazardous wastes pose many environmental issues. Waste materials that need special handling, are dangerous to our health, and/or cannot be disposed of conventionally are categorized as hazardous materials. In the United States only about 1.8 million tons of hazardous wastes were managed by recycling (metals, solvent, or other recovery), constituting only 4.4% of the total amount of hazardous waste present [7].

Due to the rapid transition towards more energy efficient displays, the disposal of Cathode Ray Tube (CRT) glass has accelerated and become a major disposal problem and global concern due to the high concentration of lead oxides embedded in the glass. A solution to reduce both the amount of raw materials consumed during concrete production and to recycle the CRT glass is needed. The challenge is that the solution needs to be safe for people and the environment. A potential solution to this environmental problem can be achieved through the practice of Industrial Ecology (IE). The goal of IE is to change the current system where raw materials are used and wastes are produced, to a reusable system where the wastes from other industries are reused as raw materials in concrete, leading to a more environmentally sustainable material. Examples of IE are seen in supplementary cementitious materials (SCMs) like fly ash and ground granulated blast-furnace slag (GGBS), byproducts of the coal and steel industry, which are used to replace 10-60% of portland cement in a concrete mixture [8]. Not only

do these byproducts reduce the impact on the environment, they also improve the quality of ordinary portland cement concrete mixtures.

This dissertation will explore the feasibility of using Cathode-Ray Tube (CRT) glass, a hazardous material, as an aggregate in concrete (CRT-Concrete) in order to promote CRT recycling as well as another way to reduce the raw material consumption in concrete mixtures. Although most concrete applications require the use of steel reinforcement, this dissertation primarily focuses on non-structural concrete applications with no steel reinforcement using a typical South Florida limestone-based concrete mixture. The reasoning behind this is that including steel reinforcement may add several unknown factors to the performance of CRT-Concrete which ultimately may alter the results of a pure CRT-Concrete mixture (i.e. the interaction between the CRT glass, the admixtures, and the steel reinforcement).

1.2 Objective

The overarching goal of this dissertation is to promote the use of secondary materials in concrete as well as bridge a much needed gap between material scientists and environmental engineers by exploring the impacts of concrete durability on leaching of contaminants. It will be achieved by studying the feasibility of CRT glass as a substitute aggregate in concrete mixtures. The main objectives of this dissertation are to:

1. Realize a novel concrete material for sustainable non-structural applications. The composite system should be able to a) no be detrimental to the environment as measured by federal requirements for pollutant leaching and, b) meet and exceed the strength and durability requirements of the concrete mixture when compared

to a control specimen. To achieve this, the use of organic biopolymers was examined.

2. Implement performance and characterization tests to evaluate the structural (i.e. compressive strength and tensile strength) and environmental (i.e. potential for pollutant release) performance of CRT-Concrete.
3. Evaluate the effects of deterioration on the leaching mechanisms of concrete using techniques such as Arrhenius aging, freeze-thaw aging, and alkali-silica reactions.

1.3 Research Significance

Concrete is a widely used material with a variety of applications around the world. However, the mining and processing of the raw materials are energy demanding and places a large burden on the environment. This dissertation focuses on reducing raw material consumption by partially replacing one of the primary materials used in concrete mixtures (sand) with a secondary material (CRT glass), thereby promoting sustainable construction materials.

Total amounts of CRT discarded yearly vary within regions. In Europe it is estimated that over 150,000 tons of CRT glass are treated yearly and that over 600,000 tons could be reached in 2013 [9]. The Florida Department of Environmental Protection (FDEP) estimates that approximately 2.7 million CRT units become available for disposal in the state on an annual basis [10]. Meanwhile, Herat [11], indicates that over 100 million CRT units are disposed nationwide. The problem is that common recycling and disposal practices such as glass smelting or electronic landfill disposals are becoming obsolete and not sustainable. The challenge is that CRT glass is a hazardous material and its

performance in concrete must be safe throughout its entire life-cycle. This research looks to study the possible impacts to people and the environment when this hazardous waste is recycled into a concrete mixture.

1.4 Outline

Articulated in three studies, this dissertation assesses the feasibility of CRT-Concrete for use in non-structural concrete applications. It begins with a detailed review focusing on the use of potentially hazardous secondary materials as aggregates in concrete mixtures and the potential impacts that may occur throughout the three phases of the material's life. The review is followed by:

Study 1 titled "Study on the Mechanical and Environmental Properties of Concrete Containing Cathode Ray Tube Glass." This study evaluates the feasibility of using CRT glass as a substitute aggregate in concrete mixtures. It focuses on the wet and dry properties of concrete including its slump and unit weight changes, compressive strength, and potential for alkali-silica reactions. Furthermore, it characterizes the leaching behavior of CRT-Concrete by comparing it to a regulatory leaching test as well as pH dependence and percolation column leaching tests;

Study 2 titled "Structural Behavior of Concrete Containing Cathode Ray Tube Glass Undergoing Accelerated Aging and Deterioration." This study seeks to characterize the structural performance of CRT-Concrete as it matures in a temperature-controlled environment and as it deteriorates in a freeze/thaw environment. This study uses an ultrasonic pulse velocity technique as well as a forced resonant frequency technique to examine how the modulus of elasticity changes as the material deteriorates. Compressive

strength tests are then used to compare the durability and structural performance of each CRT-Concrete mixture; and,

Study 3 titled “The Effects of Accelerated Aging and Deterioration on the Diffusive Properties of Concrete Containing Cathode Ray Tube Glass.” This study uses hot temperature aging and freeze/thaw testing to deteriorate the CRT-Concrete. Simultaneously, it is placed in a diffusion leaching controlled environment to quantify the release of contaminants. The objective of this study is to observe if there is any relationship between deterioration of a material and leaching of contaminants.

Chapter 2

Assessment on the use of Potentially Hazardous Secondary Aggregates in Concrete

2.1 Background

Concrete is a composite man-made material consisting of water, cement, and aggregates. It is a widely used material with a variety of applications around the world. However, the mining and processing of the raw materials is energy demanding and places a large burden on the environment. For this reason, industry and academic researchers are looking into reducing raw material consumption by replacing these primary materials with secondary (recycled or by-product) materials in concrete. Today, supplementary cementitious materials (SCMs) such as fly ash, ground granulated blast-furnace slag (GGBFS), metakaolin, along with secondary aggregates such as glass, rubber tires, and recycled concrete have paved the way to a more sustainable form of concrete. Not only do these materials reduce the need for more raw resources, they also enhance the structural integrity and durability of the concrete.

However, select secondary aggregates are known to be potentially hazardous due to their chemical composition and potential for contaminant release (i.e. leach). The challenge with using potentially hazardous secondary aggregates (PHSAs) is the lack of knowledge on the human or ecological impacts; which ultimately creates one of the main barriers to recycling [12]. To quantify the environmental performance or impact of a material, regulatory tests such as the Toxicity Characteristic Leaching Procedure (TCLP) [13] and Synthetic Precipitation Leaching Procedure (SPLP) [14] are performed. However, these tests are used for disposal of materials and not for reuse and therefore they may fail to

accurately simulate more realistic scenarios encountered during the life cycle of the material.

The assessment of PHSAs in concrete needs a life-cycle approach. Any approach focusing on one particular aspect or phase is biased or incomplete because not one single parameter or test has the ability to generalize the environmental performance of the material. The objective of this assessment is to describe the critical functions and mechanisms that affect the environmental performance of a material. It specifically focuses on water pollution because of its capability to widely spread into various sources that have a direct impact on human and ecological life. Breaking down these mechanisms into the three phases of the life cycle of a material, this assessment also discusses the coupled relationship between the durability of a material and its impacts on water pollution. The assessment is based on the premise that concrete mixtures with secondary materials should be life-cycle safe for the environment and people, while providing at least the same level of structural performance and durability as regular concrete mixtures under the similar environmental and loading conditions. To demonstrate this, the case of recycling electronic waste substitute aggregates, specifically, crushed cathode ray tube (CRT) glass from obsolete television and computer display screens, into concrete is used. CRT glass is considered a hazardous material by the U.S. Environmental Protection Agency (EPA) due to its toxicity. Embedded in the glass are large concentrations of lead oxides (10-30% by weight) to act as a shield against the radiation generated by the components that make the picture. Other heavy metal oxides like Strontium and Barium are present but at much smaller and non-hazardous concentrations. Regulations ban the disposal of CRTs in regular landfills. With approximately 2.7 million CRTs becoming

available for disposal in the state of Florida yearly and over 100 million CRTs disposed nationwide, [10,11] this environmental problem needs a solution. This dissertation originated as an answer to the concerns issued by the waste management industry in a quest to solve a hazardous waste management problem affecting the electronic waste industry, while at the same time producing a potential business opportunity for the circular, industrial economy by enabling the reuse of waste CRT glass as a potential aggregate for concrete production [15]. While concrete is typically reinforced with either steel reinforcement bars that provide improved tensile structural properties or with discrete reinforcing fibers that provide improved material ductility; this dissertation focuses on assessing the performance of un-reinforced CRT-concrete.

The idea of producing CRT-concrete with the dual purpose of using less natural resources and immobilizing hazardous CRT metals makes sense considering the relative success reported in previous work in cement-based stabilization of heavy metals from industrial wastes [16,17]. Others [18], however, report that the immobilization of Zn and Pb in cement is poor, especially at pH 4. As indicated in Table 2-1, previous studies on using concrete to contain or encapsulate CRT metals have been conducted. They can be categorized into two groups: the disposal group that intends to encapsulate CRT metals for disposal [19,20]; and the recycling group that attempts to recycle CRT as a secondary material in concrete and other products such as ceramics [21-24]. However, neither group focuses on the overall performance (structural, durability, environmental) of the composite material, which is one of the main objectives of this dissertation.

Expectedly, the durability of concrete is central to this evaluation as it directly affects the serviceability of concrete. Increased durability directly translates in improved resource

efficiency, and its lack is detrimental to concrete in all its performance dimensions. This assessment demonstrates that there is a need for a more comprehensive treatment of the viability of using concrete to encapsulate CRT glass metals, while providing a life-cycle functional, safe, and durable material alternative. Consequently, the goal of this dissertation is to evaluate the conditions, if any, for which acceptable life-cycle performance of CRT-concrete can be achieved. This chapter is organized as follows. Section 2.2, introduces the three life-cycle phases of concrete and the key factors that could have an effect on water pollution. The subsequent sections address the water pollution concerns from concrete for each one of these life-cycle phases.

2.2 Life-Cycle of Concrete

The life-cycle of concrete can be divided into three phases. Phase I focuses on the extraction of resources, transportation, and production of the material. Phase II then focuses on the use, maintenance, and repair of the material; and lastly Phase III studies the materials' end-of-life (EOL) [25]. Figure 2-1 illustrates the three overall phases of the life-cycle of concrete; the percentages in the figure come from a United States Army Corps of Engineers [26] report which analyzes the end-use of concrete in the USA.

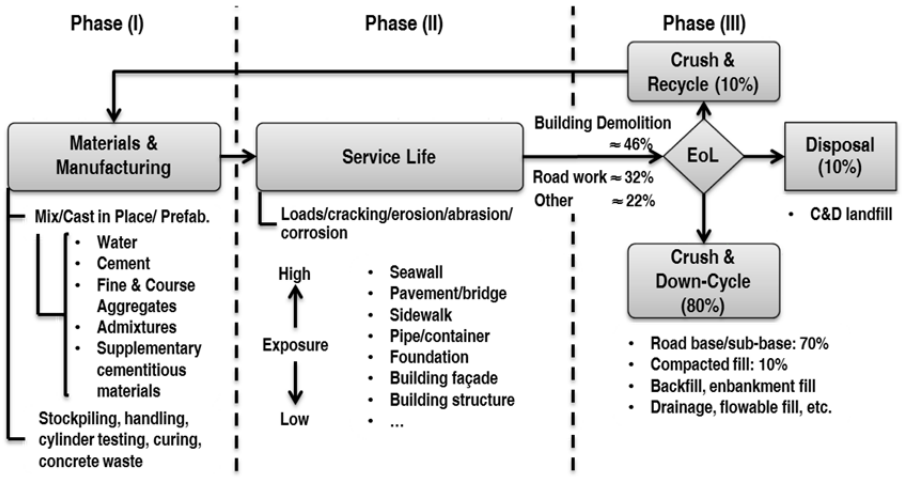

Figure 2-1 - The Life-Cycle of Concrete

There are multiple factors inherent to the design of concrete mixtures and structures as well as concrete and aggregate management that can affect the release of hazardous contaminants from concrete during its life cycle. These design-controlling and management related factors, presented in Figure 2-2, add a level of complexity to the environmental assessment of concrete containing secondary waste aggregates, termed recycled waste concrete (RWC). These factors, which occur at specific phases of the concrete life cycle, range from the source, shape, size, and chemical composition of the PHSAs used, to the structural design, production, loading, and use of the composite material. The challenge involved in predicting contaminant release is that generalization of all of these parameters into one single test may either be too conservative or not representative enough. For example, the TCLP leaching test is primarily used to test the hazardousness of a material. However, the intention of this test is to verify if the material would be hazardous if it was disposed in a municipal landfill; a scenario that exposes the material to an environmental condition that may never be observed during the materials' normal service life use.

For this reason, the subsequent sections introduce the use of proposed leaching characterization tests that assess the performance of the RWC under more realistic conditions. Furthermore, it informs the reader of how design-related and management-related factors may have an impact on water pollution during the life cycle of the material and how they can be addressed.

Table 2-1 - CRT-Concrete Studies

Study	Use of CRT	W/C Ratio	Binder	CRT Substitutio	Particle Size	Source	Additives	Tests (lead limit)	Results
[19]	CRT-Biopolymer-Concrete	0.397	Portland Cement	15.6 % of Fine Aggregate replacement	Coarse glass aggregate only (0.149-.42mm)	Color computer monitors (5883 mg/kg)	Organic biopolymers: GG, XG, Chitosan used for metal immobilization	Comp. Strength TCLP (5mg/L)	All below TCLP limit, some below drinking water limits. Compressive strength is better or comparable
[20]	Cross-linked Biopolymer CRT Concrete	0.397	Portland Cement	15.6 % of Fine Aggregate replacement	Coarse glass aggregate only (0.149-.42mm)	Color computer monitors (5883 mg/kg)	Cross-linked solutions: GG/XG, GG/BA used for metal immobilization.	Comp. Strength TCLP (5mg/L)	Cross-linked biopolymer concrete showed improved compressive strengths except for when mix water is completely subsituted with the biopolymer solution. Results below TCLP regulation and some below drinking water requirements.
[21]	CRT-Concrete with SCMs	0.6	PC, PC/PFA (35 %), PC/GGBS (50 %)	40 % of Fine Aggregate by mass	Medium grade sand according to BS 882:1992	N/A	Lithium Hydroxide, Lithium Nitrate for Alkali-Silica Reaction control	Comp. Strength ASR (<0.05%), BS EN 12457 (0.5mg/kg)	Encapsulation of lead with concrete alone above leaching limits. With GGBS and PFA leaching is below 0.1 mg/kg. Compressive strength of all specimens is higher than control. CRT glass is reactive with the alkali content of the cement and exceeds expansion limits except when mitigation techniques such as supplementary cementitious materials or additives are used.
[22]	CRT-Concrete w/ SCMs	0.45	PC, PC/FA (25 %), PC/GGBS (25%)	100 % of Fine Aggregate by mass	Medium Sand (0.15-4.75mm) Fine Sand (0.15-1.18mm)	N/A	N/A	Comp. Strength Flex. Strength ASR	Compressive and flexural strength of CRT-concrete is higher than control specimen. CRT glass has large ASR expansion values but it is mitigated with secondary cementitious materials.
[23]	CRT-Concrete w/ SCMs	0.5	Portland Cement/Fly Ash (20 %)	5,10,15 % of Fine Aggregate by mass	Coarse and fine size CRT sand	CRT (4500 mg/kg)	Darex AEA Air Entrainer	Comp. Strength TCLP, SPLP (5mg/L, 15 µg/L)	Compressive strength higher than control but decreases as percentages of CRT increase. SPLP testing show that results are below drinking water level.

SCMs - Supplementary cementitious materials, PC - Portland Cement, PFA - Pulverized fuel ash, GGBS - Granulated Blast Furnace Slag, FA - Fly Ash, GG - Guar Gum, BA - Boric Acid, XG - Xanthan Gum, ASR - Alkali Silica Reactions

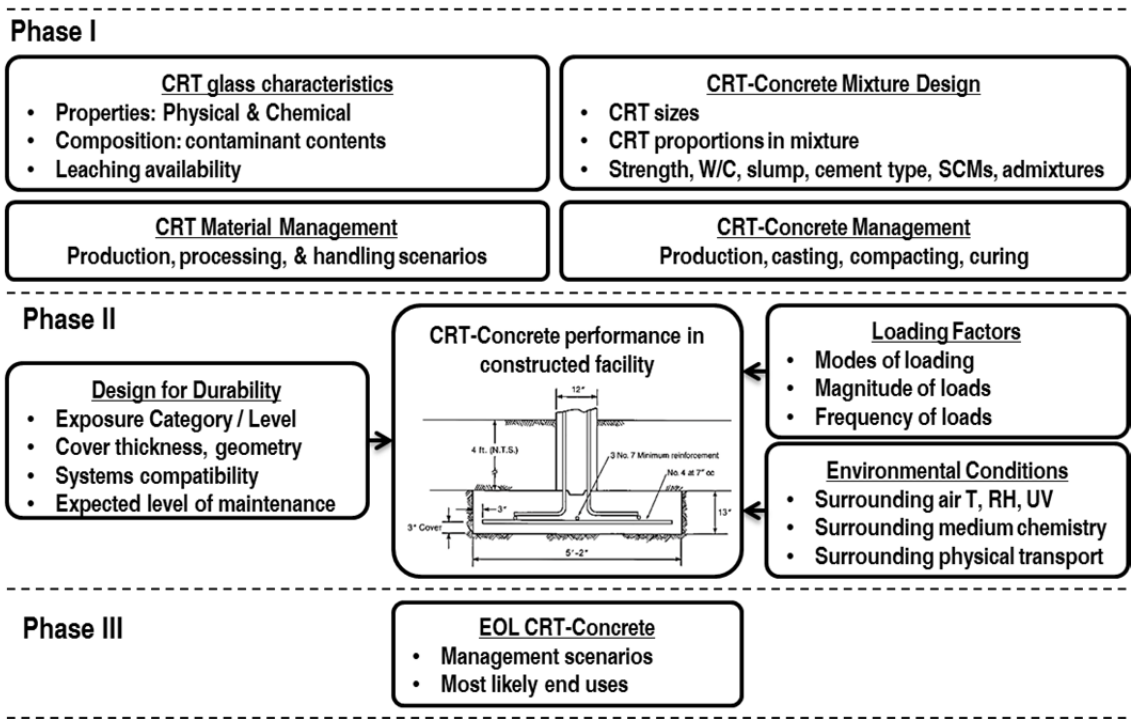

Figure 2-2 - Factors controlling the life-cycle performance of CRT-concrete

2.3 Materials and Manufacturing

To keep up with the global demand of concrete, over 10 billion tons of aggregate (sand and rock) are mined yearly [2]. Introducing a secondary material in place of the primary raw aggregates can have a positive impact on the environment. Nevertheless, researchers must ensure that the RWC is able to meet the minimum requirements for environmental and structural performance.

The workability, strength, and durability of concrete will usually determine the acceptance of a concrete mixture; and in the case of RWC, it must also meet environmental regulatory criteria. For this reason, the secondary aggregate properties and chemical composition must be well understood. An ASTM International survey [27] found that water requirement, particle size and grading, strength, absorption and specific gravity are among the most important material characteristics for concrete quality. Initial

characterization of the PHSA for potential use in concrete should focus on the size, shape, and distribution of the aggregate. These application dependent properties have a direct impact on the wet and dry properties of the RWC as well as its durability and environmental performance. To meet the particle size requirements, grinding machinery such as ball mills or hammer mills are used during processing. This process creates airborne fines that may be hazardous to the human health and proper safety equipment such as respirators and goggles may need to be worn during the production and handling of finely crushed secondary aggregates. As an example, the process of crushing CRT glass with a hammer mill produced a residue of airborne particles of glass smaller than 75μm; requiring the use of respirators, gloves, and goggles. It has been noted that certain aggregates which are silica-based and are of large diameter (greater than 4 mm) can cause a deleterious reaction with the alkali content of the cement paste [28]. This phenomenon, which will be further discussed in Section 4, is known as an Alkali-Silica Reaction (ASR) and can cause the concrete to expand, crack and spall; which consequently may increase the release of pollutants.

After a careful review of the required physical properties of the PHSA needed for a given application, grinding machinery such as ball mills or hammer mills can then be used for particle size reduction. After processing, improper storage and handling of the PHSA can lead to environmental pollution. Traditional storage solutions like outdoor stockpiling (used for coarse and fine aggregates) are no longer an option due to environmental exposure. For materials such as rubber or leaded glass, outdoor stockpiling during heavy rain or wind events may lead to leaching of hazardous species (i.e. percolation leaching) such as zinc, phenol, aniline, or lead into the ground water [19,21,29]. Although the EPA

has a regulatory test for groundwater contamination, SPLP, its procedure is not representative of the percolation leaching mechanisms which are influenced by advection. Instead, percolation leaching can be assessed using a proposed EPA test known as EPA Preliminary Method 1314 [30] where water is pumped through a column packed with the material of interest (e.g. crushed CRT) and the collected eluent is tested for the constituent of concern (e.g. lead). Using this test, PHSAs can be tested to see if they are safe to be stockpiled outdoors. Ultimately, the use of PHSAs may lead to costlier alternative storage solutions such as dry, enclosed spaces like storage silos which are used for cement and fly ash storage, or alternatively, warehouses.

In addition to the particle size of the PHSA having a direct impact on the durability and environmental performance of the RWC, the particle shape and orientation of the aggregate may influence concrete workability, strength, elasticity, and the distribution of stresses due to changes in the interlocking boundaries between the paste and the secondary aggregate particles [27]. For waste glass aggregates, several researchers concluded that the shape and texture of crushed, angular sand and glass particles reduce concrete workability, while spherical shaped aggregates increase the workability [31-35]. Lastly, the water absorption and specific gravity of the aggregate will also affect the economy of the RWC as a less absorbent aggregate with a greater specific gravity than the one being substituted will require less water for batching the concrete but will need greater amounts of the aggregate. Overall, in the first phase of a RWC material, the selection of the aggregate and the assessment of its material properties are essential as they can have a direct impact on the design of the mixture, structural performance and

durability, environmental performance (i.e. water pollution) and on the economy of the product.

2.4 Service Life

The core of the research in sustainable concrete focuses on developing high-performance concrete with higher strengths that are also lighter, durable, and environmentally friendly. Presently, several additives and substitutes for commercial ultra-high strength concretes are being used. Such additives like super-plasticizing chemical admixtures (to minimize the water to cement ratio and maintain workability), silica fume (to substitute portland cement), and metallic or organic reinforcing fibers (for improved flexibility and resistance to cracking) have drastically improved the performance of concrete. However, their benefits should not overshadow the possible detrimental effects that additives or secondary aggregates may impose on people or the environment. For instance, a recent study revealed that an admixture used in concrete produced chemical emissions during construction and service-life which resulted in negative health effects to construction workers and building occupants [36]. Therefore, central to the life-cycle performance of a RWC is the understanding of how contaminants from secondary aggregates can harm humans and the environment during its service life.

2.4.1 Overview of Environmental Assessment Methods for Waste Materials

The environmental assessment can be divided in two steps: 1) the contaminant release from the material and 2) the impact scenario that considers the migration of the contaminant to a specified receptor. Both steps involve uncertainties, however, the impact assessment involves considerable uncertainties on the actual field conditions involving

the chemical and physical dynamics of the site, and calls for detailed contaminant transport modeling and risk analysis. For contaminant release assessment, researchers have demonstrated that only a limited set of experimental methods and models are needed to obtain consistent results for a wide range of secondary construction materials [37]. These experimental methods are broken down into two types of building materials: monolithic and granular. Monolithic materials often show diffusion controlled release, whereas granular materials usually show percolation dominated release. Table 2-2 presents the models and standard test methods that could be used to assess the life-cycle environmental performance of RWC in terms of contaminant release.

Table 2-2 - Contaminant Release Assessment Methods for Secondary Construction Materials

Assessment method	pH Dependence	Percolation	Diffusion
Release control factor	Chemical pH/solubility control pH dependent	Physical: mass transfer Percolation/solubility control time-dependent	Physical: mass transfer Diffusion control time-dependent
Equation	$\tau = \frac{D^{obs} \cdot t}{r^2}$	$LS_{site} = 10\ \frac{inf \cdot t}{\rho \cdot H_{fill}}$ $M_t = (LS_{site})(S_{field\ pH})$	$M_{area}^{t} = 2 \cdot \rho \cdot C_0 \left(\frac{D^{obs} \cdot t}{\pi}\right)^{1/2}$
Parameters & boundary conditions	• Time constant, τ (-) • Equilibrium time, t (s) • Particle size, r (m^2) • Observed diffusivity, D^{obs} (m^2/s) • Expected liquid/solid (LS) ratio @ equilibrium (LS = 10)	• Anticipated LS, LS_{site}. (l/kg) • Antifipated infiltration rate, inf (cm/yr) • Time period, t (year) • Fill density, ρ, (kg/m^3) • H_{fill}, fill depth (m) • Mass release at time t, Mt, (mg/kg) • Constituent solubility at pH value corresponding to field pH, $S_{field\ pH}$ (mg/l)	• Cumulative mass of constituent release M_{area}^{t} at time t, surface area basis, (mg/m2) • Initial leachable content, C_0 (mg/kg) • Sample density, ρ, (kg/m^3) • Observed diffusivity, D^{obs} (m^2/s) • Time interval, t (s)
Output(s)	• Release (mg/kg): mg of constituent leached per kg of dry sample as a function of pH • Concentration (mg) of constituent of concern per litre of extract (mg/l)	• Cumulative release (mg/kg): mg of constituent leached per kg of dry sample (mg/kg) as a function of L/S ratio (ml/kg) • Concentration per litre of extract (mg/l)	• Cumulative release (mg/m^2): mg of constituent per square meter of exposed surface as a function of time • Release flux (mg/m^2-s) per time interval
Applications	Extreme conditions Long-term exposure with variation of pH	Granular materials: road base, embankment, fill, drainage	Monolithic materials: buildings, bridges, pipes, blocks, urban, roads
Standards USA Europe	EPA 1313 [38] CEN/TS 14429 [39]	EPA 1314 [30] CEN/TS 14405 [40]	EPA 1315 [41] EA NEN 7375 [42]
CRT-concrete life-cycle	Phases I, II, & III	Phase III	Phase II

To harmonize the environmental assessment of a wide range of secondary materials, Van der Sloot and Kosson, along with colleagues in Europe and the USA, have developed integrated frameworks [37,43]. These are hierarchical frameworks that relate knowledge gained from initial characterization leaching tests and corresponding leaching models, to simpler on-site verification tests that ensure that compliance is achieved based on previously determined characterization information. The development of harmonized leaching/release characterization tests is based on the hypothesis that the number of chemical and physical factors that control the contaminant release (i.e. dominant factors) to water is fairly limited, and these factors can be identified and quantified with few test methods. A comprehensive description of all the different factors controlling the release of contaminants from secondary materials is out of the scope of this review, however, an in-depth discussion can be found in Van der Sloot [37]. Figure 2-3 illustrates these factors.

Researchers have used these methods to group construction materials according to their characteristic release behavior and to predict their release under any scenario. When these release behaviors are presented graphically, they show similar release patterns for materials in the same group, with changes only on the absolute release values. Furthermore, a relevant report by Apul et al. [44] provides an in depth review of the movement of water in the highway environment to evaluate the implications for use of recycled materials. The report discusses simplified as well as advanced transient numerical models and water flow measuring techniques to predict the movement of water in the different pavement layers. Such models can be used and extended into fate/transport models for evaluating environmental impacts risk assessments.

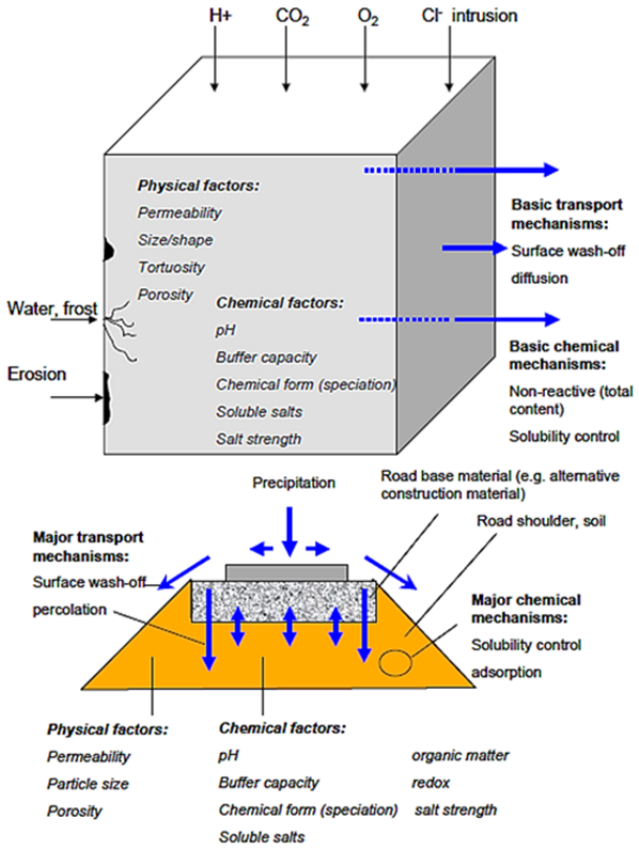

Figure 2-3 - Chemical and physical factors influencing the release of contaminants from materials [37].

Ultimately, the test methods presented in Table 2-2 are characterization tests which determine potential contaminant leaching. Although these tests are more comprehensive in comparison to the two EPA regulated leaching tests (TCLP and SPLP), they do not fully consider the effects of deterioration and its impact on release.

2.4.2 Service Life Deterioration and Environmental Performance

Concrete structures generally need to be repaired or replaced not because they are not strong enough to withstand the applied loads, but because the surrounding environment deteriorates the material and reduces its capacity [45]. Deterioration of concrete can lead to changes in release mechanisms of the RWC. Initial material deterioration during service life begins at the microscopic level in which microcracks form due to either

physical (mechanical and/or environmental loading) or chemical (deleterious physiochemical reactions, e.g. ASR) interactions. These microcracks may then become interconnected and form macrocracks which can allow rapid penetration of water with dissolved corrosive or chemically aggressive species. These cracks can lead to corrosion of the steel reinforcement, or chemical attacks that lead to a reduction of strength and stiffness, as well as serious cracking, spalling, and mass loss [46]. Table 2-3 shows the multiple application-dependent deterioration mechanisms that are involved in assessing the long-term durability of concrete. Initially, the release of a relatively new monolithic RWC specimen may be negligible due to the low diffusivity and permeability of concrete. This behavior changes as microcracks and surface cracks begin to develop and allow for water and other aggressive solutions to penetrate the material. Eventually, macrocracks and concrete spalling will expose fresh surfaces that are new potential sources for contaminant leaching. However, deterioration does not always increase the release of contaminants. For example, in concrete, where carbonation due to CO_2 can occur, the pH of the material decreases from 12 to around 8. Therefore for a pH dependent species such as lead, whose release is smaller when the pH is around the neutral range, carbonation can have a positive impact on release.

As previously described in Table 2-3, multiple complexities are involved in assessing the durability of concrete because they are application dependent and subject to multiple sources of uncertainty. In an attempt to narrow the gap between concrete durability and environmental performance, progress has been made on investigating the impact of durability factors (i.e. carbonation, intermittent wetting/drying, and freeze/thaw) on leaching of contaminants [47-50].

Table 2-3 - Summary of Main Concrete Deterioration Mechanisms

Mechanism	Agents and Exposure	Protection
Steel corrosion (main deterioration mechanism)	• Carbonation: ambient CO2 eliminates cover protection by lowering concrete pH < 9, corrosion initiates when surrounding concrete is carbonated and exposed to weather [51,52] • Chloride: seawater, groundwater, de-icing salts eliminate cover protection by lowering concrete pH < 9, which leads to corrosion initiation • Cracking bypasses steel cover protection • Water, oxygen react with steel causing cracking and spalling of cover [53]	• Alkaline concrete pH • 12.5 < pH < 13.5 • Cover thickness • Cover quality
Carbonation	• Ambient CO_2 penetrates from the surface, dissolves into concrete, reacts with hydroxides, converts them to carbonates, subsequent drop in pH < 9 • Not detrimental to concrete but eliminates alkaline steel protection • Moisture dependent, highest at: 40% < RH < 70% • Ambient CO_2 dependent: rural 0.03%, urban 0.3%, vehicle tunnels 1% [54,55]	• RH < 25% • RH > 90% • Increase Cover thickness • High strength • Low W/C
Alkali-aggregate reaction	• Alkali ions release through cement hydration react with siliceous minerals in aggregate, forms alkali-silica gel • Swelling of gel and subsequent cracking occur in presence of water • Gel goes from solid to liquid phases with water • Liquid gel is leached out by water and deposited in cracks • Reaction function of: nature and size of aggregates, moisture, pH [56,57]	• Avoid reactive aggregates • Use low alkali cements or SCM such as blast furnace slag cement
Sulfate attack	• Physical and chemical reactions • Naturally occurring sulfates of sodium, potassium, calcium, magnesium found in soils, seawater, and groundwater • Sulfates from industry and fertilizers • Release of sulfate from cement while in service [58]	• High quality concrete (low W/C) • Low permeable • Fly ash SCM
Acid attack	• Acids can be found in soils and ground water • Acids may be organic from plant decay or from industrial wastes • Liquids with pH < 6.5 attack concrete which is held together by alkaline compounds and is therefore not resistant to acids • Acid rain pH < 5.6 down to 4.3[59] • No complex chemical reactions but dissolution and disintegration of concrete	• Limit exposure to acids • Some SCMs reduce the rate of the attack
Seawater attack	• Physical abrasion from wave actions and chemical • Main durability concern: steel corrosion from sodium chloride ingress • Other minor chemical reactions: damage from sulfates, frost damage, etc.[57]	• Use SCM such as blast furnace cement
Physical abrasion/erosion	• Pavements and industrial floors • Erosion on spillways of hydraulic structures • Offshore structures subject to wave actions	• High strength concrete • Surface protection
Frost action	• Freeze-thaw (expansion-contraction) cycles • Degree of damage depends on the structure of the pore system • Damage can be avoided if pressure can be released by allowing the water to move out of the paste or to adjacent pores (air-entraining bubbles).	• Use 3%-6% air entraining admixture

Through research, coupled dissolution-diffusion models and multi-regime transport models have been developed in order to more accurately describe these changes in

behavior [60,61]. Similarly, Garrabrants and Kosson [62] are currently evaluating such a physical-chemical phenomenon from a waste management perspective by investigating the long-term contaminant release of cementitious solidification and containment of hazardous wastes. Even then, knowledge gaps continue to exist when linking durability and environmental performance as the coupled effects of the most relevant material deterioration parameters (i.e. service loading, fatigue, and weathering) on contaminant leaching have not been holistically investigated.

2.4.3 Environmental Assessment of RWC during Service Life

In order to properly assess the environmental behavior of PHSAs in concrete, test methods from Table 2-2 and the coupled dissolution-diffusion models need to be applied. Figure 2-4 displays the use of the pH Dependence and Percolation test methods and how they have been combined to assess the impact from aging of granular CRT-concrete roads on soil and groundwater, based on lead (Pb) release. The pH Dependence test results (Figure 2-4, left graph) illustrate the characteristic Pb leaching behavior from CRT-concrete as a function of pH, under equilibrium conditions (liquid/solid ratio = 10 L/kg). The percolation test method results (triangles) illustrate the Pb release until equilibrium is reached. Fresh concrete is expected to have a pH of about 12. This pH will change in time due to concrete carbonation to a pH value of about 8. Therefore, the squares in Figure 2-4 (Figure 2-4, middle graph) are extrapolations of the percolation leaching data (pH 12) and represent expected leaching due to percolation after aging (pH 8). The possible Pb release field behavior of the granular CRT-concrete is therefore expected to be somewhere between these two curves (circles). The indicative liquid to solid ratio (LS) scales under the percolation graph show LS ratios for scenarios of a road

based directly exposed to and protected from percolation. A relationship between LS rate and time can be derived using percolation equations given in Table 2-2 from the height of the road base, the infiltration rate, and the density of the material. Finally, concentration data from the percolation test (right) indicate that the concentration remains constant with varying LS ratios, which confirms a solubility controlled Pb release behavior. Overall, while the structural performance of a RWC is important, knowing the environmental behavior and performance of the material is essential. Using the tests and methods previously described, researchers and regulators will be able to more accurately predict the cumulative release, as well as the peak concentrations of potentially hazardous elements on soil and ground water.

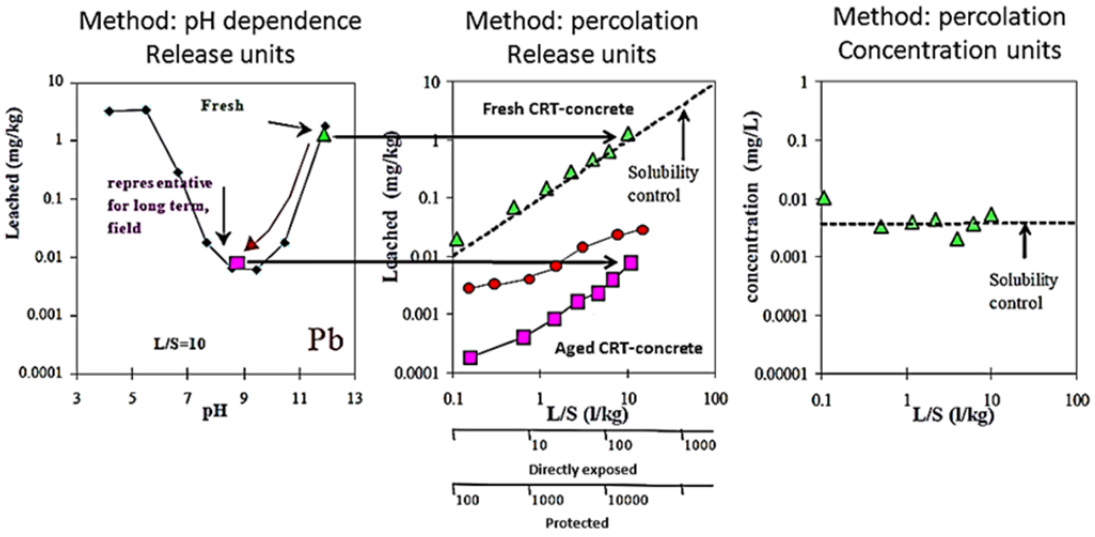

Figure 2-4- Effect of concrete carbonation on the release of Pb from granular concrete (Adapted from Van der Sloot [37])

2.5 End of Life

The environmental focus during this phase is on the reuse, recycling and down-cycling of RWC after its service life as indicated in Figure 2-1. The reuse of concrete applies only to pre-fabricated structures whose members are not monolithically connected. However, the

reuse of concrete is seldom promoted because concrete structures are custom designed for the loading conditions, and are heavy to dismantle and transport. Furthermore, the concrete structures that are often replaced are those exposed to continuous traffic such as sidewalks, curbs, roads, and highways, which are not reusable as a whole. Therefore, recycling crushed RWC as substitute construction aggregates is a more viable alternative. At the end of its life, about 80% of concrete is either recycled or down-cycled while the remaining is disposed in construction and demolition landfills [26]. With the propensity to recycle most of the concrete, one must be able to distinguish between ordinary concrete and RWC. Concrete mixtures are typically included in the construction documents; however, a visible indicator should be used as a secondary measure. To do this, colored dyes can be added during the batch or to the aggregate to help identify the RWC more easily. Special consideration to the pH of the stain or dye should be taken as it can have a negative impact on contaminant leaching for pH dependent species, especially acid-based products. Once the RWC is identified, special care should be taken when handling the material. The crushing and handling of concrete will likely expose pollutants from admixtures or secondary materials that were otherwise encapsulated in the monolithic concrete. These pollutants can be transported through air or water mediums and its release will be a function of the pH of the material and that of the environment (solubility control), similar to the release behavior during the manufacturing phase.

As indicated in Figure 2-1, potential end uses for down-cycled RWC concrete are general bulk fills, base or fill for drainage structures, pavement base and sub-base, lean-concrete bases, concrete blocks, or even bituminous concrete. While some of the end uses for

concrete may be in a monolithic form, the majority of recycled concrete is used in a granular (crushed) form. Because release is application dependent, recycled/down-cycled RWC needs to be properly assessed as different exposure conditions may expose these aggregates to rapid deterioration and possibly release of contaminants that were previously not accounted for. As an example, a monolithic concrete sidewalk can be more resilient to leaching in comparison to down cycled, crushed RWC used for base fill. Typically, these recycled aggregates will be stockpiled outdoors as they wait to be compacted in the field. For this reason, percolation column tests, pH dependence tests, and packed granular diffusion tests are essential to predict the end-of-life behavior granular recycled materials. Furthermore, more unknowns are introduced with the uncertainty of the RWC aggregate's strength and durability in a concrete mixture. In such case, the use of chemical admixtures or secondary aggregates to either improve the performance of concrete or reduce the environmental impact by recycling may result in a burden-shift to future generations and the environment if no EOL testing is conducted. Lastly, if the RWC concrete is to be discarded, then the appropriate leaching test (TCLP) needs to be conducted to verify that the material is safe for disposal as a composite. The following section describes a framework for readers to follow if interested in developing RWC.

2.6 Framework for the assessment of Recycled Waste Concrete

The multiple design and management related issues that are encountered during each phase of the life cycle of concrete were discussed in the preceding sections. However, it is desirable to develop a framework that allows for a systematic assessment on the use of

recycled waste aggregates in concrete mixtures. The proposed framework is illustrated in Figure 2-5 followed with a brief description of each step.

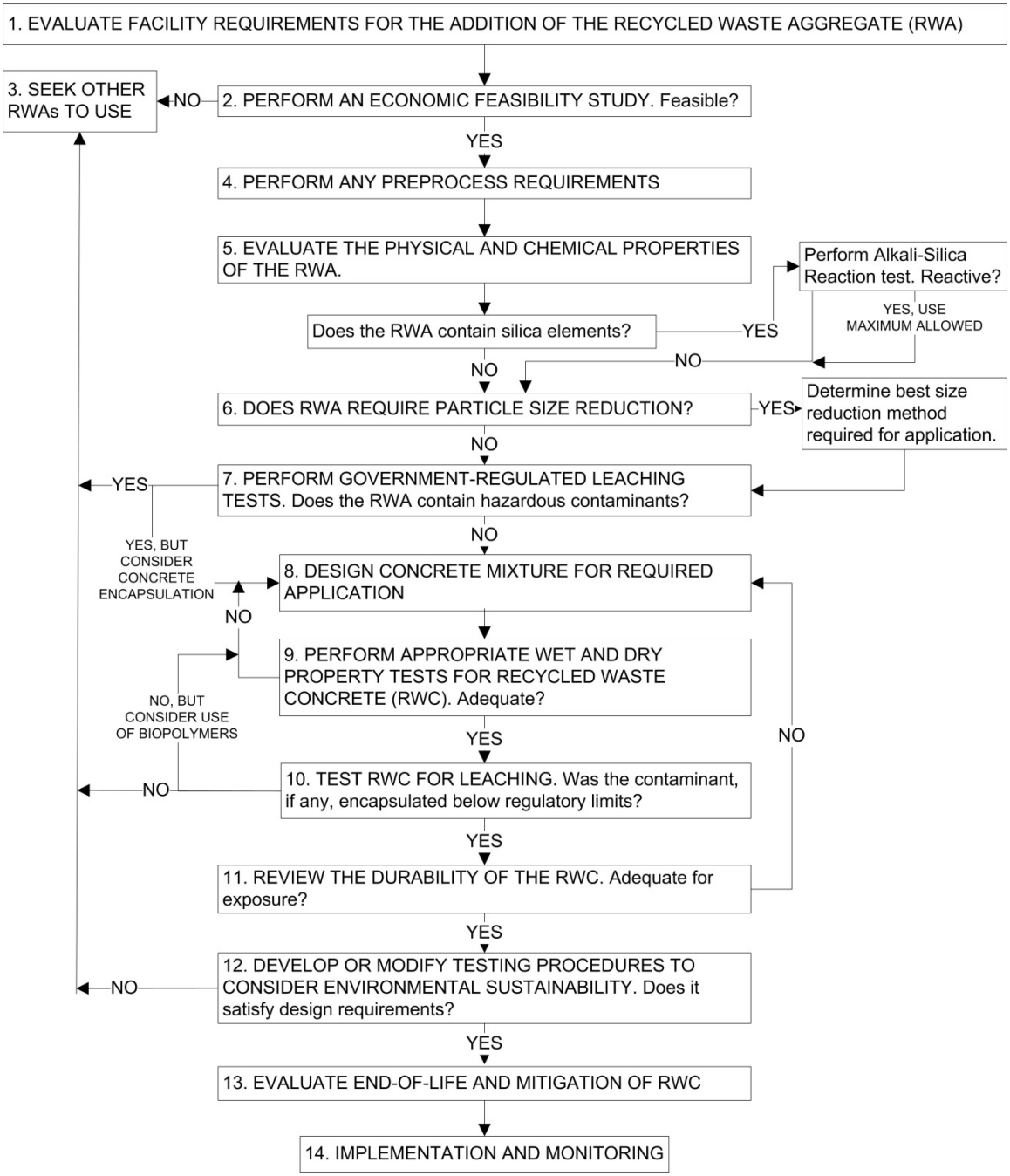

Figure 2-5 – Proposed framework for assessment and implementation of recycled waste aggregates in concrete

Step 1 - Evaluate Facility Requirements

Whether or not the concrete manufacturing plant exists or is being developed, the first step in this framework considers the facility requirements that are needed to implement the use of the recycled waste aggregate (RWA). Resource and management-related requirements should be reviewed during this step, including: storage solutions and preprocessing equipment for the RWA, permitting for handling the material, personnel training, minimum and maximum volume of RWA that can be delivered, and the development of environmental health and safety guidelines. Once these sort of requirements are established analyzed, an economic feasibility study can be developed.

Steps 2 and 3 – Perform Economic Feasibility Study

Apart from being an environmentally friendly solution, the use of RWAs in concrete may prove to be an economically feasible solution as well. While most RWAs are by-products of a current industrial process and need to be purchased (at a lower price than raw aggregates), certain recycled wastes like CRT glass will actually generate revenue just by receiving the waste. This step should review the requirements from Step 1 and compare the capital and operational costs (i.e. real estate, machinery, personnel, energy, and materials) to the savings and potential revenue generated from using the RWA. Included in the operational costs could be items such as the energy costs related to preprocess the aggregates(i.e. cleaning and size reduction), as well as any special admixtures necessary to maintain the workability of the material or biopolymer solutions used to encapsulate a contaminant. Additionally, this step requires a forecast study on the supply of the RWA that will be available and its expected supply lifetime. If the RWA is economically feasible then one can proceed with the analytical steps.

Step 4 – Perform any Preprocess Requirements

Certain recycled wastes may require dismantling, cleaning, or other processes before it can be used as a RWA. This step is essential in the framework because preprocessing and sorting of materials improves the quality of the RWA. A lack of quality control may lead to a large spread of the results in any test conducted (e.g. material characterization, strength, durability, leaching). For instance, CRT units need to be dismantled from their plastic covers, have their cathode-ray tube equipment removed, then the glass is crushed, pass through a metal separator, and finally washed. Similarly, other recycled wastes like fuel and oil filters will need to be rinsed to remove any residue and then shredded. Furthermore, processing fluorescent lights requires that the mercury vapor is removed, while other materials like Polychlorinated Biphenyl (PCB) and batteries may have their own specific preprocessing requirements.

Step 5 – Evaluate the Physical and Chemical Properties of the RWA

For proper implementation of the RWA into concrete mixtures, material (physical) properties such as: absorption, specific gravity, as well as particle shape and size distribution, must be well understood. As previously explained in Section 2.3, these properties have a direct impact on the workability and strength of a concrete mixture. Additionally, a chemical composition analysis should be conducted on the RWA to evaluate if hazardous contaminants are integrated within the material. Silica-based aggregates in concrete can be troublesome and if used, they can lead to deleterious alkali-silica reactions (ASR) when the aggregate interacts with an alkali-rich cement. If silica is found in the RWA, then it is recommended that an ASR test [63] is conducted to verify if

the aggregate is reactive with cement and what is the maximum amount of the aggregate that can be used and meet this durability guideline.

Step 6 – Particle Size Reduction for the RWA

This step is dependent on use of the RWC in the concrete mixture (e.g. replacement for the coarse, fine, or cementitious material in the concrete mixture). Particle size reduction is necessary for aggregates that do not meet the required gradation as set by the regulating agency. For example, the Florida Department of Transportation specifies that fine aggregates should have a diameter between 0.075 mm - 4.5 mm, while coarse aggregates can range from 4.5 mm to 89 mm. The selection of the crushing method is also crucial to the performance of the concrete mixture. Ball mills typically produce aggregates with rounded edges (which improve workability), while hammer mills typically leave sharp edges on the reduced aggregate (which improves the strength and adhesion of the mixture).

Step 7 – Perform Government-Regulated Leaching Tests

In addition to the chemical composition test for both hazardous and non-hazardous elements, researchers must also investigate if the elements embedded in the RWA will leach to the environment at hazardous concentrations. TCLP [13] and SPLP [14] analyses are two federally-regulated tests most commonly used to determine whether or not the material is considered hazardous. Performing these tests will determine if the RWA is a suitable candidate for use. In the case that the material is considered hazardous, two options are available: seek another RWA or consider moving forward and investigate whether encapsulating the RWA in concrete is possible. Also known as stabilization and

solidification of waste, concrete encapsulation has been successful in the disposal of radioactive waste and other hazardous waste.

Step 8 – Design Concrete Mixture for Required Application

This step considers the design of a concrete mixture containing a processed and analysed RWA. Concrete mixture design is application dependent. While a mixture can be used for multiple applications, its optimal performance is observed when the material is used for what it was designed for. Local concrete manufacturing plants may provide their mixture compositions for research purposes. Typically, investigators may ask for their most commonly used concrete mixture for the application being considered and then substitute a percent of the aggregate required with the RWA. On the other hand, custom mixture designs are possible with the help of ACI 211-1, a publication by a committee in the American Concrete Institute that addresses the selection of proportions for normal, heavyweight, and mass concrete [64].

When designing a concrete mixture, aggregate substitutions in 10% increments are suitable. The maximum amount of RWA that can be used will be controlled by ASR expansions (if any), the replacement percentage that yields a compressive strength lower than the control mixture (Step 9), or the replacement percentage that leads to leaching concentrations that are greater than the regulatory limits (Step 10); whichever is lower. Additionally, the selection of the water to cement ratio is critical to the permeability of concrete which can have a detrimental impact to its durability and environmental performance. Ratios that are kept below 0.4 may produce a concrete matrix with a permeability low enough to withstand significant hydrostatic pressures. This helps encapsulate the RWA and prevents the intrusion of water and chlorides that can

eventually deteriorate the material. Lastly, it is necessary to consideration the absorption and shape of the RWA. Aggregates that have high absorption or sharp edges will require more water to maintain its workability. Super-plasticizers and water reducing admixtures balance the requirement of water and workability but they are costly and may make the use of RWA economically unfeasible,

Step 9 – Perform Appropriate Wet and Dry Property Tests for RWC

This step determines whether the RWA is physically suitable for use in a concrete mixture. Concrete workability [65], air content [66], and 28-day compressive strength [67] measurements are the basic properties that a RWC mixture must meet to be considered a viable solution. Not only is the compressive strength vital to the safety of structure and its occupants but its air content and slump are also used by engineers and contractors as the acceptance criteria for the concrete mixture. Failure to satisfy these three basic properties will lead to a rejection of the material, a financial loss, and most importantly, delays in the project. Therefore, if the measured properties of the RWC are not close to the design value, then the mixture must be re-designed and these properties must be measured once again until the design criteria are met.

Step 10 – Test RWC for Leaching

This step, a repeat of Step 7, investigates the leaching of possible contaminants from the RWC material. This step serves as a check to evaluate if the cementitious matrix was able to bind to and encapsulate the hazardous contaminants embedded in the RWA (if any) and can be avoided if no potentially hazardous contaminants are found in Step 7. If hazardous contaminants are found to be leaching at concentrations greater than regulatory limits, the investigator can either conclude that the RWA is not suitable for use in

concrete mixtures, or, return to Step 8 and re-design the concrete mixture while considering the use of organic biopolymers [19,20,68] to bind and encapsulate heavy metal contaminants (if that is the case) within the cementitious matrix.

Step 11 – Review the Durability of the RWC

Provided that the RWC meets the structural design and environmental criteria, the next step in this framework requires an assessment of its durability. Concrete durability is exposure-dependent and its design (Step 7) should consider this. One way to address durability of a concrete material through design is by using chemical admixtures. For instance, air entraining admixtures are used to improve the freeze-thaw resistance of concrete. Similarly, corrosion-inhibiting admixtures help inhibit the corrosion of steel reinforced concrete. However, durability assessments still need to be conducted to ensure that the highest quality RWC is produced for the given application and exposure. These assessments are found in Table 2-3. Each assessment contains target values that will determine the quality of the concrete mixture (i.e. poor, acceptable, good, and excellent). If the durability rating for the RWC is satisfactory for the intended use, then the next analytical step is taken.

Step 12 – Develop or Modify Testing Procedures to Consider Environmental Sustainability

Once the RWC mixture has satisfied the basic regulatory and design requirements for structural compressive strength, environmental leaching (i.e. TCLP and SPLP) and durability, it is then recommended that the investigator focuses on implementing testing procedures that will assess if the material will become a burden shift for future generations. These testing procedures can either be existing tests as well as new or

modified versions of them. Primary to the investigation of burden shift, when using waste aggregates in concrete mixtures, is the impact to the environment (especially if the material is hazardous). Described in Section 2.4, are environmental tests methods that are not yet enforced by the Environmental Protection Agency but are highly encouraged due to their ability to characterize the behavior of the material under any exposure. These tests, along with structural and durability tests can be combined to understand the behavior of a material for any design condition. For instance, one of the main objectives of this dissertation is to understand how deterioration of a RWC specimen will affect the release of Pb. This objective was achieved by combining and modifying known durability tests (i.e. ASR and freeze-thaw tests) that periodically deteriorate a specimen with a diffusion leaching test (EPA Method 1315). By combining these two well-known test methods, new knowledge of how certain durability parameters (e.g. mass loss, loss of modulus of elasticity) affect Pb release was gathered. Additionally, empirical relationships may be developed (if they exist) if the right parameters are measured. These relationships can then be used to investigate if leaching will become a problem during the service life of the material. This is just one way of how currently available testing procedures can be combined and modified to better analyze the material. Although the RWC must meet the regulated standard tests, this step in the framework allows for flexibility with testing protocols for investigators that want to develop a RWC material that will be durable, safe for the environment, and most importantly, not a burden shift to other generations.

Step 13 – Evaluate End-of-Life Scenarios and Mitigation of RWC

Prior to the implementation of the newly created RWC, the manufacturing procedures, safety measures, and methods for identifying and mitigating the RWC need to be established. Beginning with the manufacturing of the RWC material, safety measures need to be created for the storage, processing, and handling of the RWA. This includes the proper respirators and goggles (if dealing with fine particles), or the proper permits for storage of hazardous wastes (i.e. CRT glass). Additionally, if the RWC contains hazardous RWAs, then markers within the material need to be placed to visually inform those handling the material at its end of life (discussed in Section 2.5). At its end-of-life, the material may be used as fill material or as a recycled aggregate in concrete mixtures. For fill applications, the crushed RWC should be tested for percolation leaching (explained in Table 2.2) to ensure that the aggregate will not pollute the ground water. On the other hand, if the RWC is used as an aggregate, its mechanical and environmental properties must be studied once again.

Step 14 – Implementation and Monitoring

Once the RWC mixture is finalized and the facility is built/adapted, then continuous monitoring of operational costs and field performance (i.e. leaching of contaminant) is suggested to provide data that can be used for future estimates of new facilities, material durability, and environmental impacts. In this final step, the investigator should be capable of producing specifications for maximum substitution rate of the RWA as well as be able to target specific compressive strengths. Additionally, the investigator should have a better understanding of what leaching concentrations of the constituent of concern are expected during the materials service life.

2.7 Conclusion

This assessment has presented the impact that PHSAs in concrete can have on the people and the environment throughout its three life-cycle phases. The assessment of RWC needs a holistic life-cycle view due to the numerous factors and mechanisms that affect contaminant release. While the bulk of contaminant release occurs during the service life of the material, this review discussed how to assess the impact on water pollution for special cases occurring during processing and storage of a PHSA as well as the end-use of a RWC. It is well understood that the current regulatory leaching tests (TCLP, SPLP) can under or over-predict the release of contaminants into water sources and are not representative of the materials performance during its service life. For this reason, it is encouraged that the proposed EPA tests which were noted in this chapter be used to characterize the behavior of the material in all phases of the RWC. Noting that water pollution is one of the most critical aspects for the environmental impact assessment of a RWC, this assessment also highlighted that durability and deterioration are tightly coupled with water pollution. A framework was proposed for investigators to use as a guide if they plan to work with RWAs in concrete mixtures. All things considered, a gap continues to exist when it comes to predicting the effects of deterioration on contaminant release. Modified tests methods that are hybrids of durability and characterization tests need to be explored if a more accurate understanding of the release of contaminants from PHSAs is sought.

Chapter 3

Study 1 - Study on the Mechanical and Environmental Properties of Concrete Containing Cathode Ray Tube Glass

3.1 Background

The rapid transition towards more energy efficient displays has made Cathode Ray Tube (CRT) glass a major disposal problem and global concern. Usually found in computer monitors and televisions, a typical CRT unit is composed of 63.2% screen glass, 24% cone glass, 12% ferrous metals, and 0.8% components [69]. The concern stems from the high concentrations of lead (Pb) oxide (20-25% by weight) heavy metals embedded in the CRT's neck and funnel glass for protection against X-rays. The U.S. Environmental Protection Agency (EPA) classifies CRT glass as hazardous due to its toxicity [70]. Total amounts of CRT discarded yearly vary within regions. In Europe it is estimated that over 150,000 tons of CRT glass are treated yearly and over 600,000 tons could be reached in 2013 [9]. The Florida Department of Environmental Protection (FDEP) estimates that approximately 2.7 million CRTs become available for disposal in the state on an annual basis [10]. Meanwhile, Herat [11] indicates that over 100 million CRTs are disposed nationwide. The problem is that common recycling and disposal practices such as glass smelting or electronic landfill disposals are becoming obsolete and not sustainable.

In a similar fashion concrete production can be considered an environmental concern since it is an industry where raw natural aggregates are constantly being mined. In 2010 an estimated 3.3 billion tons of cement were produced, 10 billion tons of sand and rock excavated, and 1 billion tons of water were used for concrete production [2]; these amounts reflect an increase of 51.5% in this past decade [3]. Crushed CRT-glass can help

reduce raw natural aggregate consumption as long as the structural integrity and durability of the concrete is not compromised; i.e. the silica content of the CRT glass does not cause deleterious expansions due to alkali-silica reactions (ASR). Experimental studies have found correlations between ASR and glass particle type (chemical composition), size, content, and color [71]; while other studies have concluded that up to 20% crushed recycled glass used as a fine aggregate will show no ASR expansions if used with an ordinary portland cement mixture [34,72]. The results of these studies are shown in Table 3-1. As illustrated, for applications demanding larger sizes or quantities of crushed glass aggregates the potential for ASR induced damage can be reduced or even eliminated by using supplementary cementitious materials or finely crushed glass [73-78].

Table 3-1 - ASR Expansions due to Waste Glass used as Aggregate

Study [reference]	SCMs Used	Waste Glass Size Used		
		Glass Powder (< 10 µm)	**Fine Glass (0.15-4.75mm)**	**Coarse Glass (> 4.75mm)**
[73]	PC w/25% FA	Replaced up to 30% **Below Expansion Limit***	Replaced up to 50% **Below expansion limit** (.15-4.75 mm)	50% **Below expansion limit** (4.75-12mm)
[78]	PC with 10% SF	Replaced up to 30% **Below Expansion Limit**	Replaced 40-75% **Below Expansion Limit** (.15-2.36mm)	N/A
[34]	PC w/25% GGBS-FA	N/A	Replaced up to 20% **Below Expansion Limit** (0.075-2.36mm)	N/A
[72]	PC	N/A	Replaced up to 20% **Below Expansion Limit** (0.15-2.36mm)	N/A
[33]	PC	N/A	Replaced 30-70% **Above expansion limit** (0.1-5mm and 6-20 mm)	
[28]	PC	N/A	N/A	Replaced 25-100% **Above expansion limit** (4-16mm)

SCMs – Supplementary cementitious materials, PC – Portland Cement, SF – Silica Fume, GGBS – Granulated Blast Furnace Slag, FA – Fly Ash, N/A – Not applicable. *Expansion limit is 0.1% increase of original length.

The aim of this study is to address the recycling/raw-material-consumption issue by using secondary materials, i.e. CRT glass, as a fine aggregate replacement in an ordinary portland cement concrete mixture. An organic cross-linked biopolymer solution of guar gum and boric acid was used in this study to see if it can aid in Pb encapsulation. This cross-linked biopolymer solution was first proposed by Kim [20]. The combination of Guar gum (GG), typically used in the food industry as a food thickener, and boric acid, creates a chemical structure that allows them to bind to metallic ions. Material characterization, structural and durability testing, as well as environmental tests for possible lead leaching under different exposure scenarios were conducted to investigate the performance of CRT-Concrete.

3.2 Materials and methods

3.2.1 Experimental Plan

The granulated CRT glass that was used as an aggregate replacement for concrete was analyzed for specific gravity, water absorption, particle size distribution, and Pb composition. Furthermore, due to the silica content of the CRT, ASR tests were conducted for each percent replacement. Cylindrical concrete specimens were cast with varying contents of crushed CRT (10%, 20%, and 30%) using two different mixture designs and their physical and mechanical properties were analyzed; five replicates for each mixture were tested. Lastly, Pb leaching tests were conducted using the Synthetic Precipitation Leaching Procedure (SPLP, EPA Method 1312 [14]) and two preliminary methods being proposed to the EPA, a pH dependence test and a percolation column leaching test.

3.2.2 Materials

Ordinary Type I Portland cement was used. Fine and coarse limestone aggregates were obtained from local Florida quarries. The specific gravity and absorption properties of these aggregates are shown in Table 3-2. The CRT glass used in this study was derived from both television and computer monitors and a homogeneous mix of panel and funnel glass was used. The CRT was granulated using a cross-beater mill and the metal composition of the CRT glass is shown in Table 3-3.

Table 3-2 - Physical properties of aggregates

	Specific Gravity SSD	Specific Gravity OD	Absorption (%)
#89 Limestone	2.420	2.328	3.63
#57 Limestone	2.466	2.374	3.69
Sand	2.529	2.436	3.71
Crushed CRT	3.012	3.009	0.10

Table 3-3 - Crushed CRT metal composition

Element	Results (mg/kg)	MDL (mg/kg)	PQL (mg/kg)
Barium	2580	0.017	0.051
Lead	41750	2.64	7.92
Strontium	11060	0.06	0.18

MDL - Method detection limit, PQL - Practical quantification limit

3.2.3 Mixing and Preparation

The study aimed to investigate the behavior of CRT-Concrete using two conventional concrete mixtures in South Florida plus one unconventional mix that aimed to reduce Pb leaching using organic biopolymers. Mix 1 is an ordinary non-structural mixture while Mix 3 is an ordinary normal weight structural concrete mixture. An additional mixture (Mix 2) was also prepared using the same proportions as Mix 1, but with the mixture water being partially replaced with a cross-linked biopolymer solution of GG and boric acid diluted in water. The mixture proportions can be found in Table 3-4. For this study, CRT glass was used to replace the aggregates by 10%, 20%, and 30% by volume. All

molded specimens were covered to prevent loss of moisture during the first 24 hours and then placed inside a curing room at 100% relative humidity until its 28th day. The mixture proportions used to evaluate the ASR expansion characteristic were prepared in accordance with ASTM C1260 - Standard Test Method for Potential Alkali Reactivity of Aggregates (Mortar-Bar Method) [63].

Table 3-4 - Concrete mixture design

Mix 1				
	0% CRT	10% CRT	20% CRT	30% CRT
Cement, kg/m^3	344	344	344	344
Sand , kg/m^3	977	879	782	684
Crushed CRT, kg/m^3	-	116	233	349
#89 Rock, kg/m^3	771	771	771	771
Water, kg/m^3	163	163	163	163
Water Reducer, mL/m^3	897	897	897	897
Air Entrainer, mL/m^3	116	116	116	116
Mix 2 (Mix 1 w/Biopolymers)				
	0% CRT	10% CRT	20% CRT	30% CRT
Cement, kg/m^3	344	344	344	344
Sand , kg/m^3	977	879	782	684
Crushed CRT, kg/m^3	-	116	233	349
#89 Rock, kg/m^3	771	771	771	771
Biopolymer, L/m^3	-	4.5	8.9	13.3
Water, kg/m^3	163	126	89	52
Water Reducer, mL/m^3	897	897	897	897
Air Entrainer, mL/m^3	116	116	116	116
Mix 3				
	0% CRT	10% CRT	20% CRT	30% CRT
Cement, kg/m^3	314	314	314	314
Sand , kg/m^3	869	782	695	608
Crushed CRT, kg/m^3	-	103	228	310
#57 Rock, kg/m^3	979	979	979	979
Water, kg/m^3	153	153	153	153
Water Reducer, mL/m^3	1044	1044	1044	1044

3.2.4 Tests methods

The applicability of crushed CRT as a fine aggregate replacement in concrete was examined through a series of material, mechanical, and Pb leaching tests. The tests conducted were in accordance with the methods listed in Table 3-5. Because of the

proposed application for CRT-Concrete, SPLP testing was chosen as the benchmark test. Two leaching characterization tests were also conducted in this study. For each specimen, a water sample was tested for pH, mV, and conductivity while the lead concentration was analyzed using an atomic absorption spectrometer using the flame method.

Table 3-5 - Test Methods

Test items	Test method
Crushed CRT	
Test Method for Density, Specific Gravity, and Absorption of Fine Aggregate	ASTM C128 [79]
Test Method for Sieve Analysis of Fine and Coarse Aggregates	ASTM C136 [80]
Fresh Concrete	
Test Method for Slump of Hydraulic-Cement Concrete	ASTM C143 [65]
Test Method for Density, Yield, and Air-Content of Concrete	ASTM C138 [66]
Hardened Concrete – Mechanical	
Test Method for Potential Alkali Reactivity of Aggregates (Mortar-Bar Method)	ASTM C1260 [63]
Test Method for Compressive Strength of Cylindrical Concrete Specimens	ASTM C39 [67]
Hardened Concrete - Environmental	
Synthetic Precipitation Leaching Procedure	EPA Method 1312 [14]
Liquid-Solid Partitioning as a Function of Eluate pH Using a Parallel Batch Extraction Procedure	EPA Prelim. Method 1313 [38]
Liquid-Solid Partitioning as a Function of Liquid-to-Solid Ratio Using an Up-Flow Percolation Column Procedure	EPA Prelim. Method 1314 [30]

3.2.4.1 ASR testing

For the ASR test, five mortar bars were made for each CRT percentage substitution in accordance to ASTM C1260. The specimens were cured for 24 hours, demolded, immersed in water for another 24 hours, and then stored in a 1N NaOH solution at 80°C. The change in length was recorded using a length comparator at 2-3 day intervals for 14 days. Photos showing the mixing of the specimens as well as the testing setup can be found in Figure A-1 to Figure A-3.

3.2.4.2 Compressive strength testing

Five 100 by 200 mm concrete cylinders of each mixture design and CRT percentage were tested for their 28-day compressive strength. Specimens were sulfur-capped according to ASTM C617 [81] and tested according to ASTM C39 [67] using a hydraulic testing machine and digital indicator. A photo of the sulfur capping and compressive strength testing can be found in Figure A-4 and Figure A-5.

3.2.4.3 SPLP testing

To test for lead leaching into the groundwater from the CRT-Concrete an SPLP analysis was conducted. According to EPA Method 1312, 100g samples from each of the cylinders were crushed to pass through a 9.5 mm standard sieve. The extraction fluid used was a 60/40 percent weight mixture of sulfuric and nitric acids to reagent water until the pH was 4.20 ± 0.05. The samples were tumbled at 30 ± 2 rpm for 18 ± 2 hours, filtered using a 0.7μm glass fiber filter, and acidified with nitric acid until reaching a pH < 2. A photo of the testing setup can be found in Figure A-6 and Figure A-7.

3.2.4.4 pH dependence testing

Introduced as EPA Preliminary Method 1313[38], this method characterizes the leaching behavior of a material throughout the pH spectrum. Nine target pH values were selected and 20g samples of the specimens for each pH target were crushed to pass through a 0.297 mm sieve. The sample was placed in contact with 200 ml of the extraction fluid, a combination of deionized water and 2.0 N Nitric acid, to reach the target pH value. The sample was then tumbled at 28 ± 2 rpm for 24 ± 2 hours. The eluant was filtered using 0.45μm glass fiber filter and acidified with nitric acid until reaching a pH < 2.

3.2.4.5 Percolation column testing

Introduced as EPA Preliminary Method 1314 [30], this method is a percolation column test designed to obtain liquid-solid partitioning (LSP) information as a function of liquid-solid ratio (L/S). The purpose of this test is to simulate leaching of materials being stockpiled and allows for projection towards long term leaching behavior [82]. The CRT-Concrete was reduced to a particle size smaller than a 2.38 mm sieve. A 5 x 30 cm column was then packed with the sample and sealed at both ends with a cap and a layer of fine quartz sand to prevent any solids from clogging the test setup. Deionized water was then pumped through the column and nine samples (based on the target L/S) were collected until a L/S of 10 was reached. The eluant was filtered using 0.45μm glass fiber filter and acidified with nitric acid until reaching a pH < 2. A photo of the testing setup can be found in Figure A-8 and Figure A-9 of Appendix A.

3.3 Results and discussion

3.3.1 Mechanical properties and durability testing of CRT-Concrete

Density, slump, compressive strength, and ASR tests were conducted in order to examine the fresh and hardened properties of CRT-Concrete at different replacement ratios.

3.3.1.1 Slump and Density of CRT-Concrete

All three mixtures displayed a decrease in slump as more CRT fine aggregate replacement was used. As previously reported, the decreasing trend may be due to the angular shape of the crushed CRT which creates interlocks between aggregate-aggregate and aggregate-cement particles that lessen the fluidity of the concrete and increase the demand for more water or admixtures in order to break them apart [33]. In addition, the

thick, gel-like texture of the biopolymer solution that was used in Mix 2 further decreased the slump of the concrete.

The wet density of CRT-Concrete was also measured and the results are shown in Figure 3-1. Compared to the control, the increase in density was directly proportional to the percent replacement. For Mix 1, the density increased by 0.3%, 2.2%, and 2.3%; while Mix 2 displayed a density increase of 1.9%, 2.6%, and 2.8%, for 10%, 20%, and 30% CRT replacements, respectively. Similarly, an increase in density of 0.4%, 1.5%, 1.8% was observed in Mix 3. The increase was due to the specific gravity of the crushed CRT which was 19.1% greater than that of limestone sand. Lastly, the difference in density between Mix 1 and 2 may be attributed to the addition of the biopolymer solution which was denser than water.

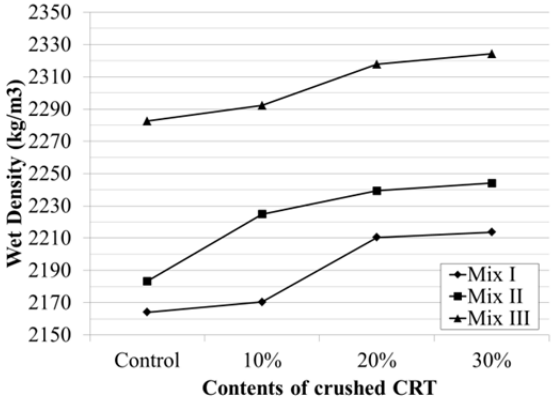

Figure 3-1 - CRT-Concrete density.

3.3.1.2 Alkali-silica reaction

The expansion of CRT-Concrete was investigated for different replacement percentages and the results are presented in Figure 3-2. As shown in the figure, there is a visible reaction between the crushed CRT and cement as deleterious expansions occur. According to the standard, expansions of less than 0.10% at 16 days after casting are

indicative of innocuous behavior, expansions of more than 0.20% are indicative of potentially deleterious expansion and expansions between 0.10 and 0.20 % may be innocuous or deleterious in field performance. Expansions on day 16 were 0.12%, 0.31%, and 0.38% for 10%, 20%, and 30% crushed CRT replacement, respectively. Given the results, it appears that CRT-Concrete can be potentially deleterious in field performance if more than 10% crushed CRT is used in the concrete. However this effect may be suppressed by using supplementary cementitious materials such as fly ash, metakaolin, or ground granulated blast-furnace slag [74-77].

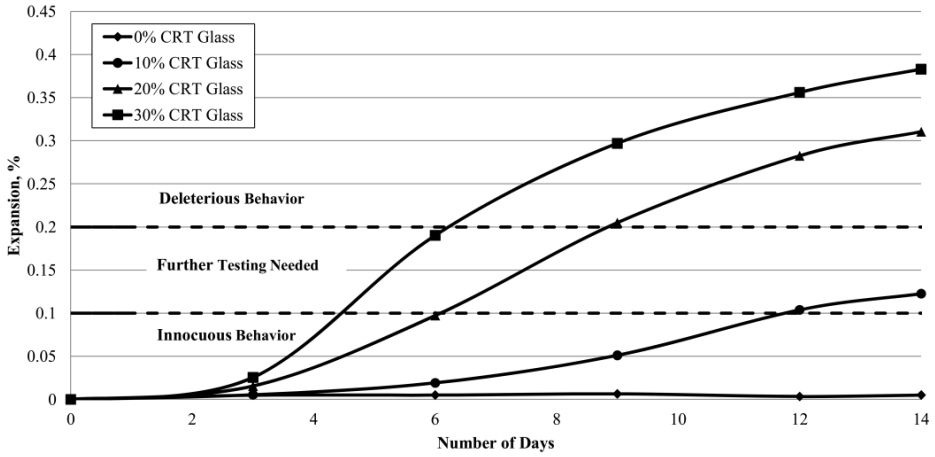

Figure 3-2 - ASR expansion of CRT-Concrete

3.3.1.3 Compressive strength

As shown in Figure 3-3, there appears to be an added benefit in using CRT in concrete as its ultimate strength increases as more crushed CRT is used. With respect to the control, Mix 1 showed 5.5%, 19.5%, and 13.2% improvements in compressive strength, while the same mixture with biopolymers showed 2.3%, 8.5%, and 5.1% strength improvements. Lastly, Mix 3 showed a similar relationship as its strength increased by 6.2%, 7.3%, and 6.1% with 10%, 20%, and 30% crushed CRT substitution, respectively.

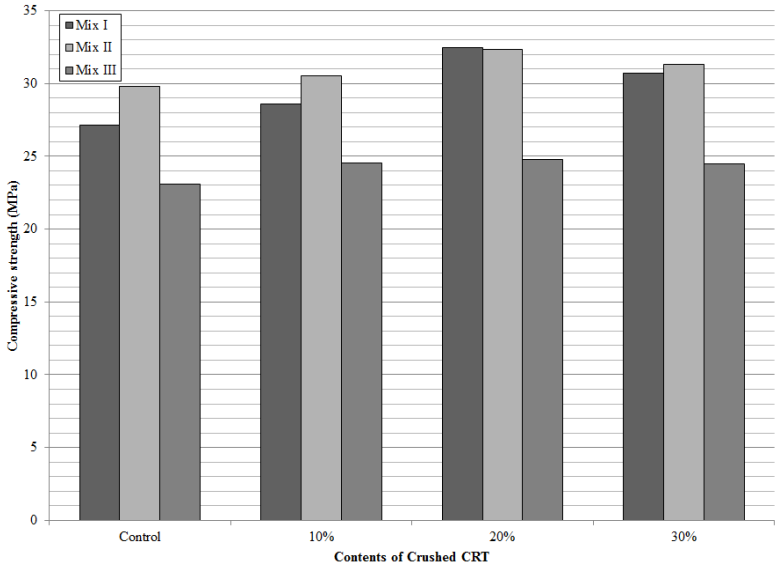

Figure 3-3 - Compressive strength of CRT-Concrete

3.3.2 Leaching Procedures for CRT-Concrete

3.3.2.1 SPLP testing

The analysis was run in triplicates using EPA Method 7000B following extraction by the SPLP procedure. To assess if the CRT-Concrete would be suitable for the environment, the drinking water standard for lead (0.015 mg/L) was used as the limit. The results presented in Table 3-6 show the benefits of using the biopolymer solution as it reduces the concentration of lead leaching from the sample and meets and exceeds the drinking water standard at CRT replacements of up to 20%. The lead concentrations for the non-biopolymer mixtures (Mix 1 and Mix 3) were above the drinking water criteria for lead and therefore further studies are needed if crushed CRT is to be used in concrete without any biopolymers. It is important to note that the leached concentration for the biopolymer mixture is higher than that of previous studies [20,23]. This is due to the CRT used in this study whose concentration of embedded lead is in the tens of thousands parts per million (ppm) instead of the several hundred ppm seen in other studies.

Table 3-6 - SPLP results

Mixture	Percent replacement	pH	Pb concentration (mg/L)
Mix I	10	12.11	0.043
	20	12.16	0.18
	30	12.1	0.338
Mix II	10	12.19	0.002
	20	12.29	0.012
	30	12.09	0.033
Mix III	10	12.25	0.016
	20	12.18	0.122
	30	12.19	0.132
CRT glass	-	-	4.169

3.3.2.2 pH dependence testing

The acid-neutralization capacity of CRT-Concrete for different percent replacements is shown in while the solubility of lead at different pH values is seen in Figure 3-5. As expected, lead leaching from the CRT-Concrete followed an amphoteric release behavior with minimum release between the pH range of 7 and 12. Furthermore, a steep increase in concentration is observed as the solution becomes more acidic. Contrary to the SPLP results, the concrete mixture containing the biopolymer solution did not have a significant effect on reducing Pb leaching when exposed to various pH values. The strong acid solution used in this test may have broken the bonds that were created between the Pb and the cross-linked biopolymer solution. Although the release appears to be high, the pH dependence test is only meant for characterization of the material and does not represent the conditions of a monolithic specimen whose release will most likely be controlled by diffusion.

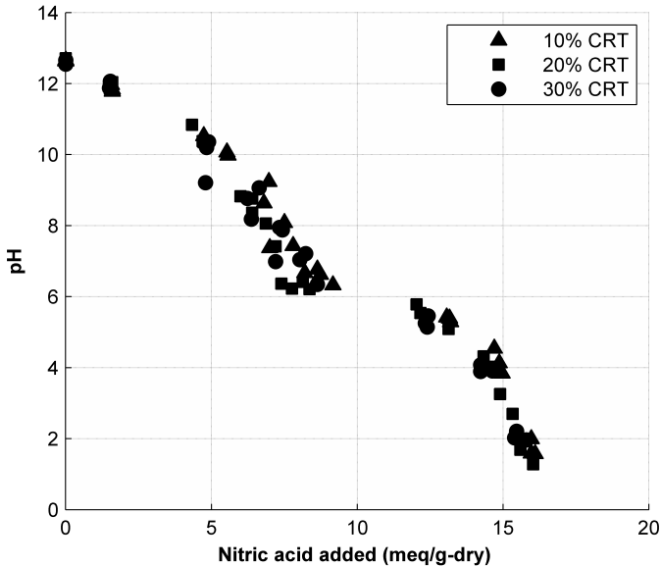

Figure 3-4 - Acid-neutralization capacity

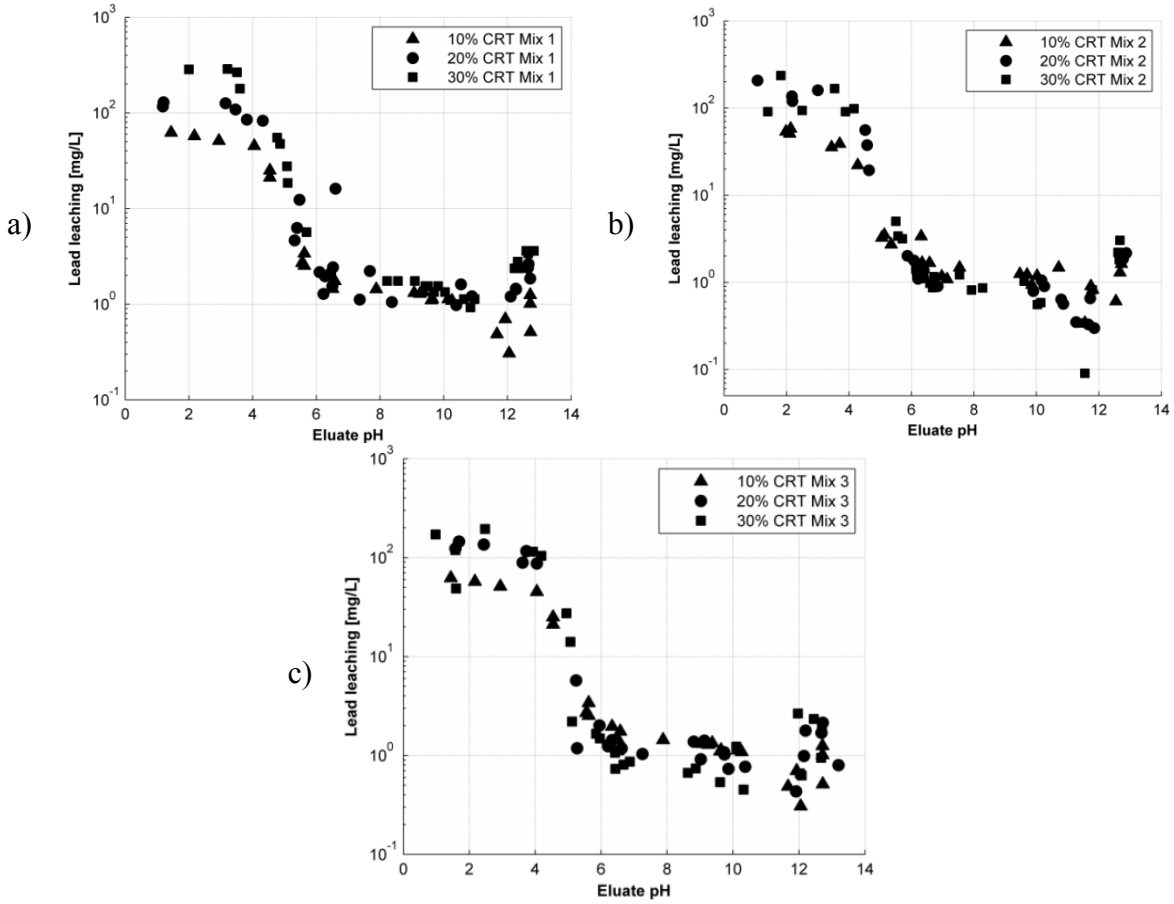

Figure 3-5 - Pb leaching vs. pH for a) Mix 1, b) Mix 2, c) Mix 3

3.3.2.3 Percolation column testing

For each mixture type and percent CRT replacement, nine extractions at selected L/S ratios were taken to investigate if any trend of lead leaching exists as the pore solution reaches equilibrium. Figure 3-6 shows the pH and conductivity of the material as a function of the L/S ratio. Throughout the experiment, the pH stabilized between 12.4 and 12.9 for all L/S ratios and its behavior was nearly constant with the exception of Mix 2 whose pH decreased as the L/S ratio increased. This could be due to the biopolymer-based pore water in the CRT-Concrete that is being released into the solution. Although the pH of the eluate remained close to constant, there was an observed decrease in the conductivity of the eluate. The change in conductivity as a function of L/S ratio was as follows; 13.6-7.3 mS/cm for Mix 1, 9.7-3.3 mS/cm for Mix 2, and 11.9-6.0 mS/cm for Mix 3. The decrease in conductivity may infer that ionic strength compounds such as calcium, sodium, potassium or lead ions were removed from the solution as time progressed, i.e. leaching decreased as time progressed.

Figure 3-7 shows the behavior of lead solubility as a function of the L/S ratio. For all the specimens tested, an increase in solubility is observed between L/S = 0 and approximately L/S = 1.8. This behavior can be due to a surface wash-out effect, in which the lead compounds located on the face of the material are initially flushed. After the wash-out phase, Mix 1 shows a slight reduction of lead solubility between 1.4-1.0 mg/L, 2.0-1.6 mg/L, and 4.0-3.1 mg/L for 10%, 20%, and 30% crushed CRT replacement, respectively. Mix 3 displayed a similar trend with results between: 1.4-0.9 mg/L, 2.6-1.9 mg/L, and 3.5-2.7 mg/L; and Mix 2 displayed a better performance with a decrease of: 1.0-0.7 mg/L, 2.2-0.9 mg/L, and 3.1-0.9 mg/L for 10%, 20%, and 30% crushed CRT

replacement, respectively. These results show the slight advantage with using biopolymer solutions to encapsulate the lead compounds in the concrete matrix for advection-controlled scenarios.

a)

b)

c)

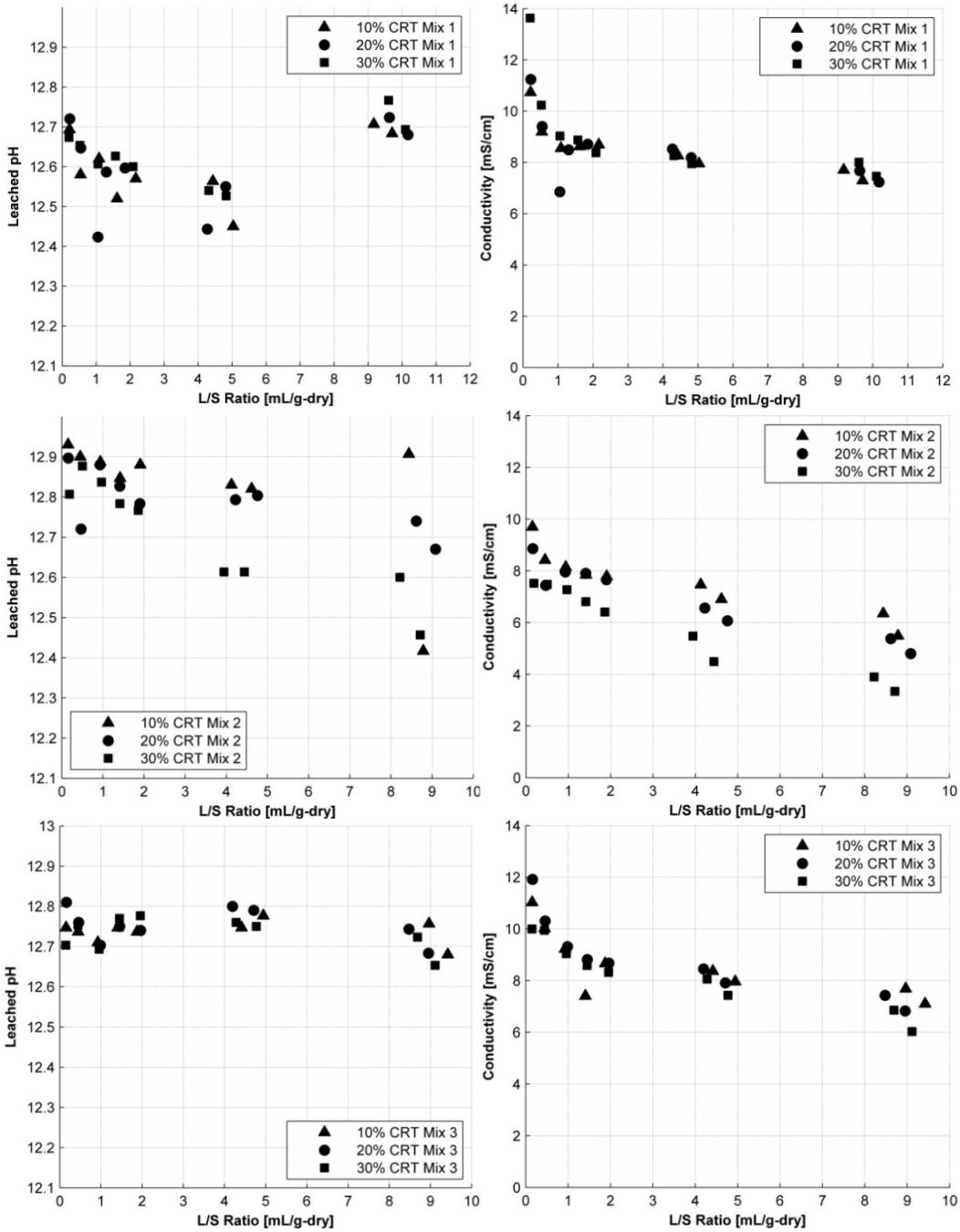

Figure 3-6 - pH and conductivity of CRT-Concrete for a) Mix 1, b) Mix 2, c) Mix 3

a)

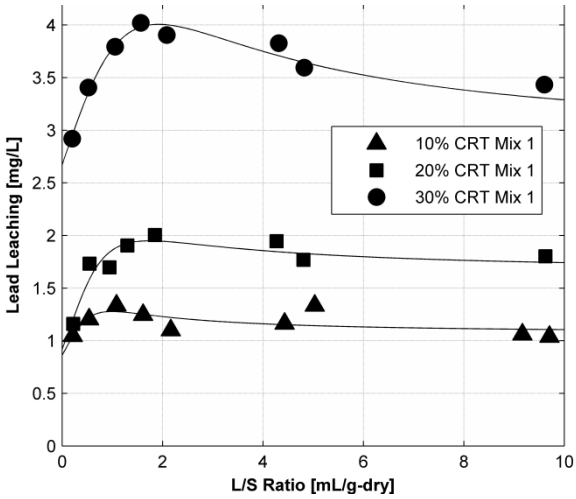

b)

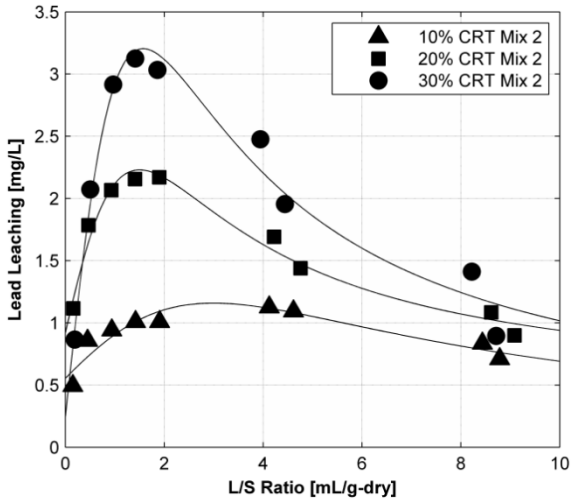

c)

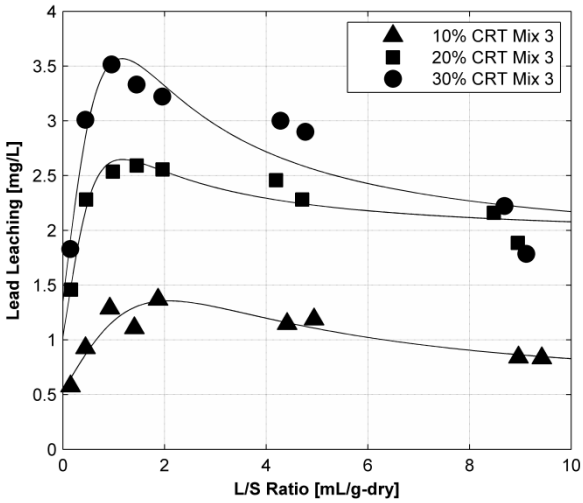

Figure 3-7 - Concentration of lead as a function of L/S ratio for a) Mix 1, b) Mix 2, c) Mix 3

3.4 Conclusions

Results for three different concrete mixtures which incorporate CRT glass as a fine aggregate replacement have been presented. Overall, the strength performance of the CRT-concrete meets and exceeds that of the control specimens. However, the workability of the CRT-concrete was adversely affected as the slump decreased as more crushed CRT was used, an issue that can be addressed with superplasticizers. Furthermore the durability of the CRT-concrete was investigated for ASR. Results show that using more than 10% CRT in concrete may lead to deleterious expansions throughout its service life. Further testing is needed to prove that supplementary cementitious materials are able to reduce expansions caused by the crushed CRT.

The implementation of CRT-Concrete for use in non-structural concrete applications is dependent on its environmental performance. Two leaching characterization tests were employed to understand the behavior of the material under different life-cycle scenarios. It was confirmed that lead leaching from CRT-Concrete is pH dependent and its minima is observed to be in the 7-12 pH range (the expected service life conditions for the concrete). This behavior is favorable for concrete materials given that as the material ages, the pH of the concrete will drop from 13 to 8 and the release of lead should therefore decrease as well. Moreover, when the material is placed under a scenario similar to a percolation column, such as crushed concrete used in stock piling or road fill, maximum concentrations of lead leaching occured during the initial surface wash-out phase and decreased shortly thereafter. Although these characterization tests were undertaken using crushed samples, they can help predict the potential behavior of the

material as environmental factors such as carbonation and material degradation can lead to cracks in the concrete that may expose inner surfaces to the leachant (water).

Lastly, an SPLP analysis was conducted for regulatory purposes. The SPLP results show that lead leaching is an order of magnitude above the drinking water criteria for Pb for certain mixtures that do not use biopolymer solutions and have high amounts of crushed CRT. The use of a cross-linked biopolymer helped reduce Pb leaching during SPLP testing to levels that were below the drinking water standard for lead. Therefore, for applications that do not consider ASR as a durability factor, up to 20% CRT can be substituted into the concrete and still be below the drinking water limits, as long as a cross-linked biopolymer solution is used.

Chapter 4

Study 2 - Structural Behavior of Concrete Containing Cathode Ray Tube Glass Undergoing Accelerated Aging and Deterioration

4.1 Background

The structural behavior of building materials is the primary concern in material characterization due to the direct relationship between performance and safety of the occupants. For this reason it is important to understand how a material behaves during its service life to avoid any unexpected behaviors. Traditionally, the compressive strength of concrete is used as the main characterization test for concrete strength. The tensile strength of concrete can also be tested; however the results are not as reliable as the compressive strength. Although these tests are used for the acceptance of the building material to be used structurally, durability tests are equally as important to assess the performance of the material throughout its lifespan. These second and third studies use Arrhenius Aging (AA), alkali-silica reactions, and Freeze/Thaw (F/T) testing techniques to deteriorate the material in different ways. Although F/T is not commonly observe in South Florida, these three testing techniques were chosen to observe how different forms of aging and deterioration (i.e. micro-crack formations from ASR, surface spalling from F/T, and changes in the internal microstructure from AA) impact the structural performance and leaching behavior of the composite material. A brief background of AA and F/T deterioration techniques are presented in the following sections.

4.1.1 Accelerated Aging and Deterioration Tests

Accelerated aging tests have gained much popularity in the field of material science due to their ability to accelerate processes and predict future performance. In the field of

Fiber-Reinforced Polymers (FRP), accelerated aging is used to study the durability of the material and its structural behavior under severe environmental and loading conditions for long periods of time. Because concrete is exposed to external agents during its life cycle, the mechanical and chemical behavior of CRT-Concrete must be well understood under weathering conditions as well.

In all accelerated tests, an acceleration factor is chosen to speed up the degradation of the test specimens. Typically, mechanical loading, voltage, current, temperature (including thermal cycling and shock), weathering (ultraviolet, radiation and humidity) and the use of high concentrations of chemicals are used as accelerating factors. Temperature is typically the most commonly used accelerating agent, however, the temperature used should not be so extreme that it may promote a behavior that would not otherwise occur under normal service conditions.

4.1.1.1 Arrhenius Steady-State Temperature Acceleration Model

Several accelerated aging techniques have been developed to predict an expected service life of a material based on the maturity of the concrete. The maturity method is a technique used to account for the combined effects of time and temperature on the strength development of concrete during the curing period, when moisture is available for cement hydration. This method provides a relatively simple approach for making reliable estimates of in-place strength during construction. A similar approach, known as the Arrhenius principle, states that the rate at which chemical degradation occurs is dependent on temperature. This principle is employed to exploit the temperature dependence of concrete and its components subjected to environmental aging at two different temperatures. In this study, two temperatures 19°C (room temperature) and

50°C (hot temperature) were used to cure and age the CRT-Concrete specimens for a total of 210 days. Photos of the testing setup can be found in Figure B-6 and Figure B-7.

4.1.1.2 Freeze-Thaw Testing

The resistance of concrete to weathering is determined by its ability to withstand the effects of freezing and thawing in the presence of water. Freeze-Thaw testing to predict the field performance of an aggregate in concrete exposed to freeze-thaw conditions is the most satisfactory used laboratory method. There are a number of freeze-thaw test procedures available, including ASTM C666 Test Method for Resistance of Concrete to Rapid Freezing and Thawing [83]. This test uses the assumption that the deterioration of concrete can be accelerated as a result of the 9% volume expansion due to the conversion of water to ice. Procedure A of the test method is utilized in this study where both freezing and thawing occurs with the specimens submerged in water. For rapid deterioration, a freezing cycle of 2 h and 45 min is used to reach a temperature of -18 ± 2°C; a thawing cycle of 2 h and 15 min is used to thaw the specimens to a temperature of 4 ± 2°C. Testing of each mixture is divided into two deterioration benchmarks. The first benchmark ends when the specimen is subjected to a total of 178 cycles or until its relative dynamic modulus of elasticity reached 80% of the initial (whichever comes first). These samples are termed “moderately deteriorated”. The second and final benchmark concludes when the specimen is subjected to 300 cycles or until its relative dynamic modulus of elasticity reaches 60% of the initial value (whichever comes first). These samples are termed “highly deteriorated”. A photograph of the testing setup is found in Figure B-8.

4.2 Materials and Method

4.2.1 Experimental Plan

The aging/deterioration techniques employed in this study are Arrhenius Aging and Freeze-Thaw testing. By placing the specimens into two fully saturated environments at approximately 19°C (room temperature) and 50°C, two objectives are met. First, AA is used to accelerate the hydration process of the cement while attempting to reach 100% saturation in the concrete. Second, the high temperature exposure on concrete may begin to deteriorate the concrete once it is fully matured. Such observations have been reported by the Federal Highway Administration [84]. Once the specimens undergo AA testing, they are then introduced to F/T cycles to further deteriorate the CRT-Concrete.

For comparison, three concrete mixtures are tested using Mix 1 from Study 1: A control mixture with no CRT glass, a concrete mixture with 10% CRT glass replacing the fine aggregate, and a concrete mixture with 20% CRT glass replacing the fine aggregate. Overall, 96 specimens were cast for each mixture and each test included five replicates. For structural performance testing, compressive strength tests, split tensile strength tests, ultrasonic pulse velocity and longitudinal resonant frequency tests are conducted. The experimental plan is shown in Figure 4-1.

4.2.2 Materials

Ordinary Type I Portland cement was used. Fine and coarse limestone aggregates were obtained from local Florida quarries. The specific gravity and absorption properties of these aggregates are shown in

Table 4-1. The CRT glass used in this study was derived from both television and computer monitors and a homogeneous mix of panel and funnel glass was used. The CRT glass is supplied by an electronics recycling facility in Marietta, Georgia. Two admixtures, an air entrainer and a superplasticizer, were used to improve the concrete workability and durability.

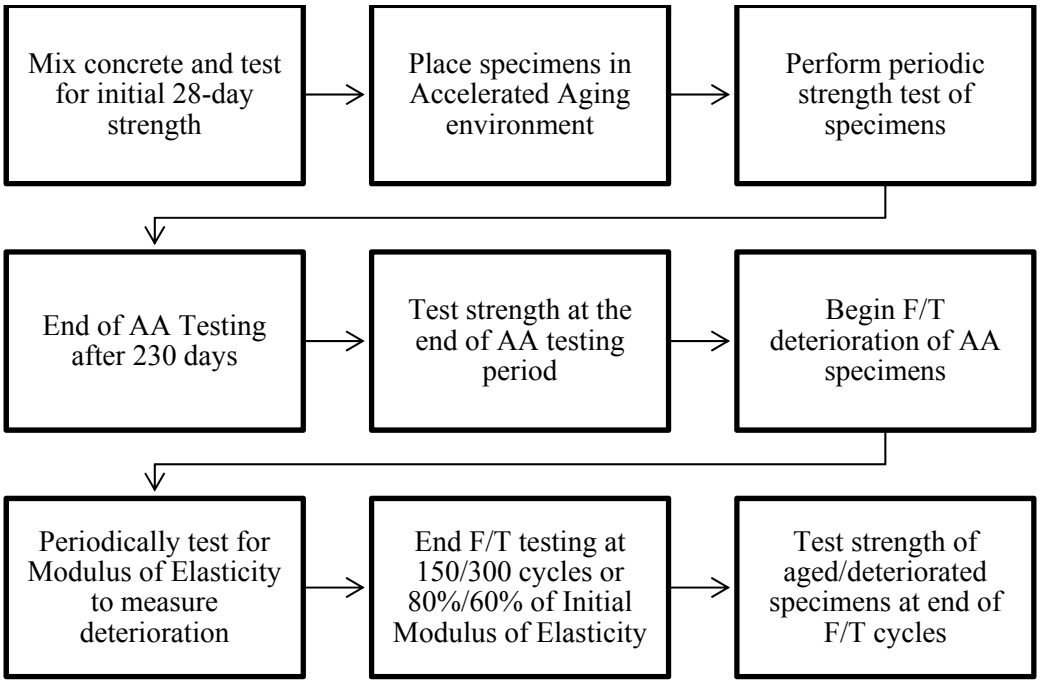

Figure 4-1 - Experimental Plan

Table 4-1 - Physical properties of aggregates

	Specific Gravity SSD	Specific Gravity OD	Absorption (%)
#89 Limestone	2.480	2.375	4.51
Sand	2.531	2.439	4.01
Crushed CRT	2.991	2.991	0.10

4.2.3 Mixing and Preparation

A commonly supplied 17 MPa concrete mixture with a maximum size coarse aggregate of 12.7 mm was used in this study (Mix 1 in Table 3-4). The mixture designs as well as all constituent materials are provided by a local concrete plant. CRT glass was used to

replace 10% and 20% of the volume of sand needed in the mixture. All molded specimens were covered to prevent loss of moisture during the first 24 hours and placed inside a curing room at 100% relative humidity until its 28th day. The mixture used to evaluate ASR expansions was prepared in accordance with ASTM C1260 - Standard Test Method for Potential Alkali Reactivity of Aggregates [63]. Photographs of the preparation and mixing of the concrete specimens are shown in Figure B-1 to Figure B-5 of Appendix B.

4.2.4 Test Methods

The sections below describe the test methods used to characterize CRT-Concrete as a structural material. Additionally, it describes the use of two test methods needed to measure the dynamic modulus of elasticity of the material.

4.2.4.1 Alkali Silica Reaction (ASR)

Five mortar bars were batched for each CRT percentage substitution in accordance to ASTM C1260 by partially substituting the required amount of fine aggregate needed in the test with crushed CRT glass. The specimens were cured for 24 hours, demolded, immersed in water for another 24 hours, and then stored in a 1N NaOH solution at 80°C. The change in length was recorded using a length comparator at 2-3 day intervals for the first 16 days and then at three predetermined intervals to investigate if expansion progressed.

4.2.4.2 Compressive Strength

In replicates of five, 100 by 200 mm concrete cylinders for each mixture and exposure environment were tested for compressive strength. The specimens were sulfur-capped

according to ASTM C617 - Standard Practice for Capping Cylindrical Concrete Specimens [81] and tested according to ASTM C39 - Standard Test Method for Compressive Strength of Cylindrical Concrete Specimens [67] using a hydraulic testing machine and digital indicator. The initial 28-day strength was recorded after the specimens cured in a moisture room. Once placed in the AA environment, two intermediate strength tests as well as a final strength test after 210 days were also recorded in order to evaluate the impact that cement hydration and deterioration had on the compressive strength. The remaining aged specimens were then placed in a F/T environment and tested for compressive strength after 178 and 300 F/T cycles.

4.2.4.3 Splitting Tensile Strength

In replicates of three, 100 by 200 mm concrete cylinders for each mixture and exposure environment were tested for split tensile strength. The specimens were tested according to ASTM C496 - Standard Test Method for Splitting Tensile Strength of Cylindrical Concrete Specimens [85] using a screw-gear testing machine and digital indicator. The initial 28-day strength was recorded after the specimens cured in a moisture room. Once placed in the AA environment, two intermediate strength tests as well as a final strength test after 210 days were also recorded. No split tensile strength testing was conducted for specimens in the F/T environment due to time constraints. A photograph of the testing setup can be found in Figure B-9.

4.2.4.4 Ultrasonic Pulse Velocity

Ultrasonic pulse velocity (UPV) testing was conducted to measure the durability and deterioration of CRT-Concrete undergoing F/T testing. ASTM C597 - Standard Test

Method for Pulse Velocity through Concrete [86] describes the procedures used to determine the propagation velocity of longitudinal stress wave pulses through concrete. The velocity of ultrasonic pulses traveling in a solid depends on the density and elastic properties of the material and allows the determination of properties such as Poisson's ratio and the Dynamic Modulus of Elasticity. Typical values of ultrasonic wave speed can range from 3500 to 5500 m/s depending on the strength of the concrete or the age at which it was tested; Table 4-2 gives a general overview of concrete quality based on pulse velocity [87].

Table 4-2 - Velocity Criterion for Concrete Quality Grading

Longitudinal Pulse Velocity (km/sec)	Concrete Quality Grading
Above 4.5	Very good to excellent
3.5 - 4.5	Good to very good, slight porosity may exist
3.0 - 3.5	Satisfactory but loss of integrity is suspected
Below 3.0	Poor or loss of integrity exists

Propagation waves (P-waves) and Shear waves (S-waves) are the two most commonly used types of waves in UPV testing. Propagation waves create compressional forces on the material due to their longitudinal oscillation (parallel to the wave propagation). Shear waves, or transverse waves, oscillate perpendicular to the direction of wave propagation and the main resisting force comes from shear effects of the material. Equations 4.1 and 4.2, describe the relationship between longitudinal and shear velocities to acquire Poisson's ratio and the Dynamic Modulus of Elasticity, respectively.

$$\nu = \frac{V_P^2 - 2V_S^2}{2(V_P^2 - V_S^2)} \tag{4.1}$$

$$E_D = 2\rho V_S^2(1+\nu) \quad (4.2)$$

Where:

ν: Poisson's Ratio

E_D: Dynamic modulus of elasticity (MPa)

ρ: Density (kg/m^3)

V_p: Velocity of Propagation wave (m/s)

V_s: Velocity of Shear wave (m/s)

The challenge in using UPV to compare the performance of a material was in detecting the initial arrival of the P and S waves. In this test, a 54 KHz transducer and a 250 KHz transducer were used to generate P and S-waves across the concrete specimen. The P-wave arrival was easily identified as the first wave received by the 54 KHz transducer. However, the S-wave arrival was slightly more difficult to identify due to the nature of the heterogeneous material. This study identified the initial arrival of the S-wave at the arrival of a wave with the largest amplitude after the P-wave arrival. A photograph of the testing setup as well as an example of the initial wave arrival is shown in Figure B-10 and Figure B-11.

4.2.4.5 Fundamental Longitudinal Resonant Frequency (FLRF)

The fundamental longitudinal resonant frequency was measured to calculate the dynamic modulus of elasticity of the specimens. The test method for Fundamental Transverse, Longitudinal, and Torsional Resonant Frequencies of Concrete Specimens, ASTM C215 [88], uses an electro-mechanical driving unit whose driving frequency is varied until the measured specimen response reaches maximum amplitude. The frequency value that causes maximum response is the resonant frequency of the specimen. This test method is

primarily intended for detecting significant changes in the dynamic modulus of elasticity of specimens that are undergoing exposure to weathering. Similar to the Ultrasonic Pulse Velocity method, the FLRF method was used to obtain values of the dynamic modulus of elasticity that will, in general, be greater than the static modulus. Equation 4.3 describes the relationship between the fundamental longitudinal resonant frequency and the dynamic modulus of elasticity. A photo of the testing setup is shown in Figure B-12.

$$E_D = 4.093\left(\frac{L}{d^2}\right)M(n')^2 \quad (4.3)$$

Where:

L: length of specimen (m)

d: diameter of specimen (m)

n': fundamental longitudinal frequency (Hz)

M: mass of specimen (kg)

4.3 Results and Discussion

4.3.1 Alkali Silica Reaction

The expansion of CRT-Concrete using different CRT glass percent substitutions was investigated and the results are presented in Figure 4-2. Important to note is that the crushed glass used in this study was slightly finer than the one used in Study 1 due to the utilization of a different grinding machine. Figure B-13 shows the particle size distribution for the CRT Glass. The use of crushed glass aggregate on the cementitious matrix causes expansions that may be deleterious. ASTM C1260 considers expansions of less than 0.10% after fourteen days as indicative of innocuous behavior, expansions of

more than 0.20% are indicative of potentially deleterious expansion and expansions between 0.10 and 0.20 % may be innocuous or deleterious in field performance.

Expansions observed on the fourteenth day of the test were 0.002%, 0.065%, and 0.149% for specimens containing 0%, 10%, and 20% CRT glass, respectively. This result reinforced the conclusion from Study 1 in which potentially deleterious field performance of CRT-Concrete may be experienced if more than 10% CRT glass is used.

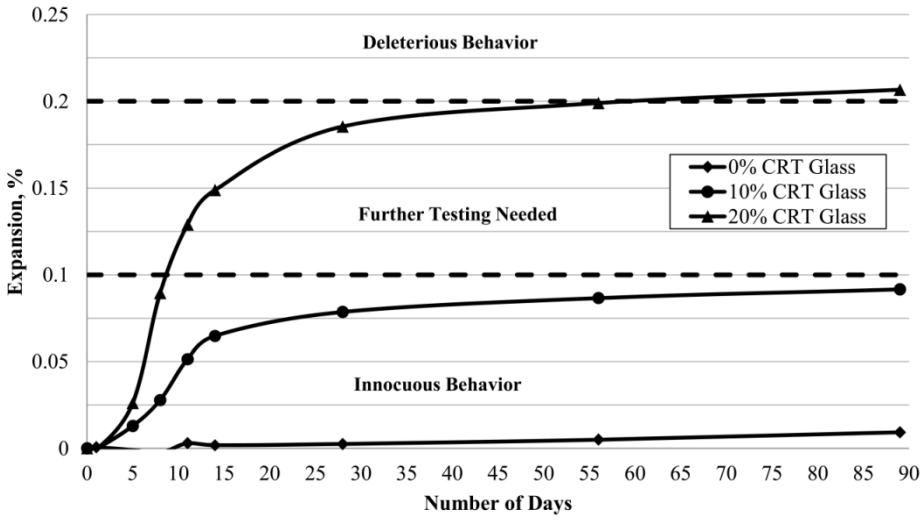

Figure 4-2 - Expansion of CRT-Concrete

The particle size of the CRT glass did have an impact on the expansion of the composite material. For 10% CRT glass replacement, the coarser glass (Study 1) displayed an average expansion of 0.12% after fourteen days of testing while the same mixture composition using finer CRT glass aggregates displayed an average expansion of only 0.065%. Similarly, a replacement of 20% resulted in an expansion of 0.31% for the coarser CRT glass aggregate specimens compared to this study's 0.15% expansion. Figure B-14 graphically presents these results. The finely crushed CRT glass evidently reduced the expansion of the CRT-Concrete composite by almost 50%. Although the magnitude of ASR expansions are dependent on many variables, in some cases the

fineness of the aggregate was found to create a more porous cement paste structure that was able to accommodate the expanding ASR gel formed, and resulted in smaller expansions [89]. Additionally, researchers have found that a pozzolanic effect may occur when glass is finely ground; ultimately helping reduce ASR-related expansions [90]. Although it is not clear if a more porous structure was created or if a pozzolanic reaction occurred in the mixture, these results reinforced the conclusions of other published work that related ASR expansions to glass particle size (see Table 3-1).

4.3.2 Compressive Strength

The compressive strength of the specimens cured under two temperatures are presented in Figure 4-3 and Figure 4-4. The 28-day compressive strength for the control specimen (0% CRT glass) was 18.6 MPa while those for the 10% and 20% CRT-Concrete mixtures were 20.5 and 24.7 MPa (an increase of 10.5% and 33.1% from the control mixture), respectively. This same trend was observed at the end of the 210-day Arrhenius Aging testing cycle. The compressive strengths of the specimens cured under the 50°C environment were 20.5% and 56.9% stronger than the control specimens while those cured under the 19°C environment were 13.7% and 29.3% (10% and 20% specimens respectively) stronger. Figure 4-5 graphically shows the strength improvement of CRT-Concrete over the control mixture at each testing interval.

The use of CRT glass in concrete improved the resistance of concrete to strength loss when the specimens were cured in a hot temperature environment. The compressive strength of the 20% CRT-Concrete mixture was reduced by only 4.0% after 210 days of exposure. Under the same conditions, a strength reduction of 18.7% and 11.2% was

observed for the control and 10% CRT mixtures, respectively. Table B-1 lists these results.

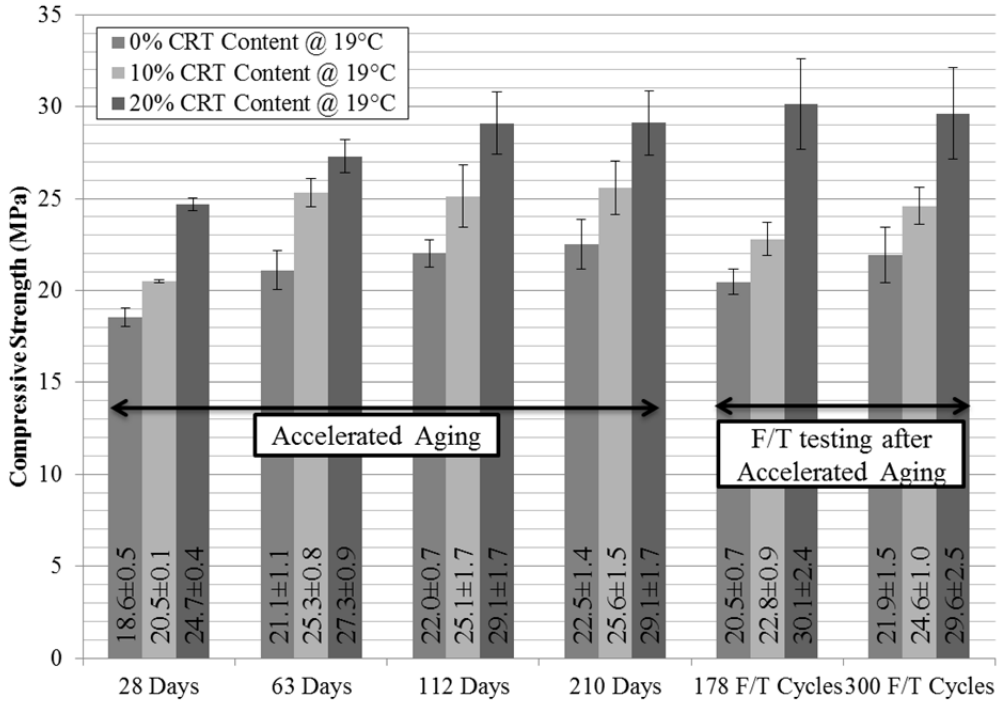

Figure 4-3 - Compressive strength of room temperature AA aged specimens

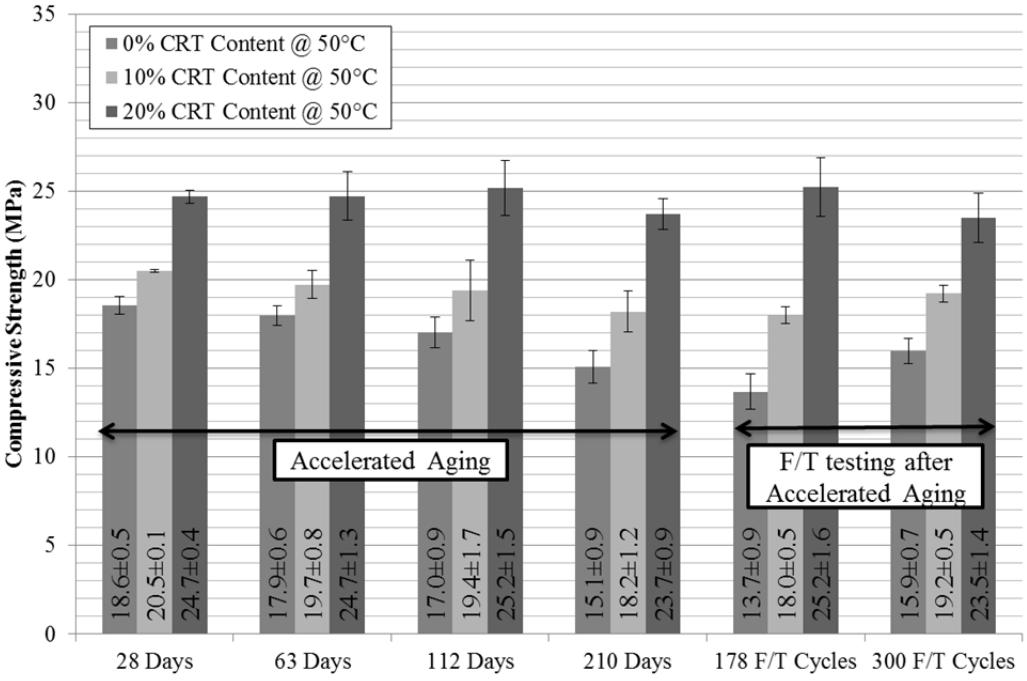

Figure 4-4 - Compressive strength of hot temperature AA aged specimens

Hot temperature curing most likely had an impact on the microstructure of the material. Literature shows that high temperature environments not only affect the rate of hydration for cement paste but also increase the porosity of the material [91,92]. A "crossover" effect [93], where an initial increase in strength due to an increased rate of hydration is followed by a decrease of strength as testing continued, was observed in this study. This behavior was not observed with the specimens cured at a room-temperature temperature, and agreed with the known behavior that the compressive strength of concrete increases as it is hydrated under normal conditions.

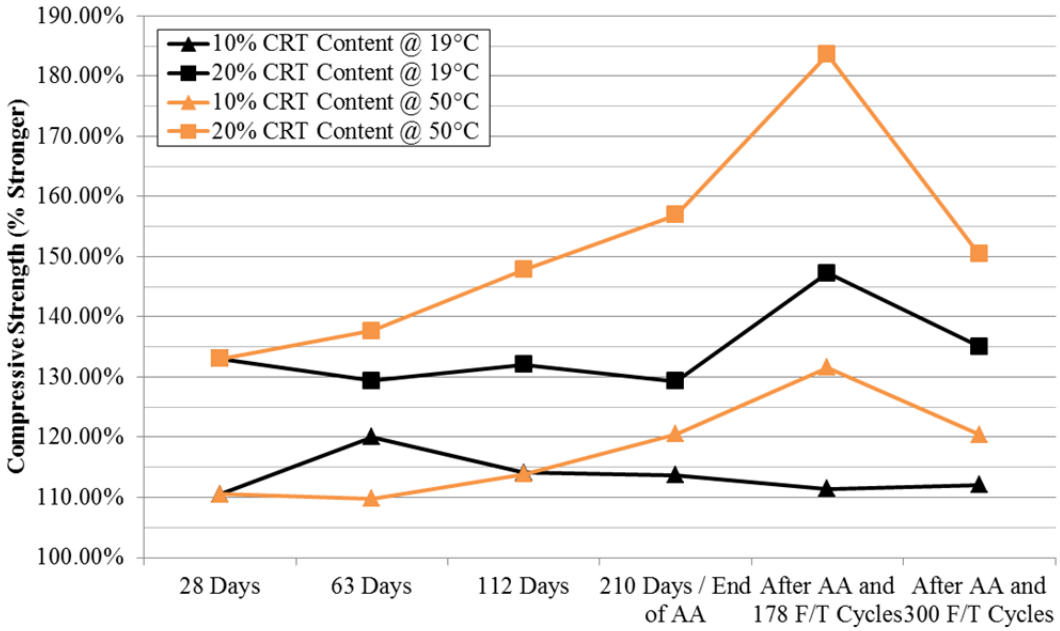

Figure 4-5 – Compressive strength of CRT-Concrete. 100% is the baseline strength from the control specimens

Freezing/Thawing had minor effects on the compressive strength of the concrete specimens cured in a room-temperature environment. Moderate deterioration (exposure to 178 F/T cycles) resulted in a loss of compressive strength (up to 11%) for the 0% and 10% CRT-Concrete mixtures, regardless of the curing temperature. However, a 6% average increase in strength was observed for the 20% CRT-Concrete mixture.

Conversely, an exposure of 300 F/T cycles did not have a similar impact on the compressive strength of the specimens. The 0% and 10% CRT-Concrete specimens cured in a room-temperature environment lost 3.5% and 4% of their initial compressive strength while the 20% specimens showed an increase of strength of 1.8%. The behavior observed in these results could be due to self-healing of concrete; this is explained in section 4.3.6. Nonetheless, adding CRT glass to concrete proves to be beneficial to the compressive strength of the material. The compressive strength test results can be found in Table B-2 and Table B-3.

4.3.3 Splitting Tensile Strength

The splitting tensile strength results for the cylindrical CRT-Concrete samples are shown in Figure 4-6 and Figure 4-7. As presented, CRT glass did not have an impact on the splitting tensile strength of the concrete mixtures. Although the 28^{th} day splitting tensile strength of CRT-Concrete (i.e. 10%, 20% CRT) was greater than the control mixture (0% CRT), the large standard deviation for each test made it difficult to make an accurate judgment of the material's performance. This was reinforced by calculating the coefficient of variation (CV) from the results. Shown in Table B-4 and Table B-5, the CV ranged between 6.6 - 19.5% for the specimens exposed to the 19°C AA environment and between 5.6 – 27.3% for the 50°C AA environment.

The large variations calculated for each test resulted in the conclusion that no further tensile testing would be conducted because no proper strength comparisons could be made between the mixtures. The variations were most likely due to the heterogeneity of concrete and other factors like the moisture condition of the specimens that may have impacted the test results [27].

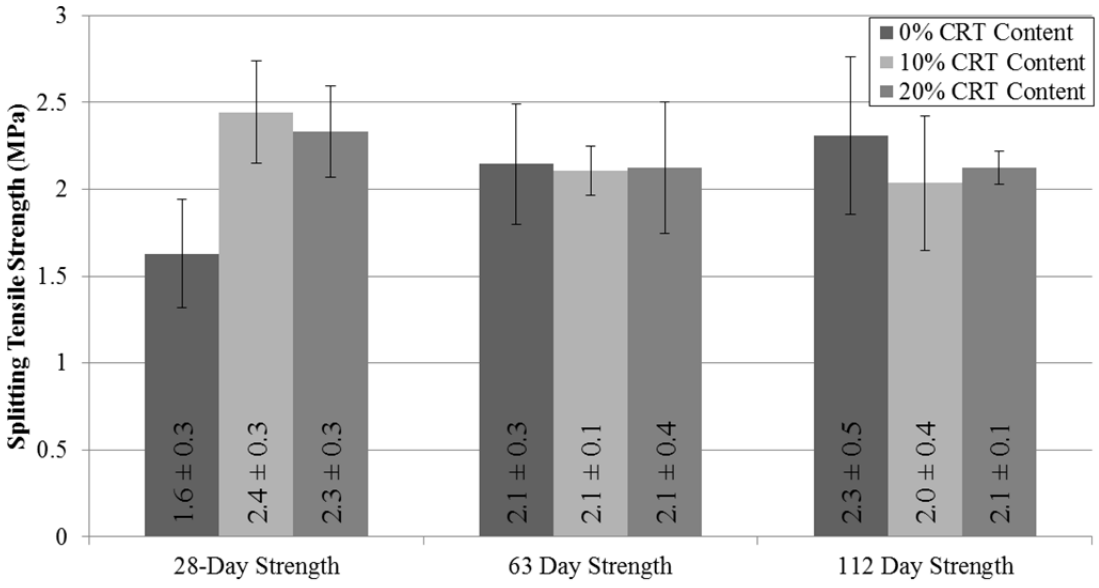

Figure 4-6 - Split tensile strength of cold temperature AA aged specimens

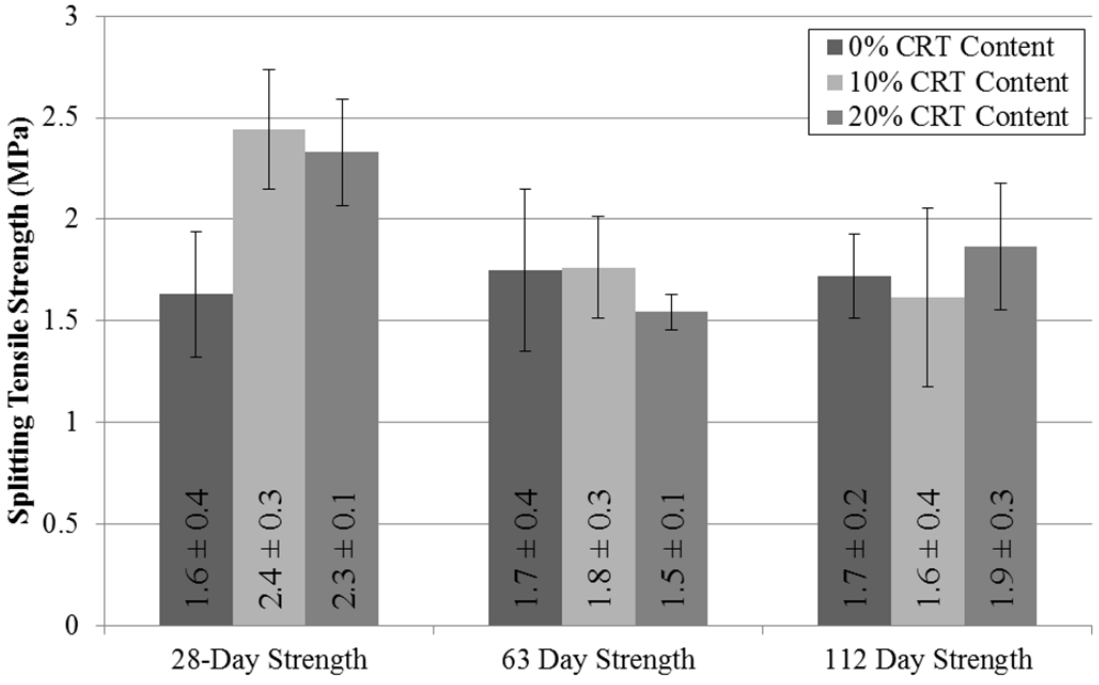

Figure 4-7 - Split tensile strength of hot temperature AA aged specimens

While all specimens were tested immediately after being removed from their AA environments, those exposed to the hot temperature environment would immediately dry once out of the water. It is possible that the effect of drying of the outer surface of the

specimen caused shrinkage and created compressive internal stresses in the material that affected the results.

4.3.4 Ultrasonic Pulse Velocity

UPV measurements were conducted to assess the Dynamic Modulus of Elasticity (E_D) of the specimens. An initial UPV measurement was conducted after the AA testing period was completed to assess if hot temperature curing had an effect on the microstructure of the material; this was used to validate the results from the compressive strength tests in section 4.3.3. Figure 4-8 shows the E_D values for all three concrete mixtures. As shown, there was a noticeable difference in E_D between the specimens that were aged in a 19°C bath as opposed to those aged in a 50°C environment. This dissimilarity confirms that AA testing had an impact on the microstructure of concrete. An average E_D reduction of 10.4%, 6.4%, and 3.9% was experienced for the 0%, 10%, and 20% CRT-concrete specimens, respectively.

Subsequent UPV measurements were taken at 25-50 F/T cycle intervals for the "moderately" deteriorated specimens (178 F/T cycles in total) and at 100 cycle intervals for the "highly" deteriorated specimens (300 F/T cycles in total) in order to investigate how curing temperature affected the durability of a material. lists the average and maximum losses of the initial dynamic modulus (after AA testing) for the "moderately" and "highly" deteriorated specimens. Up to a 9.8% loss in the dynamic modulus was observed during testing with no relationship to the amount of CRT glass in the specimen, the effect of different curing temperatures, or the number of F/T cycles.

Lastly, a relationship was hard to define due to the high sensitivity of UPV measurements to the moisture condition of the specimen. Typically, a saturated or wet specimen tends to

result in a higher UPV reading when compared to a dry specimen [94-96]. Although the specimens were air-dried for 24-hours with the assistance of two fans before UPV testing, the changing environmental conditions within the laboratory could not be controlled. Nevertheless, it was evident that moisture had a large impact on the UPV measurements and led to the inconsistent results shown in Figure 4-8 and Figure B-17.

Table 4-3 – Dynamic Modulus of Elasticity loss after F/T testing

UPV - E_D (% Change)				
	Average		Maximum	
	178 Cycles	300 Cycles	178 Cycles	300 Cycles
0% 19°C	-5.46%	-6.99%	-6.54%	-9.80%
0% 50°C	-4.61%	-6.03%	-9.83%	-9.37%
10% 19°C	-4.36%	-3.62%	-6.74%	-6.73%
10% 50°C	-4.82%	-4.29%	-6.26%	-7.03%
20% 19°C	-5.24%	-4.63%	-6.52%	-8.05%
20% 50°C	-5.73%	-6.34%	-8.32%	-7.93%

4.3.5 Fundamental Longitudinal Resonant Frequency (FLRF)

The resonant frequency of each specimen was measured and used to calculate how the dynamic modulus of elasticity changed due to F/T. The results were also used to compare the performance of the FLRF method to the UPV method. An initial measurement was recorded for each specimen to compute the effects of AA testing on the dynamic modulus of elasticity of the material. The FLRF method reinforced the conclusion from the compressive strength and UPV tests that there was a change in the microstructure of concrete when exposed to a 50°C environment. The average loss in E_D due to the rise in temperature was 11.7%, 8.4%, and 4.6% for the 0%, 10%, and 20% CRT-concrete specimens, respectively. Figure 4-9 plots the results.

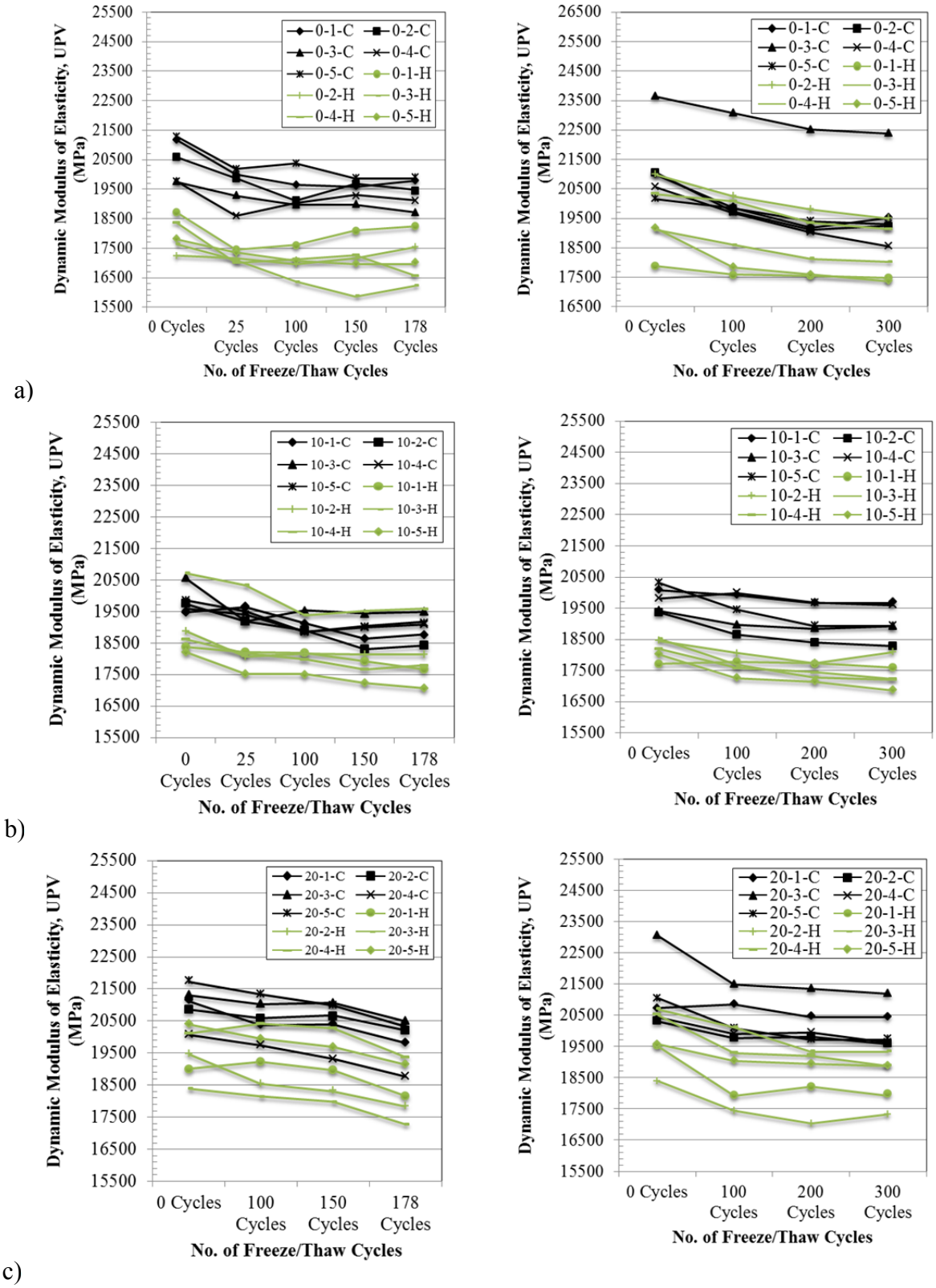

Figure 4-8 - Dynamic Modulus of Elasticity for 178 (left) and 300 (right) F/T cycles, after AA testing in 19°C (C) and 50°C (H). a) Control Mixture, b) 10% CRT-Concrete, c) 20% CRT-Concrete

Up to a 12.5% loss in the dynamic modulus was observed during testing (compared to a 10.5% loss using the UPV method). The decrease in modulus of elasticity was most likely due to the formation of microcracks within the specimens caused by the internal stresses from freezing and thawing of the water inside. However, the use of CRT glass in concrete increased the resistance of the composite to changes in its modulus of elasticity during F/T cycles.

lists the average and maximum loss of the initial dynamic modulus (after AA testing) for the "moderately" and "highly" deteriorated specimens. From the results, it is evident that the curing temperature had an impact on the F/T durability of the moderately deteriorated specimens. Conversely, this impact was not as pronounced when specimens from the same batch were exposed to almost double the amount of F/T cycles. The reasoning behind this re-strengthening or resistance to further deterioration is more likely due to concrete self-healing (discussed in section 4.3.7), and not moisture (explained in section 4.3.5) since the FLRF method is not as sensitive to moisture as the UPV Method.

Table 4-4 - Dynamic Modulus of Elasticity loss after F/T testing

LRFM - E_D (% Change)				
	Average		Maximum	
	178 Cycles	300 Cycles	178 Cycles	300 Cycles
0% 19°C	-7.55%	-8.25%	-9.45%	-10.52%
0% 50°C	-11.89%	-8.45%	-17.96%	-9.52%
10% 19°C	-5.90%	-5.99%	-10.23%	-7.81%
10% 50°C	-11.48%	-6.83%	-12.14%	-12.55%
20% 19°C	-7.15%	-6.18%	-8.75%	-6.98%
20% 50°C	-5.33%	-6.47%	-9.65%	-8.45%

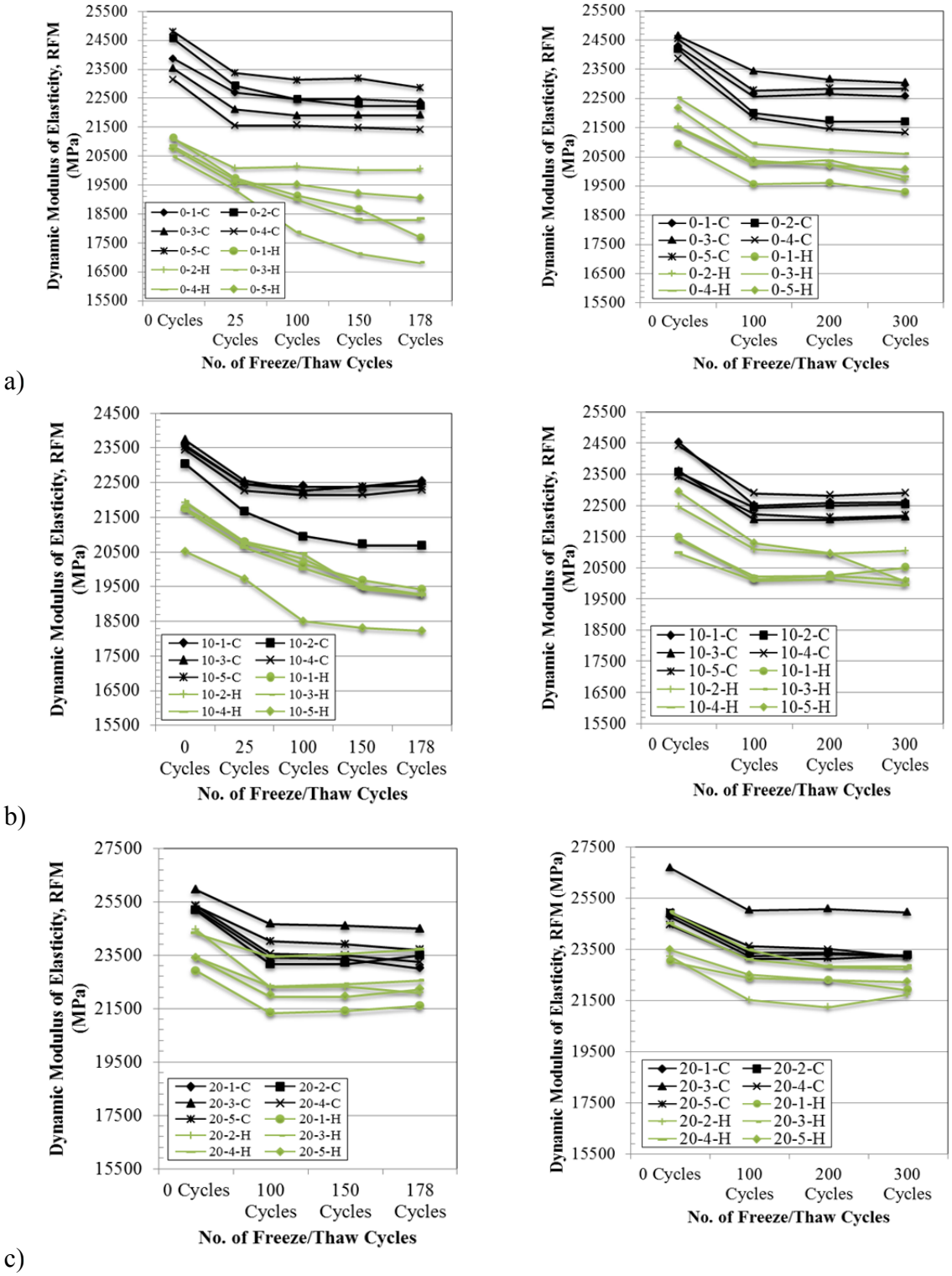

Figure 4-9 - Dynamic Modulus of Elasticity for 178 (left) and 300 (right) F/T cycles after AA testing in 19°C (C) and 50°C (H). a) Control Mixture, b) 10% CRT-Concrete, c) 20% CRT-Concrete.

4.3.5.1 Mass Loss and Durability Factor

Mass loss was measured to make comparisons in the durability and level of deterioration of each specimen and mixture. In the cast stone industry, products are accepted if their cumulative percent weight loss is less than 5% after 300 F/T cycles [97]. For concrete, this criterion does not exist, but it is important to note that these concrete mixes can be used for cast stone projects and therefore should meet these guidelines. Table 4-5 lists the average and maximum mass loss values for each concrete mixture. The specimens were all conditioned for 24 hours before weighing. Results show that the cumulative mass loss increased as the amount of CRT glass used in the mixture increased. Figure B-19 plots the mass loss for each individual specimen.

Table 4-5 - Mass loss after F/T testing

Mass Loss (% Change)				
	Average		Maximum	
	178 Cycles	300 Cycles	178 Cycles	300 Cycles
0% 19°C	-0.66%	-3.44%	-0.89%	-4.99%
0% 50°C	-0.19%	-2.11%	-1.14%	-4.73%
10% 19°C	-1.24%	-3.22%	-3.03%	-4.15%
10% 50°C	-1.69%	-2.39%	-2.18%	-5.24%
20% 19°C	-3.16%	-3.29%	-4.55%	-3.74%
20% 50°C	-2.99%	-4.39%	-4.64%	-6.16%

Although curing temperature appeared to have had an impact on mass loss, no clear trend was formed to make this comparison. Several factors including concrete self-healing and a possible change in the porosity of the material due to elevated temperatures and the amount of CRT glass present may have altered the behavior of the material and result in this inconsistency.

The Durability Factor of a concrete mixture is a calculated value used in a ranking system to compare the durability of several concrete mixtures. The DF value compares the

relative modulus of elasticity of each mixture based on their resonant frequency; it does not take into account mass loss. A DF value over 80% is considered to have a satisfactory performance against F/T cycling. Table 4-6 shows the durability factors (DF) for each mixture. Results show that all mixtures had a satisfactory or excellent durability performance. Additionally, the use of glass did not have a negative impact on the performance of the composite material. Noteworthy, the DF of the three mixtures maintained or even increased when the concrete specimens were exposed to almost double the amount of F/T cycles. This behavior could potentially be attributed to self-healing of the microcracks formed.

Table 4-6 - Durability Factor ASTM C666

Durability Factor							
178 Cycles							
Mix	Specimen 1	Specimen 2	Specimen 3	Specimen 4	Specimen 5	Average	Std. Dev.
0% 19°C	94	92	94	93	93	93	0.99
0% 50°C	84	95	82	89	92	88	5.21
10% 19°C	96	93	95	96	96	95	1.53
10% 50°C	91	88	88	89	90	89	1.18
20% 19°C	96	94	98	97	97	96	1.37
20% 50°C	96	95	98	98	97	97	1.22
300 Cycles							
Mix	Specimen 1	Specimen 2	Specimen 3	Specimen 4	Specimen 5	Average	Std. Dev.
0% 19°C	96	94	96	94	95	95	0.86
0% 50°C	94	93	93	93	92	93	0.65
10% 19°C	96	99	96	96	98	97	1.14
10% 50°C	96	95	96	96	90	95	2.75
20% 19°C	97	96	96	96	97	96	0.39
20% 50°C	100	97	96	96	97	97	1.86

4.3.6 Relationship between Material Performance and Deterioration

The previous sections showed how Arrhenius Aging and Freeze-Thaw cycling impacted the compressive strength, dynamic modulus of elasticity, and mass loss of a concrete

specimen. This section addresses the relationship, if any, between structural performance of the concrete specimens and the deterioration parameters measured. However, before any comparisons or relationships are investigated, it must be acknowledged that concrete is a living, heterogeneous material whose microstructure is forever changing. Therefore, any lack of trends or relationships could be due to many factors including the possibility of having segregation or an uneven distribution of aggregates (i.e. CRT Glass) in the specimens during concrete mixing or due to concrete self-healing.

Self-healing of concrete is a combination of chemical and physical processes. Although the primary mechanism is believed to be due to the crystallization of calcium carbonate [98-100], impurities in the water, loose concrete particles, hydration of the unreacted cementitious material, and expansions of the hydrated cementitious matrix may all seal the microscopic cracks developed [101]. Concrete self-healing, restores or improves the structural properties of an already deteriorated material. Previous work shows that the compressive strength of cracked concrete specimens was found to self-heal after weathering to more than twice the 28-day strength (after 8 years) [102]. Gray [103] also reported that self-healing improved the pullout resistance of concrete as well as its compressive strength. Nonetheless, self-healing also makes certain measurements and comparisons difficult to understand. For instance, Jacobsen and Yingzi [100,102] found that the resonant frequency of concrete improved after exposure to free moisture once Freezing/Thawing or pre-cracking tests were completed. However, while the compressive strength improved by a marginal percentage, no correlation between compressive strength and resonant frequency could be found. Additionally, Abdel-Jawad [104] also found that the ultrasonic pulse velocities improved after the material was exposed to a

moist environment and concluded that complete healing of cracks does not mean complete strength gain.

In order to understand these relationships, a general linear model (i.e. ANOVA test) was conducted to compare the effect of deterioration on the compressive strength of concrete. Three fixed variables were used (mixture composition, curing temperature, and number of F/T cycles) to see if any or all the variables had a significant statistical impact to the compressive strength results. Lastly, the dynamic modulus of elasticity was used as a covariate since there was a linear relationship between strength and modulus of elasticity. Table 4-7 shows the results from the model. Overall, the concrete mixture composition (i.e. % of CRT glass) as well as the curing temperature had a significant statistical effect on the compressive strength at the $p < 0.05$ (95^{th} percentile) confidence level. Interestingly enough, there no was significant statistical difference on compressive strength due to the number of freeze thaw cycles [$F(1,47) = 0.240$, $p = 0.626$].

Table 4-7 - General linear model (ANOVA) for compressive strength interaction

Dependent Variable: Strength

Source	Type III Sum of Squares	df	Mean Square	F	Sig.
Corrected Model	32730049.3[a]	12	2727504.110	94.904	.000
Intercept	8934.839	1	8934.839	.311	.580
Modulus	676155.975	1	676155.975	23.527	.000
Mix	3648648.932	2	1824324.466	63.478	.000
Curing	689859.411	1	689859.411	24.004	.000
FTCycles	6900.036	1	6900.036	.240	.626
Mix * Curing	392635.478	2	196317.739	6.831	.002
Mix * FTCycles	595920.976	2	297960.488	10.368	.000
Curing * FTCycles	22768.110	1	22768.110	.792	.378
Mix * Curing * FTCycles	32368.982	2	16184.491	.563	.573
Error	1350763.628	47	28739.652		
Total	660294889.6	60			
Corrected Total	34080812.95	59			

a. R Squared = .960 (Adjusted R Squared = .950)

A post-hoc analysis using the Sidak test did not clearly indicate which mixture was significantly different, concluding that every mixture was significantly different when compared to the other two. Similarly, there was no clear indication of which curing temperature had a significant statistical difference on the compressive strength of the specimens. However, the results from the ANOVA analysis are comparable to the conclusions made in section 4.3.2.

A second ANOVA test was conducted to compare the effect deterioration of concrete had on the dynamic modulus of elasticity taking into account the fixed variables: mixture composition, curing temperature, and number of F/T cycles. Table 4-8 shows the results from the model.

Table 4-8 - General linear model (ANOVA) for dynamic modulus of elasticity interaction

Dependent Variable: Modulus

Source	Type III Sum of Squares	df	Mean Square	F	Sig.
Corrected Model	156549595[a]	11	14231781.37	29.064	.000
Intercept	27793024417	1	27793024417	56758.655	.000
Mix	56258381.92	2	28129190.96	57.445	.000
Curing	82573335.94	1	82573335.94	168.630	.000
FTCycles	5211415.873	1	5211415.873	10.643	.002
Mix * Curing	7644885.901	2	3822442.951	7.806	.001
Mix * FTCycles	1544756.407	2	772378.204	1.577	.217
Curing * FTCycles	2366160.133	1	2366160.133	4.832	.033
Mix * Curing * FTCycles	950658.849	2	475329.425	.971	.386
Error	23504171.54	48	489670.241		
Total	27973078183	60			
Corrected Total	180053766.6	59			

a. R Squared = .869 (Adjusted R Squared = .840)

Results show that the concrete mixture, curing environment, and the degree of deterioration using freezing/thawing had a significant statistical effect on the dynamic modulus of elasticity at the $p < 0.05$ (95^{th} percentile) confidence level. A post-hoc

analysis using the Sidak test resulted in no clear indication as to which level of F/T deterioration had a significant statistical difference on the dynamic modulus. However, the post hoc test revealed that the 20% CRT mixture was significantly different to the remaining two mixtures. This observation supports the observations made in the previous section where the change in modulus for the 20% CRT-Concrete specimens was different in behavior and magnitude when compared to the other two mixtures.

A final ANOVA test was conducted to compare the effects of deterioration on the mass loss of the specimens. Table 4-9 shows the results from the model. As expected, the degree of deterioration under freezing/thawing had a significant statistical effect on the dynamic modulus of elasticity, agreeing with the results found in Table 4-5. However, the amount of CRT-Glass (Mix) did not have a significant impact on the mass loss, regardless of the number of F/T cycles.

Table 4-9 - General linear model (ANOVA) for mass loss interaction

Dependent Variable: Mass

Source	Type III Sum of Squares	df	Mean Square	F	Sig.
Corrected Model	71869.478[a]	11	6533.589	2.823	.006
Intercept	677521831.8	1	677521831.8	292775.298	.000
Mix	608.805	2	304.403	.132	.877
Curing	3503.704	1	3503.704	1.514	.225
FTCycles	53562.888	1	53562.888	23.146	.000
Mix * Curing	4319.889	2	2159.945	.933	.400
Mix * FTCycles	7383.445	2	3691.723	1.595	.213
Curing * FTCycles	1.568	1	1.568	.001	.979
Mix * Curing * FTCycles	2489.177	2	1244.589	.538	.587
Error	111078.524	48	2314.136		
Total	677704779.8	60			
Corrected Total	182948.002	59			

a. R Squared = .393 (Adjusted R Squared = .254)

Finally, the square of the Pearson product-moment correlation coefficient (R^2) was calculated in order to investigate if a linear relationship between compressive strength loss and loss of the dynamic modulus of elasticity or mass, existed. The R^2 value measures the correlation between two dependent variables, the closer the value is to 1.0, the higher the correlation between the two variables. Table 4-10 lists the R^2 values for four different relationships while Figure 4-10 shows a scatterplot between strength and dynamic modulus.

Table 4-10 - R^2 results for dependent variable relationships

	Correlation
Actual Strength – Actual Modulus	0.766
% Strength Loss - % Modulus Loss	0.046
% Strength Loss - % Mass Loss	0.013
% Modulus Loss - % Mass Loss	0.273

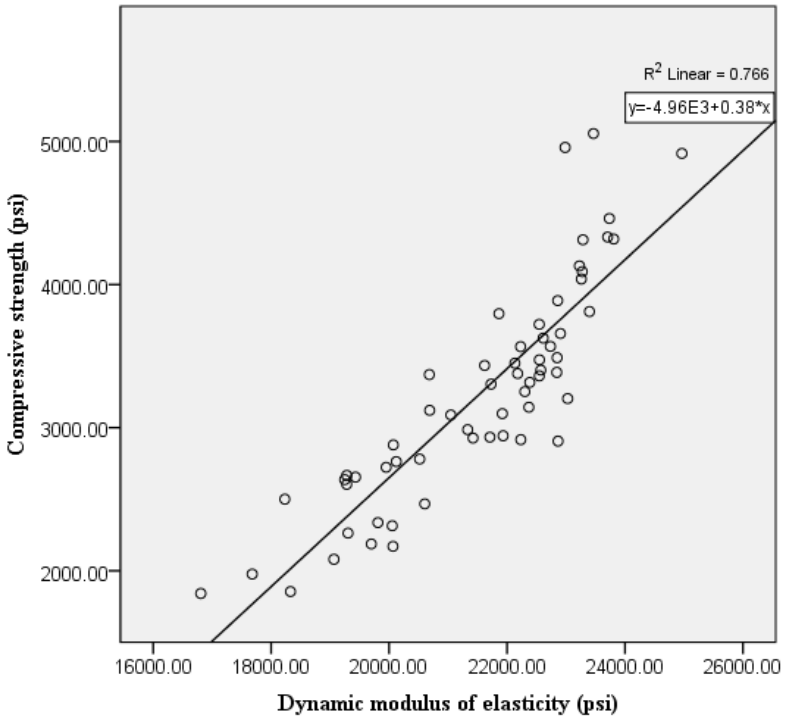

Figure 4-10 - Scatterplot of compressive strength versus dynamic modulus of elasticity

As expected, there is a strong correlation between the actual compressive strength measurements and the actual modulus of elasticity due to the experimentally-derived relationship between the two variables. However, there were no relationships and correlations that described how strength loss was related to mass and modulus loss. This conclusion agrees with the conclusions stated by Jacobsen and Yingzi [100,102] in the beginning of this section.

4.4 Conclusion

This study focused on the structural behavior of CRT-Concrete as it went through accelerated aging and deterioration tests. Substituting up to 20% of the fine aggregate with finely crushed CRT glass, three durability/deterioration tests were used to investigate how the compressive strength of the material was affected. ASR tests were used to investigate how the size particle of the CRT glass affected the expansion due to ASR reactions. Two long-term aging environments were used to understand if temperature had any impact on the microstructure of a material by comparing its change in strength. Lastly, the aged specimens were then placed in a freeze/thaw chamber where the change in dynamic modulus of elasticity, mass loss, and compressive strength were determined after an exposure of 178 and 300 F/T cycles.

The following conclusions were derived in this study:

- A finer particle size distribution in the CRT glass led to a reduction in ASR expansions. This result agreed with already published works.
- Up to 10% of the fine aggregates can be safely substituted with CRT glass as long as it satisfies the structural and environmental requirements. If more than 10%

substitution is desired, the use of supplementary cementitious materials such as fly ash, metakaolin, or ground granulated blast-furnace slag is recommended.

- CRT glass improved the 28-day strength of the concrete mixture. This was true even after 210 days of exposure to two different temperatures.
- CRT-Concrete had better strength retention than the control specimens when exposed to a hot temperature environment. However, the performance of the material was affected (i.e. early strength gain followed by long term strength loss) and therefore long-term hot temperature curing is not recommended.
- Concrete strength during the service life of the material was found to be dependent on the mixture composition and its curing temperature. The number of F/T cycles did not have a statistical impact on the strength. However, long-term F/T cycling (300 cycles) aided and improved the performance of this particular concrete mixture, most likely due to self-healing of concrete.
- The use of the Ultrasonic Pulse Velocity test method to estimate the dynamic modulus of elasticity after F/T tests is not feasible due to its high sensitivity to the moisture of the material. The resonant frequency method is recommended.
- CRT-Concrete displayed lower losses in its modulus of elasticity than the control mixture. E_D is dependent of the mixture composition, the curing temperature, and the amount of F/T exposure. Hot temperature curing accelerates the loss of E_D.
- Mass loss was most significantly impacted by the amount of F/T cycles that the specimen was exposed to.

- A linear correlation between actual strength and actual modulus was observed (R^2 = 0.766). However, no relationship between percent of strength loss compared to percent of dynamic modulus or mass loss was found at a 95% confidence interval.

Chapter 5

Study 3 - The Effects of Accelerated Aging and Deterioration on the Diffusive Properties of Concrete Containing Cathode Ray Tube Glass

5.1 Background

The leaching process takes place in two phases: the release and transport from the source to the water phase, and the transport from the concrete location to the end point of concern. There are several performance-based leaching tests that try to simulate these two phases; however, they are not enforced by the EPA. On the other hand, the leaching protocols that are enforced by the EPA do not properly address these two phases because they do not properly recreate the exposure conditions of the environment or the material's physical state (i.e. crushed vs. monolithic). In an effort to better understand the leaching process, several researchers have developed models based on diffusion controlled release to estimate long-term field performance assuming the constituents of concern are uniformly dispersed in a homogeneous matrix [61]. However, these models fail to consider the heterogeneity of concrete in the long-term leaching predictions. As previously explained in Chapter 2 of this dissertation, concrete deterioration can theoretically lead to an increase in contaminant release. Nonetheless, current environmental leaching tests do not consider deterioration effects as a parameter and can therefore be under or overestimating the release of a contaminant.

Careful consideration to the environmental impacts of a material needs to be taken when a potentially hazardous secondary aggregate like CRT glass is used. In an effort to verify if and how CRT-Concrete could be potentially hazardous to the environment, Study 1 focused on characterizing the contaminant release from CRT-Concrete (i.e. lead

leaching). Through a series of regulated as well as proposed EPA tests, multiple scenarios that are encountered throughout the life-cycle of CRT-Concrete were simulated to quantify contaminant release. Ultimately, the study showed that encapsulation of CRT glass in a concrete matrix is possible if the material and mixture proportions are adjusted.

This study focuses on the environmental performance of CRT-Concrete during its service life. Although previous researchers have looked at the interactions between concrete deterioration and leaching [49,60,61,105-108] their goal was different since they attempted to evaluate the impact of aggressive environments and leaching of constituents (cause), and how it affects the structural performance of the material (effect). This study takes the opposite approach, which is to study the effect of concrete degradation through aging (cause) and how it affects contaminant release (effect). Garrabrants and Kosson [62] are currently evaluating a similar physical-chemical phenomenon from a waste management perspective, i.e. cementitious solidification of wastes and containment of wastes with reinforced concrete structures.

There are multiple physical and chemical processes that promote aging and deterioration of concrete. Whether deterioration is due to carbonation, which can potentially lower contaminant release, or due to cyclic loading, changes in temperature, steel reinforcement corrosion, or alkali-silica reactions, the end results is the exposure of new surfaces for leaching. The complex assessment of service life contaminant leaching cannot encompass all these processes in just one test. Nevertheless, durability-leaching tests that assess leaching from granular waste materials used in highways during water infiltration coupled with freezing and thawing [109], and tests that simulate the effects of continuous and intermittent wetting and drying of concrete have been used to produce meaningful

correlations between wetting and drying, carbonation, and diffusion-based contaminant release [48]. This study takes a similar approach by coupling several commonly used durability/deterioration tests (Arrhenius aging, Freeze/Thaw, ASR testing) with a commonly used diffusion leaching tank test. The goal is to understand if there are any relationships between aging and deterioration to the leaching of contaminants in a heterogeneous material. The following subsections briefly describe the diffusion models that are used to describe this type of release behavior.

5.1.1 Leaching due to Diffusion

The purpose of the diffusion test is to simulate the leaching of inorganic components from a monolithic material under aerobic conditions as a function of time. Most of the leaching assessments and models are conducted under continuously saturated conditions which usually cause relatively minor changes in leaching chemistry. Release can be described by the diffusion model for elements that are highly soluble such as sodium and chloride, or by a shrinking front type model for pH-dependent species such as arsenic or lead. For highly soluble species the models are based on Fick's second law of diffusion which considers mass transfer taking place in response to concentration gradients between the porous material and the leachant. Diffusion is characterized by the equation below:

$$\frac{\partial C}{\partial t} = D_{obs}(\nabla^2 C) \tag{5.1}$$

Where:

C: is the bulk concentration (mg/m^3 of porous matrix)

D_{obs}: is the observed diffusivity of the species of concern (m^2/s)

t: time (s)

The rate and magnitude of release is controlled by the initial leachable concentration, C_o, and the observed diffusivity of the species of concern in the porous material, D_{obs}. Two possibilities in species concentration may occur: 1) the species of concern is not depleted over the time period of interest, or 2) the species of concern is completely depleted. For the first case, Crank [110] describes the process as a one-dimensional semi-infinite diffusion model where it is represented by the following equation:

$$M_a = 2\rho C_o \left(\frac{D_{obs} t}{\pi}\right)^{1/2} \quad (5.2)$$

Where:

M_a: Cumulative mass of the constituent released per unit surface area (mg/m^2)

C_o: Initial leachable concentration (mg/m^3 of porous matrix)

t: time interval (s)

D_{obs}: Observed diffusivity of the species of concern (m^2/s)

For species that are completely depleted or for instances where semi-infinite media cannot be assumed, 3D diffusion models and numerical techniques need to be employed to calculate a solution to the diffusion equation.

5.2 Materials and Method

5.2.1 Experimental Plan

In this study the effects of aging and deterioration on contaminant release were investigated for two elements, calcium and lead. A modified diffusion leaching procedure (also known as tank leaching) was conducted where individually mixed CRT-Concrete specimens are exposed to two different temperature environments while inside a leaching vessel. The conditions and parameters used in this modified tank leaching experiment

were the same as the ones presented in section 4.1 of this dissertation (i.e. Arrhenius Aging). At predetermined time intervals, water samples from each container were extracted and tested for the species of concern. At the conclusion of the Arrhenius Aging (AA), the specimens were then introduced to freeze-thaw cycles where further deterioration of the CRT-Concrete occurs. Once the material deteriorated to a predetermined value (first judged visually and then by calculating a loss in modulus of elasticity), they were then tested for contaminant release once again using the modified tank leaching procedure. Ultimately these values were used to compare the flux release of contaminants between the specimens before and after freeze-thaw testing.

5.2.2 Materials

This study used the same materials as those detailed in Section 4.2.2.

5.2.3 Mixing and Preparation

This study used the same concrete mixture design that was used in Study 2. Diffusion tests naturally require a large amount of water to properly conduct the test. For this reason, the dimension of the cylindrical concrete specimens used for the diffusion test was scaled down. Ten 50 mm by 100 mm CRT-Concrete cylinder samples were individually mixed per percent replacement of CRT glass. Individually mixed samples allowed each sample to have the same amount of CRT glass in the mixture. A drawback to this approach is that the lead concentration in the glass varied from sample to sample (and consequently from specimen to specimen) and therefore the assumption that the lead concentration in each specimen was the average concentration after testing 25 individual CRT glass samples was made. All molded specimens were covered to prevent loss of

moisture during the first 24 hours and then placed inside a curing room at 100% relative humidity until its 28th day. The mixture proportions used to evaluate the ASR expansion characteristic were prepared in accordance with ASTM C1260 [63].

5.2.4 Test Methods

5.2.4.1 CRT Glass Lead Availability

Two tests to quantify the total content and total availability of lead from the CRT glass used in this study were conducted. For total content, a handheld X-Ray Fluorescence (XRF) machine, see Figure C-1 in Appendix C, was used to scan the CRT glass for chemical composition. For total availability of lead, EPA method 3050B was conducted [111]. This method uses a series of strong acid digestions to dissolve almost all of the elements that could become environmentally available to leaching.

5.2.4.2 Alkali Silica Reaction

Alkali silica reactions in concrete are known to cause spider cracks and spalling of the surfaces if the reactions are deleterious. This standard durability test was slightly modified to add an environmental component that tests for changes in contaminant leaching as a function of time and percent expansion. For the ASR test, five mortar bars were individually batched for each CRT percentage substitution in accordance to ASTM C1260. The specimens were cured for 24 hours, de-molded, immersed in water for 24 hours, and then stored in a 1N NaOH solution at 80°C while periodic length measurements of the specimen were taken. The NaOH solution was replenished every time a sample of the solution was retrieved for contaminant testing while simultaneously measuring the length change of the specimen. This allowed for a direct comparison

between the percent expansion of the specimen and its release of calcium and lead. The change in length was recorded using a length comparator at 2-3 day intervals for the first 16 days, followed by a two-week interval and ending with two one-month intervals.

5.2.4.3 Modified Diffusion Test

The modified diffusion test determined the chemical properties of the heterogeneous CRT-Concrete by placing the complete sample in a leaching fluid and replenishing the solution at specified times. The concentrations of the leached components in the successive eluate fractions were measured. Then, the leached quantity per unit area or weight was calculated for each element considered (i.e. lead and calcium). Using this data, the effective diffusion coefficient was calculated and used to model the leaching behavior. In this study, a modified diffusion test based on EPA Draft Method 1315 [41] was conducted by adding the concept of AA. The idea that temperature has a direct impact on the chemical behavior of a material was achieved by placing the CRT-Concrete diffusion samples into individual leaching vessels at two different temperatures (approximately 19°C and 50°C). The temperature limit of 50°C was selected after an extensive literature review that suggested that the maximum temperature for concrete curing and aging is 60°C since anything higher would change the kinetics, leaching and the nano-structure of the material [93,112].

Similar to Study 2, three CRT-Concrete mixtures (0%, 10%, 20% CRT glass) with ten specimens each were tested. Five specimens for each mixture were maintained at 19°C for the duration of the diffusion test in their individual containers, while the remaining five specimens were maintained at the elevated temperature of 50°C. Individual containers with a total liquid volume of deionized water equal to a liquid-to-surface-area

of 9 ± 1 mL/cm^2 or 1700 mL, prevented cross contamination between specimens and promoted diffusion leaching.

Andac [113] believed that diffusion tests could be reproduced more accurately if the pH of the diffusion test was controlled. This is especially true when testing concrete materials since the pH of the unbuffered water quickly rises due to the alkalinity of the concrete (between a pH of 11 and 13). The concern is that an alkaline environment does not promote concrete degradation. In fact, this protective environment protects calcium from being dissolved and ultimately protects the steel reinforcement. By being able to more accurately control the pH of the solution, calcium leaching is promoted and the material beings to deteriorate. For this reason, carbon dioxide gas was bubbled into each container until the pH of the solution dropped to 7 ± 0.5. This value was initially checked daily but as time progressed, weekly bubbling of CO_2 was sufficient to maintain the pH.

This AA portion of the experiment lasted approximately 8 months in order to promote full cement hydration and long-term leaching data. Periodically, the leaching solution (deionized water) was replenished and the specimens were weighed while the previous solution was tested for pH, conductivity, calcium, and lead. The sampling time for this portion of the test is shown in Table 5-1. A photograph of the sample and setup created for this experiment are shown Figure C-2 and Figure C-3. Following the AA portion of the modified leaching procedure was the introduction of freeze-thaw cycles to the specimens to promote further deterioration. Periodically, ultrasonic pulse velocity tests and fundamental resonant frequency tests (explained in Section 4.2.4) were conducted to measure the change in modulus of elasticity of each specimen.

Table 5-1 - Schedule of Eluate Renewals for AA-Diffusion Testing

Interval Label	Interval Duration (h)	Interval Duration (d)	Cumulative Leaching Time (d)
T01	2±0.25	-	0.08
T02	23.0±0.5	-	1
T03	23.0±0.5	-	2
T04	-	7±0.1	9
T05	-	7±0.1	16
T06	-	7±0.1	23
T07	-	14±0.1	37
T08	-	14±0.1	51
T09	-	28±0.1	79
T10	-	28±0.1	107
T11	-	28±0.1	135
T12	-	95±0.1	230

Freeze-thaw deterioration was completed when the specimens had visually deteriorated (i.e. spalling of the surfaces) or had lost a similar percentage of their initial modulus of elasticity as compared to Study 2. At this point, the specimens were placed back into the modified diffusion tank test to see if there was any change in release behavior (i.e. flux release). The sampling time for this portion of the test is shown in Table 5-2.

Table 5-2 - Schedule of Eluate Renewals during F/T Testing

Interval Label	Interval Duration (h)	Interval Duration (d)	Cumulative Leaching Time (d)
First F/T Run			
T12	2±0.5	-	0.08
T13	23.0±0.5	-	1.08
T14	-	7±0.1	8
T15	-	21±0.1	29
Second F/T Run			
T16	2±0.5	-	0.08
T17	23.0±0.5	-	1.08
T18	-	7±0.1	8
T19	-	21±0.1	29

5.3 Results and Discussion

5.3.1 CRT Glass Lead Availability Results

Presented in Table 5-3 are the averaged results from both EPA Method 3050B and the XRF analysis. The full set of results are reported in Appendix C. Twenty five randomly selected glass samples were tested from a well-mixed, CRT funnel and panel glass source. The samples were scanned with the handheld XRF equipment to measure total lead contents. These samples were then tested for total lead availability. Results show that the CRT glass had an average available lead content of 0.41% and a total lead content of 5.56%. The discrepancy in the results was due to the nature of the tests conducted. While one method uses X-Ray technology to record the total content of lead present in a sample, the other method relies more on leaching from the surface of the material. However, the results for total lead content are comparable with other CRT studies [19-21,69,70].

Table 5-3 - Lead Availability in CRT Glass

Lead Testing	Lead (mg/kg)	Percent Lead
Lead available for leaching (EPA Method 3050B)	4,121	0.41%
Total lead content (XRF)	55,568	5.56%

5.3.2 Leaching due to Alkali Silica Reaction Expansions

Lead

The objective of this experiment was to see if any correlation exists between expansion of the concrete and leaching. This modified version of ASTM C1260 required that the solution be replenished at every sampling interval in order to avoid saturation of the solution with the constituent of concern. Figure 5-1 displays the lead concentrations at consecutive intervals of: (1) 1-day, (1) 2-day, (4) 3-day, (1) 14-day, and (1) 28-days. The

numbers parentheses represent how many tests were conducted for that particular time interval.

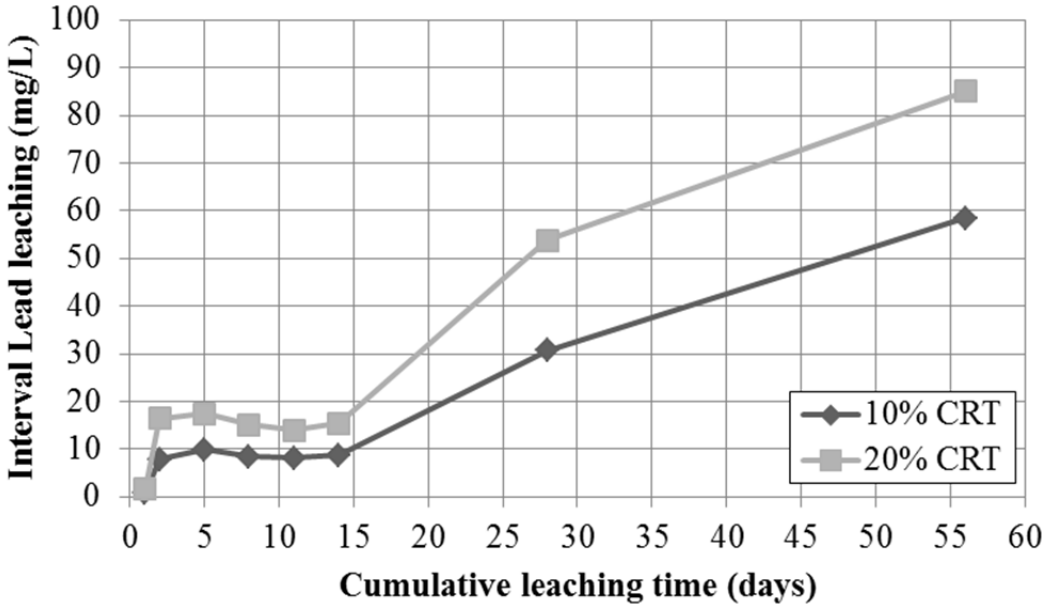

Figure 5-1 – Lead interval leaching concentrations

The modified ASR-leaching test resulted in leaching concentrations that were almost equal during the 2-day and 3-day leaching intervals. To understand its significance, the mass flux release was plotted. Figure 5-2 plots the mass flux release of lead for each leaching interval using the generalized mean of the square root of the cumulative leaching time to describe each leaching interval. This is the standard form to report time in cumulative leaching tests [41]. The results gathered from this plot showed a mass flux release that was relatively constant throughout the 2 and 3-day leaching intervals. The significance of this observation is that saturation of the leaching solution with lead occurred during testing and therefore the interval period should be shortened if the relationship between expansion and leaching was sought after.

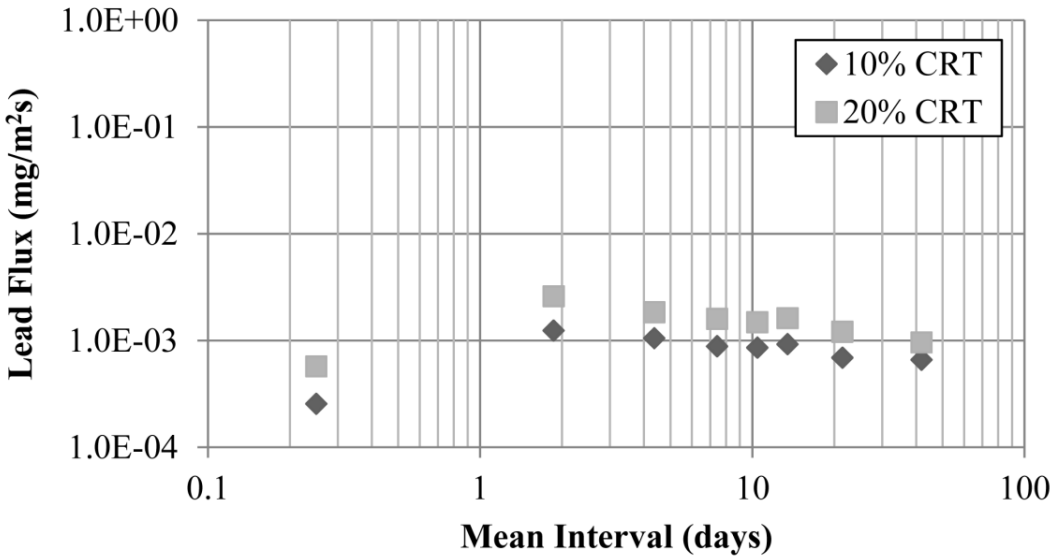

Figure 5-2 - Mass flux of Lead

The saturation of the leaching solution with Pb ions led to a lack of relationship between mortar-bar expansion and Pb release. Figure 5-3 shows the plot of the average release versus expansion of the mortar bar per leaching interval. Once again, it is clear from this plot that no relationship could be derived because of the saturated solution. The increased contact time between the specimen and the strong basic solution allowed for dissolution of the specimen to occur. This was observed after a prolonged exposure of 14 and 28 days which led to an increase in release. However, these values cannot be used to correlate expansion and leaching because a change in the release mechanism (dissolution instead of diffusion) occurred and the possibility that a portion of the solution evaporated during these longer-than-normal leaching intervals which could be the reason why the concentrations increased. Finally, although it may be possible to find a correlation between contaminant leaching and specimen expansion by reducing the leaching interval to 1 day or less, this procedure is not feasible since replenishing the solution and testing a large number of samples is labor and material intensive.

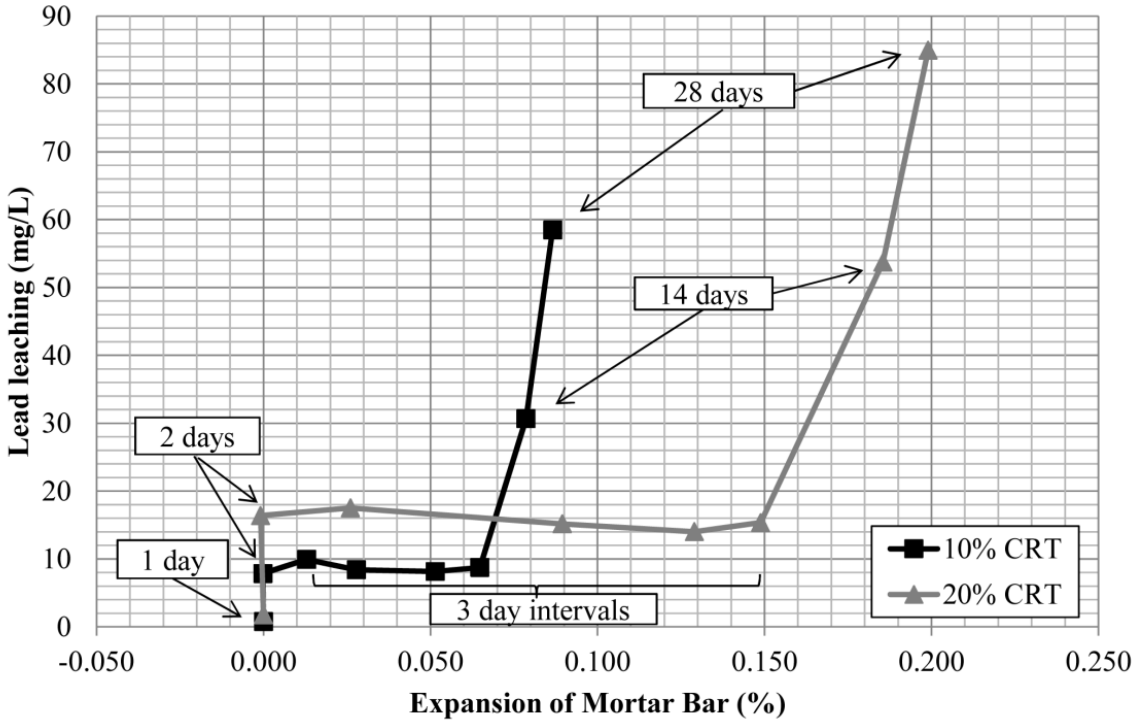

Figure 5-3 - Average lead leaching with respect to the expansion of CRT mortar bars

Calcium

Calcium is one of the main elements in both the cement and aggregates used in this concrete mixture. Being so, it is important to understand how the release of this element if affected by outside parameters such as ASR. Figure 5-4 displays the interval release concentrations for calcium. The modified ASR-leaching test resulted in erratic calcium leaching concentrations with a trend that was consistent throughout all three mixtures. The 14 and 28-day interval leaching samples for the control mixture were not tested because no relationship between expansion and leaching could be determined since the control mixtures do not have any significant expansions.

Figure 5-5 displays calcium mass flux for each leaching interval. Similar to the mass flux of lead, the results gathered from this plot show that calcium release was constant

throughout the 2 and 3-day leaching intervals and decreased during the 14 and 28-day intervals. These results essentially mean that the solution was saturated during the 2 and 3-day leaching intervals and calcium dissolution occurred so rapidly in the early stages of leaching that eventually its availability at the exposed surfaces of the specimen started to deplete; resulting in a lower mass flux release during the 14 and 28-day leaching intervals.

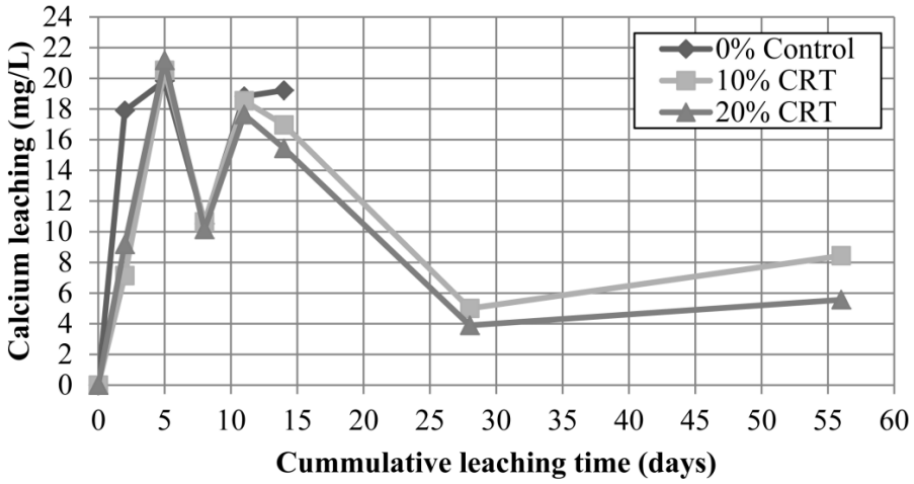

Figure 5-4 - Calcium interval leaching concentrations

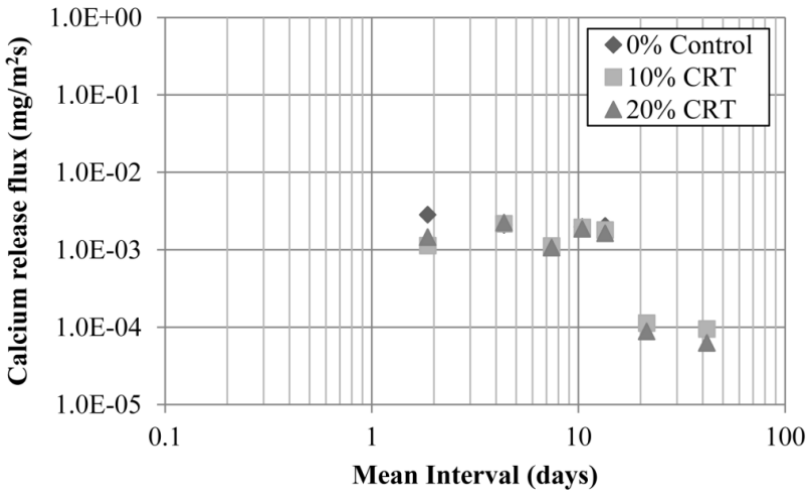

Figure 5-5 - Mass flux of Calcium

Figure 5-6 shows the plot of the average calcium release versus the average expansion of the mortar bar. The erratic behavior presented in the plot shows that calcium leaching

was independent and no relationship to the expansion of the mortar bars existed. This is further proven by observing a similar magnitude and behavior of release from the control mixture which did not expand due to the absence of the CRT glass. The significance of the similar behavior observed in all three mixtures is that calcium release was driven more by dissolution of the material and not by diffusion. Individual results as well as the pH and conductivity of each solution used in this test are reported in Figure C-4 to Figure C-24.

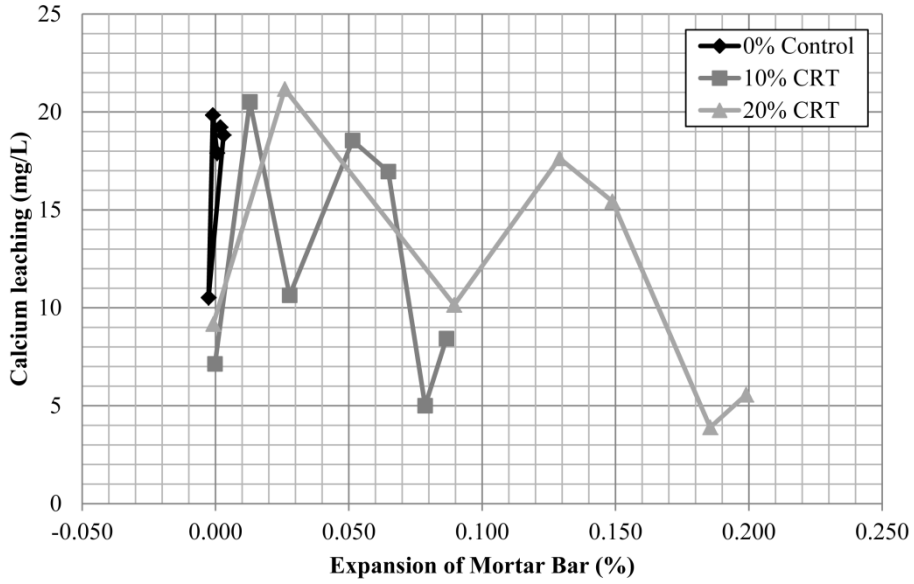

Figure 5-6 - Average calcium leaching with respect to the expansion of CRT mortar bars

5.3.3 Modified Diffusion Test

The modified method of the tank diffusion test bubbled carbon dioxide gas into the leaching solution to maintain the pH as close to neutral as possible. Initial adjustments of the pH required daily CO_2 bubbling for approximately the first two months. After this period, the CO_2 gas neutralized the outer layer of the specimens and only weekly followed by monthly pH adjustments were necessary. Figure 5-7 displays the average pH that the specimens were exposed to throughout the experiment. Points where the pH

dropped below 6.5 are due to acid residue from acid washing; similarly, parts where the pH rose above 9 are because the leaching solution was recently replenished with a fresh solution and no CO_2 bubbling occurred during that period.

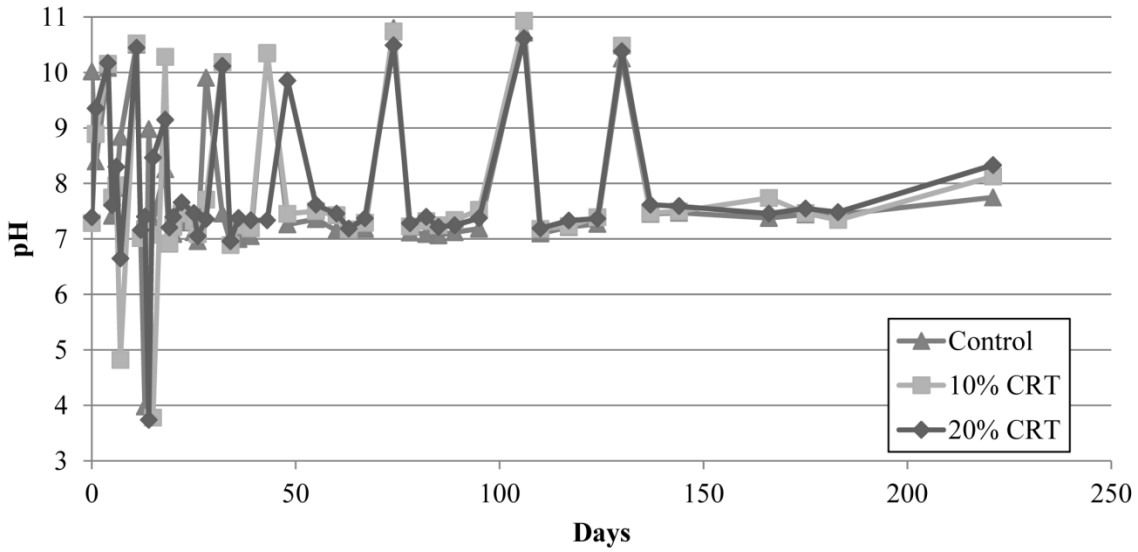

Figure 5-7 - Timetable of the pH swing.

5.3.3.1 Lead

Sixteen samples were acquired at predetermined time intervals for this modified diffusion test procedure. The minimum detection limit for the equipment used to analyze the lead samples was 0.0011 mg/L. For visual presentation as well as modeling reasons, the samples that were undetected by the equipment were assumed to have the minimum concentration that the equipment could read. Figure 5-8 displays the interval lead release that was observed for 10% and 20% substitution with CRT glass under both the 19°C room temperature environment (cold) and the 50°C environment (hot). As expected, the hot environment accelerated the release of lead; however, this appeared to be more dependent on the interval leaching period which showed a greater difference in release occurring during the short time intervals. The difference in release was less noticeable

during the 14 and 28-day leaching intervals. After approximately 80 days, the specimens in the hot temperature environment exhibited color changes in the surface as well as small amounts of spalled concrete residue in the containers, both possible signs of deterioration. These effects are shown in Figure C-30 and Figure C-31 of Appendix C.

a)

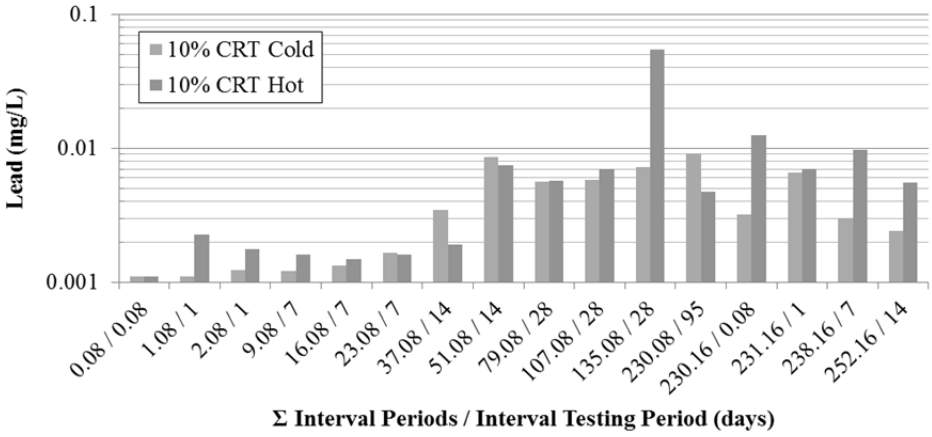

b)

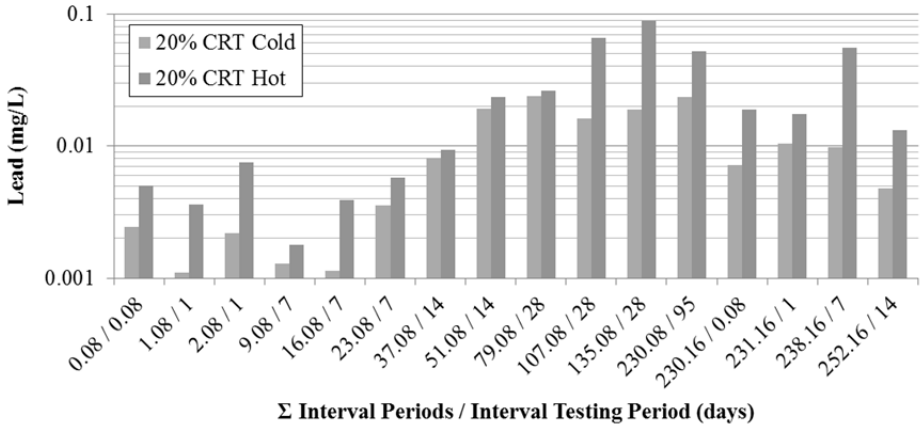

Figure 5-8 - Average lead interval release of lead: a) 10% CRT b) 20% CRT

Mass transport is often characterized in terms of the mass flux or cumulative mass released as a function of time. Mass flux, which defines the mass released across an exposed surface area over a period of time, is expected to be highest in the beginning of the experiment, since most of the contaminants lying on the surface are washed out, and then gradually decrease. Figure 5-9 shows the behavior of CRT-Concrete for both environments. Release wise, there was almost no difference (between the cold and hot

environments) in mass flux release for the 10% CRT glass specimens, this was possibly due to a low amount of leachable lead available from the CRT glass. Conversely, the 20% CRT specimens showed a difference in mass flux release at the two different temperatures. However, when an Analysis of Variance (ANOVA) test was conducted to compare the difference in mass flux between the two temperatures, no statistical significance was found for both the 10% and 20% mixtures at a 95% confidence interval. The peak fluxes observed towards the end of the plots were due to freeze/thaw deterioration which is explained in Section 5.3.4.

a)

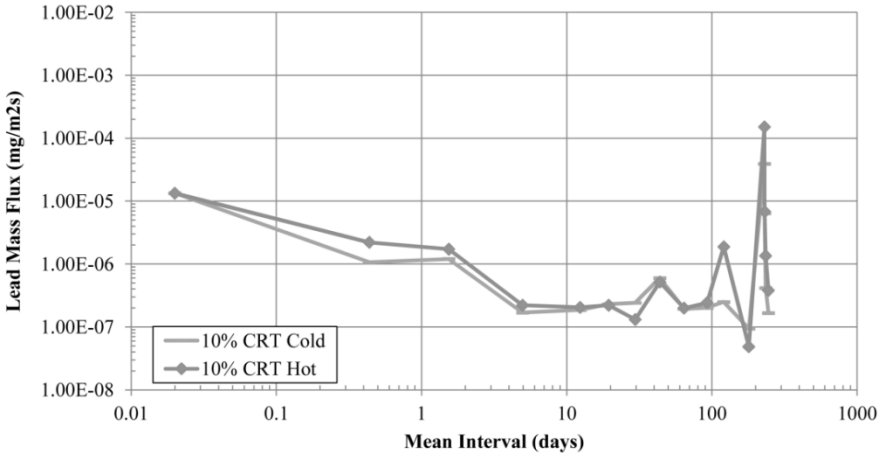

b)

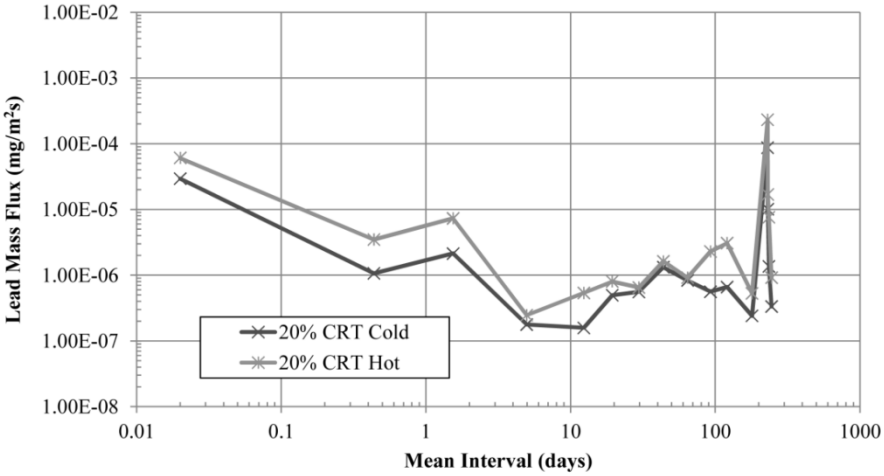

Figure 5-9 - Average lead mass flux release a) 10% CRT b) 20% CRT

Figure 5-10 shows the total cumulative leaching that occurred throughout the duration of the experiment. Overall, the hot temperature environment had a significant statistical

impact on the cumulative contaminant release from the specimens [p = 0.019 and 0.002 for 10% and 20% respectively]. Comparing the effect of temperature on the release, the 10% CRT specimens displayed an average increase in release of 51.9% per leaching interval in the hot temperature environment while the 20% CRT specimens had an average increase of 128.3%.

a)

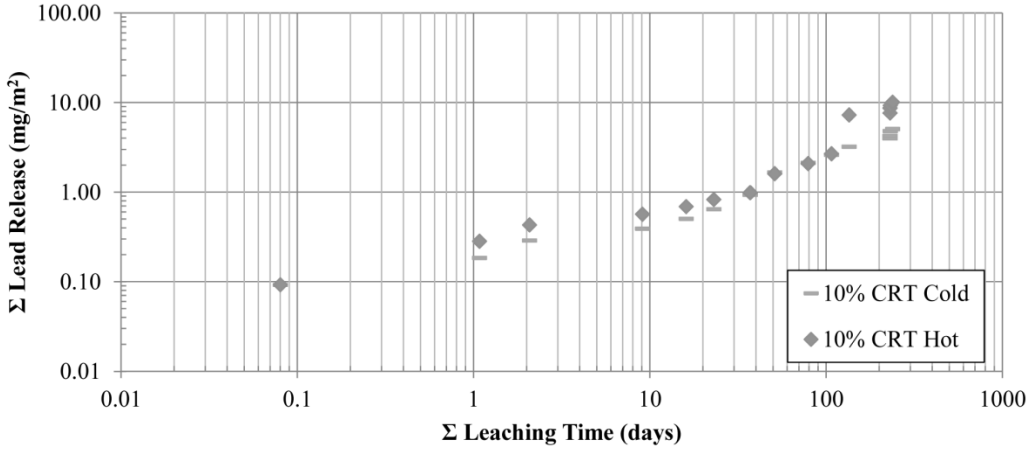

b)

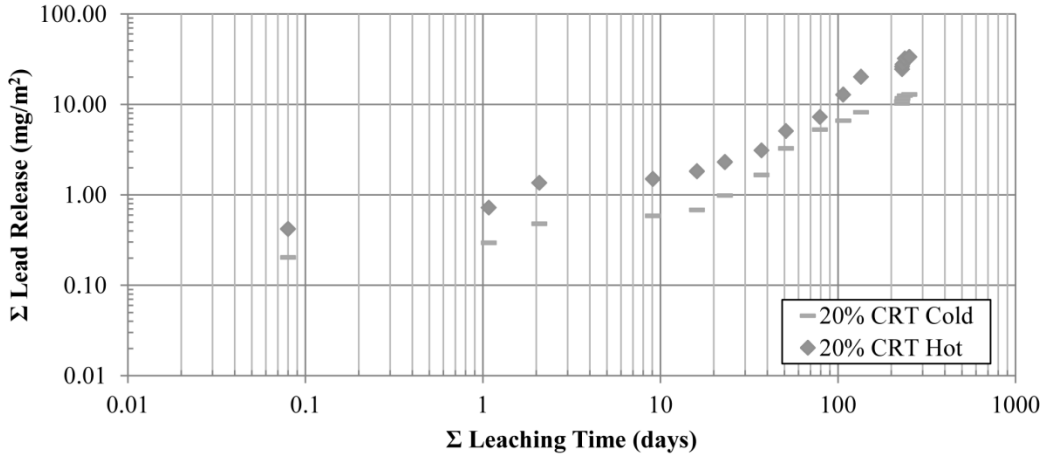

Figure 5-10 - Average lead cumulative release a) 10% CRT b) 20% CRT

The slope of Figure 5-10 determines the release mechanism of the system. The European Committee for Standardization (CEN) states that for fully diffusion-controlled leaching, the slope should be exactly 0.5. However, diffusion leaching can be also observed at slopes between 0.35 and 0.65 [42]. Furthermore, any slope that is below 0.35 may indicate either surface wash-off or depletion (depending on the time interval) and any

slope above 0.65 is considered to be dissolution or delayed diffusion if it occurs in the initial leaching intervals. For the 10% CRT specimens exposed to the cold environment, surface wash-off occurred during the initial leaching interval (average slope of 0.27) and then progressed to a mixture of diffusion and dissolution controlled leaching (average slope varied from 0.63 to 1.04 for the latter intervals). On the other hand, the specimens aged under the hot environment did not experience any surface wash-off; which later progressed to a mixture of diffusion and dissolution controlled leaching (slopes varied from 0.80 to 1.87). In the case of the 20% CRT specimens, both the cold and hot temperature specimens exhibited surface wash-off during the initial leaching interval (slope of 0.17 and 0.21 respectively) followed by a period of diffusion controlled leaching for the 7 and 14 day intervals.

The intervals whose slopes were within 0.5 ± 0.15 were used to calculate the diffusivity coefficient. The diffusivity coefficient was adjusted for the difference in temperature between the room temperature specimens and the hot temperature environment. Results show that the hot temperature specimens had a higher rate of leaching as shown by the lower pD values, this trend was consistent between the 10% and 20% CRT specimens. Overall, a very low mobility in lead release occurred regardless of the temperature environment.

Table 5-4 shows the average diffusivity observed for both lead and calcium along with a pD value (which is defined as the negative log of the average diffusivity) that was used to determine the rate of leaching. The higher the pD value, the lower the rate of leaching. Values of pD that are greater than 12.5 indicate a component with low mobility, while a pD value between 11 and 12.5 describe a component with average mobility.

The diffusivity coefficient was adjusted for the difference in temperature between the room temperature specimens and the hot temperature environment. Results show that the hot temperature specimens had a higher rate of leaching as shown by the lower pD values, this trend was consistent between the 10% and 20% CRT specimens. Overall, a very low mobility in lead release occurred regardless of the temperature environment.

Table 5-4 - Average diffusivity coefficient

	Lead			Calcium		
	Average Diffusivity (m^2/s)	Std. Deviation of Diffusivity	pD = -log(D_{avg})	Average Diffusivity (m^2/s)	Std. Deviation of Diffusivity	pD = -log(D_{avg})
0% CRT Cold	-	-	-	4.11E-18	7.13E-19	17.4
0% CRT Hot	-	-	-	7.66E-18	2.42E-18	17.1
10% CRT Cold	5.29E-21	2.32E-21	20.3	5.86E-18	2.02E-18	17.2
10% CRT Hot	9.12E-19	1.99E-18	18.0	9.36E-18	2.45E-18	17.0
20% CRT Cold	4.01E-20	2.04E-20	19.4	3.73E-18	5.13E-19	17.4
20% CRT Hot	6.41E-19	5.11E-19	18.2	6.24E-18	2.09E-18	17.2

For each specimen, Crank's solution to Fick's Second Law of Diffusion for radial specimens (see section 5.1.1) was plotted using the diffusivity coefficient that was experimentally derived in order to compare the prediction of the model to the results. Figure 5-11 shows the cumulative release of lead for selected specimens along with a plot of Crank's solution (results for all specimens can be found in Figure C-25 and Figure C-26). A sample named "D10-1C" would indicate the first (out of five) 10% CRT diffusion sample that was exposed to a room temperature (cold) environment. Similarly, "D20-5H" would represent the fifth (20% CRT) diffusion sample exposed to the hot temperature environment.

As shown, Crank's solution agreed fairly well with the experimental data that was acquired. Primarily, this was because the diffusivity coefficient that was used in the model is the averaged experimental value that was gathered for that particular specimen. Nevertheless, Crank's solution to Fick's Second Law allowed for a comparison to be

made between the diffusion model and the release behavior of this modified accelerated diffusion leaching test.. The values that exceeded the predicted value of the model were considered to be due to surface wash-off (if it occurred during the early leaching interval) or dissolution; while the values that closely followed the slope of the model were considered to be controlled by diffusion leaching. The intervals where the curve skewed and did not match the slope of the model were most likely due to factors like CO_2 bubbling to lower pH of eluate, erosion or dissolution of the specimen.

Crank's model appeared to work well for the long-term leaching data where the effects of surface wash-off and the CO_2 began to disappear and diffusion began to control. Additionally, since temperature impacts the release of lead, Crank's model was a more accurate predictor of diffusion release under room temperature conditions. For the hot temperature specimens, a change in release was observed approximately one week after the initiation of the experiment and continued for another two weeks. Although the behavior skewed away from the model and was not representative of diffusion leaching, Crank's model conservatively overestimated the release.

a)

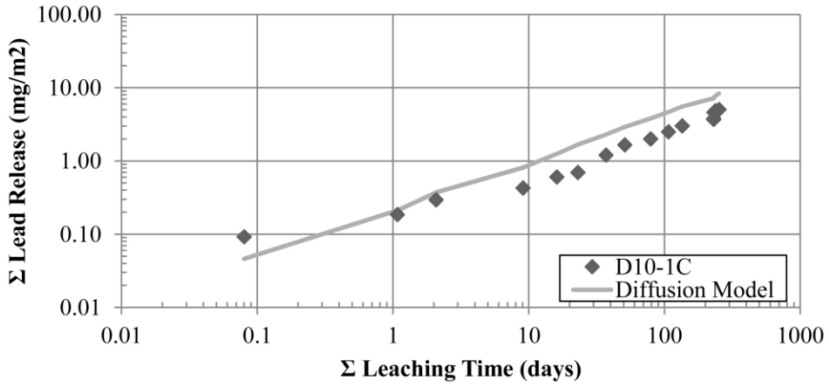

b)

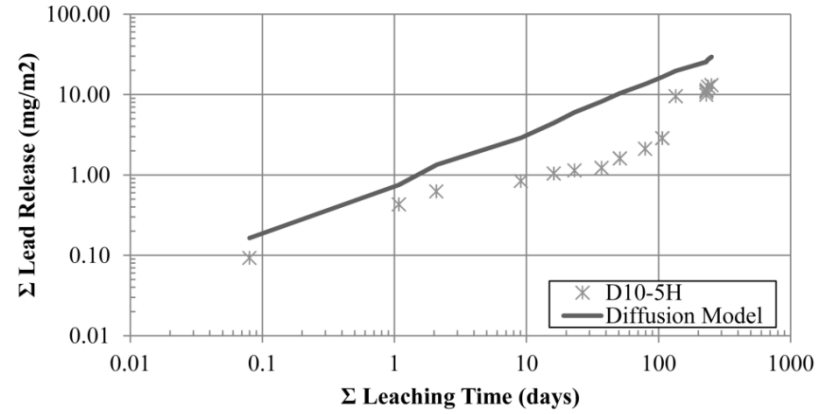

c)

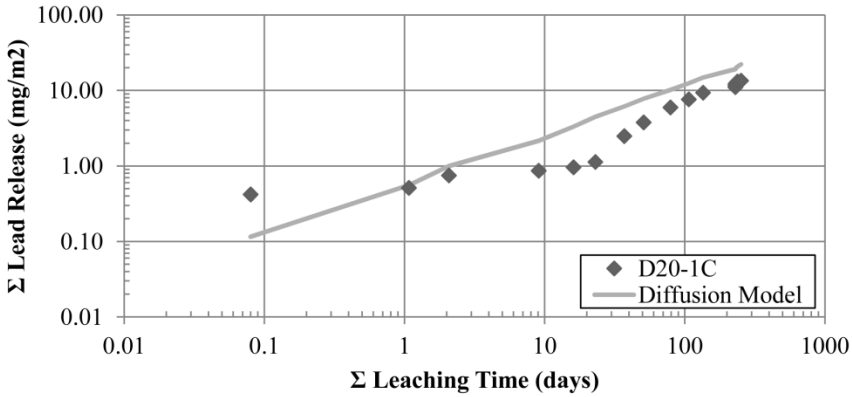

d)

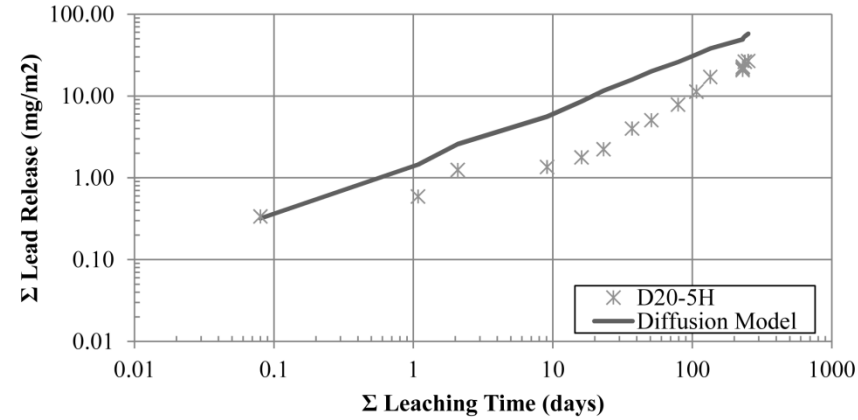

Figure 5-11 - Cumulative release plotted with Crank's Diffusion Equation solution

5.3.3.2 Calcium

The sixteen samples that were obtained for lead analysis were also analyzed for calcium. The minimum detection limit for the equipment used to analyze the calcium samples was 0.0036 mg/L. Figure 5-12 displays the interval calcium release that was observed for the control specimens as well as the 10% and 20% CRT-Concrete specimens. Similar to the

lead release case, calcium leaching was dependent on temperature. Initially, the hot temperature cured specimens released more calcium then the cold specimens. However, this behavior stopped during the longer leaching intervals, an indication that calcium on the outer surface may have been depleted.

a)

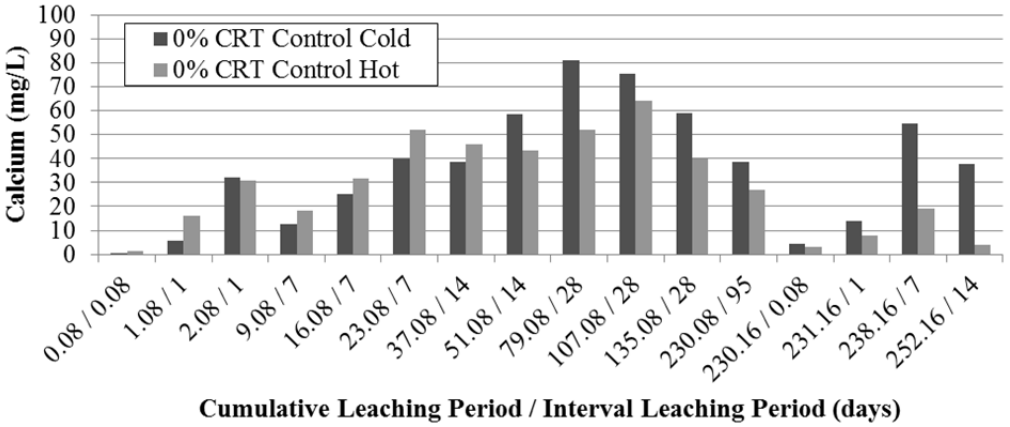

b)

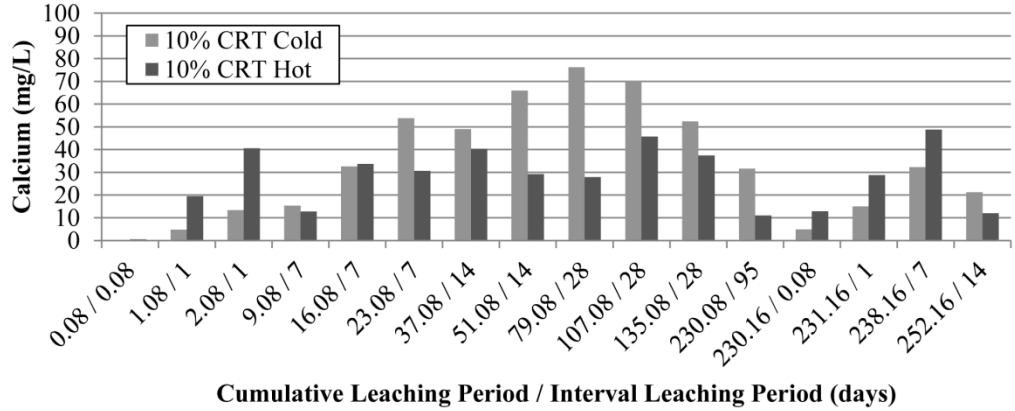

c)

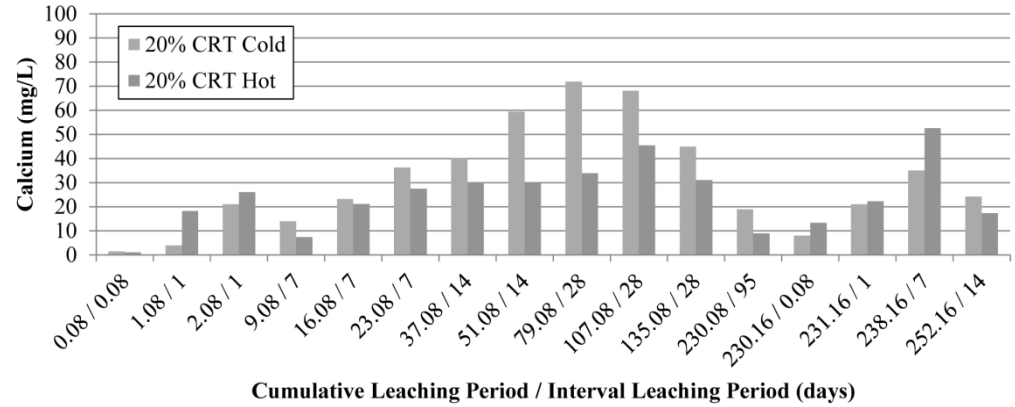

Figure 5-12 - Average calcium interval release a) Control b) 10% CRT c) 20% CRT

Mass transport is often characterized in terms of the mass flux or cumulative mass released as a function of time. Figure 5-13 shows the mass flux of CRT-Concrete for both environments. Although temperature did have an impact on the mass flux release of calcium, there was little to no difference in the magnitude of the release between all three concrete mixtures. Concurrent to the interval leaching behavior, the mass flux release of the CRT-Concrete specimens exposed to the hot environment was initially higher than its cold environment counterpart.

a)

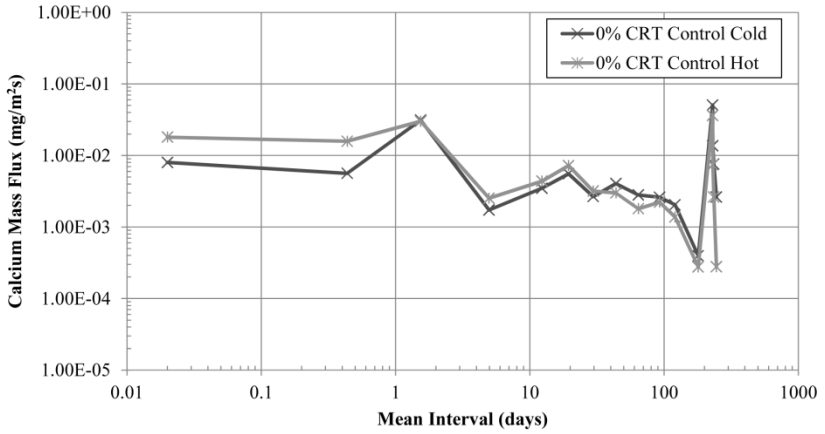

b)

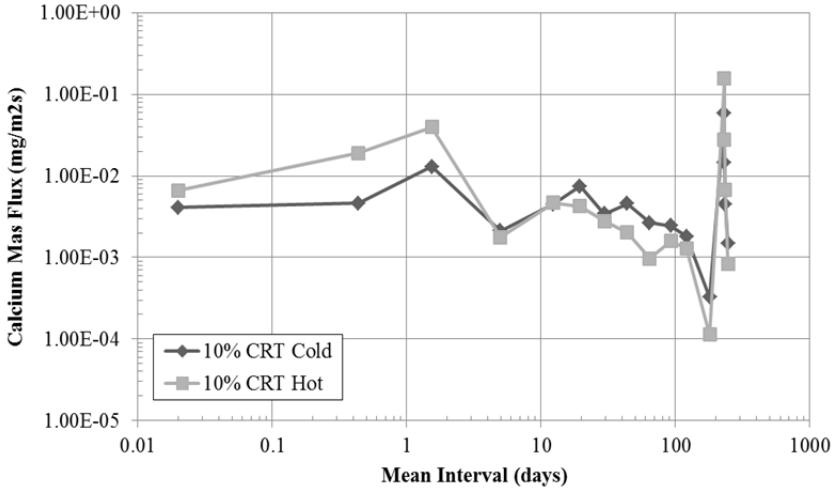

c)

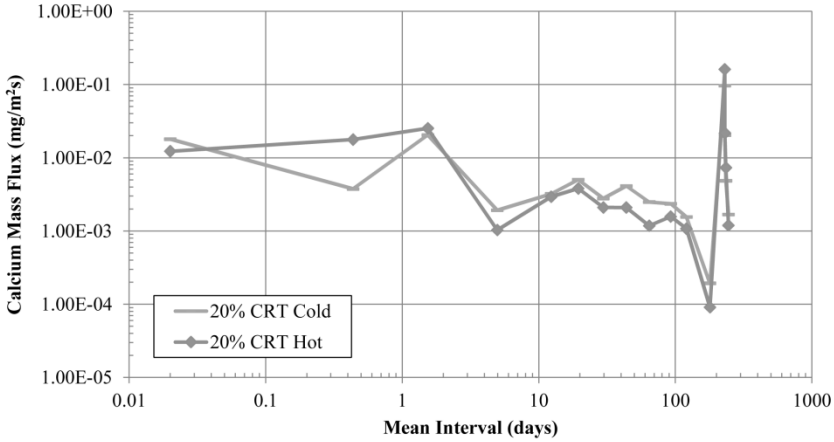

Figure 5-13 - Average calcium mass flux release a) 10% CRT b) 20% CRT

The overall impact of the hot temperature environment on leaching was not as expected. Figure 5-14 shows the cumulative leaching that occurred throughout the experiment. While the results for both the cold and hot environments are in the same order of magnitude, the average cumulative sum of calcium released from the hot specimens was 19.9% to 21.3% lower than their cold environment counterparts, effectively showing that temperature had a minor effect on the initial release of calcium but ultimately did not impact the release of calcium in this test.

a)

b)

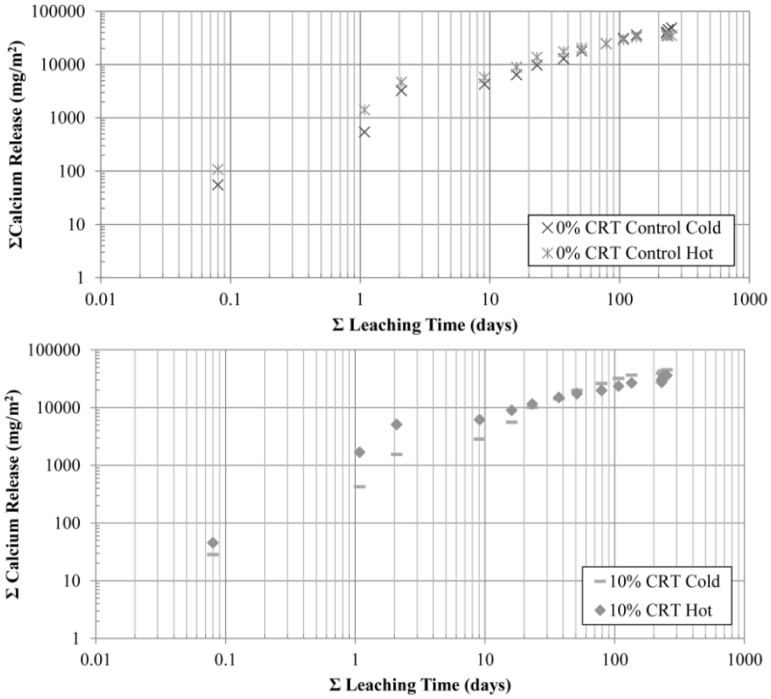

c)

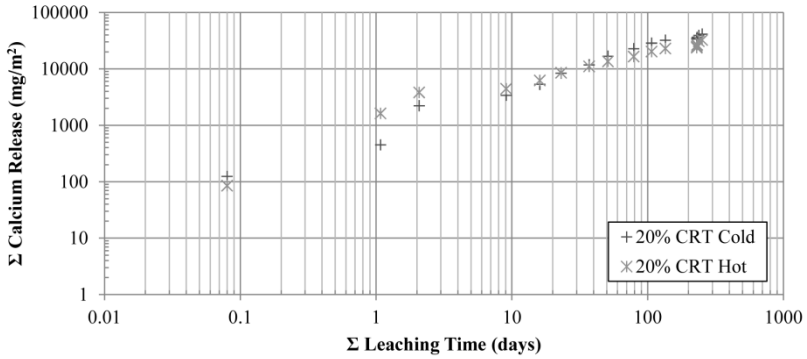

Figure 5-14 - Average cumulative calcium release a) 10% CRT b) 20% CRT

The final observation made from calcium leaching was its correlation to Crank's Diffusion model. The diffusivity coefficient was adjusted for the difference in temperature between the room temperature specimens and the hot temperature environment. Results show that the hot temperature specimens had a higher rate of leaching as shown by the lower pD values, this trend was consistent between the 10% and 20% CRT specimens. Overall, a very low mobility in lead release occurred regardless of the temperature environment.

Table 5-4 (in Section 5.3.3.1) shows the average diffusivity observed for calcium along with the pD value which was used to determine the rate of leaching. Results show that there was no difference in calcium leaching between the hot and cold temperature environments, supporting the conclusion previously made. Although its pD value is lower than that of lead, calcium release is still considered to have low mobility regardless of the temperature environment.

Crank's solution to Fick's Second Law of Diffusion for radial specimens (see section 5.1.1) was plotted using the diffusivity coefficient that was experimentally derived in order to compare the prediction of the model to the calcium release results. Figure 5-15 shows the cumulative release of calcium for selected specimens along with a plot of

Crank's solution (results for all specimens are found in Figure C-27 - Figure C-29). As shown, Crank's solution agreed fairly well with the experimental data that was acquired. Both the hot and room temperature specimens had similar release mechanisms that were not affected by the change in temperature. The results showed that calcium leaching from an accelerated and modified diffusion test can be conservatively estimated using Crank's solution.

a)

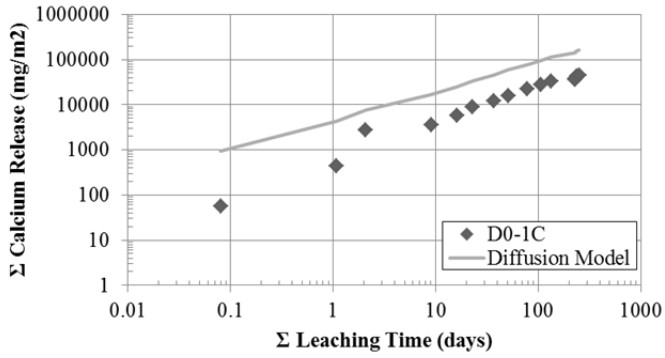

b)

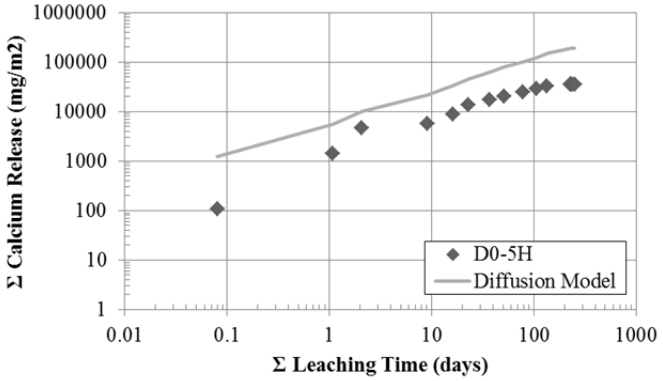

c)

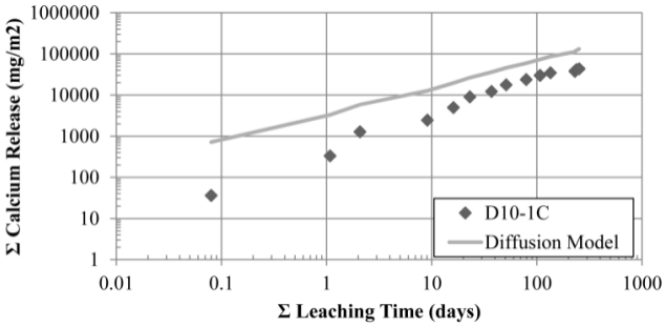

d)

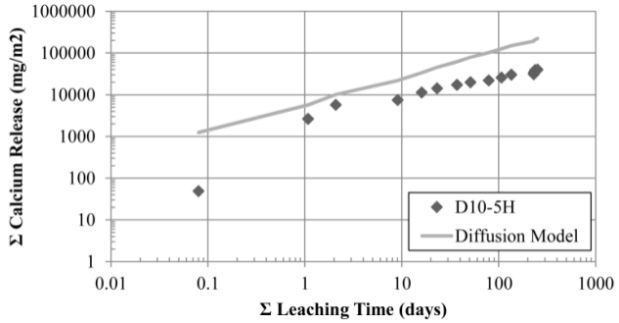

e)

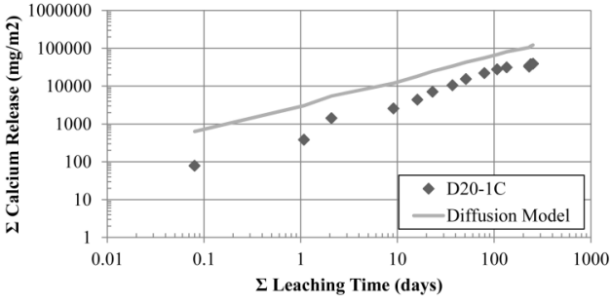

f)

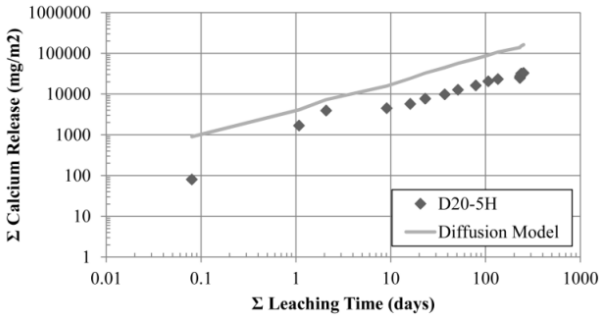

Figure 5-15 - Cumulative calcium release plotted with Crank's Diffusion Equation solution

5.3.4 Effects of Freezing/Thawing Deterioration on Leaching

The specimens that were aged using Arrhenius Aging were placed in a freeze/thaw chamber to physically deteriorate them. Table 5-5 shows the average mass retained and modulus of elasticity that was observed. Individual results are reported in Table C-3 to Table C-5. An ANOVA analysis was implemented to verify if the impacts to leaching had any statistical significance based on the interactions of the three mixtures used, the curing environments, and the level of deterioration. A P-value less than 0.05 means that there was a probability greater than 95% that the source (Mix, Curing Temperature, Deterioration) had a significant impact on leaching. Results show that deterioration (F/T

testing) had a significant statistical impact on the initial release of lead (0.08 and 1-day leaching intervals).

Table 5-5 - Average loss in mass and modulus of elasticity after F/T testing

Specimen ID	Avg. Modulus of Elasticity Loss (%)	Avg. Mass Retained (%)
Control Specimen (Cold)	94.56%	81.04%
Control Specimen (Hot)*	90.24%	84.95%
10% CRT-Concrete (Cold)	91.38%	91.38%
10% CRT-Concrete (Hot)	82.53%	82.53%
20% CRT-Concrete (Cold)	95.68%	79.93%
20% CRT-Concrete (Hot)	93.13%	83.46%

*One specimen was available for testing

This was confirmed by observing an F-value for deterioration that exceeds the critical value at the 5% significance level; therefore rejecting the null hypothesis that deterioration had no effect on the mass flux release. Table 5-6 shows the results of the ANOVA test for lead for all leaching intervals.

Table 5-6 - Analysis of Variance for Lead

LEAD	Flux 0.08 Days			Flux 1 Day			Flux 7 Days			Flux 14 Days		
Source	F-Value	P-Value	% of Total Variation	F-Value	P-Value	% of Total Variation	F-Value	P-Value	% of Total Variation	F-Value	P-Value	% of Total Variation
Mix	0.829	0.459	0.00	1.171	0.392	1.20	1.328	0.368	9.56	-	-	0.00
Curing	0.870	0.486	0.00	0.338	0.732	0.00	12.603	0.019	53.61	-	-	11.74
Deterioration	26.499	0.000	83.58	21.907	0.000	79.73	1.340	0.277	2.35	-	-	15.96
Error	-	-	16.42	-	-	19.07	-	-	34.48	-	-	72.30
Total	-	-	-	-	-	-	-	-	-	-	-	-

In contrast, the effects of deterioration on mass flux release during the 7 and 14-day leaching intervals were not as significant; instead, the curing method (the temperature of the water) had a more significant effect on the release of lead. These results were likely due to the initial surface wash-off that occurred during the early leaching intervals which was not observed in the later intervals.

Deterioration of the specimens had a statistically significant effect on the mass flux release of calcium. In this case, however, all four leaching intervals were affected by

deterioration and the curing temperature did not have much of an impact on the results, an observation that was explained in Section 5.3.3.2. The results for the ANOVA analysis for calcium are found in the Table 5-7. Although the ANOVA analysis shows that deterioration did have an impact on flux release, it does not explain if the impact is positive or negative nor does it explain the source.

Table 5-7 - Analysis of Variance for Calcium

CALCIUM	Flux 0.08 Days			Flux 1 Day			Flux 7 Days			Flux 14 Days		
Source	F-Value	P-Value	% of Total Variation	F-Value	P-Value	% of Total Variation	F-Value	P-Value	% of Total Variation	F-Value	P-Value	% of Total Variation
Mix	0.160	0.860	0.00	0.020	0.981	0.00	3.600	0.157	17.69	0.72	0.551	0.00
Curing	0.380	0.772	0.00	2.390	0.166	36.70	0.550	0.665	0.00	0.75	0.558	0.00
Deterioration	36.780	0.000	89.20	16.090	0.000	49.18	15.570	0.000	63.45	5.84	0	52.78
Error	-	-	10.80	-	-	14.12	-	-	18.87	-	-	47.22
Total	-	-	-	-	-	-	-	-	-	-	-	-

Freeze-thaw testing and the equations used to measure the deterioration (modulus of elasticity) of the specimen relied on mass loss. Therefore, a possible relationship between mass loss and the change in mass flux was important to investigate. Table C-6 to Table C-10 list in descending order the mass retained in each specimen and the corresponding change in mass flux for each leaching interval. Ideally, higher mass loss should reflect a greater increase in contaminant mass flux. Instead, the results show that there were no apparent relationships between them both. This phenomenon was most likely due to the heterogeneity of the material and the little amount of CRT glass present in the material. In other words, any surfaces that may have spalled may have uncovered little to no excess CRT glass therefore no relationship could be observed. Calcium on the other hand, did show an increase in release for the more deteriorated specimens, initially. This leads to conclusion that the release flux was not dependent on the amount of mass loss but on the content of the surfaces that were exposed.

Figure 5-16 and Figure 5-17 compares the average mass flux during four different leaching intervals for both lead and calcium release before and after F/T. On average, the overall lead mass flux for all leaching intervals increased once the specimens were deteriorated. Furthermore, the deteriorated cold specimens released more lead during the initial leaching intervals (0.08 and 1 day) than the hot non-deteriorated specimens; an increase that was attributed to new surface exposure.

Calcium appeared to have a slightly similar behavior. Once again, the initial leaching intervals proved that the newly exposed surfaces on the specimens increased flux release due to the surface wash-off effect. However, during the latter leaching interval at 14 days, the mass flux for the deteriorated samples (10 and 20% specimens) was actually lower than their non-deteriorated counterparts. This result possibly hints at depletion occurring in the surface of the material.

a)

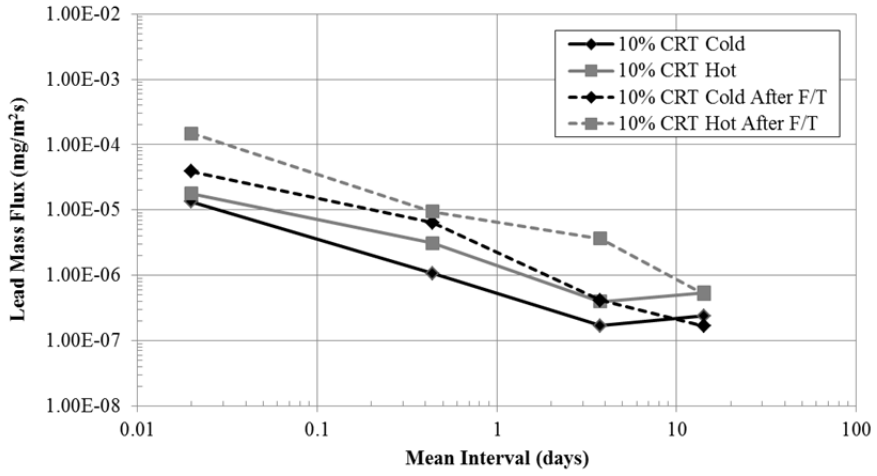

b)

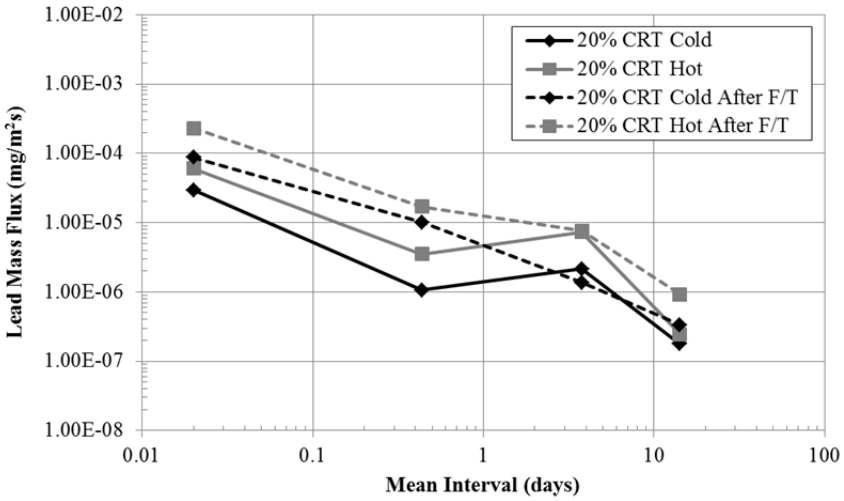

Figure 5-16 - Comparison of lead mass flux release before and after freezing and thawing.

a)

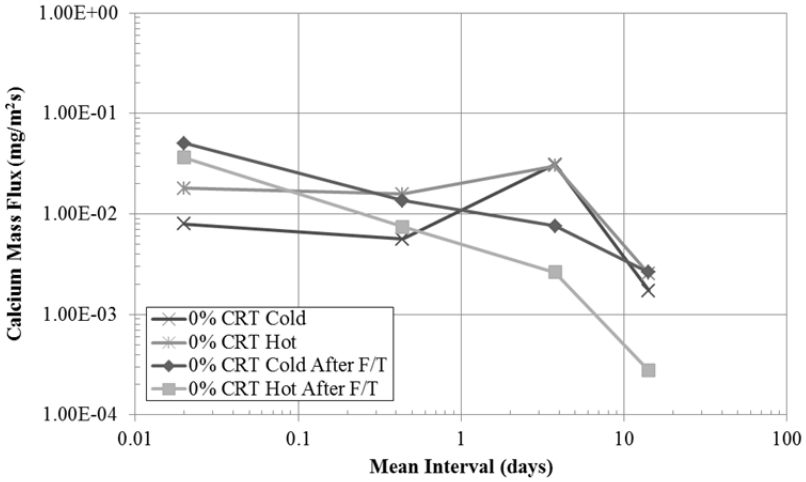

b)

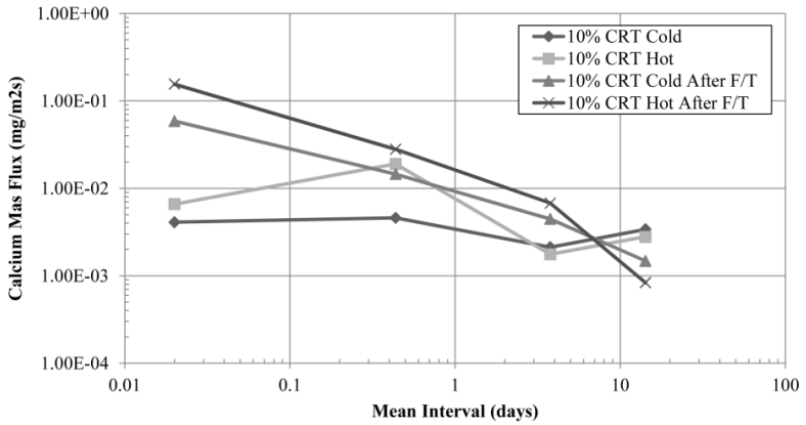

c)

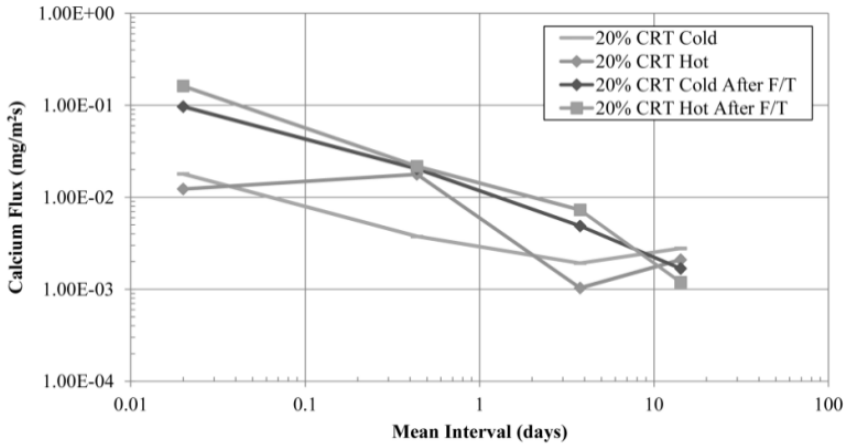

Figure 5-17 - Comparison of calcium mass flux release before and after freezing and thawing

5.4 Conclusions

This study focused on the environmental behavior of CRT-Concrete during its service life and the effects that durability and deterioration factors have on the release of lead and calcium. Substituting up to 20% of the fine aggregates needed for concrete with finely crushed CRT glass, three different durability/deterioration mechanisms were evaluated for their impact on leaching. Micro-cracking of the concrete matrix was achieved through ASR expansions, temperature dependency was evaluated using Arrhenius Aging, and surface deterioration and mass loss was promoted using F/T cycling.

ASR expansions were forced in the concrete specimens to observe if a correlation between lead and calcium release existed as the material expanded and cracked. The standard test was modified to include periodic refreshing and sampling of the solution for specimens in individual testing environments. Periodic sampling of the solution ranged from 1 day to 4 weeks. Although concentrations of calcium and lead were recorded at each testing interval, no correlation between expansion of the specimen and leaching could be made. This was due to the quick saturation of the leaching solution with the contaminant of interest (saturation occurred within two days of testing). Although

shorter time intervals could be tested, it will simply not be feasible due to the laborious task of preparing multiple solutions daily.

Temperature was observed to evaluate its impacts on leaching of lead and calcium. A modified diffusion tank test was developed to include Arrhenius Aging. This experiment exposed CRT-Concrete specimens to a solution of deionized water at two different temperature environments for 230 days. The modified diffusion tank test was also modified to simulate CRT-Concrete under service-life conditions (i.e. a concrete slab surrounded by neutral-pH ground water). Results show that diffusion leaching of lead was observed for the room temperature specimens and the release concentrations were in good agreement with the theoretical results acquired using Fick's second law of diffusio. When compared to a control group of specimens at 19°C, the hot temperature environment (50°C) resulted with a larger calculated diffusivity coefficient proving that the hot temperature did have an effect negative effect on lead leaching (increased rate of release). Additionally, lead leaching for the hot temperature specimens was not completely controlled by diffusion since the results skewed away from Crank's model, showing the effects of temperature. Calcium leaching on the other hand closely followed the model results and its diffusive behavior was not affected by either temperature or pH changes. One item to note is that after about 80 days of cumulative leaching in hot water, the CRT-Concrete specimens began to show signs of deterioration (change in surface color, concrete pieces in the containers). These signs of minor deterioration correlated with leaching intervals that showed an increase in release of both lead and calcium. As expected, the specimens containing 20% of CRT glass released more lead than those with only 10% CRT glass. Although the release mechanism of lead in the hot temperature

specimens was not completely diffusion controlled, due to its dependency on temperature and possibly other unknown factors, Crank's model is able to conservatively predict its release. From the data recorded in this dissertation (pH, conductivity and temperature of the solution, mass loss of the specimens, and lead/calcium concentrations) no significant relationship between the parameters and the change in release were found. Therefore, to more accurately model this behavior, more parameters and tests would need to be recorded to properly develop a numerical or theoretical model. For example, measurements of the surface pH and internal temperature of the specimens, CO_2 concentrations in the solution and penetration depth, and the porosity of the material would also need to be recorded.

Finally, surface deterioration and mass loss from F/T cycling was promoted to see if they had any correlations to a change in contaminant leaching. Specimens undergoing approximately 9-20% mass loss or 5-10% loss in modulus of elasticity exhibited an increase in lead and calcium mass flux release when compared to their non-deteriorated counterparts. An ANOVA analysis was used to confirm that deterioration (and not the concrete mixtures or curing temperature) had the greatest impact in the variance of the leaching results. From this, it was concluded that mass loss aided in the increase of release but was not the sole reason. Mass loss led to new surface exposures; however, an increase in mass loss did not always translate to an increase in contaminant release. This was most likely due to the heterogeneity of concrete and the comparatively small amounts of CRT glass replacements which made it difficult to find a relationship between mass loss and release of contaminants.

The following conclusions were derived in this study:

- The results acquired from the modified diffusion tank-leaching experiment were in good agreement with the theoretical Fick's Second Law of Diffusion, further enforcing that the modified experiments conducted did not alter the release behavior of the species and that Crank's Model can be used to predict Lead and Calcium leaching for specimens in a neutral pH environment.
- Surface deterioration of a CRT-Concrete specimen due to F/T cycling increased the release of contaminants into the environment by showing an increase in flux release for the deteriorated specimens. The increase in release was random and was not dependent on the mass loss of the specimen, but possibly dependent on the distribution of the CRT aggregate.
- Temperature had a direct impact on the leaching of contaminants. Hot temperatures (50°C) changed the microstructure of the material and in turn accelerated the release of contaminants (i.e. increase in lead leaching).
- No relationship between ASR expansions and contaminant release was found. This was due to the rapid saturation of the solution used in the experiment with the contaminant of interest.

Although deterioration has been found to increase contaminant leaching, the EPA regulated tests for disposal (TCLP) and use (SPLP) are considered a worst case scenario test (too conservative) because the material is granulated and not monolithic like in the diffusion test. The conclusions made in this study should be used to further investigate how the proposed environment for the material will affect the contaminant release, and potentially be used to create less conservative and more realistic tests.

Chapter 6

Conclusion

6.1 Discussion

This thesis aimed at studying the feasibility of recycling a hazardous waste product into a concrete matrix and in turn developing a new sustainable material for use in non-structural concrete applications. While Cathode-Ray Tube glass is considered a hazardous waste material due to its lead content, concrete has the capability of successfully encapsulating the lead within the composite material thereby reducing environmental impacts. While this dissertation showed that with the help of organic biopolymers, lead leaching can be encapsulated and be below the EPA regulatory limit for drinking water, it also took the research one step further and analyzed how the composite material would behave at its end of life or if certain durability factors began to deteriorate the material during its service life. Additionally, Chapter 2 laid out a framework of the physical and chemical impacts that concrete mixtures may experience when using substitute waste aggregates. Covering the three phases of the life-cycle of concrete, researchers who are interested in using waste materials (e.g. rubber tires, plastics, etc.) as aggregates in concrete mixtures, may now understand how handling, mitigation, durability, strength and environmental performance of the material can be affected throughout the life of the material, and how to address them.

Apart from the framework, this dissertation was split into three studies in order to holistically understand the structural and environmental behavior of the concrete during its entire life cycle. The first objective was to understand the CRT-Concrete material itself and how different factors (i.e. wet properties of concrete, structural strength,

durability, and environmental safety) were impacted with the addition of CRT glass to a conventional concrete mixture. Once this objective was well understood, a second study was performed to understand how the structural integrity of CRT-Concrete would change if it were subjected to two different aging/durability tests. Finally, the third objective of this dissertation was to analyze how deterioration of concrete can impact the release mechanism (leaching) of the material. Its results can then be used to study how a proposed environment for CRT-Concrete will affect the durability and strength of the material as well as its environmental performance. The following sections summarize the conclusions drawn from each objective.

6.2 Objective I

The first objective of this dissertation looked at the structural and environmental concerns with using CRT glass in concrete mixtures. It concluded that partially substituting fine aggregates in concrete mixtures with CRT glass was feasible both structurally and environmentally. While the workability of the CRT-Concrete was adversely affected as more crushed CRT was used, the strength performance of the CRT-concrete meets and exceeds that of the control specimens. A concern with using silica-based aggregates is the potential for deleterious expansions in the concrete to occur due to alkali-silica reactions. Results show that using more than 10% CRT glass in concrete may lead to deleterious expansions throughout its service life and therefore glass substitution should be limited to 10% or supplementary cementitious materials should be used if higher replacement ratios are considered. Lastly, it was confirmed that lead leaching from CRT-Concrete was pH dependent and its minima was observed to be in the 7-12 pH range (the expected service life conditions for the concrete). This behavior is favorable for concrete materials given

that as the material ages, the pH of the concrete will drop from 13 to 8 and the release of lead should therefore decrease as well. Moreover, when the material was placed under a scenario similar to a percolation column, such as crushed concrete used in stock piling or road fill, maximum concentrations of lead leaching occurred during the initial surface wash-out phase and decreased shortly thereafter. Finally, an SPLP analysis was conducted for regulatory purposes. For normal concrete mixtures with CRT glass, Pb leaching concentrations were greater than the drinking water limit. However, the addition of a cross-linked biopolymer solution to the concrete mixture helped encapsulate the Pb ions and up to 20% CRT glass substituting the fine aggregate in the concrete mixture was found to have SPLP Pb concentrations lower than the drinking water limit.

6.3 Objective II

The second objective of this dissertation was to understand how the durability and strength of CRT-Concrete was impacted during and after deterioration. Several material properties were investigated as the specimens were exposed to a long-term temperature controlled curing environment and through Freeze/Thaw cycling. Overall, the structural performance and durability of CRT-Concrete was comparable and at times better than the control concrete mixture. ASR expansions were found to be dependent on the particle size of the glass aggregate. Up to a 50% reduction in expansion was observed simply by using a finer aggregate. Deleterious ASR expansions occurred when 20% CRT glass was used as an aggregate. Therefore, it is recommended that up to 10% CRT glass can be safely used as a fine aggregate substitute if no supplementary cementitious materials such as fly ash, metakaolin, or ground granulated blast-furnace slag were used.

Deterioration was measured by the change in mass and dynamic modulus of elasticity. This study concluded that ultrasonic pulse velocity testing is not feasible for determining the modulus of elasticity of a material because it is sensitive to the moisture condition of the material. Instead, taking longitudinal resonant frequency measurements proved to be a more feasible and accurate method for determining the modulus of elasticity.

The compressive strength of CRT-Concrete was higher than the control specimen after 28-days at normal curing conditions and after 210 days under 19°C and 50°C curing temperatures. F/T cycling did not have a significant impact on the compressive strength of the material. Instead, an ANOVA analysis concluded that the mixture composition as well as the curing temperature had a significant impact on the compressive strength of the composite. Self-healing of the microcracks formed was believed to have occurred given that specimens that were treated to 300 F/T cycles were stronger than those that were exposed to only 178 F/T. However, more testing on this phenomenon is suggested.

The final objective of this study was to find if any relationship between compressive strength, loss of modulus of elasticity, and loss of mass existed. Although a linear relationship between the actual modulus of elasticity and the actual strength of the material was found, no correlation between the percent loss in the modulus of elasticity and the percent loss in compressive strength was found at a 95% confidence interval, this may change if a lower confidence interval is selected. In conclusion, the structural properties of CRT-Concrete were comparable to the control conventional concrete mixture. The durability of CRT-Concrete also proved to be equal or at times better than the control mixture but special considerations should be given to ASR expansions and how much CRT glass is used. Although no direct relationships were found between

deterioration and strength, a better understanding of the performance of CRT-Concrete throughout an accelerated service life was developed.

6.4 Objective III

The final objective of this dissertation was to understand how leaching was influenced with the deterioration of the concrete matrix. Three different durability/deterioration mechanisms were used to investigate the impact to leaching. Micro-cracking of the concrete matrix was achieved through ASR expansions, leaching dependency due to temperature was measured using Arrhenius Aging, and surface deterioration and mass loss was promoted using F/T cycling. It was found that the results acquired from the modified diffusion tank-leaching experiment were in good agreement with the theoretical Fick's Second Law of Diffusion, further enforcing that the modified experiments conducted did not alter the release behavior of the species.

Additionally, surface deterioration from F/T cycling increased the release of contaminants from CRT-Concrete into the environment by displaying an increase in flux release. The increase in release was random and was not dependent on the mass loss of the specimen, but possibly dependent on the distribution of the CRT aggregate. Furthermore, temperature had a direct impact on the leaching of contaminants. Hot temperatures (50°C) changed the microstructure of the material and in turn accelerated the release of contaminants (i.e. increase in lead leaching). Lastly, no relationship between ASR expansions and contaminant release was found. This was due to the rapid saturation of the solution used in the experiment with the contaminant of interest.

6.5 Overall Conclusion

This thesis explored how the many factors that impact the development, performance, and durability of conventional concrete affect the integrity of concrete containing CRT glass aggregates. From a holistic life cycle point of view, this dissertation developed a guideline for researchers who are interested in substituting similar potentially hazardous materials into concrete mixtures. Additionally, it used new performance-based leaching experiments that are currently being presented to the EPA (by Vanderbilt University) for potential enforcement, to assess how leaching of lead is controlled during different life cycle scenarios. Furthermore, this dissertation looked at how the structural performance of the material was affected with the addition of CRT glass and compared the durability of a conventional concrete mixture to that of a CRT-Concrete mixture. An accelerated aging technique was used along with freezing/thawing of the concrete specimens in order to age and deteriorate the materials. This process allowed the understanding of strength development and leaching dependency due to deterioration and mass loss of the material. From a structural performance view, CRT-Concrete has proven to meet and exceed the performance of conventional concrete. Additionally, up to 10% CRT was found to be feasible in order to control ASR expansions. From an environmental stand point, the Pb results of the SPLP test for crushed CRT-Concrete that used the organic biopolymer solution were lower than the drinking water limit for Pb. A maximum of 20% CRT glass replacing the fine aggregate in the specified concrete mixture was found to meet the SPLP requirements. For ordinary CRT-Concrete mixtures without the biopolymer solution, Pb leaching was above drinking water limits.

All in all, the amount of CRT glass substitution is controlled by ASR expansions and lead leaching. For this dissertation, up to 10% CRT glass (with the use of organic biopolymers) should be used in order to avoid ASR cracks. This CRT-Concrete mixture should primarily be used in non-structural concrete applications, where moisture exposure is limited; until more testing is conducted (i.e. chloride ion penetration, reinforced CRT-Concrete, sulfate resistance, leaching reaction to different types of aggregates and concrete mixtures, etc.). Finally, Table 6-1 shows that there is enough CRT glass available to meet up to 91% of the total yearly U.S. demand for concrete until at least the year 2020, if the suggested concrete mixture substituting 10% of the fine aggregate is used.

Table 6-1 – CRT demand in Ready-Mixed concrete production

U.S. Yearly disposal of CRT units, by volume [11]	100 x 10^6 CRT units/yr
U.S. Yearly disposal of CRT units, by mass (assume 30 pounds of glass/unit)	1.4 x 10^6 tons/yr
U.S. Yearly Concrete production volume (2006) [114]	454.6 x 10^6 yd^3/yr
U.S. Yearly Concrete production mass (2006)	30.9 x 10^6 tons/yr
Yearly demand for CRT glass if 10% substitution is used (approximately 5% of the overall mass)	1.545 x 10^6 tons/yr
CRT supply expectancy, year [115]	2020

6.6 Further Investigations

This dissertation presents a large step towards the use of hazardous waste materials as aggregates in concrete. Although most of the factors that impact concrete strength, durability, and leaching were studied in this dissertation, there are still more items that can be studied.

The following are suggested items for further investigation:

- Examine the effects of the CRT glass particle size on leaching. Are larger particles more prone to contaminant release? What effects does powdered CRT glass have on the release of lead as opposed to crushed CRT glass?
- Investigate the effects of other durability parameters that affect concrete and their impact to contaminant release (i.e. corrosion of reinforcement bars, carbonation, and sulfate attacks).
- Investigate if CRT-Concrete self-healing occurs and if it behaves better than conventional concrete.
- Use larger replacement percentages of CRT glass to reduce scarcity of glass in the concrete matrix and have a better understanding of the impacts of deterioration/mass loss on leaching.
- Further explore the use of cross-linked biopolymers in CRT-Concrete mixtures and evaluate the maximum substitution percentage for CRT glass that can still be encapsulated in the composite material and meet the Pb drinking water limits.
- Evaluate if the use of boric acid in the biopolymer admixture solution is toxic for drinking water standards.
- Develop a numerical or theoretical model to more accurately describe the release behavior of lead when exposed to a change in pH and an elevated temperature. Consider recording parameters such as: surface pH, internal temperature and porosity of the specimen, CO_2 penetration depth and concentrations in the solution.

- Explore the hazards of producing and commercializing such material. What are the health impacts to producing granulated CRT glass? How is CRT glass dust/powder controlled, used, or disposed?
- Study the implementation and financial feasibility of using such material and if there is a demand in the market.

References

Reference List

[1] United Nations, The World At Six Billion, United Nations Population Division. (1999).

[2] P.K. Mehta, Greening of the Concrete Industry for Sustainable Development, Concr. Int. (2002).

[3] USGS, Cement Statistics and Information, (2011).

[4] USEPA, Municipal Solid Waste, (2011).

[5] World Business Council for Sustainable Development, Recycling Concrete, The Cement Sustainability Initiative. (2009).

[6] A. Abbas, G. Fathifazl, O.B. Isgor, A.G. Razaqpur, B. Fournier, S. Foo, Environmental Benefits of Green Concrete, EIC Climate Change Technology, 2006 IEEE. (2006) 1-8.

[7] USEPA, Hazardous Waste Recycling, (2010).

[8] A. Bilodeau, Durability of Concrete Incorporating High Volumes of Fly-Ash From Sources in the US, ACI Mater. J. 91 (1994) 3-12.

[9] EERA,
Position paper on CRT treatment, European Electronics Recyclers Association. (2008).

[10] FDEP, Focus on Televisions and Computer Monitors: Lead (Pb), National Safety Council's EPR2 Electronics Baseline Report. (2008).

[11] S. Herat, Recycling of Cathode Ray Tubes (CRTs) in Electronic Waste, Clean Soil, Air, Water. 36 (2008) 19-24.

[12] ASTSWMO, Association of State and Territorial Solid Waste Management Officials Beneficial Use Survey, ASTSWMO. April 2000 (2000) 4.

[13] USEPA, EPA Method 1311 - Toxicity Characteristic Leaching Procedure, (1992).

[14] USEPA, EPA Method 1312 - Synthetic Precipitation Leaching Procedure, (1994).

[15] H. Florida, Hinkley Center for Solid and Hazardous Waste Management, 2011 (2011).

[16] D.M. Montgomery, C.J. Sollars, R. Perry, Cement-based solidification for the safe disposal of heavy metal contaminated sewage sludge, Waste Manage. Res. 6 (1988) 217-226.

[17] M.F.M. Zain, M.N. Islam, S.S. Radin, S.G. Yap, Cement-based solidification for the safe disposal of blasted copper slag, Cement and Concrete Composites. 26 (2004) 845-851.

[18] I. Olmo, E. Chacón, A. Irabien, Leaching Behavior of Lead, Chromium (III), and Zinc in Cement/Metal Oxides Systems, J. Environ. Eng. 129 (2003) 532-538.

[19] D. Kim, Evaluation of biopolymer-modified concrete systems for disposal of cathode ray tube glass, J. Air Waste Manage. Assoc. 55 (2005) 961-969.

[20] D. Kim, M. Quinlan, T.F. Yen, Encapsulation of lead from hazardous CRT glass wastes using biopolymer cross-linked concrete systems, Waste Manage. 29 (2009) 321-328.

[21] C. Morrison, Reuse of CRT glass as aggregate in concrete, Proceedings of the International Conference on Sustainable Waste Management and Recycling: Glass Waste. (2004) 91-98.

[22] Z. Hui, W. Sun, Study of properties of mortar containing cathode ray tubes (CRT) glass as replacement for river sand fine aggregate, Constr. Build. Mater. 25 (2011) 4059-4064.

[23] Hazardous Substance & Waste Management Research, Inc., The Use of Cathode Ray Tube (CRT) Glass in theManufacturing of Pre-stress and Pre-cast Concrete Products, Final Report for the Florida Department of Environmental Protection. (2008).

[24] F. Andreola, L. Barbieri, A. Corradi, I. Lancellotti, CRT glass state of the art: A case study: Recycling in ceramic glazes, Journal of the European Ceramic Society. 27 (2007) 1623-1629.

[25] R. Mora, G. Bitsuamlak, M. Horvat, Integrated life-cycle design of building enclosures, Build. Environ. 46 (2011) 1469-1479.

[26] US Army Corps of Engineers, Reuse of Concrete Materials from Building Demolition, Public Works Technical Bulletin 200-1-27, (2004).

[27] ASTM International, Significance of Tests and Properties of Concrete and Concrete-Making Materials, in: J. Lamond, J. Pielert (Eds.), ASTM International, 2006, pp. 30-35.

[28] I.B. Topçu, M. Canbaz, Properties of concrete containing waste glass, Cem. Concr. Res. 34 (2004) 267-274.

[29] L. Lim, R. Walker,
An Assessment of Chemical Leaching, Releases to Air and Temperature at Crumb-Rubber Infilled Synthetic Turf Fields, (2009).

[30] EPA Draft Method 1314, Liquid-solid partitioning as a function of liquid-solid ratio for constituents in solid materials using an up-flow percolation column procedure, EPA SW-846 Update V. Rev. 0 (2012).

[31] H. Donza, O. Cabrera, E.F. Irassar, High-strength concrete with different fine aggregate, Cem. Concr. Res. 32 (2002) 1755-1761.

[32] S.S. Jamkar, C.B.K. Rao, Index of Aggregate Particle Shape and Texture of coarse aggregate as a parameter for concrete mix proportioning, Cem. Concr. Res. 34 (2004) 2021-2027.

[33] S.B. Park, B.C. Lee, J.H. Kim, Studies on mechanical properties of concrete containing waste glass aggregate, Cem. Concr. Res. 34 (2004) 2181-2189.

[34] C.H. Chen, R. Huang, J.K. Wu, C.C. Yang, Waste E-glass particles used in cementitious mixtures, Cem. Concr. Res. 36 (2006) 449-456.

[35] Y. Choi, D. Moon, J. Chung, S. Cho, Effects of waste PET bottles aggregate on the properties of concrete, Cem. Concr. Res. 35 (2005) 776-781.

[36] T. Lindgren, A case of indoor air pollution of ammonia emitted from concrete in a newly built office in Beijing, Build. Environ. 45 (2010) 596-600.

[37] H.A. Van der Sloot, J.J. Dijkstra, Development of Horizontally Standardized Leaching Tests for Construction Materials: A Material Based or Release Based Approach? Identical leaching mechanisms for different materials, ECN-C--04-060. (2004).

[38] EPA Method 1313, Liquid-solid partitioning as a function of extract pH in solid materials using a parallel batch procedure, EPA SW-846 Update V. (2012).

[39] CEN/TC 292, CEN/TS 14429: Characterization of waste. Leaching behaviour tests. Influence of pH on leaching with initial acid/base addition, (2006).

[40] CEN/TC 292, CEN/TS 14405: Characterization of waste. Leaching behaviour tests. Up-flow percolation test (under specified conditions), (2004).

[41] EPA Draft Method 1315, Mass transfer rates of constituents in monolithic or compacted granular materials using a semi-dynamic tank leaching procedure, EPA SW-846 Update V. Rev. 0 (2012).

[42] CEN/TC 292, EA NEN 7375: Leaching characteristics of moulded or monolithic building and waste materials. Determination of leaching of inorganic components with the diffusion test, (2005).

[43] D.S. Kosson, A.C. Garrabrants, Leaching Environmental Assessment Framework, 2011 (2010).

[44] D. Apul, K. Gardner, T. Eighmy, J. Benoit, L. Brannaka, A Review of water movement in the highway environment: Implications for recycled materials use, Recycled Materials Resource Center - Environmental Technology Building. (2002).

[45] C. Lobo, New perspective on concrete durability, Concrete InFocus. Spring 2007 (2007) 24-30.

[46] TRB - Basic Research and Emerging Technologies Related to Concrete Committee, Control of Cracking in Concrete - State of the Art, October 2006. (2006).

[47] A.C. Garrabrants, F. Sanchez, D.S. Kosson, Changes in constituent equilibrium leaching and pore water characteristics of a Portland cement mortar as a result of carbonation, Waste Manage. 24 (2004) 19-36.

[48] C. Gervais, A.C. Garrabrants, F. Sanchez, R. Barna, P. Moszkowicz, D.S. Kosson, The effects of carbonation and drying during intermittent leaching on the release of inorganic constituents from a cement-based matrix, Cem. Concr. Res. 34 (2004) 119-131.

[49] F. Sanchez, A.C. Garrabrants, D.S. Kosson, Effects of Intermittent Wetting on Concentration Profiles and Release from a Cement-Based Waste Matrix, Environ. Eng. Sci. 20 (2003) 135-153.

[50] F. Sanchez, M.K. Langley White, A. Hoang, Leaching from granular cement-based materials during infiltration/wetting coupled with freezing and thawing, J. Environ. Manage. 90 (2009) 983-993.

[51] A. Bentur, S. Diamond, N. Berke, Steel Corrosion in Concrete: Fundamentals and Civil Engineering Practice, E&FN Spon, London, 1997.

[52] R.E. Melchers, C.Q. Li, W. Lawanwisut, Probabilistic modeling of structural deterioration of reinforced concrete beams under saline environment corrosion, Struct. Saf. 30 (2008) 447-460.

[53] ACI 222 committee, ACI 222R-96 Corrosion of metals in concrete, (1996).

[54] L. Basheer, J. Kropp, D.J. Cleland, Assessment of the durability of concrete from its permeation properties: a review, Constr. Build. Mater. 15 (2001) 93-103.

[55] R. Polder, P. Pedeferri, L. Bertolini, B. Elsener, Corrosion of Steel in Concrete : Prevention, Diagnosis, Repair, Wiley-VCH, Weinheim ; [Cambridge] :, 2004.

[56] W. Touma, Alkali-Silica Reaction in Portland Cement Concrete: Testing Methods and Mitigation Alternatives, Alkali-silica reaction in portland cement concrete: Testing methods and mitigation alternatives. (2000).

[57] T. Siemes, P. R., Design of concrete structures for durability, Delft University of Technology. 43 (1998) 227-244.

[58] M. Djuric, Sulfate corrosion of portland cement-pure and blended with 30% of fly ash, Cem. Concr. Res. 26 (1996) 1295-1300.

[59] USEPA, Acid Rain, 2011 (2011).

[60] A.C. Garrabrants, F. Sanchez, D.S. Kosson, Leaching model for a cement mortar exposed to intermittent wetting and drying, AICHE J. 49 (2003) 1317-1333.

[61] F. Sanchez, I.W. Massry, T. Eighmy, D.S. Kosson, Multi-regime transport model for leaching behavior of heterogeneous porous materials, Waste Manage. 23 (2003) 219-224.

[62] A.C. Garrabrants, D.S. Kosson, Conceptual models and approaches to estimating long-term contaminant release from near surface disposal of cementitious and other waste forms, Powerpoint Presentation. (2006).

[63] ASTM C1260-07, Standard Test Method for Potential Alkali Reactivity of Aggregates (Mortar-Bar Method), ASTM International. (2007).

[64] ACI 211 Committee, **Standard Practice for Selecting Proportions for Normal, Heavyweight, and Mass Concrete (Reapproved 2009)**, ACI. (1991).

[65] ASTM C143-10, Standard Test Method for Slump of Hydraulic-Cement Concrete, ASTM International. (2010).

[66] ASTM C138-10, Standard Test Method for Density (Unit Weight), Yield, and Air Content (Gravimetric) of Concrete, ASTM International. (2010).

[67] ASTM C39-10, Standard Test Method for Compressive Strength of Cylindrical Concrete Specimens, ASTM International. (2010).

[68] D. Romero, J. James, R. Mora, C.D. Hays, Study on the mechanical and environmental properties of concrete containing cathode ray tube glass aggregate, Waste Management. (2013).

[69] N. Menad, Cathode ray tube recycling, Resour. Conserv. Recycling. 26 (1999) 143-154.

[70] F. Méar, P. Yot, M. Cambon, M. Ribes, The characterization of waste cathode-ray tube glass, Waste Manage. 26 (2006) 1468-1476.

[71] W. Jin, C. Meyer, S. Baxter, "Glascrete" - Concrete with glass aggregate, ACI Mater. J. 97 (2000) 208-213.

[72] Z.Z. Ismail, E.A. AL-Hashmi, Recycling of waste glass as a partial replacement for fine aggregate in concrete, Waste Manage. 29 (2009) 655-659.

[73] A. Shayan, A. Xu, Value-added utilisation of waste glass in concrete, Cem. Concr. Res. 34 (2004) 81-89.

[74] T. Ramlochan, M. Thomas, K.A. Gruber, The effect of metakaolin on alkali-silica reaction in concrete, Cem. Concr. Res. 30 (2000) 339-344.

[75] M.H. Shehata, M.D.A. Thomas, The effect of fly ash composition on the expansion of concrete due to alkali–silica reaction, Cem. Concr. Res. 30 (2000) 1063-1072.

[76] M.H. Shehata, M.D.A. Thomas, Use of ternary blends containing silica fume and fly ash to suppress expansion due to alkali–silica reaction in concrete, Cem. Concr. Res. 32 (2002) 341-349.

[77] P.M. Gifford, J.E. Gillott, Alkali-silica reaction (ASR) and alkali-carbonate reaction (ACR) in activated blast furnace slag cement (ABFSC) concrete, Cem. Concr. Res. 26 (1996) 21-26.

[78] A. Shayan, A. Xu, Performance of glass powder as a pozzolanic material in concrete: A field trial on concrete slabs, Cem. Concr. Res. 36 (2006) 457-468.

[79] ASTM C128, Standard Test Method for Density, Specific Gravity, and Absorption of Fine Aggregate, ASTM International. (2007).

[80] ASTM C136-06, Standard Test Method for Sieve Analysis of Fine and Coarse Aggregates, ASTM International. (2006).

[81] ASTM C617-11, Standard Practice for Capping Cylindrical Concrete Specimens, ASTM International. (2011).

[82] H.A. Van der Sloot, Leaching Test Methods, 2011 (2007).

[83] ASTM C666-08, Standard Test Method for Resistance of Concrete to Rapid Freezing and Thawing, ASTM International. (2008).

[84] T. Eighmy, R. Cook, A. Coviello, J. Spear, K. Hover, A Predictive Approach for Long-Term Performance of Recycled Materials Using Accelerated Aging, FHWA-RD-01-022. 1 (2001).

[85] ASTM C496-11, Standard Test Method for Splitting Tensile Strength of Cylindrical Concrete Specimens, ASTM International. (2011).

[86] ASTM C597-09, Standard Test Method for Pulse Velocity Through Concrete, ASTM International. (2009).

[87] BIS 1331 (Part 1), Non-Destructive Testing of Concrete - Methods of Test: Part 1 - Ultrasonic Pulse Velocity, BIS. (1992 (2004)).

[88] ASTM C215-08, Standard Test Method for Fundamental Transverse, Longitudinal, and Torsional Resonant Frequencies of Concrete Specimens, ASTM International. (2008).

[89] R. Idir, M. Cyr, A. Tagnit-Hamou, Use of fine glass as ASR inhibitor in glass aggregate mortars, Constr. Build. Mater. 24 (2010) 1309-1312.

[90] Y. Shao, T. Lefort, S. Moras, D. Rodriguez, Studies on concrete containing ground waste glass, Cem. Concr. Res. 30 (2000) 91-100.

[91] K.O. Kjellsen, R.J. Detwiler, O.E. Gjørv, Development of microstructures in plain cement pastes hydrated at different temperatures, Cem. Concr. Res. 21 (1991) 179-189.

[92] K.O. Kjellsen, Heat curing and post-heat curing regimes of high-performance concrete: Influence on microstructure and C-S-H composition, Cem. Concr. Res. 26 (1996) 295-307.

[93] R. Pinto, S. Hobbs, K. Hover, Accelerated Aging of Concrete: A Literature Review, FHWA. (2002).

[94] J.H. Bungey, The validity of ultrasonic pulse velocity testing of in-place concrete for strength, NDT International. 13 (1980) 296-300.

[95] M. Shariq, J. Prasad, A. Masood, Studies in ultrasonic pulse velocity of concrete containing GGBFS, Constr. Build. Mater. 40 (2013) 944-950.

[96] Y.A. Abdel-Jawad, M. Afaneh, Factors affecting the relationship between ultrasonic pulse velocity and concrete compressive strength, Indian Concrete J. 71 (1997) 373-376.

[97] Cast Stone Institute, Freeze-Thaw durability: Technical Bulletin #40, CSI. 2013 (2012) 1.

[98] S. Qian, J. Zhou, M.R. de Rooij, E. Schlangen, G. Ye, K. van Breugel, Self-healing behavior of strain hardening cementitious composites incorporating local waste materials, Cement and Concrete Composites. 31 (2009) 613-621.

[99] C. Edvardsen, Water permeability and autogenous healing of cracks in concrete, ACI Mater. J. 96 (1999) 448-454.

[100] Y. Yang, M.D. Lepech, E. Yang, V.C. Li, Autogenous healing of engineered cementitious composites under wet–dry cycles, Cem. Concr. Res. 39 (2009) 382-390.

[101] M. Wu, B. Johannesson, M. Geiker, A review: Self-healing in cementitious materials and engineered cementitious composite as a self-healing material, Constr. Build. Mater. 28 (2012) 571-583.

[102] S. Jacobsen, E.J. Sellevold, Self healing of high strength concrete after deterioration by freeze/thaw, Cem. Concr. Res. 26 (1996) 55-62.

[103] R.J. Gray, Autogenous healing of fibre/matrix interfacial bond in fibre-reinforced mortar, Cem. Concr. Res. 14 (1984) 315-317.

[104] Y. Abdel-Jawad, R. Haddad, Effect of early overloading of concrete on strength at later ages, Cem. Concr. Res. 22 (1992) 927-936.

[105] A. Saetta, Deterioration of Reinforced Concrete Structures due to Chemical–Physical Phenomena: Model-Based Simulation, J. Mat. in Civ. Engrg. 17 (2005).

[106] F. Bangert, S. Grasberger, D. Kuhl, G. Meschke, Environmentally induced deterioration of concrete: physical motivation and numerical modeling, Eng. Fract. Mech. 70 (2003) 891-910.

[107] C.L. Bellégo, G. Pijaudier-Cabot, B. Gérard, J. Dubé, L. Molez, Coupled Mechanical and Chemical Damage in Calcium Leached Cementitious Structures, J. Engrg. Mech. 129 (2003).

[108] C. Carde, R. François, Aging damage model of concrete behavior during the leaching process, Materials and Structures. 30 (1997) 465-472.

[109] M.K.L. White, Leaching from Granular Waste Materials Used in Highway Infrastructures During Infiltration Coupled with Freezing and Thawing, Thesis. (2005).

[110] J. Crank, The Mathematics of Diffusion, (1975).

[111] USEPA, EPA Method 3050B - Acid Digestion of Sediments, Sludges, and Soils, (1996).

[112] R.D. Spence, C. Shi, Stabilization and Solidification of Hazardous, Radioactive, and Mixed Wastes, 1st ed., CRC Press, 2004.

[113] M. Andac, F.P. Glasser, Long-term leaching mechanisms of Portland cement-stabilized municipal solid waste fly ash in carbonated water, Cem. Concr. Res. 29 (1999) 179-186.

[114] National Ready Mix Concrete Association, U.S. Ready Mixed Concrete Production, NRMCA. 2013.

[115] J.R. Mueller, M.W. Boehm, C. Drummond, Direction of CRT waste glass processing: Electronics recycling industry communication, Waste Manage. 32 (2012) 1560-1565.

Appendix A

Appendix A Study I

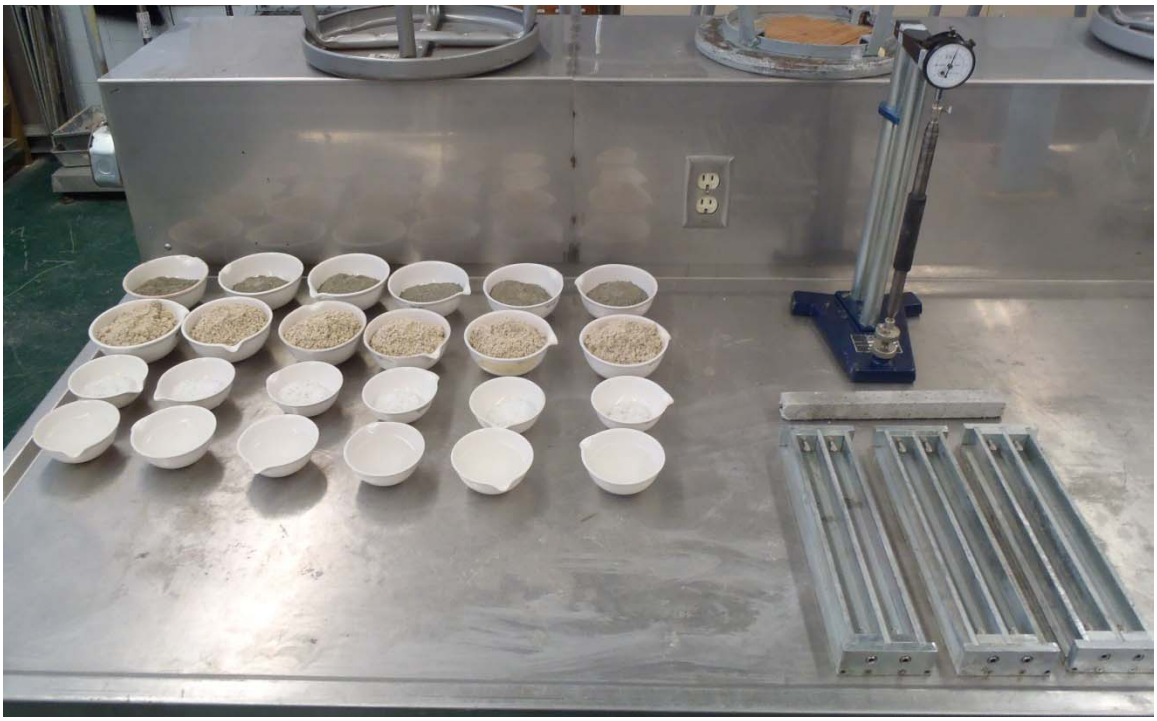

Figure A-1 - Setup for mixing ASR specimens

Figure A-2 - Fresh ASR Specimen in Mold

Figure A-3 - ASR specimen being measured

Figure A-4 - Sulfur capping specimens for Compressive Strength Test

Figure A-5 - Compressive Strength Test

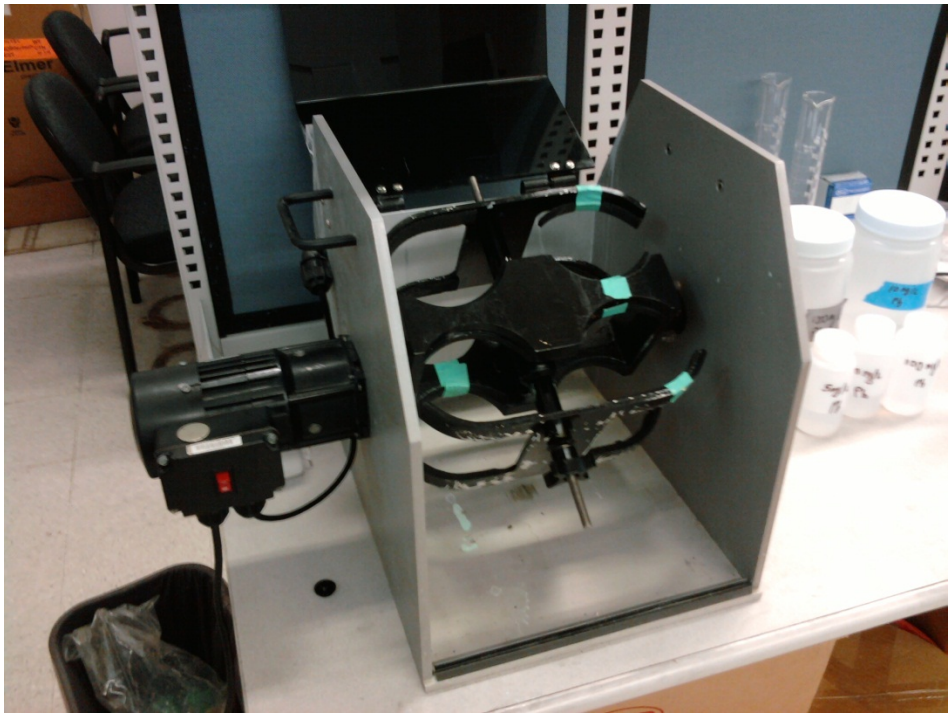

Figure A-6 - SPLP Testing Equipment

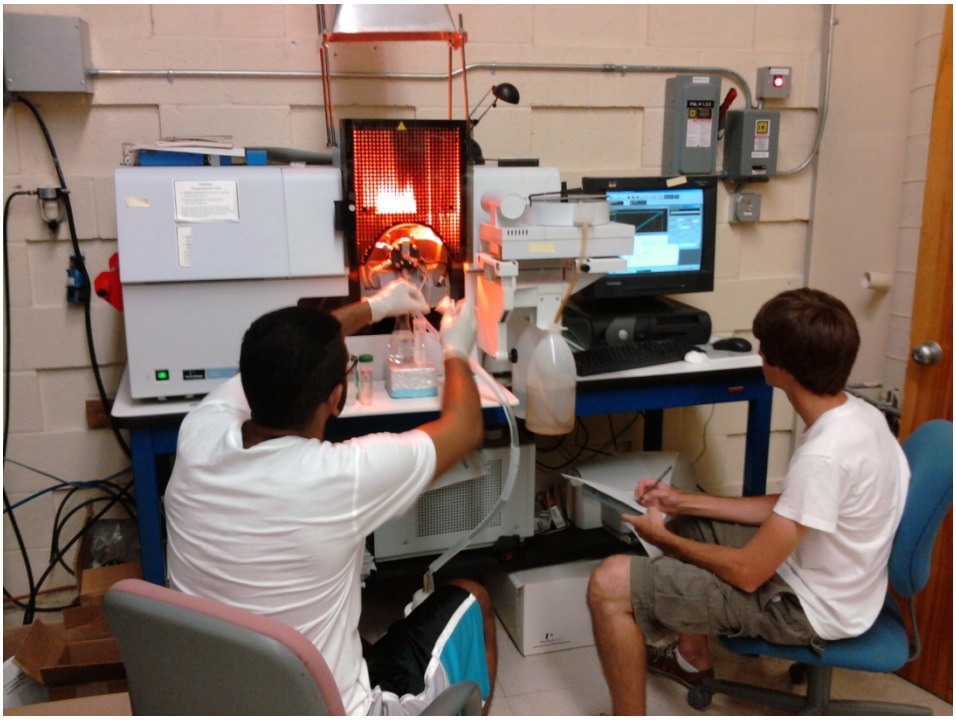

Figure A-7 - Atomic Absorption Spectrometer for constituent detection

Figure A-8 - EPA Draft Method 1314 Percolation column setup

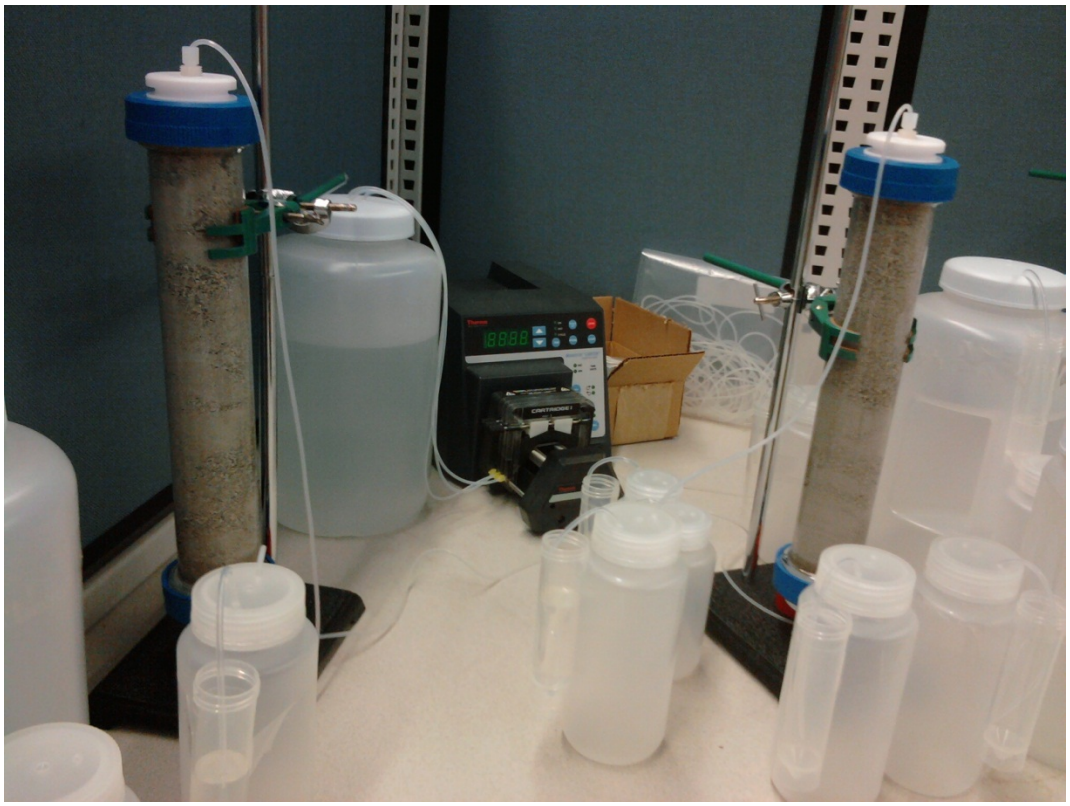

Figure A-9 - EPA Draft Method 1314 Percolation Column setup closeup

Table A-1 - CRT-Concrete compression test results

Mix ID	Control (MPa)	10% CRT (MPa)	20% CRT (MPa)	30% CRT (MPa)
Mix I	27.1	28.6	32.4	30.7
Mix II	29.8	30.5	32.4	31.3
Mix III	23.1	24.5	24.8	24.5

PreMethod 1313 LeachXS™ Lite Data Template

METHOD 1313 MASTER DATA LIST

QC Flags	
J	Value greater than calibration
E	Value between MDL and ML
U	Value less than MDL
U1/2	Value less than MDL (shown at 1/2 MDL)

	Code	Description *(optional)*
Project ID	CRT	Auto-inserted from "Title Sheet"
Material ID	Mix 1 10%	Auto-inserted from "Title Sheet"
Test ID	1313	

	Acid Type	Base Type
Test Rep A	HNO3	KOH
Test Rep B	HNO3	NaOH
Test Rep C	HNO3	NaOH

	Pb
MDL	0.15
ML	0.2
Analytical Method	*AAS-Flame*
Analysis Date	18-Jun-10
Analytical Lab Name	Diego
Eluate Composition	14

Sample ID	"As Tested" Solid g	Moisture Content g-H_2O/g	Water Added mL	Acid Added mL	Acid Stength N	Base Added mL	Base Stength N	Acid Added meq/g-dry	Eluate pH s.u.	Eluate Cond. mS/cm	Eluate ORP mV	Lead Pb mg/L
Mix 1 10%-1313-T01-A	21.19	0.06	198.81	-	-	-	-	0.00	12.58			0.51
Mix 1 10%-1313-T02-A	21.19	0.06	182.81	16.0000	2.00	-	-	1.60	12.10			0.31
Mix 1 10%-1313-T03-A	21.19	0.06	143.81	55.0000	2.00	-	-	5.50	10.74			1.13
Mix 1 10%-1313-T04-A	21.19	0.06	119.81	79.0000	2.00	-	-	7.90	6.56			1.13
Mix 1 10%-1313-T05-A	21.19	0.06	110.81	88.0000	2.00	-	-	8.80	7.72			1.75
Mix 1 10%-1313-T06-A	21.19	0.06	100.81	98.0000	2.00	-	-	9.80	6.25			1.96
Mix 1 10%-1313-T07-A	21.19	0.06	66.81	132.0000	2.00	-	-	13.20	5.29			3.40
Mix 1 10%-1313-T08-A	21.19	0.06	49.81	149.0000	2.00	-	-	14.90	4.80			21.07
Mix 1 10%-1313-T09-A	21.19	0.06	33.81	165.0000	2.00	-	-	16.50	0.49			57.12
Mix 1 10%-1313-T01-B	21.72	0.08	198.28	-	-			0.00	12.63			1.01
Mix 1 10%-1313-T02-B	21.72	0.08	182.28	16.0000	2.00	-	-	1.60	12.03			0.49
Mix 1 10%-1313-T03-B	21.72	0.08	143.28	55.0000	2.00	-	-	5.50	9.65			1.10
Mix 1 10%-1313-T04-B	21.72	0.08	119.28	79.0000	2.00	-	-	7.90	8.99			1.29
Mix 1 10%-1313-T05-B	21.72	0.08	110.28	88.0000	2.00	-	-	8.80	7.83			1.33
Mix 1 10%-1313-T06-B	21.72	0.08	100.28	98.0000	2.00	-	-	9.80	6.94			1.45
Mix 1 10%-1313-T07-B	21.72	0.08	66.28	132.0000	2.00	-	-	13.20	5.56			2.70
Mix 1 10%-1313-T08-B	21.72	0.08	49.28	149.0000	2.00	-	-	14.90	4.40			24.97
Mix 1 10%-1313-T09-B	21.72	0.08	33.28	165.0000	2.00	-	-	16.50	1.05			51.11
Mix 1 10%-1313-T01-C	21.74	0.08	198.26	-	-	-	-	0.00	12.58			1.25
Mix 1 10%-1313-T02-C	21.74	0.08	182.26	16.00	2.00	-	-	1.60	11.84			0.70
Mix 1 10%-1313-T03-C	21.74	0.08	142.26	56.00	2.00	-	-	4.40	10.73			1.08
Mix 1 10%-1313-T04-C	21.74	0.08	131.26	67.00	2.00	-	-	7.90	6.75			1.31
Mix 1 10%-1313-T05-C	21.74	0.08	123.26	75.00	2.00	-	-	8.80	6.55			1.44
Mix 1 10%-1313-T06-C	21.74	0.08	115.26	83.00	2.00	-	-	9.80	6.34			1.49
Mix 1 10%-1313-T07-C	21.74	0.08	66.26	132.00	2.00	-	-	13.20	5.10			2.53
Mix 1 10%-1313-T08-C	21.74	0.08	48.26	150.00	2.00	-	-	14.90	3.77			45.07
Mix 1 10%-1313-T09-C	21.74	0.08	37.26	161.00	2.00	-	-	16.50	1.15			62.09
Mix 1 10%-1313-B01-A			200.00	-	2.00	-	-	-	4.57			
Mix 1 10%-1313-B02-A			35.00	165.00	-	-	-	-	0.00			
Mix 1 10%-1313-B03-A					2.00	-	-	-	0.00			

Figure A-10 - EPA Method 1313 Results for Mix 1 10% CRT

PreMethod 1313 LeachXS™ Lite Data Template

METHOD 1313 MASTER DATA LIST

QC Flags	
J	Value greater than calibration
E	Value between MDL and ML
U	Value less than MDL
U1/2	Value less than MDL (shown at 1/2 MDL)

	Code	Description *(optional)*
Project ID	CRT	Auto-inserted from "Title Sheet"
Material ID	Mix 1 20%	Auto-inserted from "Title Sheet"
Test ID	1313	

	Acid Type	Base Type
Test Rep A	HNO3	NaOH
Test Rep B	HNO3	NaOH
Test Rep C	HNO3	NaOH

	Pb
MDL	0.15
ML	0.2
Analytical Method	*AAS-Flame*
Analysis Date	18-Jun-10
Analytical Lab Name	Diego
Eluate Composition	14

Sample ID	"As Tested" Solid g	Moisture Content g-H_2O/g	Water Added mL	Acid Added mL	Acid Stength N	Base Added mL	Base Stength N	Acid Added meq/g-dry	Eluate pH s.u.	Eluate Cond. mS/cm	Eluate ORP mV	Lead Pb mg/L
Mix 1 20%-1313-T01-A	21.74	0.0800	198.2609	-	-	-	-	0.00	12.71	0.00	0.00	1.86
Mix 1 20%-1313-T02-A	21.74	0.0800	182.2609	16.0000	2.00	-	-	1.60	12.27	0.00	0.00	1.43
Mix 1 20%-1313-T03-A	21.74	0.0800	143.2609	55.0000	2.00	-	-	5.50	10.88	0.00	0.00	1.21
Mix 1 20%-1313-T04-A	21.74	0.0800	119.2609	79.0000	2.00	-	-	7.90	7.36	0.00	0.00	1.12
Mix 1 20%-1313-T05-A	21.74	0.0800	110.2609	88.0000	2.00	-	-	8.80	8.37	0.00	0.00	1.05
Mix 1 20%-1313-T06-A	21.74	0.0800	100.2609	98.0000	2.00	-	-	9.80	6.22	0.00	0.00	1.28
Mix 1 20%-1313-T07-A	21.74	0.0800	66.2609	132.0000	2.00	-	-	13.20	5.32	0.00	0.00	4.65
Mix 1 20%-1313-T08-A	21.74	0.0800	49.2609	149.0000	2.00	-	-	14.90	3.82	0.00	0.00	84.93
Mix 1 20%-1313-T09-A	21.74	0.0800	33.2609	165.0000	2.00	-	-	16.50	1.18	0.00	0.00	116.71
Mix 1 20%-1313-T01-B	20.86	0.0410	199.1449	-	-	-	-	0.00	12.66	0.00	0.00	2.64
Mix 1 20%-1313-T02-B	20.86	0.0410	183.1449	16.0000	2.00	-	-	1.60	12.10	0.00	0.00	1.20
Mix 1 20%-1313-T03-B	20.86	0.0410	144.1449	55.0000	2.00	-	-	5.50	10.54	0.00	0.00	1.61
Mix 1 20%-1313-T04-B	20.86	0.0410	120.1449	79.0000	2.00	-	-	7.90	7.68	0.00	0.00	2.23
Mix 1 20%-1313-T05-B	20.86	0.0410	111.1449	88.0000	2.00	-	-	8.80	6.60	0.00	0.00	16.13
Mix 1 20%-1313-T06-B	20.86	0.0410	105.1449	94.0000	2.00	-	-	9.40	6.52	0.00	0.00	2.43
Mix 1 20%-1313-T07-B	20.86	0.0410	67.1449	132.0000	2.00	-	-	13.20	5.47	0.00	0.00	12.36
Mix 1 20%-1313-T08-B	20.86	0.0410	50.1449	149.0000	2.00	-	-	14.90	3.15	0.00	0.00	126.25
Mix 1 20%-1313-T09-B	20.86	0.0410	41.1449	158.0000	2.00	-	-	15.80	1.20	0.00	0.00	129.17
Mix 1 20%-1313-T01-C	21.48	0.069	198.52	-	-	-	-	0.00	12.64	8.71	-322.70	2.40
Mix 1 20%-1313-T02-C	21.48	0.069	182.52	16.00	2.00	-	-	1.60	12.26	16.88	-303.00	1.46
Mix 1 20%-1313-T03-C	21.48	0.069	143.52	55.00	2.00	-	-	5.50	10.39	33.68	-196.00	0.98
Mix 1 20%-1313-T04-C	21.48	0.069	123.52	75.00	2.00	-	-	7.50	6.50	43.37	30.50	1.54
Mix 1 20%-1313-T05-C	21.48	0.069	110.52	88.00	2.00	-	-	8.80	6.27	59.04	40.40	1.96
Mix 1 20%-1313-T06-C	21.48	0.069	106.52	92.00	2.00	-	-	9.20	6.10	62.14	50.40	2.16
Mix 1 20%-1313-T07-C	21.48	0.069	66.52	132.00	2.00	-	-	13.20	5.39	64.25	92.00	6.29
Mix 1 20%-1313-T08-C	21.48	0.069	51.52	147.00	2.00	-	-	14.70	4.32	68.22	154.60	82.77
Mix 1 20%-1313-T09-C	21.48	0.069	46.52	152.00	2.00	-	-	15.20	3.46	70.32	204.80	108.55
Mix 1 20%-1313-B01-A	-	-	200.00	-	-	-	-	-	0.00	0.00	0.00	
Mix 1 20%-1313-B02-A	-	-	35.00	165.00	2.00	-	-	-	0.00	0.00	0.00	
Mix 1 20%-1313-B03-A	-	-	-	-	-	-	-	-	0.00	0.00	0.00	

Figure A-11 - EPA Method 1313 Results for Mix 1 20% CRT

PreMethod 1313 LeachXS™ Lite Data Template

METHOD 1313 MASTER DATA LIST

QC Flags	
J	Value greater than calibration
E	Value between MDL and ML
U	Value less than MDL
U1/2	Value less than MDL (shown at 1/2 MDL)

	Code	Description *(optional)*
Project ID	ABC	Auto-inserted from "Title Sheet"
Material ID	Mix 1 30%	Auto-inserted from "Title Sheet"
Test ID	1313	

	Acid Type	Base Type
Test Rep A	HNO3	KOH
Test Rep B	HNO3	NaOH
Test Rep C	HNO3	NaOH

	Pb
MDL	0.15
ML	0.2
Analytical Method	*AAS-Flame*
Analysis Date	18-Jun-10
Analytical Lab Name	Diego
Eluate Composition	14

Sample ID	"As Tested" Solid g	Moisture Content g-H_2O/g	Water Added mL	Acid Added mL	Acid Stength N	Base Added mL	Base Stength N	Acid Added meq/g-dry	Eluate pH s.u.	Eluate Cond. mS/cm	Eluate ORP mV	Lead Pb mg/L
Mix 1 30%-1313-T01-A	21.74	0.0800	198.2609	-	-	-	-	0.00	12.59	6.93	-322.60	3.61
Mix 1 30%-1313-T02-A	21.74	0.0800	182.2609	16.0000	2.00	-	-	1.60	12.22	13.80	-301.10	2.37
Mix 1 30%-1313-T03-A	21.74	0.0800	143.2609	55.0000	2.00	-	-	5.50	10.63	40.34	-210.40	1.13
Mix 1 30%-1313-T04-A	21.74	0.0800	125.2609	73.0000	2.00	-	-	7.30	9.82	42.00	-164.00	1.54
Mix 1 30%-1313-T05-A	21.74	0.0800	114.2609	84.0000	2.00	-	-	8.40	8.22	56.63	-72.50	1.75
Mix 1 30%-1313-T06-A	21.74	0.0800	106.2609	92.0000	2.00	-	-	9.20	6.47	60.21	22.70	1.96
Mix 1 30%-1313-T07-A	21.74	0.0800	66.2609	132.0000	2.00	-	-	13.20	5.10	63.33	109.40	18.48
Mix 1 30%-1313-T08-A	21.74	0.0800	51.2609	147.0000	2.00	-	-	14.70	3.60	67.69	197.20	178.76
Mix 1 30%-1313-T09-A	21.74	0.0800	38.2609	160.0000	2.00	-	-	16.00	2.00	77.28	290.70	284.56
Mix 1 30%-1313-T01-B	21.28	0.0600	198.7234	-	-	-	-	0.00	12.65	7.17	-326.40	3.40
Mix 1 30%-1313-T02-B	21.28	0.0600	182.7234	16.0000	2.00	-	-	1.60	12.32	13.42	-307.60	2.78
Mix 1 30%-1313-T03-B	21.28	0.0600	143.7234	55.0000	2.00	-	-	5.50	10.97	36.99	-232.60	1.13
Mix 1 30%-1313-T04-B	21.28	0.0600	123.7234	75.0000	2.00	-	-	7.50	9.69	47.58	-160.40	1.34
Mix 1 30%-1313-T05-B	21.28	0.0600	114.7234	84.0000	2.00	-	-	8.40	9.50	51.56	-148.00	1.54
Mix 1 30%-1313-T06-B	21.28	0.0600	107.7234	91.0000	2.00	-	-	9.10	8.56	56.16	-95.10	1.75
Mix 1 30%-1313-T07-B	21.28	0.0600	66.7234	132.0000	2.00	-	-	13.20	4.86	62.03	118.90	47.46
Mix 1 30%-1313-T08-B	21.28	0.0600	51.7234	147.0000	2.00	-	-	14.70	4.77	64.98	124.40	55.05
Mix 1 30%-1313-T09-B	21.28	0.0600	38.7234	160.0000	2.00	-	-	16.00	3.21	68.56	214.90	287.36
Mix 1 30%-1313-T01-C	21.74	0.080	198.26	-	-	-	-	0.00	12.83	7.01	-334.90	3.61
Mix 1 30%-1313-T02-C	21.74	0.080	182.26	16.00	2.00	-	-	1.60	12.37	13.59	-309.60	2.37
Mix 1 30%-1313-T03-C	21.74	0.080	143.26	55.00	2.00	-	-	5.50	10.84	31.40	-223.70	0.93
Mix 1 30%-1313-T04-C	21.74	0.080	123.26	75.00	2.00	-	-	7.50	10.04	39.59	-178.80	1.34
Mix 1 30%-1313-T05-C	21.74	0.080	114.26	84.00	2.00	-	-	8.40	9.42	42.70	-143.70	1.54
Mix 1 30%-1313-T06-C	21.74	0.080	107.26	91.00	2.00	-	-	9.10	9.09	45.48	-125.30	1.75
Mix 1 30%-1313-T07-C	21.74	0.080	66.26	132.00	2.00	-	-	13.20	5.69	59.39	70.40	5.67
Mix 1 30%-1313-T08-C	21.74	0.080	51.26	147.00	2.00	-	-	14.70	5.08	65.42	100.10	27.59
Mix 1 30%-1313-T09-C	21.74	0.080	38.26	160.00	2.00	-	-	16.00	3.51	68.07	197.20	265.16
Mix 1 30%-1313-B01-A	-	-	200.00	-	-	-	-	-	0.00	0.00	0.00	
Mix 1 30%-1313-B02-A	-	-	40.00	160.00	2.00	-	-	-	0.00	0.00	0.00	
Mix 1 30%-1313-B03-A	-	-	-	-	-	-	-	-	0.00	0.00	0.00	

Figure A-12 - EPA Method 1313 Results for Mix 1 30% CRT

PreMethod 1313 LeachXS™ Lite Data Template

METHOD 1313 MASTER DATA LIST

QC Flags

J	Value greater than calibration
E	Value between MDL and ML
U	Value less than MDL
U1/2	Value less than MDL (shown at 1/2 MDL)

	Code	Description *(optional)*
Project ID	CRT	Auto-inserted from "Title Sheet"
Material ID	Mix 2 10%	Auto-inserted from "Title Sheet"
Test ID	1313	

	Acid Type	Base Type
Test Rep A	HNO3	KOH
Test Rep B	HNO3	KOH
Test Rep C	HNO3	KOH

	Pb
MDL	0.15
ML	0.2
Analytical Method	*AAS-Flame*
Analysis Date	
Analytical Lab Name	Diego
Eluate Composition	14

Sample ID	"As Tested" Solid g	Moisture Content g-H_2O/g	Water Added mL	Acid Added mL	Acid Stength N	Base Added mL	Base Stength N	Acid Added meq/g-dry	Eluate pH s.u.	Eluate Cond. mS/cm	Eluate ORP mV	Lead Pb mg/L
Mix 2 10%-1313-T01-A	20.72	0.0349	199.2760	-	-	-	-	0.00	12.72	7.93	-330.60	1.63
Mix 2 10%-1313-T02-A	20.72	0.0349	183.2760	16.0000	2.00	-	-	1.60	11.80	14.87	-281.00	0.82
Mix 2 10%-1313-T03-A	20.72	0.0349	143.2760	56.0000	2.00	-	-	5.60	10.02	40.90	-184.30	1.19
Mix 2 10%-1313-T04-A	20.72	0.0349	132.2760	67.0000	2.00	-	-	6.70	7.14	47.81	-25.50	1.09
Mix 2 10%-1313-T05-A	20.72	0.0349	124.2760	75.0000	2.00	-	-	7.50	6.97	52.39	-15.60	1.17
Mix 2 10%-1313-T06-A	20.72	0.0349	116.2760	83.0000	2.00	-	-	8.30	6.31	56.49	22.30	3.37
Mix 2 10%-1313-T07-A	20.72	0.0349	67.2760	132.0000	2.00	-	-	13.20	5.13	78.38	91.60	3.51
Mix 2 10%-1313-T08-A	20.72	0.0349	49.2760	150.0000	2.00	-	-	15.00	3.70	84.22	173.70	38.75
Mix 2 10%-1313-T09-A	20.72	0.0349	42.2760	157.0000	2.00	-	-	15.70	2.10	81.97	259.50	50.75
Mix 2 10%-1313-T01-B	20.93	0.0446	199.0667	-	-	-	-	0.00	12.54	7.78	-321.00	0.61
Mix 2 10%-1313-T02-B	20.93	0.0446	183.0667	16.0000	2.00	-	-	1.60	11.55	14.87	-267.40	0.34
Mix 2 10%-1313-T03-B	20.93	0.0446	144.0667	55.0000	2.00	-	-	5.50	9.85	41.33	-175.40	0.94
Mix 2 10%-1313-T04-B	20.93	0.0446	139.0667	60.0000	2.00	-	-	6.00	9.70	44.28	-167.30	1.23
Mix 2 10%-1313-T05-B	20.93	0.0446	136.0667	63.0000	2.00	-	-	6.30	9.47	46.03	-154.80	1.25
Mix 2 10%-1313-T06-B	20.93	0.0446	124.0667	75.0000	2.00	-	-	7.50	7.54	52.87	-48.30	1.48
Mix 2 10%-1313-T07-B	20.93	0.0446	68.0667	131.0000	2.00	-	-	13.10	5.05	78.45	95.50	3.26
Mix 2 10%-1313-T08-B	20.93	0.0446	50.0667	149.0000	2.00	-	-	14.90	3.44	85.26	187.70	35.47
Mix 2 10%-1313-T09-B	20.93	0.0446	42.0667	157.0000	2.00	-	-	15.70	1.98	88.37	267.30	53.69
Mix 2 10%-1313-T01-C	21.05	0.050	198.95	-	-	-	-	0.00	12.67	7.84	-327.70	1.30
Mix 2 10%-1313-T02-C	21.05	0.050	183.95	15.00	2.00	-	-	1.50	11.74	14.45	-278.10	0.90
Mix 2 10%-1313-T03-C	21.05	0.050	156.95	42.00	2.00	-	-	4.20	10.71	32.73	-222.30	1.48
Mix 2 10%-1313-T04-C	21.05	0.050	134.95	64.00	2.00	-	-	6.40	6.30	45.04	22.40	1.40
Mix 2 10%-1313-T05-C	21.05	0.050	127.95	71.00	2.00	-	-	7.10	6.58	50.26	6.50	1.67
Mix 2 10%-1313-T06-C	21.05	0.050	122.95	76.00	2.00	-	-	7.60	6.34	53.38	20.70	1.67
Mix 2 10%-1313-T07-C	21.05	0.050	70.95	128.00	2.00	-	-	12.80	5.35	76.31	79.00	2.72
Mix 2 10%-1313-T08-C	21.05	0.050	53.95	145.00	2.00	-	-	14.50	4.28	82.75	143.00	22.11
Mix 2 10%-1313-T09-C	21.05	0.050	41.95	157.00	2.00	-	-	15.70	2.13	86.63	259.50	57.93
Mix 2 10%-1313-B01-A	-	-	200.00	-	-	-	-	-	0.00	0.00	0.00	
Mix 2 10%-1313-B02-A	-	-	43.00	157.00	2.00	-	-	-	0.00	0.00	0.00	
Mix 2 10%-1313-B03-A	-	-	-	-	-	-	-	-	0.00	0.00	0.00	
	-	-	-	-	-	-	-	-				

Figure A-13 - EPA Method 1313 Results for Mix 2 10% CRT

PreMethod 1313 LeachXS™ Lite Data Template

METHOD 1313 MASTER DATA LIST

QC Flags	
J	Value greater than calibration
E	Value between MDL and ML
U	Value less than MDL
U1/2	Value less than MDL (shown at 1/2 MDL)

	Code	Description *(optional)*
Project ID	CRT	Auto-inserted from "Title Sheet"
Material ID	Mix 2 20%	Auto-inserted from "Title Sheet"
Test ID	1313	

	Acid Type	Base Type
Test Rep A	HNO3	KOH
Test Rep B	HNO3	KOH
Test Rep C	HNO3	KOH

	Pb
MDL	0.1500
ML	0.2
Analytical Method	*AAS-Flame*
Analysis Date	
Analytical Lab Name	Diego
Eluate Composition	14

Sample ID	"As Tested" Solid g	Moisture Content g-H_2O/g	Water Added mL	Acid Added mL	Acid Stength N	Base Added mL	Base Stength N	Acid Added meq/g-dry	Eluate pH s.u.	Eluate Cond. mS/cm	Eluate ORP mV	Lead Pb mg/L
Mix 2 20%-1313-T01-A	21.05	0.0500	198.9474	-	-	-	-	0.00	12.87	7.93	-337.80	2.18
Mix 2 20%-1313-T02-A	21.05	0.0500	182.9474	16.0000	2.00	-	-	1.60	11.66	14.88	-272.50	0.33
Mix 2 20%-1313-T03-A	21.05	0.0500	150.9474	48.0000	2.00	-	-	4.80	6.68	36.10	2.10	0.94
Mix 2 20%-1313-T04-A	21.05	0.0500	138.9474	60.0000	2.00	-	-	6.00	6.21	44.23	26.30	1.10
Mix 2 20%-1313-T05-A	21.05	0.0500	133.9474	65.0000	2.00	-	-	6.50	6.37	47.52	18.20	1.14
Mix 2 20%-1313-T06-A	21.05	0.0500	127.9474	71.0000	2.00	-	-	7.10	6.20	50.89	28.20	1.23
Mix 2 20%-1313-T07-A	21.05	0.0500	68.9474	130.0000	2.00	-	-	13.00	4.64	77.18	122.30	19.36
Mix 2 20%-1313-T08-A	21.05	0.0500	50.9474	148.0000	2.00	-	-	14.80	3.00	84.90	212.60	160.22
Mix 2 20%-1313-T09-A	21.05	0.0500	42.9474	156.0000	2.00	-	-	15.60	1.07	91.21	319.50	207.58
Mix 2 20%-1313-T01-B	21.04	0.0495	198.9583	-	-	-	-	0.00	12.77	0.00	0.00	1.87
Mix 2 20%-1313-T02-B	21.04	0.0495	184.9583	14.0000	2.00	-	-	1.40	11.85	0.00	0.00	0.30
Mix 2 20%-1313-T03-B	21.04	0.0495	174.9583	24.0000	2.00	-	-	2.40	11.27	0.00	0.00	0.35
Mix 2 20%-1313-T04-B	21.04	0.0495	166.9583	32.0000	2.00	-	-	3.20	10.86	0.00	0.00	0.57
Mix 2 20%-1313-T05-B	21.04	0.0495	158.9583	40.0000	2.00	-	-	4.00	10.25	0.00	0.00	0.90
Mix 2 20%-1313-T06-B	21.04	0.0495	152.9583	46.0000	2.00	-	-	4.60	9.90	0.00	0.00	0.79
Mix 2 20%-1313-T07-B	21.04	0.0495	100.9583	98.0000	2.00	-	-	9.80	6.08	0.00	0.00	1.78
Mix 2 20%-1313-T08-B	21.04	0.0495	62.9583	136.0000	2.00	-	-	13.60	4.58	0.00	0.00	37.56
Mix 2 20%-1313-T09-B	21.04	0.0495	46.9583	152.0000	2.00	-	-	15.20	2.19	0.00	0.00	120.36
Mix 2 20%-1313-T01-C	21.22	0.058	198.78	-	-	-	-	0.00	12.66	7.84	-326.10	2.07
Mix 2 20%-1313-T02-C	21.22	0.058	184.78	14.00	2.00	-	-	1.40	11.72	13.81	-275.50	0.66
Mix 2 20%-1313-T03-C	21.22	0.058	166.78	32.00	2.00	-	-	3.20	10.79	26.74	-225.00	0.64
Mix 2 20%-1313-T04-C	21.22	0.058	152.78	46.00	2.00	-	-	4.60	10.16	35.88	-191.00	1.06
Mix 2 20%-1313-T05-C	21.22	0.058	142.78	56.00	2.00	-	-	5.60	6.84	42.15	-8.10	0.90
Mix 2 20%-1313-T06-C	21.22	0.058	128.78	70.00	2.00	-	-	7.00	6.39	50.31	17.20	1.38
Mix 2 20%-1313-T07-C	21.22	0.058	96.78	102.00	2.00	-	-	10.20	5.87	66.98	48.20	2.02
Mix 2 20%-1313-T08-C	21.22	0.058	59.78	139.00	2.00	-	-	13.90	4.52	81.80	128.80	56.00
Mix 2 20%-1313-T09-C	21.22	0.058	46.78	152.00	2.00	-	-	15.20	2.17	86.38	255.60	136.66
Mix 2 20%-1313-B01-A	-	-	200.00	-	-	-	-	-	0.00	0.00	0.00	
Mix 2 20%-1313-B02-A	-	-	44.00	156.00	2.00	-	-	-	0.00	0.00	0.00	
Mix 2 20%-1313-B03-A	-	-	-	-	-	-	-	-	0.00	0.00	0.00	
	-	-	-	-	-	-	-	-	-			

Figure A-14 - EPA Method 1313 Results for Mix 2 20% CRT

PreMethod 1313 LeachXS™ Lite Data Template

METHOD 1313 MASTER DATA LIST

QC Flags

J	Value greater than calibration
E	Value between MDL and ML
U	Value less than MDL
U1/2	Value less than MDL (shown at 1/2 MDL)

	Code	Description *(optional)*
Project ID	CRT	Auto-inserted from "Title Sheet"
Material ID	Mix 2 30%	Auto-inserted from "Title Sheet"
Test ID	1313	

	Acid Type	Base Type
Test Rep A	HNO3	KOH
Test Rep B	HNO3	KOH
Test Rep C	HNO3	KOH

	Pb
MDL	0.15
ML	0.2
Analytical Method	*AAS-Flame*
Analysis Date	
Analytical Lab Name	Diego
Eluate Composition	14

Sample ID	"As Tested" Solid g	Moisture Content g-H_2O/g	Water Added mL	Acid Added mL	Acid Stength N	Base Added mL	Base Stength N	Acid Added meq/g-dry	Eluate pH s.u.	Eluate Cond. mS/cm	Eluate ORP mV	Lead Pb mg/L
Mix 2 30%-1313-T01-A	21.01	0.0480	198.9897	-	-	-	-	0.00	12.61	7.16	-325.10	2.20
Mix 2 30%-1313-T02-A	21.01	0.0480	184.9897	14.0000	2.00	-	-	1.40	11.79	13.31	-280.10	0.82
Mix 2 30%-1313-T03-A	21.01	0.0480	160.9897	38.0000	2.00	-	-	3.80	10.14	30.28	-190.30	0.58
Mix 2 30%-1313-T04-A	21.01	0.0480	150.9897	48.0000	2.00	-	-	4.80	9.61	35.96	-162.10	1.03
Mix 2 30%-1313-T05-A	21.01	0.0480	140.9897	58.0000	2.00	-	-	5.80	7.54	42.79	-48.40	1.22
Mix 2 30%-1313-T06-A	21.01	0.0480	133.9897	65.0000	2.00	-	-	6.50	6.72	46.70	-1.20	1.16
Mix 2 30%-1313-T07-A	21.01	0.0480	88.9897	110.0000	2.00	-	-	11.00	5.57	69.78	65.90	3.39
Mix 2 30%-1313-T08-A	21.01	0.0480	58.9897	140.0000	2.00	-	-	14.00	4.16	80.37	148.50	98.14
Mix 2 30%-1313-T09-A	21.01	0.0480	46.9897	152.0000	2.00	-	-	15.20	1.40	86.79	298.60	90.84
Mix 2 30%-1313-T01-B	21.08	0.0510	198.9224	-	-	-	-	0.00	12.67	7.61	-325.50	3.03
Mix 2 30%-1313-T02-B	21.08	0.0510	184.9224	14.0000	2.00	-	-	1.40	11.55	13.03	-266.70	0.09
Mix 2 30%-1313-T03-B	21.08	0.0510	161.9224	37.0000	2.00	-	-	3.70	10.03	29.35	-181.50	0.56
Mix 2 30%-1313-T04-B	21.08	0.0510	148.9224	50.0000	2.00	-	-	5.00	8.28	37.68	-90.40	0.86
Mix 2 30%-1313-T05-B	21.08	0.0510	142.9224	56.0000	2.00	-	-	5.60	7.92	41.46	-70.10	0.82
Mix 2 30%-1313-T06-B	21.08	0.0510	134.9224	64.0000	2.00	-	-	6.40	6.59	46.37	6.20	0.98
Mix 2 30%-1313-T07-B	21.08	0.0510	88.9224	110.0000	2.00	-	-	11.00	5.50	66.70	70.00	5.02
Mix 2 30%-1313-T08-B	21.08	0.0510	58.9224	140.0000	2.00	-	-	14.00	3.54	80.19	182.80	167.42
Mix 2 30%-1313-T09-B	21.08	0.0510	49.9224	149.0000	2.00	-	-	14.90	1.82	85.11	276.20	235.78
Mix 2 30%-1313-T01-C	20.69	0.033	199.31	-	-	-	-	0.00	12.65	7.37	-327.70	1.82
Mix 2 30%-1313-T02-C	20.69	0.033	186.31	13.00	2.00	-	-	1.30	11.44	12.32	-261.20	0.34
Mix 2 30%-1313-T03-C	20.69	0.033	163.31	36.00	2.00	-	-	3.60	6.68	29.11	1.00	0.87
Mix 2 30%-1313-T04-C	20.69	0.033	150.31	49.00	2.00	-	-	4.90	6.23	37.73	26.40	1.10
Mix 2 30%-1313-T05-C	20.69	0.033	143.31	56.00	2.00	-	-	5.60	6.20	42.14	28.00	1.31
Mix 2 30%-1313-T06-C	20.69	0.033	135.31	64.00	2.00	-	-	6.40	6.14	46.56	32.00	1.43
Mix 2 30%-1313-T07-C	20.69	0.033	89.31	110.00	2.00	-	-	11.00	5.71	70.09	58.00	3.16
Mix 2 30%-1313-T08-C	20.69	0.033	59.31	140.00	2.00	-	-	13.99	3.89	81.40	163.80	90.82
Mix 2 30%-1313-T09-C	20.69	0.033	51.31	148.00	2.00	-	-	14.79	2.50	84.29	238.70	93.82
Mix 2 30%-1313-B01-A	-	-	200.00	-	-	-	-	-				0
Mix 2 30%-1313-B02-A	-	-	48.00	152.00	2.00	-	-	-				0
Mix 2 30%-1313-B03-A	-	-		-	-	-	-	-				
	-	-	-	-	-	-	-	-				

Figure A-15 - EPA Method 1313 Results for Mix 2 30% CRT

PreMethod 1313 LeachXS™ Lite Data Template

METHOD 1313 MASTER DATA LIST

QC Flags	
J	Value greater than calibration
E	Value between MDL and ML
U	Value less than MDL
U1/2	Value less than MDL (shown at 1/2 MDL)

	Code	Description *(optional)*
Project ID	CRT	Auto-inserted from "Title Sheet"
Material ID	Mix 3 10%	Auto-inserted from "Title Sheet"
Test ID	1313	

	Acid Type	Base Type
Test Rep A	HNO3	NaOH
Test Rep B	HNO3	NaOH
Test Rep C	HNO3	NaOH

	Pb
MDL	0.15
ML	0.2
Analytical Method	*AAS-Flame*
Analysis Date	18-Jun-10
Analytical Lab Name	Diego
Eluate Composition	14

Sample ID	"As Tested" Solid g	Moisture Content g-H_2O/g	Water Added mL	Acid Added mL	Acid Stength N	Base Added mL	Base Stength N	Acid Added meq/g-dry	Eluate pH s.u.	Eluate Cond. mS/cm	Eluate ORP mV	Lead Pb mg/L
Mix 3 10%-1313-T01-A	21.28	0.0600	198.7234	-	-	-	-	0.00	12.72	7.25	-339.20	0.51
Mix 3 10%-1313-T02-A	21.28	0.0600	182.7234	16.0000	2.00	-	-	1.60	12.05	15.10	-291.90	0.31
Mix 3 10%-1313-T03-A	21.28	0.0600	142.7234	56.0000	2.00	-	-	5.60	10.14	41.28	-184.10	1.13
Mix 3 10%-1313-T04-A	21.28	0.0600	133.7234	65.0000	2.00	-	-	6.50	9.64	46.33	-155.70	1.13
Mix 3 10%-1313-T05-A	21.28	0.0600	110.7234	88.0000	2.00	-	-	8.80	6.58	53.72	21.90	1.75
Mix 3 10%-1313-T06-A	21.28	0.0600	104.7234	94.0000	2.00	-	-	9.40	6.33	60.37	32.50	1.96
Mix 3 10%-1313-T07-A	21.28	0.0600	66.7234	132.0000	2.00	-	-	13.20	5.62	73.53	74.20	3.40
Mix 3 10%-1313-T08-A	21.28	0.0600	51.7234	147.0000	2.00	-	-	14.70	4.54	76.35	137.90	21.07
Mix 3 10%-1313-T09-A	21.28	0.0600	41.7234	157.0000	2.00	-	-	15.70	2.17	79.85	274.90	57.12
Mix 3 10%-1313-T01-B	21.48	0.0690	198.5177	-	-	-	-	0.00	12.71	6.25	-330.40	1.01
Mix 3 10%-1313-T02-B	21.48	0.0690	182.5177	16.0000	2.00	-	-	1.60	11.67	12.17	-272.70	0.49
Mix 3 10%-1313-T03-B	21.48	0.0690	142.5177	56.0000	2.00	-	-	5.60	9.61	41.10	-157.60	1.10
Mix 3 10%-1313-T04-B	21.48	0.0690	131.5177	67.0000	2.00	-	-	6.70	9.25	47.59	-137.50	1.29
Mix 3 10%-1313-T05-B	21.48	0.0690	128.5177	70.0000	2.00	-	-	7.00	9.37	49.68	-144.40	1.33
Mix 3 10%-1313-T06-B	21.48	0.0690	112.5177	86.0000	2.00	-	-	8.60	6.51	58.56	17.30	1.45
Mix 3 10%-1313-T07-B	21.48	0.0690	66.5177	132.0000	2.00	-	-	13.20	5.55	64.11	79.00	2.70
Mix 3 10%-1313-T08-B	21.48	0.0690	50.5177	148.0000	2.00	-	-	14.80	4.54	69.21	133.10	24.97
Mix 3 10%-1313-T09-B	21.48	0.0690	41.5177	157.0000	2.00	-	-	15.70	2.94	84.83	226.20	51.11
Mix 3 10%-1313-T01-C	21.46	0.068	198.54	-	-	-	-	0.00	12.71	7.76	-330.30	1.25
Mix 3 10%-1313-T02-C	21.46	0.068	182.54	16.00	2.00	-	-	1.60	11.93	14.96	-287.40	0.70
Mix 3 10%-1313-T03-C	21.46	0.068	142.54	56.00	2.00	-	-	5.60	10.26	41.15	-193.90	1.08
Mix 3 10%-1313-T04-C	21.46	0.068	131.54	67.00	2.00	-	-	6.70	9.07	46.88	-127.60	1.31
Mix 3 10%-1313-T05-C	21.46	0.068	123.54	75.00	2.00	-	-	7.50	7.88	52.30	-60.80	1.44
Mix 3 10%-1313-T06-C	21.46	0.068	115.54	83.00	2.00	-	-	8.30	6.48	57.13	18.80	1.49
Mix 3 10%-1313-T07-C	21.46	0.068	66.54	132.00	2.00	-	-	13.20	5.62	65.88	70.00	2.53
Mix 3 10%-1313-T08-C	21.46	0.068	48.54	150.00	2.00	-	-	15.00	4.05	74.63	162.00	45.07
Mix 3 10%-1313-T09-C	21.46	0.068	37.54	161.00	2.00	-	-	16.10	1.44	91.54	315.30	62.09
Mix 3 10%-1313-B01-A	-	-	200.00	-	-	-	-	-	0.00	0.00	0.00	
Mix 3 10%-1313-B02-A	-	-	43.00	157.00	2.00	-	-	-	0.00	0.00	0.00	
Mix 3 10%-1313-B03-A	-	-	-	-	-	-	-	-	0.00	0.00	0.00	

Figure A-16 - EPA Method 1313 Results for Mix 3 10% CRT

PreMethod 1313 LeachXS™ Lite Data Template

METHOD 1313 MASTER DATA LIST

QC Flags	
J	Value greater than calibration
E	Value between MDL and ML
U	Value less than MDL
U1/2	Value less than MDL (shown at 1/2 MDL)

	Code	Description *(optional)*
Project ID	CRT	Auto-inserted from "Title Sheet"
Material ID	Mix 3 20%	Auto-inserted from "Title Sheet"
Test ID	1313	

	Acid Type	Base Type
Test Rep A	HNO3	NAOH
Test Rep B	HNO3	NAOH
Test Rep C	HNO3	NAOH

	Pb
MDL	0.15
ML	0.2
Analytical Method	*AAS-Flame*
Analysis Date	
Analytical Lab Name	Diego
Eluate Composition	14

Sample ID	"As Tested" Solid g	Moisture Content g-H_2O/g	Water Added mL	Acid Added mL	Acid Stength N	Base Added mL	Base Stength N	Acid Added meq/g-dry	Eluate pH s.u.	Eluate Cond. mS/cm	Eluate ORP mV	Lead Pb mg/L
Mix 3 20%-1313-T01-A	21.53	0.0707	198.4715	-	-	-	-	0.00	12.68	8.54	-328.70	1.70
Mix 3 20%-1313-T02-A	21.53	0.0707	182.4715	16.0000	2.00	-	-	1.60	11.91	15.62	-285.20	0.43
Mix 3 20%-1313-T03-A	21.53	0.0707	143.4715	55.0000	2.00	-	-	5.50	9.86	40.84	-171.40	0.73
Mix 3 20%-1313-T04-A	21.53	0.0707	131.4715	67.0000	2.00	-	-	6.70	9.02	47.94	-124.70	0.92
Mix 3 20%-1313-T05-A	21.53	0.0707	122.4715	76.0000	2.00	-	-	7.60	6.21	53.18	34.40	1.27
Mix 3 20%-1313-T06-A	21.53	0.0707	116.4715	82.0000	2.00	-	-	8.20	6.21	56.70	34.60	1.24
Mix 3 20%-1313-T07-A	21.53	0.0707	66.4715	132.0000	2.00	-	-	13.20	5.24	78.77	92.60	5.73
Mix 3 20%-1313-T08-A	21.53	0.0707	48.4715	150.0000	2.00	-	-	15.00	3.62	84.97	187.30	89.25
Mix 3 20%-1313-T09-A	21.53	0.0707	38.4715	160.0000	2.00	-	-	16.00	1.58	90.14	306.80	123.55
Mix 3 20%-1313-T01-B	21.69	0.0780	198.3080	-	-	-	-	0.00	12.72	7.80	-330.90	2.14
Mix 3 20%-1313-T02-B	21.69	0.0780	182.3080	16.0000	2.00	-	-	1.60	12.15	15.57	-299.60	0.99
Mix 3 20%-1313-T03-B	21.69	0.0780	144.3080	54.0000	2.00	-	-	5.40	9.74	40.71	-165.10	1.03
Mix 3 20%-1313-T04-B	21.69	0.0780	131.3080	67.0000	2.00	-	-	6.70	7.25	48.26	-22.70	1.04
Mix 3 20%-1313-T05-B	21.69	0.0780	124.3080	74.0000	2.00	-	-	7.40	6.62	52.13	11.00	1.18
Mix 3 20%-1313-T06-B	21.69	0.0780	118.3080	80.0000	2.00	-	-	8.00	6.33	56.42	27.50	1.43
Mix 3 20%-1313-T07-B	21.69	0.0780	67.3080	131.0000	2.00	-	-	13.10	5.95	69.83	50.90	2.01
Mix 3 20%-1313-T08-B	21.69	0.0780	50.3080	148.0000	2.00	-	-	14.80	3.73	80.31	180.00	116.27
Mix 3 20%-1313-T09-B	21.69	0.0780	40.3080	158.0000	2.00	-	-	15.80	1.69	87.56	302.20	145.69
Mix 3 20%-1313-T01-C	21.46	0.068	198.54	-	-	-	-	0.00	13.20	8.23	-357.60	0.80
Mix 3 20%-1313-T02-C	21.46	0.068	182.54	16.00	2.00	-	-	1.60	12.20	15.34	-301.70	1.78
Mix 3 20%-1313-T03-C	21.46	0.068	147.54	51.00	2.00	-	-	5.10	10.37	38.83	-200.00	0.77
Mix 3 20%-1313-T04-C	21.46	0.068	133.54	65.00	2.00	-	-	6.50	9.73	46.94	-164.30	1.08
Mix 3 20%-1313-T05-C	21.46	0.068	128.54	70.00	2.00	-	-	7.00	9.13	49.88	-130.70	1.41
Mix 3 20%-1313-T06-C	21.46	0.068	126.54	72.00	2.00	-	-	7.20	8.81	51.06	-112.50	1.38
Mix 3 20%-1313-T07-C	21.46	0.068	67.54	131.00	2.00	-	-	13.10	5.27	78.56	90.40	1.18
Mix 3 20%-1313-T08-C	21.46	0.068	51.54	147.00	2.00	-	-	14.70	4.05	84.19	161.50	87.33
Mix 3 20%-1313-T09-C	21.46	0.068	42.54	156.00	2.00	-	-	15.60	2.44	87.13	256.50	135.73
Mix 3 20%-1313-B01-A	-	-	200.00	-	-	-	-	-	0.00	0.00	0.00	
Mix 3 20%-1313-B02-A	-	-	40.00	160.00	2.00	-	-	-	0.00	0.00	0.00	
Mix 3 20%-1313-B03-A	-	-	-	-	-	-	-	-	0.00	0.00	0.00	

Figure A-17 - EPA Method 1313 Results for Mix 2 20% CRT

PreMethod 1313 LeachXS™ Lite Data Template

METHOD 1313 MASTER DATA LIST

QC Flags

J	Value greater than calibration
E	Value between MDL and ML
U	Value less than MDL
U1/2	Value less than MDL (shown at 1/2 MDL)

	Code	Description *(optional)*
Project ID	CRT	Auto-inserted from "Title Sheet"
Material ID	Mix 3 30%	Auto-inserted from "Title Sheet"
Test ID	1313	

	Acid Type	Base Type
Test Rep A	HNO3	NaOH
Test Rep B	HNO4	NaOH
Test Rep C	HNO5	NaOH

	Pb
MDL	
ML	
Analytical Method	*AAS-Flame*
Analysis Date	
Analytical Lab Name	Diego
Eluate Composition	14

Sample ID	"As Tested" Solid g	Moisture Content g-H_2O/g	Water Added mL	Acid Added mL	Acid Stength N	Base Added mL	Base Stength N	Acid Added meq/g-dry	Eluate pH s.u.	Eluate Cond. mS/cm	Eluate ORP mV	Lead Pb mg/L
Mix 3 30%-1313-T01-A	21.69	0.0780	198.3080	-	-	-	-	0.00	12.67	7.77	-328.20	0.95
Mix 3 30%-1313-T02-A	21.69	0.0780	182.3080	16.0000	2.00	-	-	1.60	11.97	15.82	-289.40	2.65
Mix 3 30%-1313-T03-A	21.69	0.0780	144.3080	54.0000	2.00	-	-	5.40	10.10	40.68	-184.60	1.23
Mix 3 30%-1313-T04-A	21.69	0.0780	112.3080	86.0000	2.00	-	-	8.60	6.42	58.82	22.60	1.06
Mix 3 30%-1313-T05-A	21.69	0.0780	106.3080	92.0000	2.00	-	-	9.20	5.96	61.97	48.40	1.48
Mix 3 30%-1313-T06-A	21.69	0.0780	96.3080	102.0000	2.00	-	-	10.20	5.85	65.91	56.50	1.66
Mix 3 30%-1313-T07-A	21.69	0.0780	67.3080	131.0000	2.00	-	-	13.10	5.12	78.47	98.60	2.20
Mix 3 30%-1313-T08-A	21.69	0.0780	43.3080	155.0000	2.00	-	-	15.50	1.60	89.73	304.90	48.71
Mix 3 30%-1313-T09-A	21.69	0.0780	36.3080	162.0000	2.00	-	-	16.20	0.98	102.00	341.30	171.44
Mix 3 30%-1313-T01-B	21.62	0.0750	198.3784	-	-	-	-	0.00	12.70	8.29	-330.40	1.82
Mix 3 30%-1313-T02-B	21.62	0.0750	182.3784	16.0000	2.00	-	-	1.60	12.08	14.56	-295.60	0.63
Mix 3 30%-1313-T03-B	21.62	0.0750	145.3784	53.0000	2.00	-	-	5.30	10.32	33.29	-197.60	0.45
Mix 3 30%-1313-T04-B	21.62	0.0750	131.3784	67.0000	2.00	-	-	6.70	8.63	45.07	-103.00	0.67
Mix 3 30%-1313-T05-B	21.62	0.0750	124.3784	74.0000	2.00	-	-	7.40	8.87	50.72	-110.20	0.74
Mix 3 30%-1313-T06-B	21.62	0.0750	117.3784	81.0000	2.00	-	-	8.10	6.68	55.60	7.90	0.81
Mix 3 30%-1313-T07-B	21.62	0.0750	68.3784	130.0000	2.00	-	-	13.00	5.07	74.97	100.60	14.07
Mix 3 30%-1313-T08-B	21.62	0.0750	58.3784	140.0000	2.00	-	-	14.00	4.19	77.47	152.40	104.19
Mix 3 30%-1313-T09-B	21.62	0.0750	46.3784	152.0000	2.00	-	-	15.20	2.48	84.16	256.90	194.36
Mix 3 30%-1313-T01-C	21.69	0.078	198.31	-	-	-	-	0.00	12.45	8.37	-316.60	2.34
Mix 3 30%-1313-T02-C	21.69	0.078	182.31	16.00	2.00	-	-	1.60	12.03	15.91	-293.80	0.66
Mix 3 30%-1313-T03-C	21.69	0.078	145.31	53.00	2.00	-	-	5.30	9.61	40.02	-157.60	0.54
Mix 3 30%-1313-T04-C	21.69	0.078	132.31	66.00	2.00	-	-	6.60	6.87	47.76	-10.10	0.87
Mix 3 30%-1313-T05-C	21.69	0.078	122.31	76.00	2.00	-	-	7.60	6.55	53.44	8.20	1.13
Mix 3 30%-1313-T06-C	21.69	0.078	118.31	80.00	2.00	-	-	8.00	6.43	55.42	15.10	0.73
Mix 3 30%-1313-T07-C	21.69	0.078	70.31	128.00	2.00	-	-	12.80	4.95	76.87	105.90	27.34
Mix 3 30%-1313-T08-C	21.69	0.078	58.31	140.00	2.00	-	-	14.00	3.93	81.48	161.30	114.83
Mix 3 30%-1313-T09-C	21.69	0.078	44.31	154.00	2.00	-	-	15.40	1.58	87.91	289.30	119.18
Mix 3 30%-1313-B01-A	-	-	200.00	-	-	-	-	-	0.00	0.00	0.00	
Mix 3 30%-1313-B02-A	-	-	38.00	162.00	2.00	-	-	-	0.00	0.00	0.00	
Mix 3 30%-1313-B03-A	-	-	-	-	-	-	-	-	0.00	0.00	0.00	

Figure A-18 - EPA Method 1313 Results for Mix 3 30% CRT

PreMethod 1314 LeachXS™ Lite Data Template — PreMethod 1314 LeachXS™ Lite D

METHOD 1314 MASTER DATA LIST

QC Flags

J	Value greater than calibration
E	Value between MDL and ML
U	Value less than MDL
U1/2	Value less than MDL (shown at 1/2 MDL)

	Code	Description *(optional)*
Project ID	CRT	Auto-inserted from "Title Sheet"
Material ID	Mix 1 10%	Auto-inserted from "Title Sheet"
Test ID	1314	

Bed Diameter	4.8	[cm]
Bed Height	28	[cm]
Volume	507	[cm^3]
Eluant Composition	DI Water	

	Pb
MDL	0.1500
ML	0.2
Analytical Method	*AAS-Flame*
Analysis Date	
Analytical Lab Name	Diego
Eluate Composition	14

Sample ID	Fraction #	"As Tested" Solid g	Moisture Content g-H_2O/g	Flow Rate mL/h	Starting Temp. °C	Σ Eluate @ Begin mL	Σ Eluate @ End mL	ΣLS Ratio @ End mL/g-dry	Eluate pH s.u.	Eluate Cond. mS/cm	Eluate ORP mV	Lead Pb mg/L
Mix 1 10%-1314-T01-A	1	649.40	0.047	645.46	19	0.00	140.65	0.23	12.26	9.86	-304.90	1.04
Mix 1 10%-1314-T02-A	2	649.40	0.047	636.84		140.65	331.05	0.53	12.03	7.64	-291.20	1.63
Mix 1 10%-1314-T03-A	3	649.40	0.047	643.40		331.05	651.65	1.05	12.27	7.19	-304.70	1.71
Mix 1 10%-1314-T04-A	4	649.40	0.047	625.74		651.65	963.45	1.56	12.08	8.83	-292.80	1.90
Mix 1 10%-1314-T05-A	5	649.40	0.047	673.50		963.45	1302.25	2.10	12.20	8.65	-299.90	1.77
Mix 1 10%-1314-T06-A	6	649.40	0.047	592.18		1302.25	2777.65	4.49	12.12	8.12	-293.90	1.62
Mix 1 10%-1314-T07-A	7	649.40	0.047	624.60		2777.65	3090.95	4.99	12.21	7.64	-299.90	1.62
Mix 1 10%-1314-T08-A	8	649.40	0.047	602.53		3090.95	5793.05	9.36	12.73	6.88	-330.00	1.01
Mix 1 10%-1314-T09-A	9	649.40	0.047	675.31		5793.05	6129.55	9.90	12.65	6.64	-326.30	0.95
Mix 1 10%-1314-T01-B	1	614.50	0.059	547.60	19	0.00	109.00	0.19	12.99	10.85	-344.90	1.24
Mix 1 10%-1314-T02-B	2	614.50	0.059	710.03		109.00	321.00	0.56	12.90	9.52	-340.30	1.07
Mix 1 10%-1314-T03-B	3	614.50	0.059	695.90		321.00	667.30	1.15	12.81	8.82	-335.10	1.07
Mix 1 10%-1314-T04-B	4	614.50	0.059	672.59		667.30	1002.00	1.73	12.78	8.59	-333.40	1.17
Mix 1 10%-1314-T05-B	5	614.50	0.059	672.99		1002.00	1336.90	2.31	12.79	8.49	-333.50	0.82
Mix 1 10%-1314-T06-B	6	614.50	0.059	449.05		1336.90	2454.20	4.24	12.90	8.23	-341.20	0.95
Mix 1 10%-1314-T07-B	7	614.50	0.059			2454.20						
Mix 1 10%-1314-T08-B	8	614.50	0.059	557.33			4950.30	8.56	12.72	8.07	-330.90	1.04
Mix 1 10%-1314-T09-B	9	614.50	0.059	644.05		4950.30	5270.80	9.12	12.70	7.56	-329.20	1.32
Mix 1 10%-1314-T01-C	1	642.70	0.045	609.68	19	0.00	134.30	0.22	12.83	11.49	-336.50	0.85
Mix 1 10%-1314-T02-C	2	642.70	0.045	635.03		134.30	320.40	0.52	12.81	10.43	-335.50	0.91
Mix 1 10%-1314-T03-C	3	642.70	0.045	638.91		320.40	640.30	1.04	12.78	9.65	-333.60	1.22
Mix 1 10%-1314-T04-C	4	642.70	0.045	626.17		640.30	951.90	1.55	12.70	8.44	-329.60	0.67
Mix 1 10%-1314-T05-C	5	642.70	0.045	647.27		951.90	1274.00	2.08	12.72	8.93	-329.70	0.71
Mix 1 10%-1314-T06-C	6	642.70	0.045	611.78		1274.00	2796.20	4.56	12.67	8.45	-328.10	0.92
Mix 1 10%-1314-T07-C	7	642.70	0.045	630.99		2796.20	3110.20	5.07	12.69	8.27	-329.20	1.05
Mix 1 10%-1314-T08-C	8	642.70	0.045	617.99		3110.20	5878.00	9.58	12.67	8.17	-328.90	1.13
Mix 1 10%-1314-T09-C	9	642.70	0.045	636.82		5878.00	6194.90	10.09	12.70	7.68	-326.00	0.84
Mix 1 10%-1314-B01-A	QA/QC	-	-	-		-	-	-	-	-	-	

Figure A-19 - EPA Method 1314 Results for Mix 1 10% CRT

PreMethod 1314 LeachXS™ Lite Data Template — **PreMethod 1314 LeachXS™ Lite**

METHOD 1314 MASTER DATA LIST

QC Flags	
J	Value greater than calibration
E	Value between MDL and ML
U	Value less than MDL
U1/2	Value less than MDL (shown at 1/2 MDL)

	Code	Description *(optional)*
Project ID	CRT	Auto-inserted from "Title Sheet"
Material ID	Mix 1 20%	Auto-inserted from "Title Sheet"
Test ID	1314	

Bed Diameter	4.8	[cm]
Bed Height	28	[cm]
Volume	507	[cm^3]
Eluant Composition	DI Water	

	Pb
MDL	0.15
ML	0.2
Analytical Method	*AAS-Flame*
Analysis Date	
Analytical Lab Name	Diego
Eluate Composition	14

Sample ID	Fraction #	"As Tested" Solid g	Moisture Content g-H_2O/g	Flow Rate mL/h	Starting Temp. °C	Σ Eluate @ Begin mL	Σ Eluate @ End mL	ΣLS Ratio @ End mL/g-dry	Eluate pH s.u.	Eluate Cond. mS/cm	Eluate ORP mV	Lead Pb mg/L
Mix 1 20%-1314-T01-A	1	647.00	0.055	693.82	19	0.00	151.81	0.25	12.30	10.92	-306.50	1.35
Mix 1 20%-1314-T02-A	2	647.00	0.055	704.63		151.81	362.31	0.59	12.20	8.44	-300.70	2.10
Mix 1 20%-1314-T03-A	3	647.00	0.055	573.41		362.31	647.81	1.06	12.09	7.50	-294.40	2.52
Mix 1 20%-1314-T04-A	4	647.00	0.055	523.40		647.81	908.41	1.49	12.17	8.09	-297.80	2.48
Mix 1 20%-1314-T05-A	5	647.00	0.055	662.79		908.41	1242.61	2.03	12.24	8.86	-302.10	2.60
Mix 1 20%-1314-T06-A	6	647.00	0.055	609.45		1242.61	2759.81	4.51	11.95	8.60	-285.10	2.55
Mix 1 20%-1314-T07-A	7	647.00	0.055	640.22		2759.81	3082.21	5.04	12.23	8.41	-301.10	2.44
Mix 1 20%-1314-T08-A	8	647.00	0.055	585.44		3082.21	5705.61	9.33	12.79	7.63	-333.70	2.35
Mix 1 20%-1314-T09-A	9	647.00	0.055	636.79		5705.61	6016.61	9.84	12.68	7.35	-327.50	2.19
Mix 1 20%-1314-T01-B	1	608.00	0.049	547.60	19	0.00	109.00	0.19	13.01	11.01	-346.10	0.83
Mix 1 20%-1314-T02-B	2	608.00	0.049	700.66		109.00	318.20	0.55	12.93	9.43	-341.50	1.39
Mix 1 20%-1314-T03-B	3	608.00	0.049			318.20			12.42	3.41	-314.30	0.86
Mix 1 20%-1314-T04-B	4	608.00	0.049	620.94			627.20	1.08	12.87	8.37	-338.20	1.77
Mix 1 20%-1314-T05-B	5	608.00	0.049	690.88		627.20	971.00	1.68	12.85	8.32	-337.40	1.82
Mix 1 20%-1314-T06-B	6	608.00	0.049	616.44		971.00	2504.80	4.33	12.64	8.31	-326.50	1.80
Mix 1 20%-1314-T07-B	7	608.00	0.049	627.58		2504.80	2817.10	4.87	12.73	7.83	-331.50	1.64
Mix 1 20%-1314-T08-B	8	608.00	0.049	658.05		2817.10	5764.30	9.96	12.69	7.41	-329.00	1.77
Mix 1 20%-1314-T09-B	9	608.00	0.049	665.36		5764.30	6095.40	10.54	12.66	6.93	-326.30	1.45
Mix 1 20%-1314-T01-C	1	642.70	0.045	622.86	19	0.00	139.40	0.23	12.85	11.79	-337.80	1.30
Mix 1 20%-1314-T02-C	2	642.70	0.045	557.57		139.40	302.80	0.49	12.81	10.35	-335.60	1.71
Mix 1 20%-1314-T03-C	3	642.70	0.045	671.07		302.80	638.80	1.04	12.76	9.66	-332.50	1.71
Mix 1 20%-1314-T04-C	4	642.70	0.045	356.29		638.80	816.10	1.33	12.72	9.02	-330.60	1.47
Mix 1 20%-1314-T05-C	5	642.70	0.045	625.56		816.10	1127.40	1.84	12.70	8.96	-329.20	1.59
Mix 1 20%-1314-T06-C	6	642.70	0.045	525.17		1127.40	2434.10	3.97	12.74	8.65	-330.40	1.49
Mix 1 20%-1314-T07-C	7	642.70	0.045	672.99		2434.10	2769.00	4.51	12.69	8.32	-329.40	1.23
Mix 1 20%-1314-T08-C	8	642.70	0.045	694.45		2769.00	5879.20	9.58	12.69	7.99	-329.90	1.29
Mix 1 20%-1314-T09-C	9	642.70	0.045	698.51		5879.20	6226.80	10.15	12.70	7.44	-326.10	1.34
Mix 1 20%-1314-B01-A	QA/QC	-	-	-		-	-	-	-	-	-	

Figure A-20 - EPA Method 1314 Results for Mix 1 20% CRT

PreMethod 1314 LeachXS™ Lite Data Template — PreMethod 1314 LeachXS™ Lite

METHOD 1314 MASTER DATA LIST

QC Flags

J	Value greater than calibration
E	Value between MDL and ML
U	Value less than MDL
U1/2	Value less than MDL (shown at 1/2 MDL)

	Code	Description *(optional)*
Project ID	CRT	Auto-inserted from "Title Sheet"
Material ID	Mix 1 30%	Auto-inserted from "Title Sheet"
Test ID	1314	

Bed Diameter	4.8	[cm]
Bed Height	28	[cm]
Volume	507	[cm^3]
Eluant Composition	DI Water	

	Pb
MDL	0.15
ML	0.2
Analytical Method	*AAS-Flame*
Analysis Date	
Analytical Lab Name	Diego
Eluate Composition	14

Sample ID	Fraction #	"As Tested" Solid g	Moisture Content g-H_2O/g	Flow Rate mL/h	Starting Temp. °C	Σ Eluate @ Begin mL	Σ Eluate @ End mL	ΣLS Ratio @ End mL/g-dry	Eluate pH s.u.	Eluate Cond. mS/cm	Eluate ORP mV	Lead Pb mg/L
Mix 1 30%-1314-T01-A	1	649.40	0.042	619.20	19	0.00	135.34	0.22	12.22	12.53	-301.70	2.05
Mix 1 30%-1314-T02-A	2	649.40	0.042	675.90		135.34	337.34	0.54	12.14	8.61	-299.10	3.04
Mix 1 30%-1314-T03-A	3	649.40	0.042	587.23		337.34	629.84	1.01	12.16	7.60	-298.50	3.55
Mix 1 30%-1314-T04-A	4	649.40	0.042	520.38		629.84	889.04	1.43	12.34	8.56	-307.70	3.83
Mix 1 30%-1314-T05-A	5	649.40	0.042	592.71		889.04	1187.54	1.91	12.25	7.37	-302.70	3.87
Mix 1 30%-1314-T06-A	6	649.40	0.042	536.84		1187.54	2524.54	4.06	12.12	7.37	-294.30	3.48
Mix 1 30%-1314-T07-A	7	649.40	0.042	584.01		2524.54	2818.04	4.53	12.13	7.10	-295.10	3.37
Mix 1 30%-1314-T08-A	8	649.40	0.042	654.82		2818.04	5753.54	9.25	12.90	7.83	-334.20	2.94
Mix 1 30%-1314-T09-A	9	649.40	0.042	649.67		5753.54	6077.14	9.77	12.71	7.28	-329.30	2.82
Mix 1 30%-1314-T01-B	1	621.10	0.069	505.90	19	0.00	100.70	0.17	12.85	12.64	-337.10	2.28
Mix 1 30%-1314-T02-B	2	621.10	0.069	647.40		100.70	294.00	0.51	13.00	10.65	-345.50	2.67
Mix 1 30%-1314-T03-B	3	621.10	0.069	681.03		294.00	632.90	1.09	12.91	9.55	-340.70	3.12
Mix 1 30%-1314-T04-B	4	621.10	0.069	682.04		632.90	972.30	1.68	12.80	8.71	-333.60	3.36
Mix 1 30%-1314-T05-B	5	621.10	0.069	649.88		972.30	1295.70	2.24	12.81	8.55	-335.00	3.34
Mix 1 30%-1314-T06-B	6	621.10	0.069	597.76		1295.70	2783.00	4.81	12.76	8.44	-333.20	3.16
Mix 1 30%-1314-T07-B	7	621.10	0.069	602.26		2783.00	3082.70	5.33	12.73	8.10	-331.60	3.06
Mix 1 30%-1314-T08-B	8	621.10	0.069	623.58		3082.70	5875.50	10.16	12.72	7.78	-330.80	3.08
Mix 1 30%-1314-T09-B	9	621.10	0.069	655.31		5875.50	6201.60	10.72	12.65	7.01	-326.40	2.49
Mix 1 30%-1314-T01-C	1	633.95	0.058	573.07	19	0.00	127.90	0.21	12.95	15.73	-343.00	4.43
Mix 1 30%-1314-T02-C	2	633.95	0.058	620.02		127.90	309.60	0.52	12.82	11.45	-336.20	4.51
Mix 1 30%-1314-T03-C	3	633.95	0.058	643.71		309.60	631.90	1.06	12.75	9.94	-332.50	4.71
Mix 1 30%-1314-T04-C	4	633.95	0.058	635.39		631.90	948.10	1.59	12.74	9.34	-331.40	4.88
Mix 1 30%-1314-T05-C	5	633.95	0.058	622.52		948.10	1257.90	2.11	12.74	9.21	-331.60	4.51
Mix 1 30%-1314-T06-C	6	633.95	0.058	470.69		1257.90	2429.10	4.07	12.74	8.98	-330.50	4.84
Mix 1 30%-1314-T07-C	7	633.95	0.058	646.04		2429.10	2750.60	4.61	12.72	8.65	-330.90	4.36
Mix 1 30%-1314-T08-C	8	633.95	0.058	639.14		2750.60	5613.20	9.40	12.68	8.42	-328.90	4.29
Mix 1 30%-1314-T09-C	9	633.95	0.058	487.29		5613.20	5855.70	9.81	12.72	8.09	-330.00	4.10
Mix 1 30%-1314-B01-A	QA/QC	-	-	-		-	-	-	-	-	-	

Figure A-21 - EPA Method 1314 Results for Mix 1 30% CRT

PreMethod 1314 LeachXS™ Lite Data Template — PreMethod 1314 LeachXS™ Lite

METHOD 1314 MASTER DATA LIST

QC Flags

J	Value greater than calibration
E	Value between MDL and ML
U	Value less than MDL
U1/2	Value less than MDL (shown at 1/2 MDL)

	Code	Description *(optional)*
Project ID	CRT	Auto-inserted from "Title Sheet"
Material ID	Mix 2 10%	Auto-inserted from "Title Sheet"
Test ID	1314	

Bed Diameter	4.8	[cm]
Bed Height	28	[cm]
Volume	507	[cm^3]
Eluant Composition	DI Water	

	Pb
MDL	0.1500
ML	0.2
Analytical Method	*AAS-Flame*
Analysis Date	
Analytical Lab Name	Diego
Eluate Composition	14

Sample ID	Fraction #	"As Tested" Solid g	Moisture Content g-H_2O/g	Flow Rate mL/h	Starting Temp. °C	Σ Eluate @ Begin mL	Σ Eluate @ End mL	ΣLS Ratio @ End mL/g-dry	Eluate pH s.u.	Eluate Cond. mS/cm	Eluate ORP mV	Lead Pb mg/L
Mix 2 10%-1314-T01-A	1	636.07	0.057	293.92	19	0.00	61.44	0.10	12.77	7.04	-325.50	0.20
Mix 2 10%-1314-T02-A	2	636.07	0.057	609.48		61.44	245.13	0.41	12.88	7.86	-331.70	0.56
Mix 2 10%-1314-T03-A	3	636.07	0.057	549.89		245.13	520.28	0.87	12.87	7.82	-331.20	0.71
Mix 2 10%-1314-T04-A	4	636.07	0.057	526.68		520.28	782.89	1.30	12.78	7.69	-327.50	0.98
Mix 2 10%-1314-T05-A	5	636.07	0.057	537.54		782.89	1054.47	1.76	12.85	7.65	-330.20	1.01
Mix 2 10%-1314-T06-A	6	636.07	0.057	480.43		1054.47	2204.40	3.67	12.68	7.30	-320.60	1.03
Mix 2 10%-1314-T07-A	7	636.07	0.057	459.43		2204.40	2478.32	4.13	12.76	6.66	-324.90	1.11
Mix 2 10%-1314-T08-A	8	636.07	0.057	453.01		2478.32	4509.90	7.52	12.94	6.19	-333.20	1.01
Mix 2 10%-1314-T09-A	9	636.07	0.057	537.81		4509.90	4755.48	7.93	11.69	5.52	-265.00	0.88
Mix 2 10%-1314-T01-B	1	671.97	0.048	552.02	19	0.00	110.36	0.17	13.03	12.23	-340.10	0.39
Mix 2 10%-1314-T02-B	2	671.97	0.048	635.09		110.36	300.81	0.47	12.90	8.74	-332.80	0.78
Mix 2 10%-1314-T03-B	3	671.97	0.048	637.65		300.81	619.51	0.97	12.88	8.41	-331.70	0.94
Mix 2 10%-1314-T04-B	4	671.97	0.048	642.26		619.51	940.51	1.47	12.87	7.95	-331.00	0.96
Mix 2 10%-1314-T05-B	5	671.97	0.048	628.03		940.51	1261.01	1.97	12.86	7.95	-330.60	0.99
Mix 2 10%-1314-T06-B	6	671.97	0.048	630.92		1261.01	2834.81	4.43	12.84	7.74	-329.30	1.16
Mix 2 10%-1314-T07-B	7	671.97	0.048	682.00		2834.81	3172.97	4.96	12.85	7.43	-330.10	1.20
Mix 2 10%-1314-T08-B	8	671.97	0.048	612.85		3172.97	5929.52	9.27	12.87	7.13	-330.80	0.98
Mix 2 10%-1314-T09-B	9	671.97	0.048	673.20		5929.52	6266.12	9.79	12.78	6.18	-326.20	0.79
Mix 2 10%-1314-T01-C	1	685.92	0.050	574.93	19	0.00	114.92	0.18	12.99	9.82	-337.00	0.89
Mix 2 10%-1314-T02-C	2	685.92	0.050	627.60		114.92	303.09	0.47	12.92	8.65	-333.20	1.23
Mix 2 10%-1314-T03-C	3	685.92	0.050	663.78		303.09	634.79	0.97	12.91	8.20	-332.90	1.18
Mix 2 10%-1314-T04-C	4	685.92	0.050	651.38		634.79	960.29	1.47	12.89	7.90	-332.60	1.08
Mix 2 10%-1314-T05-C	5	685.92	0.050	667.99		960.29	1294.09	1.99	12.93	7.76	-334.10	1.03
Mix 2 10%-1314-T06-C	6	685.92	0.050	594.35		1294.09	2779.10	4.26	12.97	7.36	-336.00	1.19
Mix 2 10%-1314-T07-C	7	685.92	0.050	632.22		2779.10	3095.03	4.75	12.85	6.62	-329.50	0.98
Mix 2 10%-1314-T08-C	8	685.92	0.050	546.26		3095.03	5551.77	8.52	12.91	5.72	-336.30	0.52
Mix 2 10%-1314-T09-C	9	685.92	0.050	144.18		5551.77	5623.82	8.63	12.78	4.76	-323.80	0.46
Mix 2 10%-1314-B01-A	QA/QC	-	-	-		-	-	-	-	-	-	

Figure A-22 - EPA Method 1314 Results for Mix 2 10% CRT

PreMethod 1314 LeachXS™ Lite Data Template — PreMethod 1314 LeachXS™ Lite

METHOD 1314 MASTER DATA LIST

QC Flags

J	Value greater than calibration
E	Value between MDL and ML
U	Value less than MDL
U1/2	Value less than MDL (shown at 1/2 MDL)

	Code	Description *(optional)*
Project ID	CRT	Auto-inserted from "Title Sheet"
Material ID	Mix 2 20%	Auto-inserted from "Title Sheet"
Test ID	1314	

Bed Diameter	4.8	[cm]
Bed Height	28	[cm]
Volume	507	[cm^3]
Eluant Composition	DI Water	

	Pb
MDL	0.1500
ML	0.2
Analytical Method	*AAS-Flame*
Analysis Date	
Analytical Lab Name	Diego
Eluate Composition	14

Sample ID	Fraction #	"As Tested" Solid g	Moisture Content g-H_2O/g	Flow Rate mL/h	Starting Temp. °C	Σ Eluate @ Begin mL	Σ Eluate @ End mL	ΣLS Ratio @ End mL/g-dry	Eluate pH s.u.	Eluate Cond. mS/cm	Eluate ORP mV	Lead Pb mg/L
Mix 2 20%-1314-T01-A	1	623.50	0.038	276.65	19	0.00	57.83	0.10	12.85	7.77	-330.20	0.56
Mix 2 20%-1314-T02-A	2	623.50	0.038	627.00		57.83	246.80	0.41	12.91	8.64	-330.20	1.46
Mix 2 20%-1314-T03-A	3	623.50	0.038	547.29		246.80	520.65	0.87	12.91	8.26	-332.10	1.84
Mix 2 20%-1314-T04-A	4	623.50	0.038	558.95		520.65	799.35	1.33	12.74	8.15	-324.40	1.87
Mix 2 20%-1314-T05-A	5	623.50	0.038	578.76		799.35	1091.76	1.82	12.58	7.91	-318.80	2.04
Mix 2 20%-1314-T06-A	6	623.50	0.038	569.06		1091.76	2453.84	4.09	12.70	7.38	-321.50	1.80
Mix 2 20%-1314-T07-A	7	623.50	0.038	549.38		2453.84	2781.39	4.64	12.85	6.23	-328.10	1.44
Mix 2 20%-1314-T08-A	8	623.50	0.038	530.30		2781.39	5159.59	8.60	12.63	5.36	-318.00	0.95
Mix 2 20%-1314-T09-A	9	623.50	0.038	546.55		5159.59	5409.16	9.02	12.60	4.31	-316.00	0.63
Mix 2 20%-1314-T01-B	1	664.80	0.038	539.04	19	0.00	107.76	0.17	12.95	10.83	-335.90	1.86
Mix 2 20%-1314-T02-B	2	664.80	0.038	585.40		107.76	283.30	0.44	12.37	5.84	-303.80	2.18
Mix 2 20%-1314-T03-B	3	664.80	0.038	562.05		283.30	564.20	0.88	12.85	7.95	-329.80	2.41
Mix 2 20%-1314-T04-B	4	664.80	0.038	642.49		564.20	885.30	1.38	12.88	8.24	-331.00	2.75
Mix 2 20%-1314-T05-B	5	664.80	0.038	629.22		885.30	1204.70	1.88	12.89	7.97	-332.30	2.69
Mix 2 20%-1314-T06-B	6	664.80	0.038	621.66		1204.70	2755.40	4.31	12.88	7.75	-351.40	2.22
Mix 2 20%-1314-T07-B	7	664.80	0.038	688.42		2755.40	3096.74	4.84	12.86	7.41	-330.30	1.99
Mix 2 20%-1314-T08-B	8	664.80	0.038	601.32		3096.74	5801.42	9.07	12.88	6.76	-331.40	1.51
Mix 2 20%-1314-T09-B	9	664.80	0.038	613.82		5801.42	6108.33	9.55	12.76	5.75	-325.10	1.17
Mix 2 20%-1314-T01-C	1	674.50	0.034	687.31	19	0.00	137.39	0.21	12.89	7.98	-331.70	0.93
Mix 2 20%-1314-T02-C	2	674.50	0.034	719.74		137.39	353.20	0.54	12.88	7.84	-331.10	1.72
Mix 2 20%-1314-T03-C	3	674.50	0.034	641.34		353.20	673.70	1.03	12.88	7.66	-331.10	1.94
Mix 2 20%-1314-T04-C	4	674.50	0.034	621.73		673.70	984.40	1.51	12.86	7.32	-329.80	1.84
Mix 2 20%-1314-T05-C	5	674.50	0.034	621.73		984.40	1295.10	1.99	12.88	7.11	-330.90	1.78
Mix 2 20%-1314-T06-C	6	674.50	0.034	594.52		1295.10	2780.61	4.27	12.80	4.56	-326.70	1.05
Mix 2 20%-1314-T07-C	7	674.50	0.034	687.34		2780.61	3124.10	4.79	12.70	4.57	-321.00	0.89
Mix 2 20%-1314-T08-C	8	674.50	0.034	490.03		3124.10	5328.07	8.18	12.71	4.01	-321.50	0.79
Mix 2 20%-1314-T09-C	9	674.50	0.034	668.89		5328.07	5662.34	8.69	12.65	4.34	-319.40	0.90
Mix 2 20%-1314-B01-A	QA/QC	-	-	-		-	-	-	-	-	-	

Figure A-23 - EPA Method 1314 Results for Mix 2 20% CRT

PreMethod 1314 LeachXS™ Lite Data Template — PreMethod 1314 LeachXS™ Lite

METHOD 1314 MASTER DATA LIST

QC Flags

J	Value greater than calibration
E	Value between MDL and ML
U	Value less than MDL
U1/2	Value less than MDL (shown at 1/2 MDL)

	Code	Description *(optional)*
Project ID	CRT	Auto-inserted from "Title Sheet"
Material ID	Mix 2 30%	Auto-inserted from "Title Sheet"
Test ID	1314	

Bed Diameter	4.8	[cm]
Bed Height	28	[cm]
Volume	507	[cm^3]
Eluant Composition	DI Water	

	Pb
MDL	0.15
ML	0.2
Analytical Method	*AAS-Flame*
Analysis Date	
Analytical Lab Name	Diego
Eluate Composition	14

Sample ID	Fraction #	"As Tested" Solid g	Moisture Content g-H_2O/g	Flow Rate mL/h	Starting Temp. °C	Σ Eluate @ Begin mL	Σ Eluate @ End mL	ΣLS Ratio @ End mL/g-dry	Eluate pH s.u.	Eluate Cond. mS/cm	Eluate ORP mV	Lead Pb mg/L
Mix 2 30%-1314-T01-A	1	625.70	0.041	439.06	19	0.00	91.78	0.15	12.73	6.94	-323.60	0.24
Mix 2 30%-1314-T02-A	2	625.70	0.041	605.40		91.78	274.24	0.46	12.89	7.63	-332.10	1.00
Mix 2 30%-1314-T03-A	3	625.70	0.041	555.63		274.24	552.26	0.92	12.82	7.36	-328.40	1.90
Mix 2 30%-1314-T04-A	4	625.70	0.041	562.24		552.26	832.60	1.39	12.72	6.76	-322.10	2.25
Mix 2 30%-1314-T05-A	5	625.70	0.041	526.75		832.60	1098.73	1.83	12.67	6.23	-319.00	2.04
Mix 2 30%-1314-T06-A	6	625.70	0.041	446.53		1098.73	2167.53	3.61	12.39	5.04	-304.50	1.72
Mix 2 30%-1314-T07-A	7	625.70	0.041	461.66		2167.53	2442.78	4.07	12.47	3.77	-308.80	1.28
Mix 2 30%-1314-T08-A	8	625.70	0.041	424.90		2442.78	4348.32	7.25	12.46	3.30	-308.40	0.90
Mix 2 30%-1314-T09-A	9	625.70	0.041	631.34		4348.32	4636.61	7.73	12.29	3.20	-299.40	0.51
Mix 2 30%-1314-T01-B	1	663.50	0.036	626.96	19	0.00	125.33	0.20	12.85	8.34	-330.30	0.85
Mix 2 30%-1314-T02-B	2	663.50	0.036	631.64		125.33	314.73	0.49	12.90	7.64	-332.60	2.33
Mix 2 30%-1314-T03-B	3	663.50	0.036	648.92		314.73	639.03	1.00	12.88	7.72	-331.40	3.53
Mix 2 30%-1314-T04-B	4	663.50	0.036	636.31		639.03	957.03	1.50	12.83	7.58	-328.70	4.04
Mix 2 30%-1314-T05-B	5	663.50	0.036	625.60		957.03	1274.63	1.99	12.84	7.39	-329.40	4.34
Mix 2 30%-1314-T06-B	6	663.50	0.036	591.59		1274.63	2750.32	4.30	12.81	7.13	-328.10	3.93
Mix 2 30%-1314-T07-B	7	663.50	0.036	661.43		2750.32	3078.28	4.81	12.79	6.41	-326.60	3.45
Mix 2 30%-1314-T08-B	8	663.50	0.036	582.28		3078.28	5697.33	8.91	12.72	5.60	-322.80	2.54
Mix 2 30%-1314-T09-B	9	663.50	0.036	664.46		5697.33	6029.56	9.43	12.63	4.56	-317.80	1.77
Mix 2 30%-1314-T01-C	1	673.50	0.032	688.22	19	0.00	137.57	0.21	12.84	7.28	-329.20	1.50
Mix 2 30%-1314-T02-C	2	673.50	0.032	744.20		137.57	360.71	0.55	12.84	7.16	-329.00	2.89
Mix 2 30%-1314-T03-C	3	673.50	0.032	551.10		360.71	636.11	0.98	12.81	6.73	-327.20	3.32
Mix 2 30%-1314-T04-C	4	673.50	0.032	491.86		636.11	881.91	1.35	12.80	6.09	-326.30	3.08
Mix 2 30%-1314-T05-C	5	673.50	0.032	525.48		881.91	1144.51	1.76	12.79	5.62	-326.20	2.72
Mix 2 30%-1314-T06-C	6	673.50	0.032	563.00		1144.51	2551.26	3.92	12.64	4.26	-318.00	1.78
Mix 2 30%-1314-T07-C	7	673.50	0.032	670.46		2551.26	2886.31	4.43	12.58	3.29	-314.50	1.13
Mix 2 30%-1314-T08-C	8	673.50	0.032	590.17		2886.31	5540.65	8.50	12.62	2.80	-315.30	0.80
Mix 2 30%-1314-T09-C	9	673.50	0.032	627.82		5540.65	5854.39	8.98	12.45	2.26	-307.30	0.40
Mix 2 30%-1314-B01-A	QA/QC	-	-	-		-	-	-	-	-	-	

Figure A-24 - EPA Method 1314 Results for Mix 2 30% CRT

PreMethod 1314 LeachXS™ Lite Data Template — **PreMethod 1314 LeachXS™ Lite**

METHOD 1314 MASTER DATA LIST

QC Flags

J	Value greater than calibration
E	Value between MDL and ML
U	Value less than MDL
U1/2	Value less than MDL (shown at 1/2 MDL)

	Code	Description *(optional)*
Project ID	CRT	Auto-inserted from "Title Sheet"
Material ID	Mix 3 10%	Auto-inserted from "Title Sheet"
Test ID	1314	

Bed Diameter	4.8	[cm]
Bed Height	28	[cm]
Volume	507	[cm^3]
Eluant Composition	DI Water	

	Pb
MDL	0.15
ML	0.2
Analytical Method	*AAS-Flame*
Analysis Date	
Analytical Lab Name	Diego
Eluate Composition	14

Sample ID	Fraction #	"As Tested" Solid g	Moisture Content g-H_2O/g	Flow Rate mL/h	Starting Temp. °C	Σ Eluate @ Begin mL	Σ Eluate @ End mL	ΣLS Ratio @ End mL/g-dry	Eluate pH s.u.	Eluate Cond. mS/cm	Eluate ORP mV	Lead Pb mg/L
Mix 3 10%-1314-T01-A	1	661.50	0.058	189.06	19	0.00	37.70	0.06	12.70	11.34	-324.70	0.78
Mix 3 10%-1314-T02-A	2	661.50	0.058	592.77		37.70	215.00	0.35	12.69	10.61	-329.10	1.00
Mix 3 10%-1314-T03-A	3	661.50	0.058	569.10		215.00	498.70	0.80	12.67	9.44	-328.20	1.44
Mix 3 10%-1314-T04-A	4	661.50	0.058	607.01		498.70	801.30	1.29	12.73	9.01	-331.70	0.80
Mix 3 10%-1314-T05-A	5	661.50	0.058	608.42		801.30	1104.60	1.77	12.70	8.87	-330.40	1.51
Mix 3 10%-1314-T06-A	6	661.50	0.058	611.99		1104.60	2630.00	4.22	12.68	8.55	-327.20	1.06
Mix 3 10%-1314-T07-A	7	661.50	0.058	644.12		2630.00	2951.10	4.74	12.82	8.08	-335.00	1.32
Mix 3 10%-1314-T08-A	8	661.50	0.058	643.05		2951.10	5836.20	9.37	12.68	7.96	-326.70	0.52
Mix 3 10%-1314-T09-A	9	661.50	0.058	677.42		5836.20	6173.90	9.91	12.59	7.37	-322.00	0.62
Mix 3 10%-1314-T01-B	1	668.70	0.059	616.69	19	0.00	122.80	0.20	12.71	10.84	-330.10	0.51
Mix 3 10%-1314-T02-B	2	668.70	0.059	622.38		122.80	308.70	0.49	12.70	9.96	-328.40	0.97
Mix 3 10%-1314-T03-B	3	668.70	0.059	602.70		308.70	612.20	0.97	12.63	9.29	-327.20	1.08
Mix 3 10%-1314-T04-B	4	668.70	0.059	614.28		612.20	918.00	1.46	12.64	8.77	-326.40	1.30
Mix 3 10%-1314-T05-B	5	668.70	0.059	625.93		918.00	1229.60	1.95	12.64	8.89	-326.20	1.31
Mix 3 10%-1314-T06-B	6	668.70	0.059	617.06		1229.60	2763.80	4.39	12.70	8.62	-329.40	1.14
Mix 3 10%-1314-T07-B	7	668.70	0.059	654.60		2763.80	3091.10	4.91	12.69	8.30	-328.90	1.09
Mix 3 10%-1314-T08-B	8	668.70	0.059	578.54		3091.10	5683.20	9.03	12.70	7.93	-329.70	1.14
Mix 3 10%-1314-T09-B	9	668.70	0.059	622.51		5683.20	5993.10	9.52	12.66	7.39	-327.70	1.12
Mix 3 10%-1314-T01-C	1	634.46	0.038	547.84	19	0.00	120.60	0.20	12.83	10.89	-330.00	0.44
Mix 3 10%-1314-T02-C	2	634.46	0.038	634.53		120.60	303.91	0.50	12.82	9.49	-328.60	0.81
Mix 3 10%-1314-T03-C	3	634.46	0.038	615.22		303.91	606.82	0.99	12.83	8.94	-328.70	1.35
Mix 3 10%-1314-T04-C	4	634.46	0.038	590.91		606.82	901.48	1.48	12.87	4.44	-331.60	1.23
Mix 3 10%-1314-T05-C	5	634.46	0.038	512.98		901.48	1157.28	1.90	12.87	8.23	-331.30	1.29
Mix 3 10%-1314-T06-C	6	634.46	0.038	668.12		1157.28	2823.08	4.63	12.86	7.94	-330.40	1.24
Mix 3 10%-1314-T07-C	7	634.46	0.038	672.01		2823.08	3158.18	5.17	12.82	7.49	-328.60	1.16
Mix 3 10%-1314-T08-C	8	634.46	0.038	451.39		3158.18	5183.95	8.49	12.89	7.17	-332.00	0.86
Mix 3 10%-1314-T09-C	9	634.46	0.038	414.12		5183.95	5390.45	8.83	12.79	6.54	-326.70	0.76
Mix 3 10%-1314-B01-A	QA/QC	-	-	-		-	-	-	-	-	-	

Figure A-25 - EPA Method 1314 Results for Mix 3 10% CRT

PreMethod 1314 LeachXS™ Lite Data Template — PreMethod 1314 LeachXS™ Lite

METHOD 1314 MASTER DATA LIST

QC Flags

J	Value greater than calibration
E	Value between MDL and ML
U	Value less than MDL
U1/2	Value less than MDL (shown at 1/2 MDL)

	Code	Description *(optional)*
Project ID	CRT	Auto-inserted from "Title Sheet"
Material ID	Mix 3 20%	Auto-inserted from "Title Sheet"
Test ID	1314	

Bed Diameter	4.8	[cm]
Bed Height	28	[cm]
Volume	507	[cm^3]
Eluant Composition	DI Water	

	Pb
MDL	0.15
ML	0.2
Analytical Method	*AAS-Flame*
Analysis Date	
Analytical Lab Name	Diego
Eluate Composition	14

Sample ID	Fraction #	"As Tested" Solid g	Moisture Content g-H_2O/g	Flow Rate mL/h	Starting Temp. °C	Σ Eluate @ Begin mL	Σ Eluate @ End mL	ΣLS Ratio @ End mL/g-dry	Eluate pH s.u.	Eluate Cond. mS/cm	Eluate ORP mV	Lead Pb mg/L
Mix 3 20%-1314-T01-A	1	660.80	0.057	243.23	19	0.00	48.50	0.08	12.71	11.19	-330.30	2.16
Mix 3 20%-1314-T02-A	2	660.80	0.057	563.01		48.50	216.90	0.35	12.72	11.16	-330.90	2.60
Mix 3 20%-1314-T03-A	3	660.80	0.057	660.97		216.90	546.40	0.88	12.68	9.74	-328.70	2.72
Mix 3 20%-1314-T04-A	4	660.80	0.057	559.27		546.40	825.20	1.32	12.70	9.01	-330.40	2.60
Mix 3 20%-1314-T05-A	5	660.80	0.057	638.91		825.20	1143.70	1.84	12.68	8.81	-329.00	2.73
Mix 3 20%-1314-T06-A	6	660.80	0.057	465.59		1143.70	2304.20	3.70	12.82	8.80	-335.00	2.63
Mix 3 20%-1314-T07-A	7	660.80	0.057	646.93		2304.20	2626.70	4.22	12.85	8.36	-336.40	2.32
Mix 3 20%-1314-T08-A	8	660.80	0.057	633.38		2626.70	5468.40	8.78	12.64	7.75	-324.70	1.72
Mix 3 20%-1314-T09-A	9	660.80	0.057	676.62		5468.40	5805.70	9.32	12.61	6.94	-323.50	1.47
Mix 3 20%-1314-T01-B	1	660.25	0.047	572.02	19	0.00	113.90	0.18	12.76	12.10	-333.00	0.28
Mix 3 20%-1314-T02-B	2	660.25	0.047	623.41		113.90	300.10	0.48	12.70	10.14	-330.00	1.62
Mix 3 20%-1314-T03-B	3	660.25	0.047	646.96		300.10	625.90	0.99	12.68	9.42	-328.90	2.21
Mix 3 20%-1314-T04-B	4	660.25	0.047	639.62		625.90	944.30	1.50	12.65	8.95	-327.10	2.30
Mix 3 20%-1314-T05-B	5	660.25	0.047	653.68		944.30	1269.70	2.02	12.62	8.72	-325.30	2.16
Mix 3 20%-1314-T06-B	6	660.25	0.047	633.50		1269.70	2844.80	4.52	12.67	8.15	-327.60	1.81
Mix 3 20%-1314-T07-B	7	660.25	0.047	691.20		2844.80	3190.40	5.07	12.65	7.32	-326.80	1.52
Mix 3 20%-1314-T08-B	8	660.25	0.047	592.09		3190.40	5843.10	9.29	12.61	6.44	-325.00	1.79
Mix 3 20%-1314-T09-B	9	660.25	0.047	647.45		5843.10	6165.40	9.80	12.55	5.59	-322.00	1.24
Mix 3 20%-1314-T01-C	1	634.46	0.038	609.39	19	0.00	134.15	0.22	12.96	12.45	-336.00	1.93
Mix 3 20%-1314-T02-C	2	634.46	0.038	695.53		134.15	335.08	0.55	12.86	9.62	-330.60	2.62
Mix 3 20%-1314-T03-C	3	634.46	0.038	661.43		335.08	660.74	1.08	12.75	8.78	-330.20	2.68
Mix 3 20%-1314-T04-C	4	634.46	0.038	548.34		660.74	934.17	1.53	12.90	8.49	-332.90	2.87
Mix 3 20%-1314-T05-C	5	634.46	0.038	616.06		934.17	1241.37	2.03	12.92	8.51	-333.80	2.78
Mix 3 20%-1314-T06-C	6	634.46	0.038	571.26		1241.37	2665.67	4.37	12.91	8.41	-333.20	2.93
Mix 3 20%-1314-T07-C	7	634.46	0.038	583.57		2665.67	2956.67	4.84	12.87	8.06	-331.40	3.01
Mix 3 20%-1314-T08-C	8	634.46	0.038	344.24		2956.67	4501.56	7.38	12.98	8.11	-337.00	2.96
Mix 3 20%-1314-T09-C	9	634.46	0.038	444.80		4501.56	4723.36	7.74	12.89	7.96	-332.30	2.95
Mix 3 20%-1314-B01-A	QA/QC	-	-	-		-	-	-	-	-	-	

Figure A-26 - EPA Method 1314 Results for Mix 3 20% CRT

PreMethod 1314 LeachXS™ Lite Data Template — PreMethod 1314 LeachXS™ Lite

METHOD 1314 MASTER DATA LIST

QC Flags

J	Value greater than calibration
E	Value between MDL and ML
U	Value less than MDL
U1/2	Value less than MDL (shown at 1/2 MDL)

	Code	Description *(optional)*
Project ID	CRT	Auto-inserted from "Title Sheet"
Material ID	Mix 3 30%	Auto-inserted from "Title Sheet"
Test ID	1314	

Bed Diameter	4.8	[cm]
Bed Height	28	[cm]
Volume	507	[cm^3]
Eluant Composition	DI Water	

	Pb
MDL	0.15
ML	0.2
Analytical Method	*AAS-Flame*
Analysis Date	
Analytical Lab Name	Diego
Eluate Composition	14

Sample ID	Fraction #	"As Tested" Solid g	Moisture Content g-H_2O/g	Flow Rate mL/h	Starting Temp. °C	Σ Eluate @ Begin mL	Σ Eluate @ End mL	ΣLS Ratio @ End mL/g-dry	Eluate pH s.u.	Eluate Cond. mS/cm	Eluate ORP mV	Lead Pb mg/L
Mix 3 30%-1314-T01-A	1	662.90	0.060	122.87	19	0.00	24.50	0.04	12.45	8.09	-316.10	2.09
Mix 3 30%-1314-T02-A	2	662.90	0.060	549.98		24.50	189.00	0.30	12.69	10.84	-329.20	3.23
Mix 3 30%-1314-T03-A	3	662.90	0.060	611.63		189.00	493.90	0.79	12.68	9.38	-328.40	3.60
Mix 3 30%-1314-T04-A	4	662.90	0.060	569.31		493.90	777.70	1.25	12.72	8.87	-331.40	3.38
Mix 3 30%-1314-T05-A	5	662.90	0.060	631.89		777.70	1092.70	1.75	12.72	8.49	-331.30	3.15
Mix 3 30%-1314-T06-A	6	662.90	0.060	541.66		1092.70	2442.80	3.92	12.71	8.27	-328.90	3.01
Mix 3 30%-1314-T07-A	7	662.90	0.060	597.99		2442.80	2740.90	4.40	12.75	7.83	-331.30	3.20
Mix 3 30%-1314-T08-A	8	662.90	0.060	546.46		2740.90	5192.60	8.33	12.71	7.41	-328.40	2.40
Mix 3 30%-1314-T09-A	9	662.90	0.060	585.15		5192.60	5484.30	8.80	12.62	6.48	-324.00	1.70
Mix 3 30%-1314-T01-B	1	661.70	0.049	543.34	19	0.00	108.20	0.17	12.73	10.45	-331.50	1.28
Mix 3 30%-1314-T02-B	2	661.70	0.049	607.28		108.20	289.60	0.46	12.71	9.60	-330.60	2.53
Mix 3 30%-1314-T03-B	3	661.70	0.049	614.84		289.60	599.20	0.95	12.71	8.92	-330.00	3.41
Mix 3 30%-1314-T04-B	4	661.70	0.049	616.46		599.20	906.10	1.44	12.71	8.65	-330.00	3.24
Mix 3 30%-1314-T05-B	5	661.70	0.049	640.36		906.10	1224.90	1.95	12.71	8.39	-330.10	3.17
Mix 3 30%-1314-T06-B	6	661.70	0.049	606.41		1224.90	2732.60	4.34	12.69	8.15	-328.70	2.84
Mix 3 30%-1314-T07-B	7	661.70	0.049	639.60		2732.60	3052.40	4.85	12.68	7.61	-327.90	2.75
Mix 3 30%-1314-T08-B	8	661.70	0.049	577.89		3052.40	5641.70	8.97	12.63	6.69	-325.90	2.02
Mix 3 30%-1314-T09-B	9	661.70	0.049	614.45		5641.70	5947.60	9.45	12.58	5.71	-323.40	1.58
Mix 3 30%-1314-T01-C	1	640.24	0.038	638.32	19	0.00	140.52	0.23	12.93	11.46	-334.30	2.13
Mix 3 30%-1314-T02-C	2	640.24	0.038	718.58		140.52	348.11	0.57	12.86	9.40	-330.60	3.28
Mix 3 30%-1314-T03-C	3	640.24	0.038	704.00		348.11	694.73	1.13	12.69	8.82	-320.90	3.54
Mix 3 30%-1314-T04-C	4	640.24	0.038	656.34		694.73	1021.74	1.66	12.88	8.24	-332.00	3.37
Mix 3 30%-1314-T05-C	5	640.24	0.038	628.83		1021.74	1335.04	2.17	12.90	8.07	-333.00	3.34
Mix 3 30%-1314-T06-C	6	640.24	0.038	596.27		1335.04	2820.44	4.58	12.88	7.75	-331.20	3.16
Mix 3 30%-1314-T07-C	7	640.24	0.038	599.72		2820.44	3119.24	5.06	12.82	6.86	-328.30	2.76
Mix 3 30%-1314-T08-C	8	640.24	0.038	508.43		3119.24	5399.05	8.77	12.83	6.48	-328.90	2.26
Mix 3 30%-1314-T09-C	9	640.24	0.038	402.83		5399.05	5599.75	9.09	12.76	5.90	-325.40	2.08
Mix 3 30%-1314-B01-A	QA/QC	-	-	-		-	-	-	-	-	-	

Figure A-27 - EPA Method 1314 Results for Mix 3 30% CRT

Appendix B

Appendix B Study 2

Figure B-1 - Setup for concrete mixing

Figure B-2 - Materials for concrete mixing

Figure B-3 - Concrete mixing with 9 cubic foot mixer

Figure B-4 - Casted cyclinders

Figure B-5 - Cylinders curing in moisture room

Figure B-6 - Arrhenius Aging setup

Figure B-7 - Arrhenius Aging setup

Figure B-8 - Freeze / Thaw testing setup

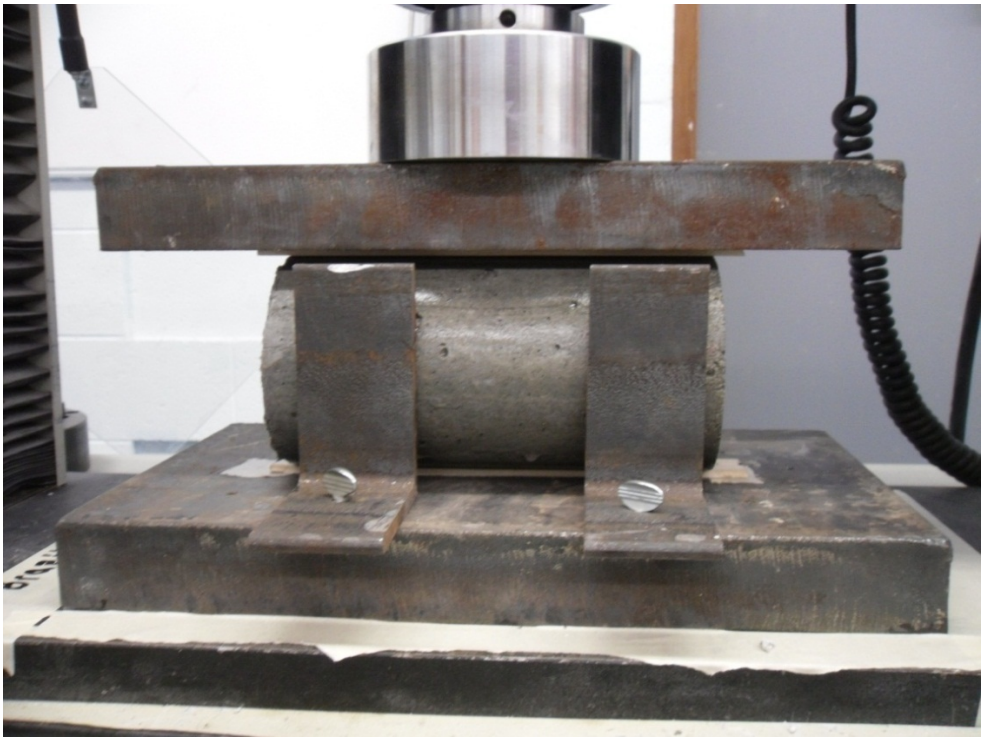

Figure B-9 - Splitting Tensile Strength test setup

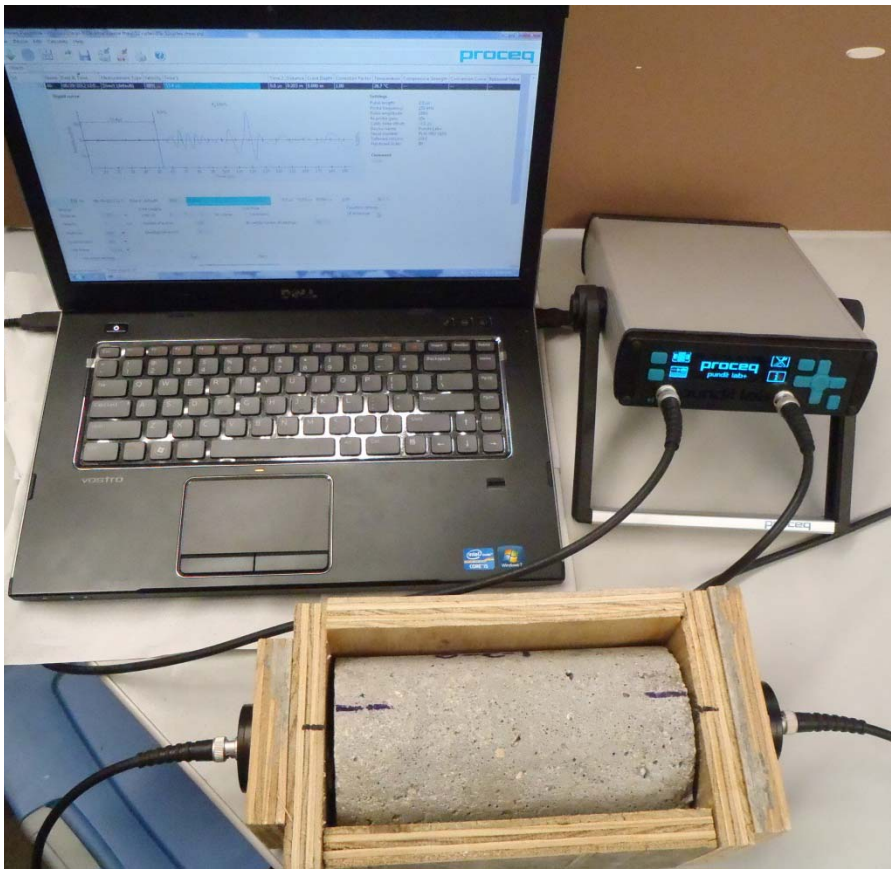

Figure B-10 - UPV testing equipment

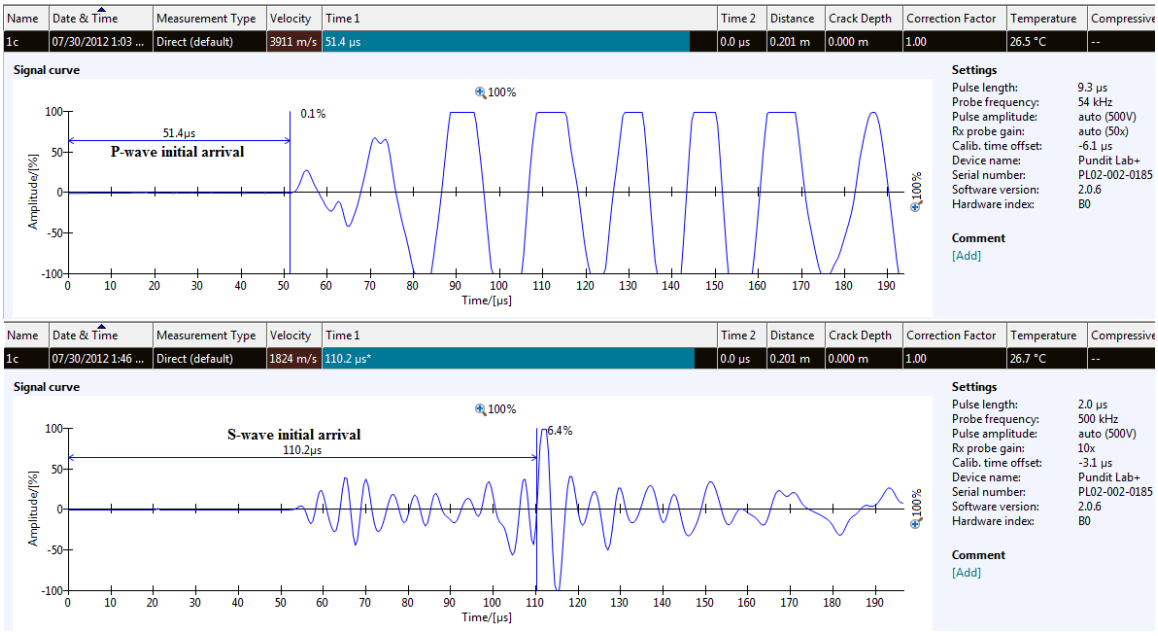

Figure B-11 – P-wave and S-wave arrival times using UPV

Figure B-12 - Fundamental longitudinal resonant frequency testing

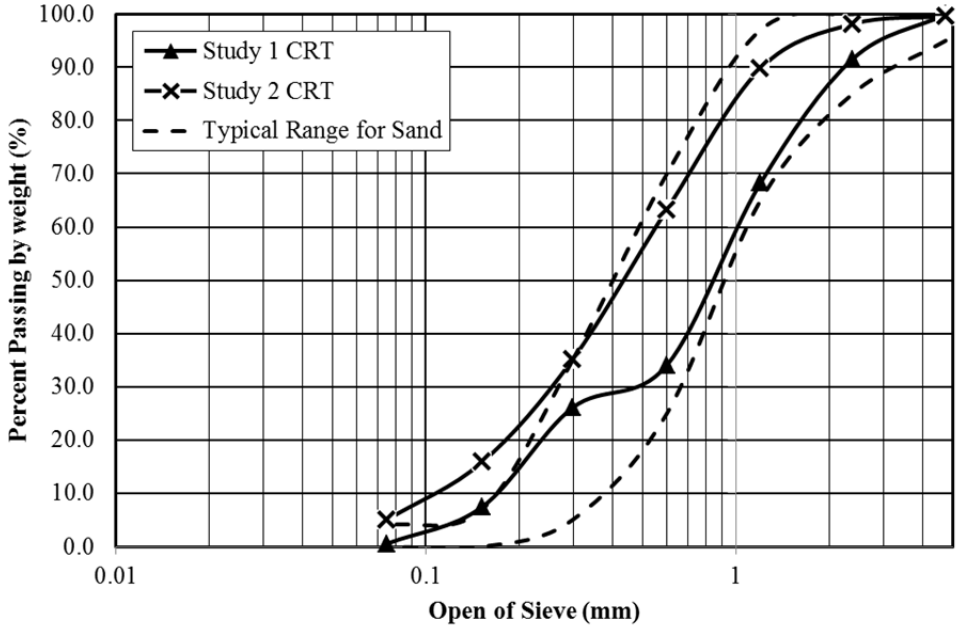

Figure B-13 - CRT glass particle size distribution

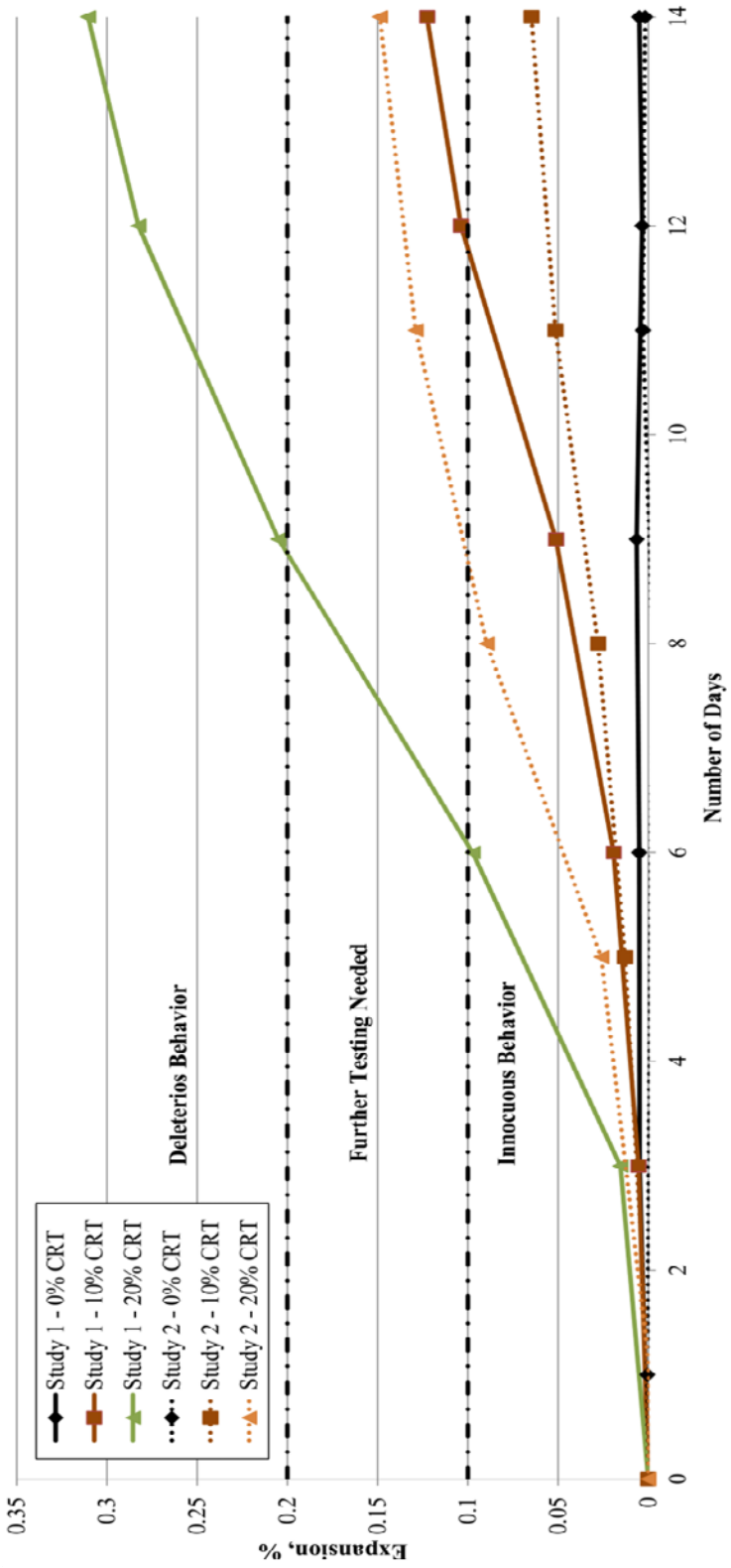

Figure B-14 - Comparison of ASR results between studies

Table B-1- Strength development of specimens at 19°C Arrhenius Aging

Strength Development 19°C						
	28 Days	63 Days	112 Days	210 Days / End of AA	After AA and 178 F/T Cycles	After AA and 300 F/T Cycles
0% CRT	100.00%	113.76%	118.71%	121.30%	110.25%	118.24%
10% CRT	100.00%	123.60%	122.55%	124.81%	111.13%	119.93%
20% CRT	100.00%	110.59%	117.82%	117.89%	122.03%	120.02%
Strength Development 50°C						
	28 Days	63 Days	112 Days	210 Days / End of AA	After AA and 178 F/T Cycles	After AA and 300 F/T Cycles
0% CRT	100.00%	96.82%	91.79%	81.39%	73.75%	85.97%
10% CRT	100.00%	96.23%	94.58%	88.78%	87.84%	93.69%
20% CRT	100.00%	100.15%	101.99%	96.00%	101.77%	95.08%

Table B-2 - Summary of strength tests with standard deviation and coefficient of variation (Cold AA)

19°C	28 Days			63 Days			112 Days		
	Strength (MPa)	Std. Dev.	CV	Strength (MPa)	Std. Dev.	CV	Strength (MPa)	Std. Dev.	CV
0% CRT Content	18.6	0.504	0.027	21.1	1.080	0.032	22.0	0.738	0.051
10% CRT Content	20.5	0.089	0.004	25.3	0.769	0.039	25.1	1.690	0.088
20% CRT Content	24.7	0.363	0.015	27.3	0.919	0.054	29.1	1.703	0.062
	210 Days / End of AA			After AA and 178 F/T Cycles			After AA and 300 F/T Cycles		
	Strength (MPa)	Std. Dev.	CV	Strength (MPa)	Std. Dev.	CV	Strength (MPa)	Std. Dev.	CV
0% CRT Content	22.5	1.368	0.061	20.5	0.683	0.072	21.9	1.506	0.045
10% CRT Content	25.6	1.450	0.063	22.8	0.903	0.026	24.6	1.006	0.024
20% CRT Content	29.1	1.749	0.037	30.1	1.626	0.075	29.6	2.488	0.058

Table B-3 - Summary of strength tests with standard deviation and coefficient of variation (Hot AA)

50°C	28 Days			63 Days			112 Days		
	Strength (MPa)	Std. Dev.	CV	Strength (MPa)	Std. Dev.	CV	Strength (MPa)	Std. Dev.	CV
0% CRT Content	18.6	0.504	0.027	18.0	0.570	0.032	17.0	0.862	0.051
10% CRT Content	20.5	0.089	0.004	19.7	0.778	0.039	19.4	1.697	0.088
20% CRT Content	24.7	0.363	0.015	24.7	1.347	0.054	25.2	1.550	0.062
	210 Days / End of AA			After AA and 178 F/T Cycles			After AA and 300 F/T Cycles		
	Strength (MPa)	Std. Dev.	CV	Strength (MPa)	Std. Dev.	CV	Strength (MPa)	Std. Dev.	CV
0% CRT Content	15.1	0.918	0.061	13.7	0.983	0.072	16.0	0.712	0.045
10% CRT Content	18.2	1.151	0.063	18.0	0.462	0.026	19.2	0.458	0.024
20% CRT Content	23.7	0.868	0.037	25.1	1.891	0.075	24.0	1.395	0.058

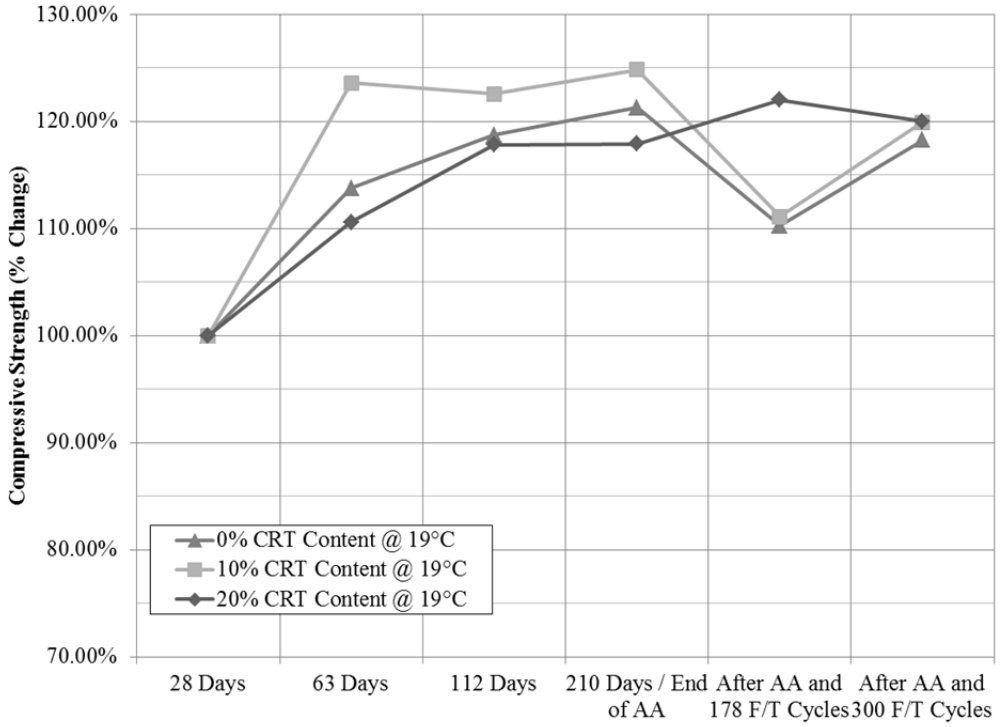

Figure B-15 Compressive strength development 19°C

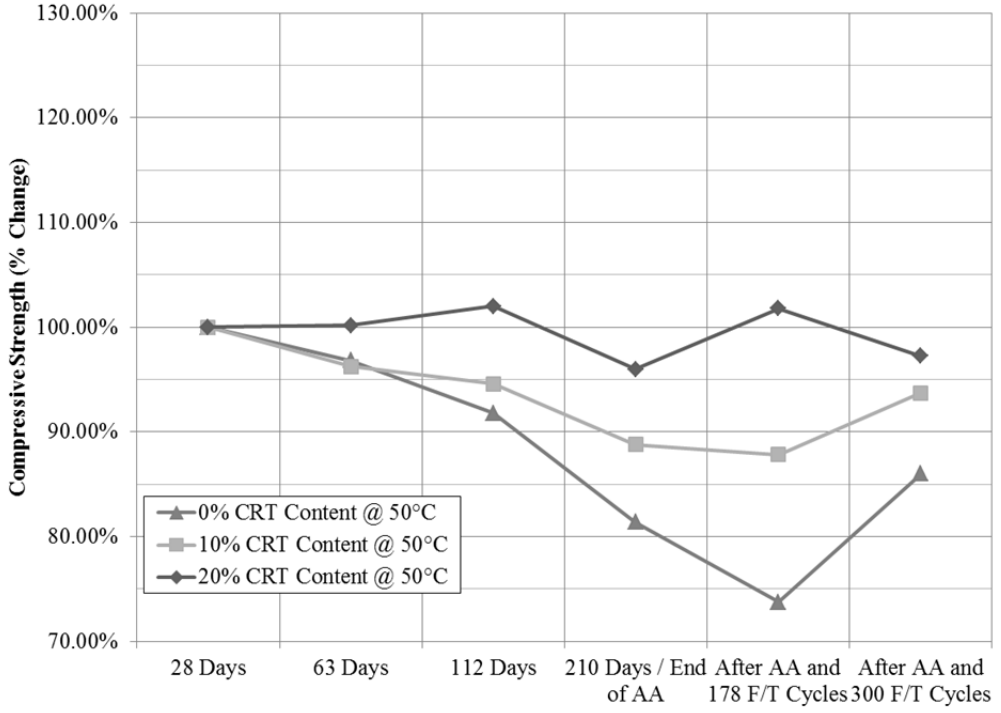

Figure B-16 - Compressive strength development 50°C

Table B-4 – Summary of Splitting Tensile Strength results for CRT-Concrete (Cold AA)

	28 Days			63 Day Strength			112 Day Strength		
	Strength (MPa)	Std. Dev.	CV	Strength (MPa)	Std. Dev.	CV	Strength (MPa)	Std. Dev.	CV
0% CRT Content	1.6	0.311	0.191	2.1	0.347	0.162	2.3	0.451	0.195
10% CRT Content	2.4	0.295	0.121	2.1	0.139	0.066	2.0	0.387	0.190
20% CRT Content	2.3	0.262	0.112	2.1	0.377	0.178	2.1	0.097	0.046

Table B-5 - Summary of Splitting Tensile Strength results for CRT-Concrete under (Hot AA)

	28 Days			63 Day Strength			112 Day Strength		
	Strength (MPa)	Std. Dev.	CV	Strength (MPa)	Std. Dev.	CV	Strength (MPa)	Std. Dev.	CV
0% CRT Content	1.6	0.399	0.191	1.7	0.399	0.228	1.7	0.208	0.121
10% CRT Content	2.4	0.251	0.121	1.8	0.251	0.142	1.6	0.441	0.273
20% CRT Content	2.3	0.086	0.112	1.5	0.086	0.056	1.9	0.313	0.168

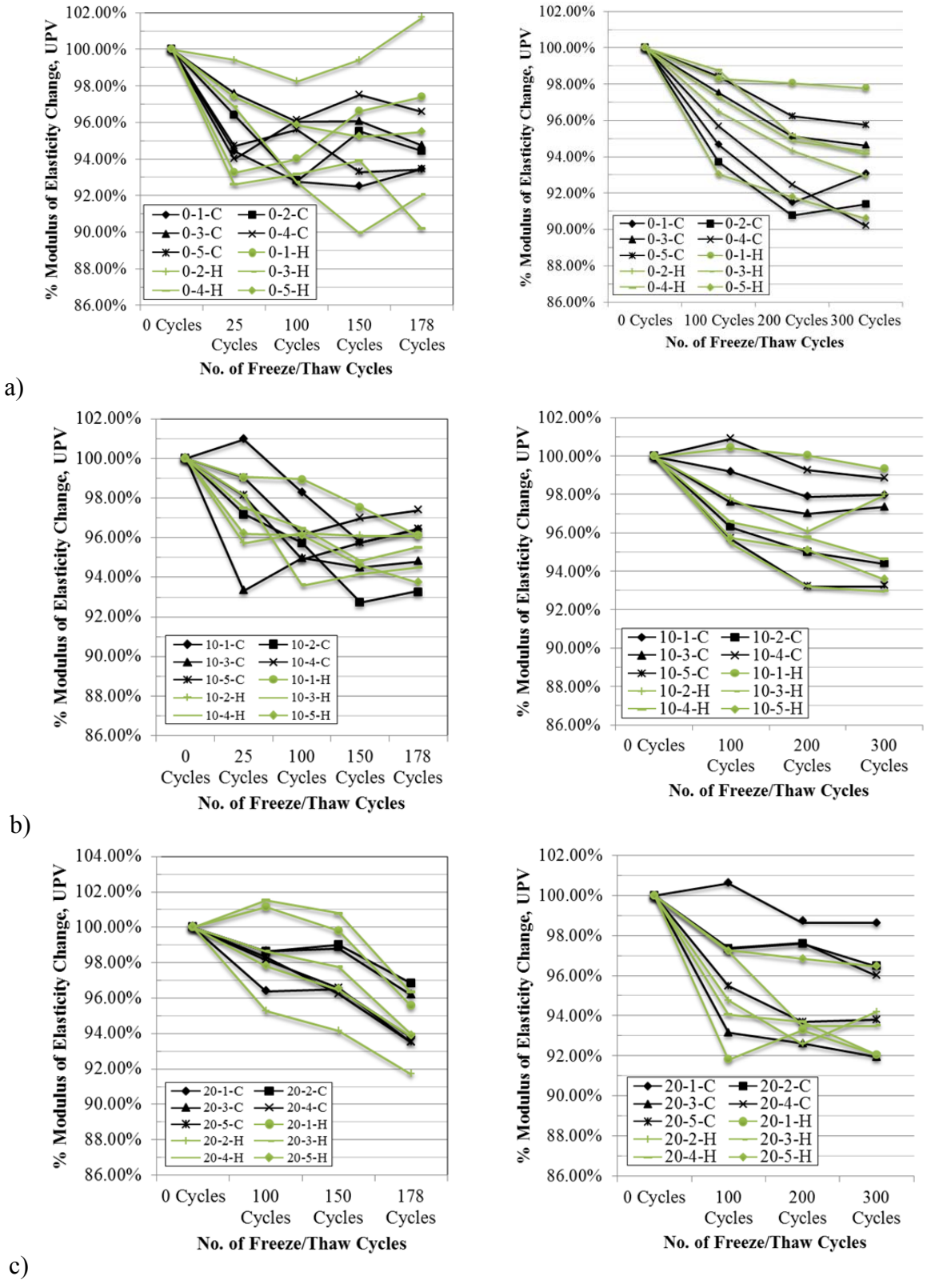

Figure B-17 - Percent change in the Dynamic Modulus of Elasticity for 178 (left) and 300 (right) F/T cycles.

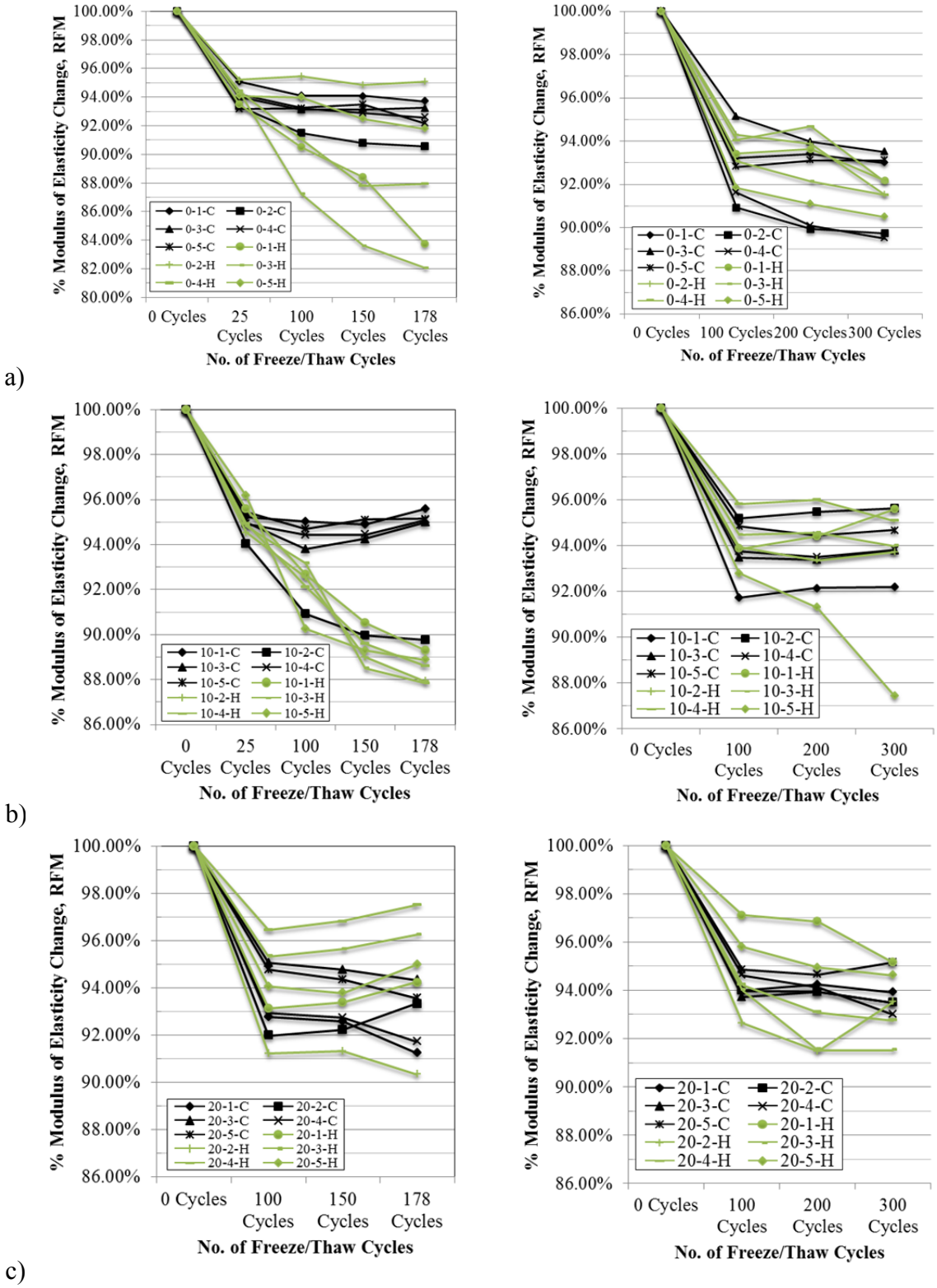

Figure B-18 - Percent change in the Dynamic Modulus of Elasticity for 178 (left) and 300 (right) F/T cycles.

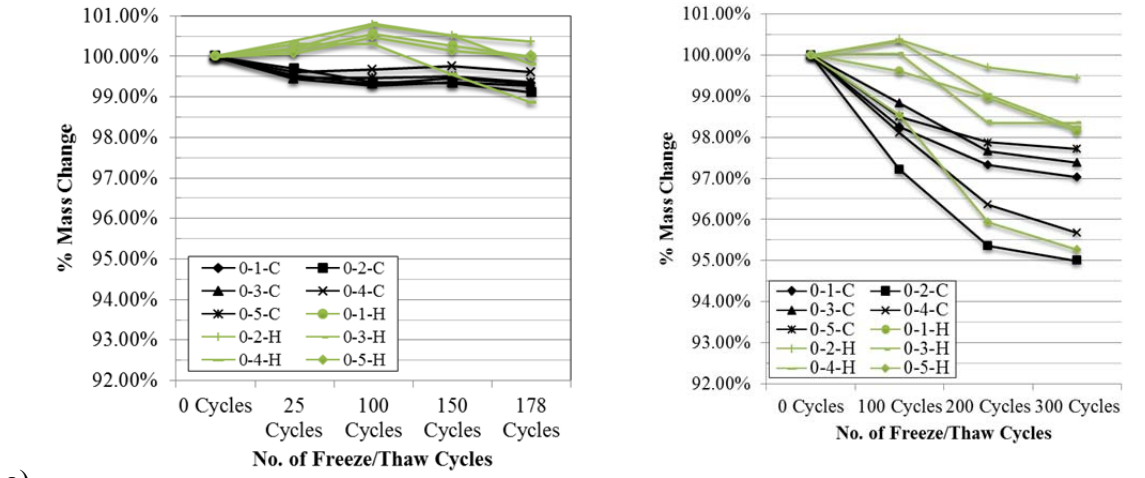

a)

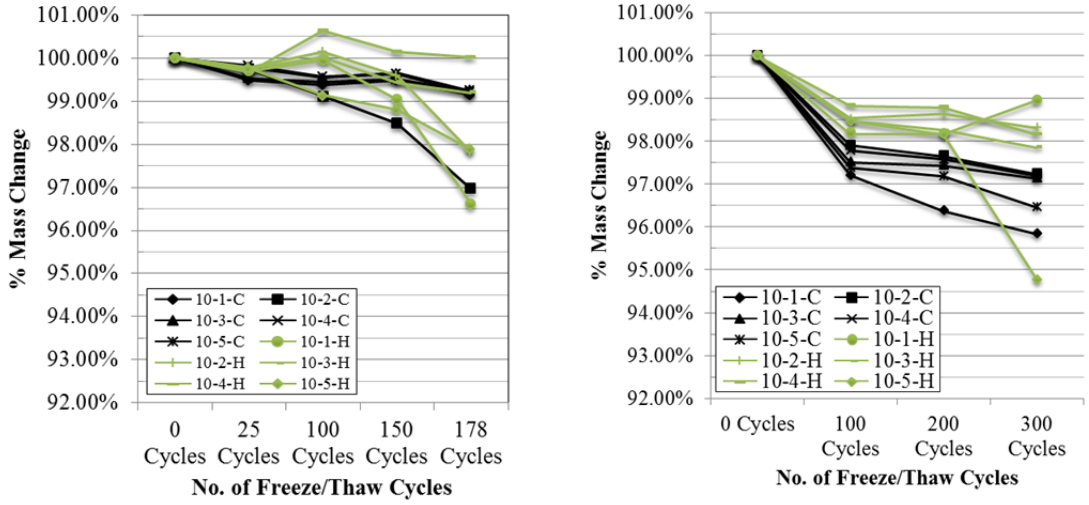

b)

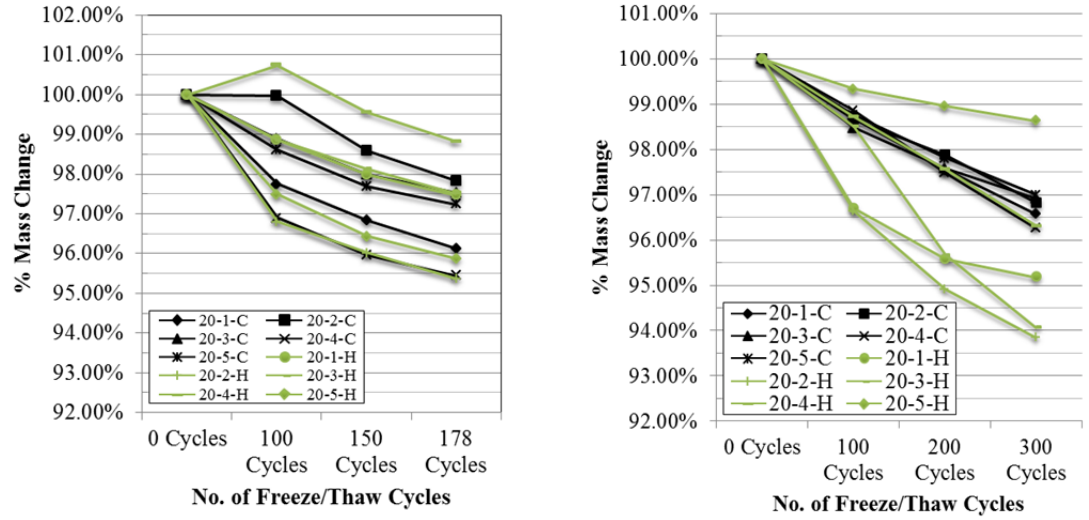

c)

Figure B-19 - Percent change in mass for 178 (left) and 300 (right) F/T cycles.

Appendix C

Appendix C Study 3

Figure C-1 - XRF testing of CRT glass

Figure C-2 - Diffusion leaching specimen

Figure C-3 - Modified diffusion leaching test setup

Table C-1 - Lead availability of CRT glass by EPA Method 3050B

Sample ID	Lead (mg/kg)	Sample ID	Lead (mg/kg)
CRT-1	4936	CRT-14	3893
CRT-2	4614	CRT-15	2806
CRT-3	2806	CRT-16	2724
CRT-4	5325	CRT-17	4122
CRT-5	6130	CRT-18	4147
CRT-6	6727	CRT-19	2526
CRT-7	3619	CRT-20	2310
CRT-8	4508	CRT-21	2719
CRT-9	4430	CRT-22	6050
CRT-10	4428	CRT-23	3652
CRT-11	6881	CRT-24	2377
CRT-12	6429	CRT-25	3051
CRT-13	1818	**AVERAGE**	4121

Table C-2 - Total lead content of CRT glass using XRF

Sample ID	Pb (mg/kg)	Pb +/-	Sample ID	Pb (mg/kg)	Pb +/-	Sample ID	Pb (mg/kg)	Pb +/-
CRT 1	52894	1331	**CRT 9**	50638	1161	**CRT 17**	46637	1031
CRT 1	51543	1150	**CRT 9**	54752	1236	**CRT 17**	50063	1094
CRT 1	58350	1169	**CRT 9**	59611	1232	**CRT 17**	55528	1306
CRT 2	58858	1377	**CRT 10**	56176	1231	**CRT 18**	52003	1236
CRT 2	53580	1162	**CRT 10**	58417	1271	**CRT 18**	53579	2876
CRT 2	56321	1295	**CRT 10**	62434	1413	**CRT 18**	57203	1356
CRT 3	59842	939	**CRT 11**	57820	1336	**CRT 19**	47666	1046
CRT 3	56130	695	**CRT 11**	54817	1277	**CRT 19**	58881	1371
CRT 3	58091	933	**CRT 11**	63028	1438	**CRT 19**	53395	1216
CRT 4	56739	1298	**CRT 12**	60064	1421	**CRT 20**	47857	1053
CRT 4	58750	1361	**CRT 12**	58034	1383	**CRT 20**	59130	1327
CRT 4	58132	1210	**CRT 12**	55364	1229	**CRT 20**	58158	1453
CRT 5	61296	1407	**CRT 13**	58213	1391	**CRT 21**	57018	1361
CRT 5	57561	1371	**CRT 13**	62566	1514	**CRT 21**	54969	1315
CRT 5	57443	1366	**CRT 13**	62107	1432	**CRT 21**	47740	1173
CRT 6	50767	1138	**CRT 14**	53628	1277	**CRT 22**	61885	1504
CRT 6	57359	1252	**CRT 14**	58896	1411	**CRT 22**	50851	1213
CRT 6	57469	1314	**CRT 14**	57680	1361	**CRT 22**	54444	1276
CRT 7	49743	1151	**CRT 15**	49052	951	**CRT 23**	51804	1151
CRT 7	50357	1167	**CRT 15**	52164	1208	**CRT 23**	49129	1136
CRT 7	55070	1297	**CRT 15**	58056	1374	**CRT 23**	50391	1133
CRT 8	58527	1338	**CRT 16**	48995	1250	**CRT 24**	55645	1266
CRT 8	59678	1361	**CRT 16**	56073	1315	**CRT 24**	58269	1340
CRT 8	54215	1050	**CRT 16**	55904	1370	**CRT 24**	55471	1305

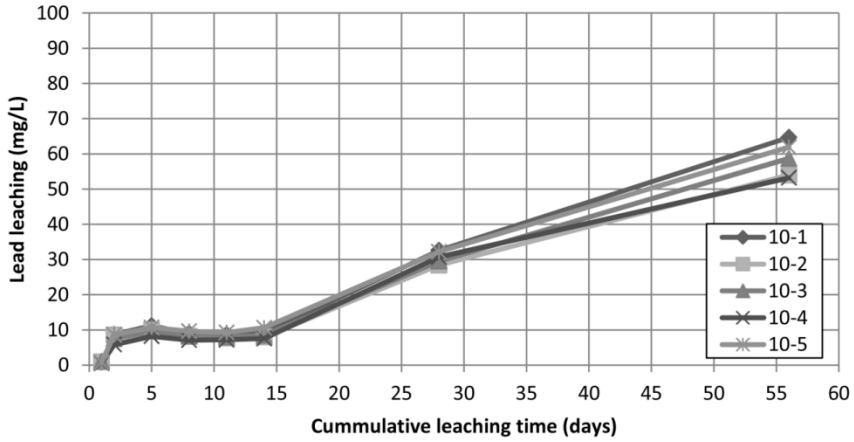

Figure C-4 - Interval lead leaching for 10% ASR CRT mixture

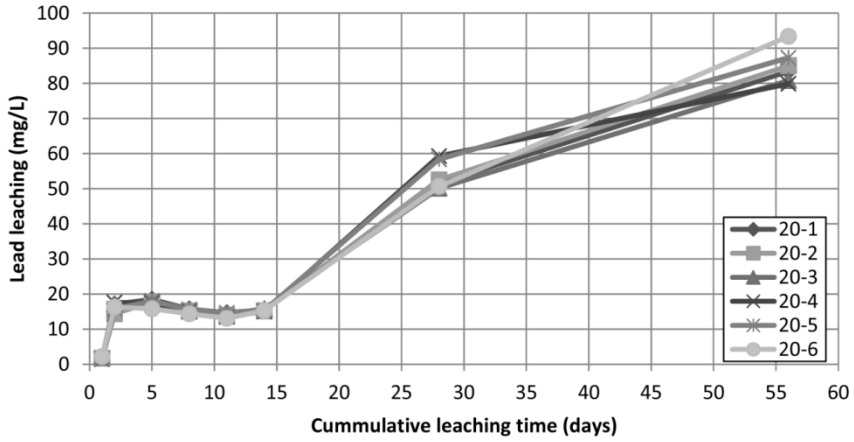

Figure C-5 - Interval lead leaching for 20% ASR CRT mixture

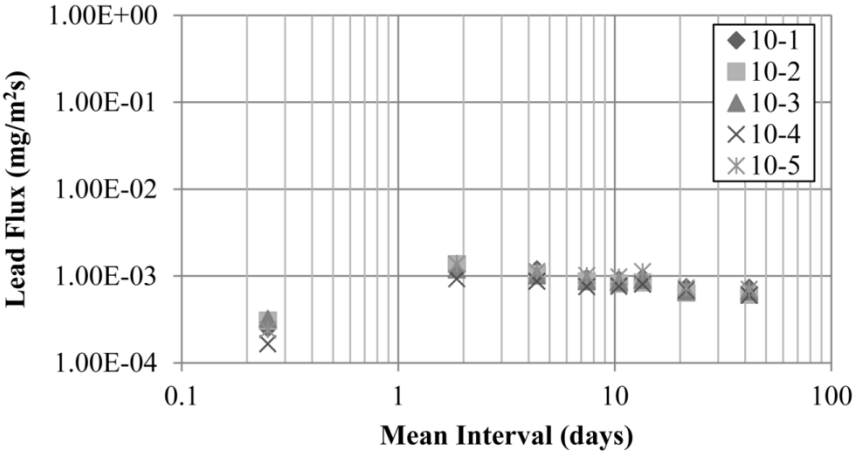

Figure C-6 - Mass flux for lead in 10% ASR CRT mixture

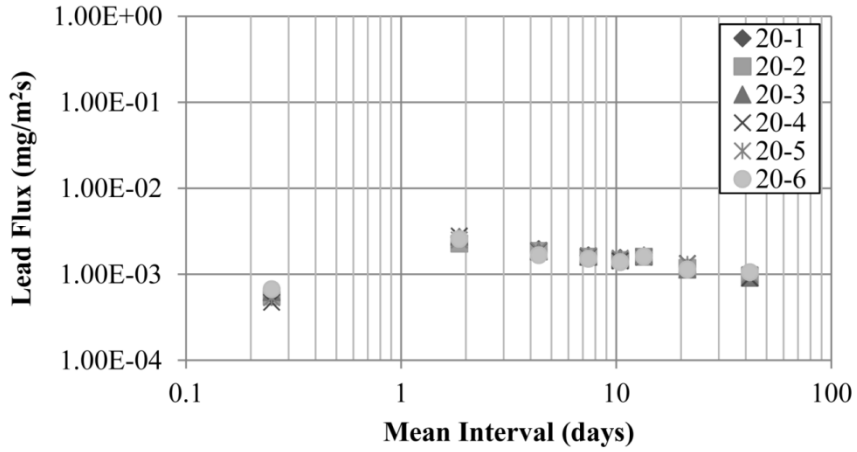

Figure C-7 - Mass flux for lead in 20% ASR CRT mixture

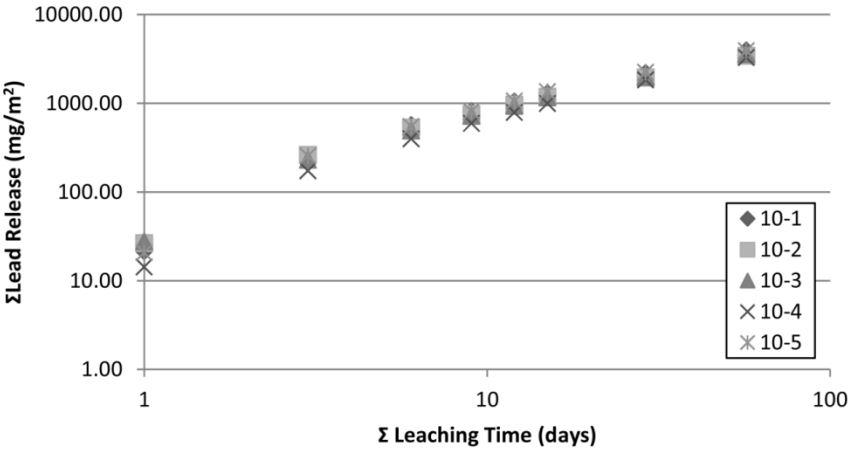

Figure C-8 - Cumulative lead leaching for 10% ASR CRT Mixture

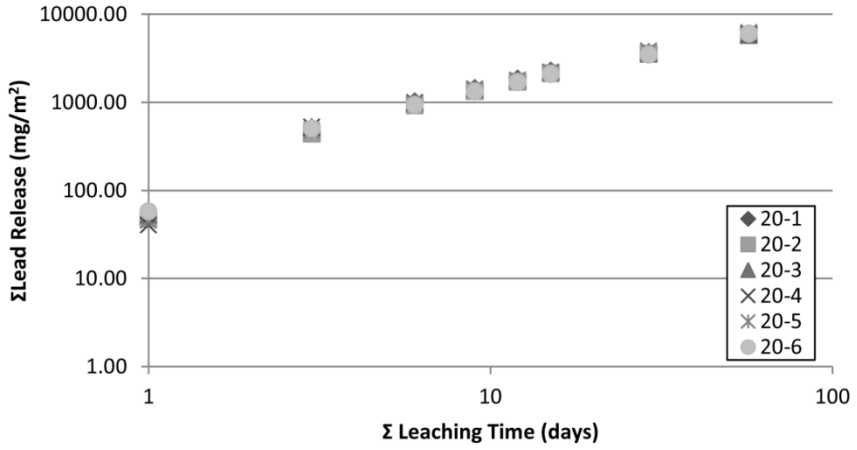

Figure C-9 - Cumulative lead leaching for 20% ASR CRT Mixture

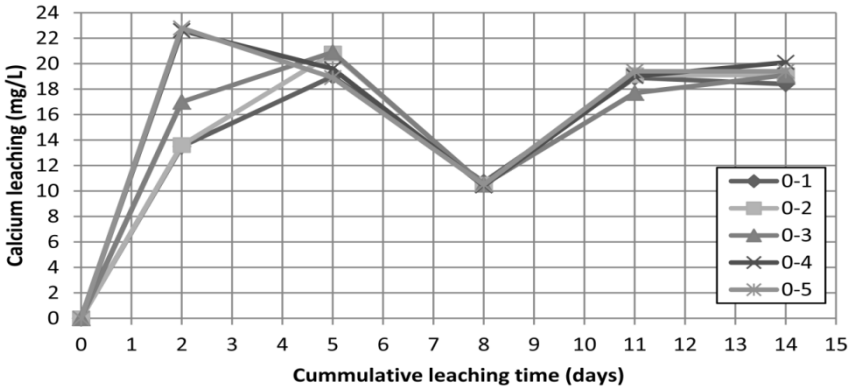

Figure C-10 - Interval calcium leaching for 0% ASR CRT mixture

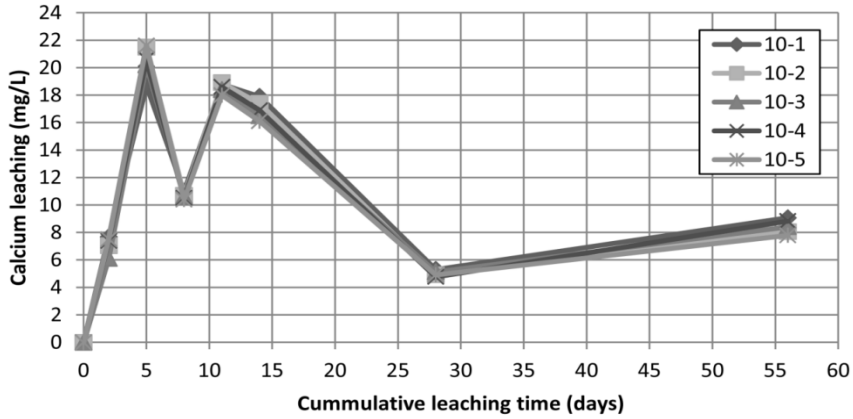

Figure C-11 - Interval calcium leaching for 10% ASR CRT mixture

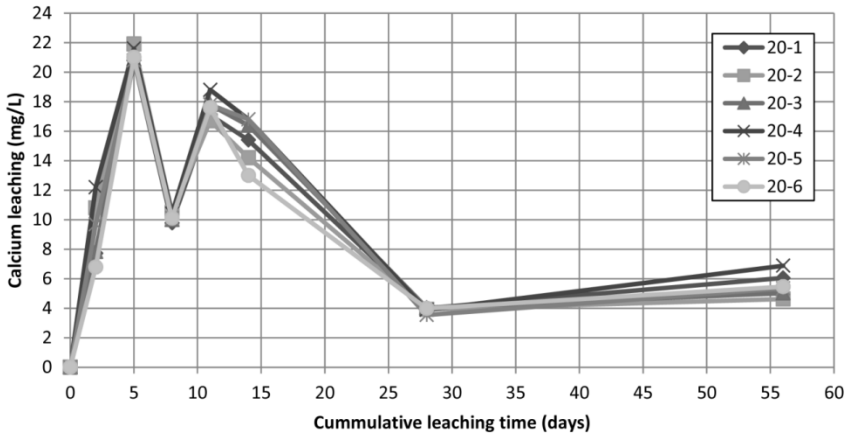

Figure C-12 - Interval calcium leaching for 20% ASR CRT mixture

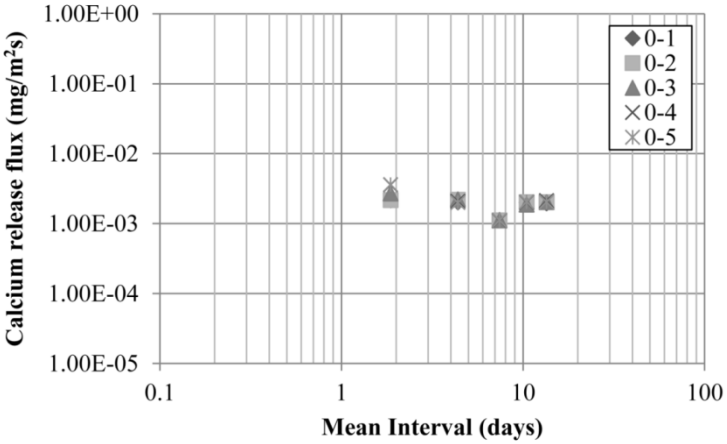

Figure C-13 - Mass flux for calcium in 0% ASR CRT mixture

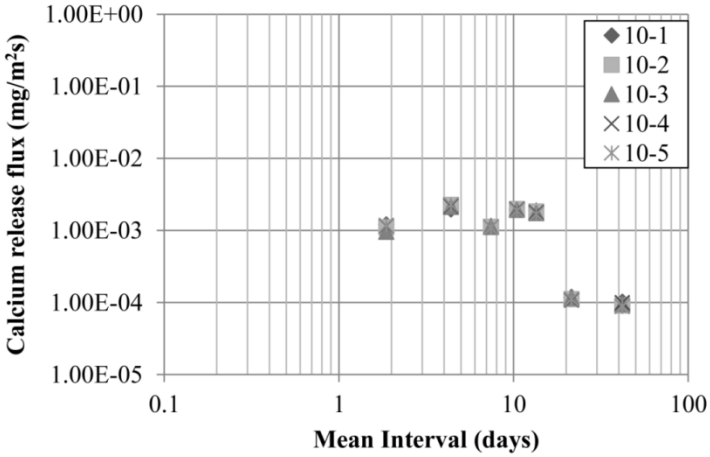

Figure C-14 - Mass flux for calcium in 10% ASR CRT mixture

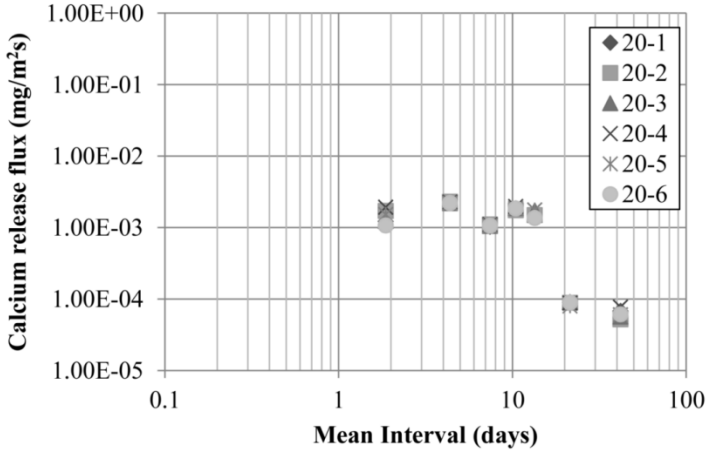

Figure C-15 - Mass flux for calcium in 20% ASR CRT mixture

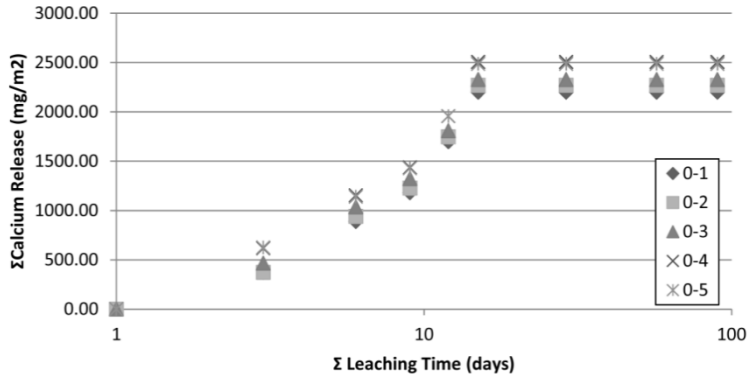

Figure C-16 - Cumulative calcium leaching for 0% ASR CRT mixture

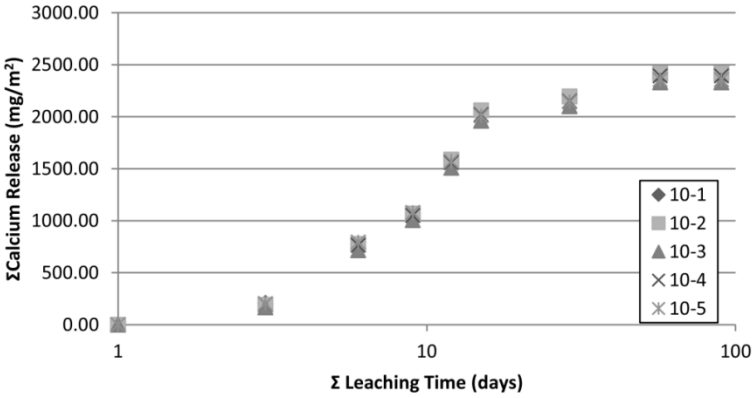

Figure C-17 - Cumulative calcium leaching for 10% ASR CRT mixture

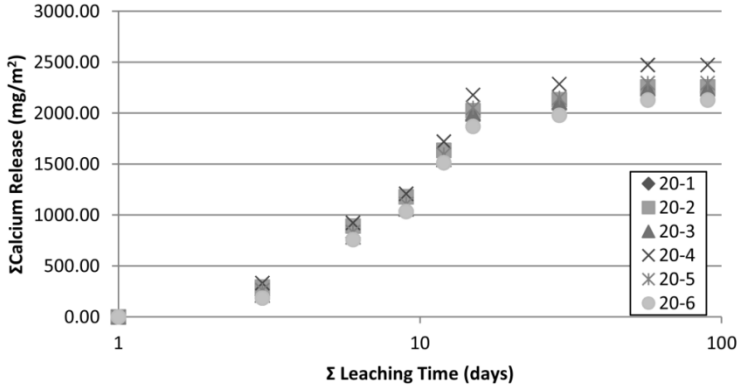

Figure C-18 - Cumulative calcium leaching for 20% ASR CRT mixture

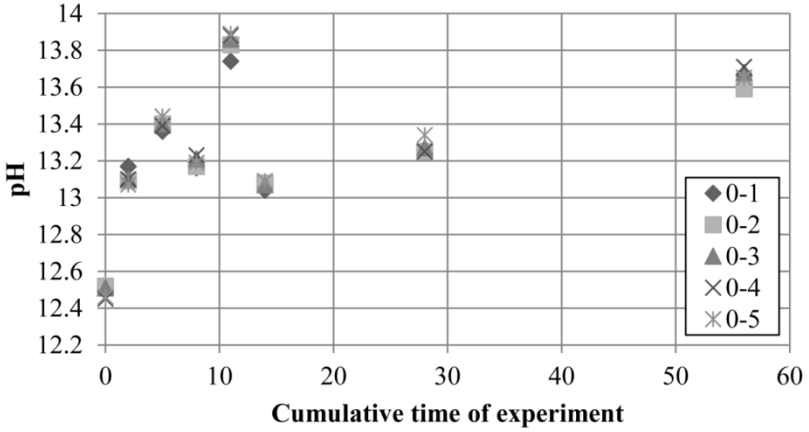

Figure C-19 - pH for ASR 0% ASR CRT Mixture

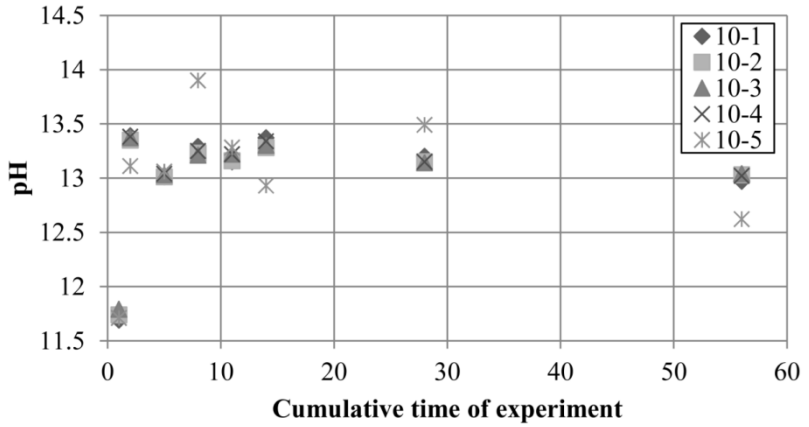

Figure C-20 - pH for ASR 10% ASR CRT Mixture

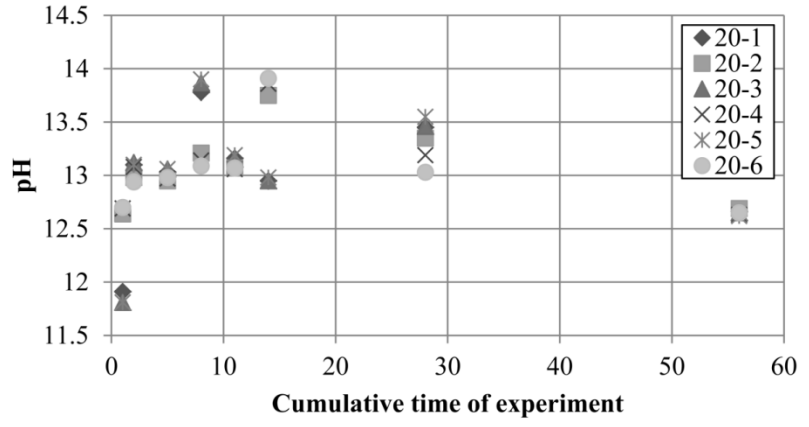

Figure C-21 - pH for ASR 20% ASR CRT Mixture

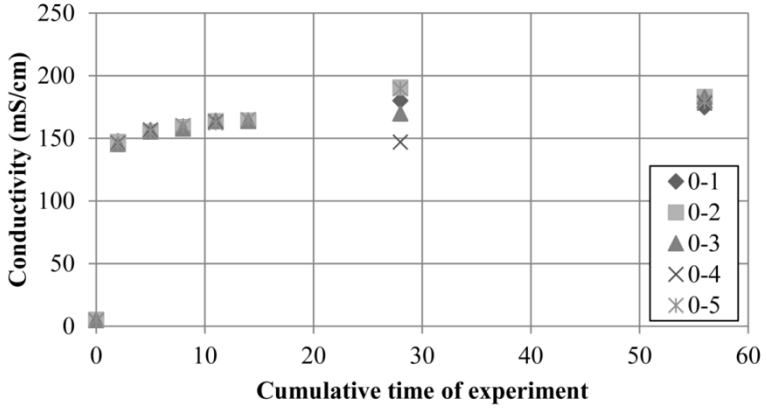

Figure C-22 - Conductivity for ASR 0% ASR CRT Mixture

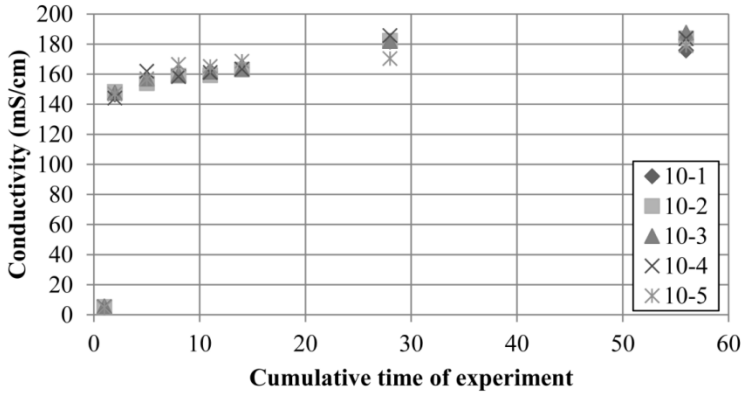

Figure C-23 - Conductivity for ASR 10% ASR CRT Mixture

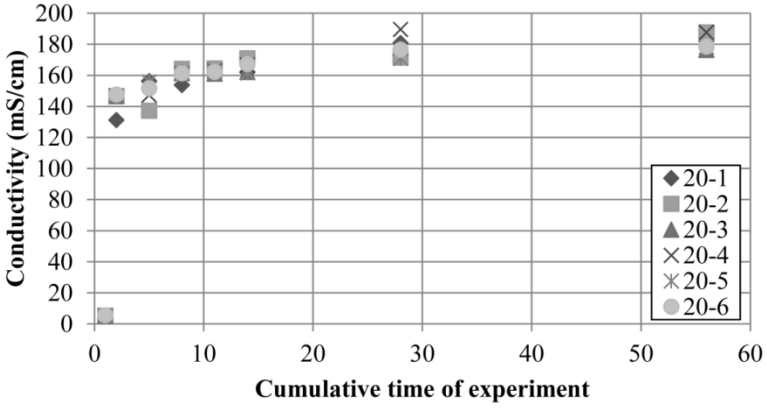

Figure C-24 - Conductivity for ASR 20% ASR CRT Mixture

a)

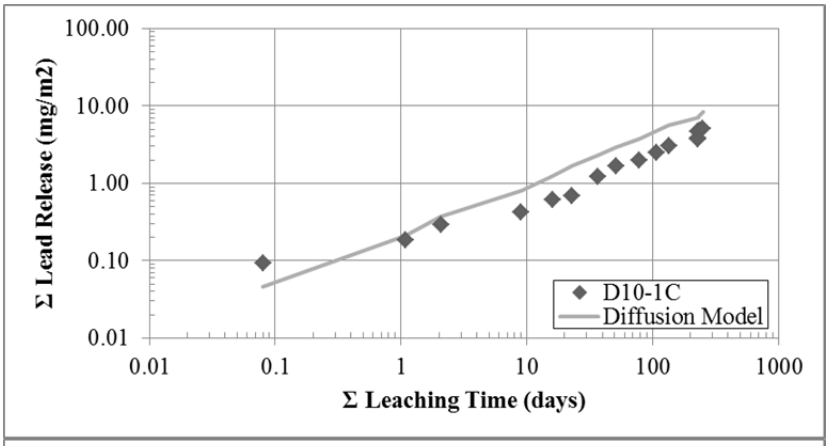
100.00
10.00
1.00
0.10
0.01
Σ Lead Release (mg/m2)
0.01
0.1
1
10
100
1000
Σ Leaching Time (days)
D10-1C
Diffusion Model

b)

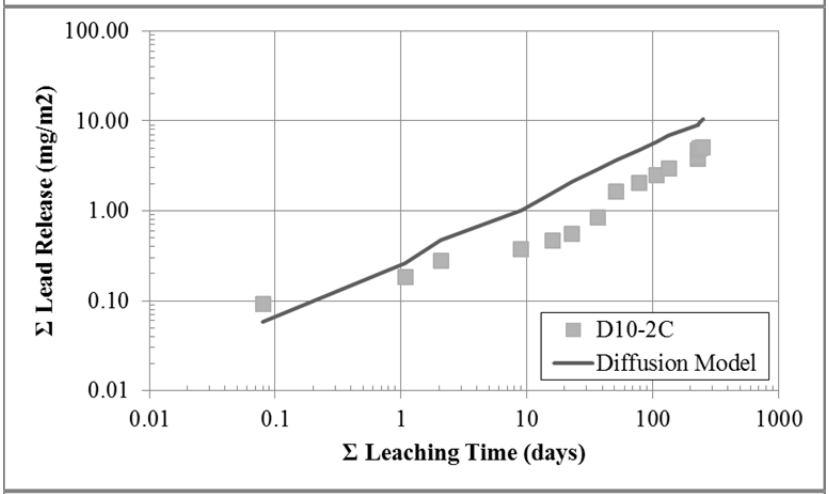
100.00
10.00
1.00
0.10
0.01
Σ Lead Release (mg/m2)
0.01
0.1
1
10
100
1000
Σ Leaching Time (days)
D10-2C
Diffusion Model

c)

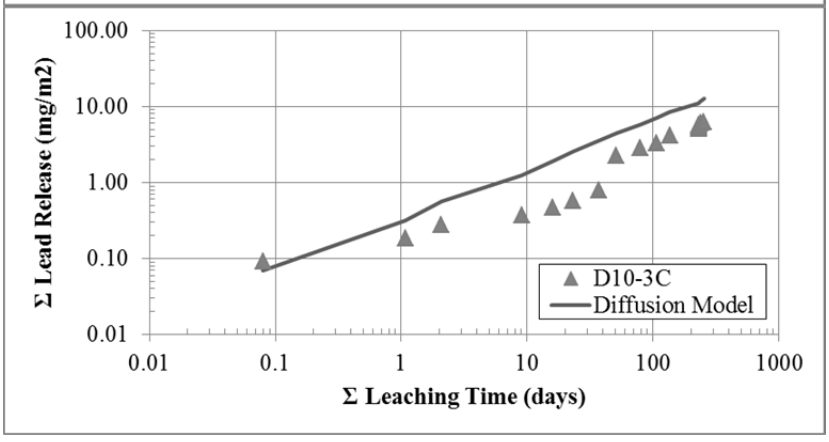
100.00
10.00
1.00
0.10
0.01
Σ Lead Release (mg/m2)
0.01
0.1
1
10
100
1000
Σ Leaching Time (days)
D10-3C
Diffusion Model

d)

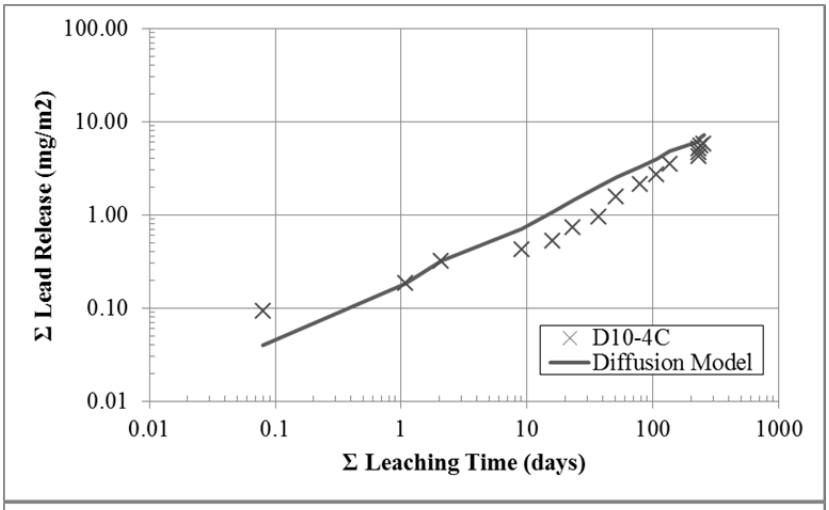
100.00
10.00
1.00
0.10
0.01
Σ Lead Release (mg/m2)
0.01
0.1
1
10
100
1000
Σ Leaching Time (days)
D10-4C
Diffusion Model

e)

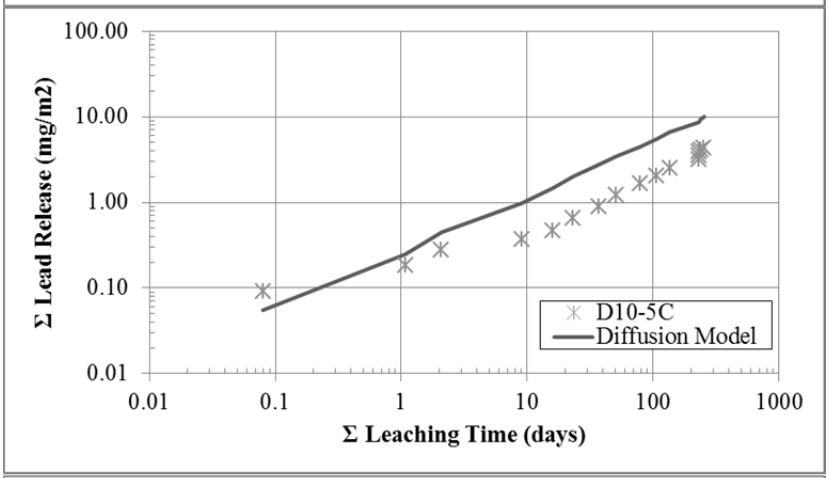
100.00
10.00
1.00
0.10
0.01
Σ Lead Release (mg/m2)
0.01
0.1
1
10
100
1000
Σ Leaching Time (days)
D10-5C
Diffusion Model

f)

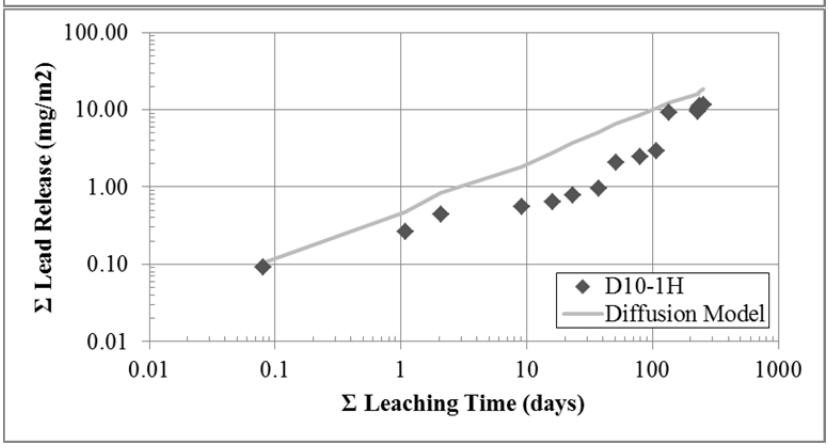
100.00
10.00
1.00
0.10
0.01
Σ Lead Release (mg/m2)
0.01
0.1
1
10
100
1000
Σ Leaching Time (days)
D10-1H
Diffusion Model

g)

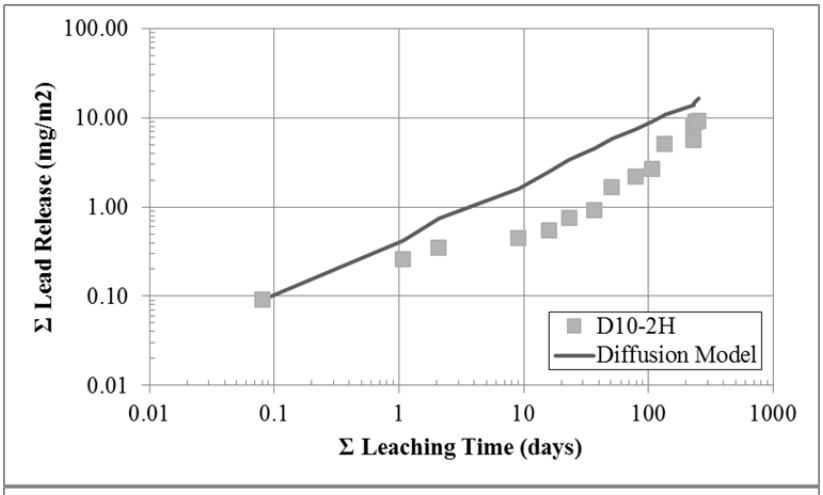
100.00
10.00
1.00
0.10
0.01
Σ Lead Release (mg/m2)
0.01
0.1
1
10
100
1000
Σ Leaching Time (days)
D10-2H
Diffusion Model

h)

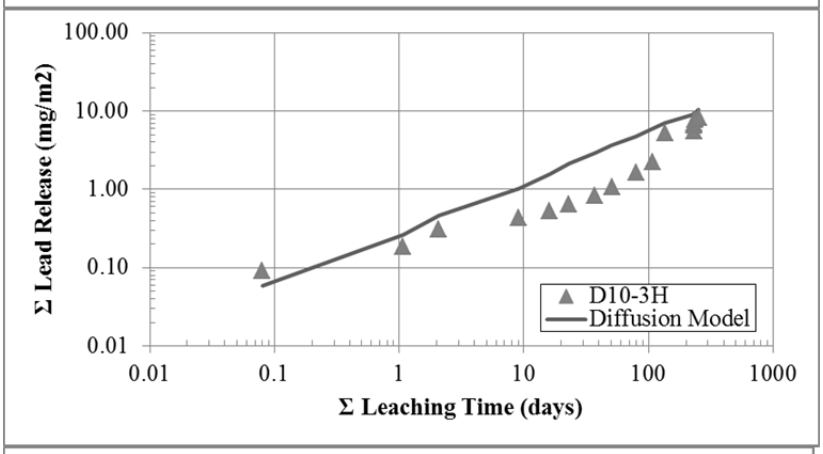
100.00
10.00
1.00
0.10
0.01
Σ Lead Release (mg/m2)
0.01
0.1
1
10
100
1000
Σ Leaching Time (days)
D10-3H
Diffusion Model

i)

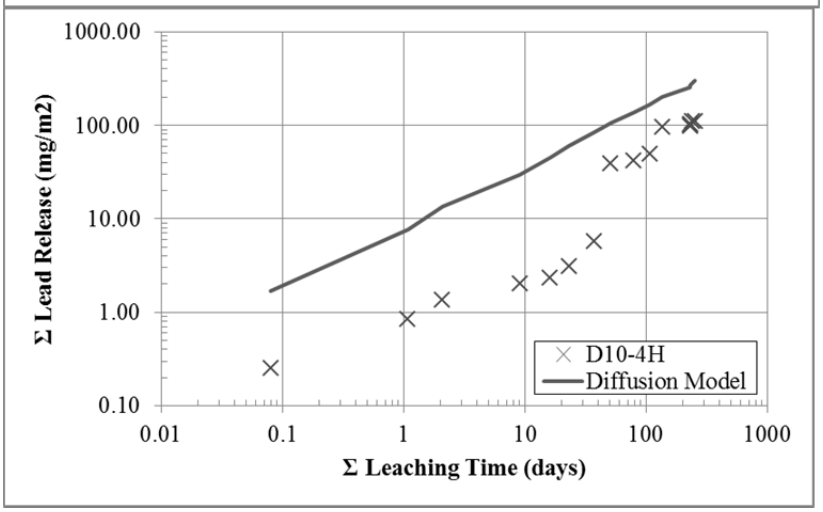
1000.00
100.00
10.00
1.00
0.10
Σ Lead Release (mg/m2)
0.01
0.1
1
10
100
1000
Σ Leaching Time (days)
D10-4H
Diffusion Model

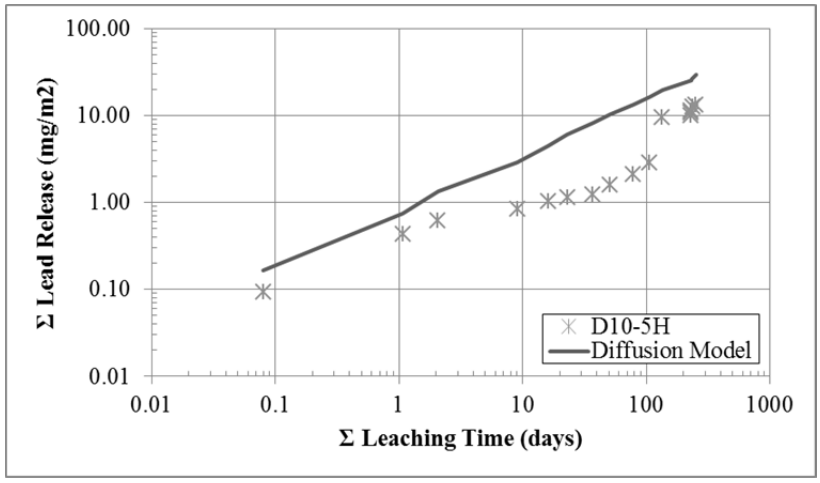

j)

Figure C-25 - 10% CRT Lead Diffusion specimens. (A-E: Cold, F-J: Hot environment)

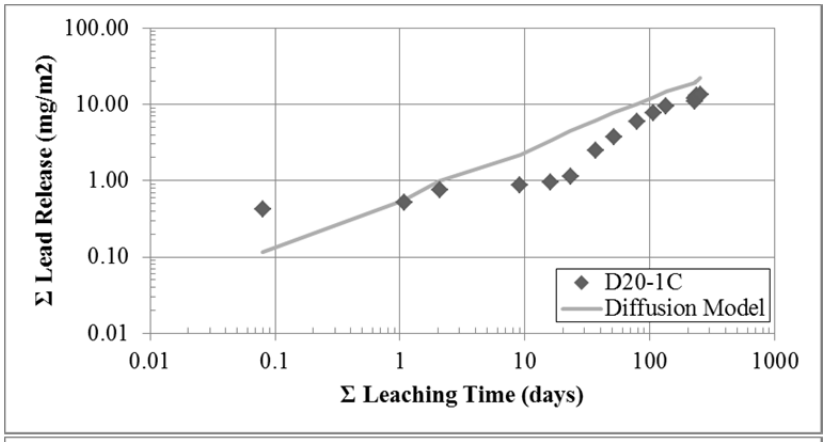

a)

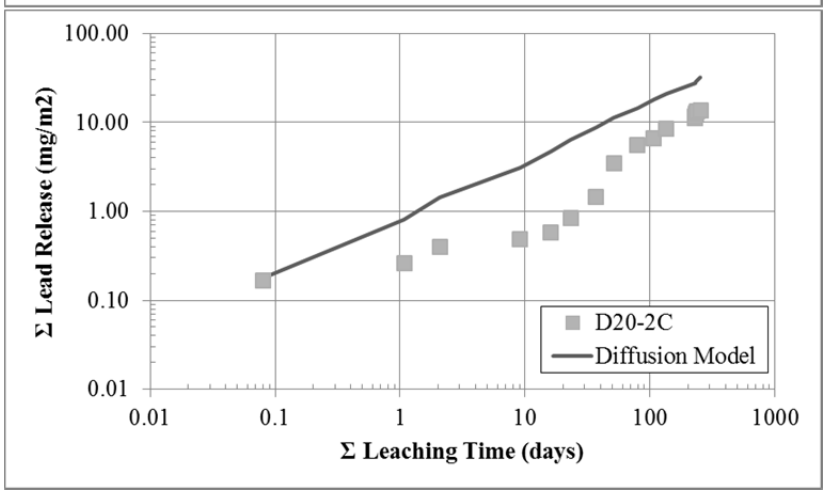

b)

c)

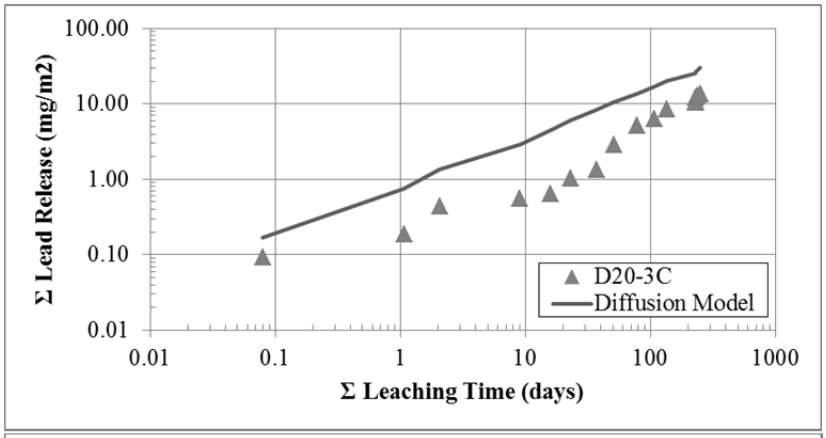
100.00
10.00
1.00
0.10
0.01
Σ Lead Release (mg/m2)
0.01
0.1
1
10
100
1000
Σ Leaching Time (days)
D20-3C
Diffusion Model

d)

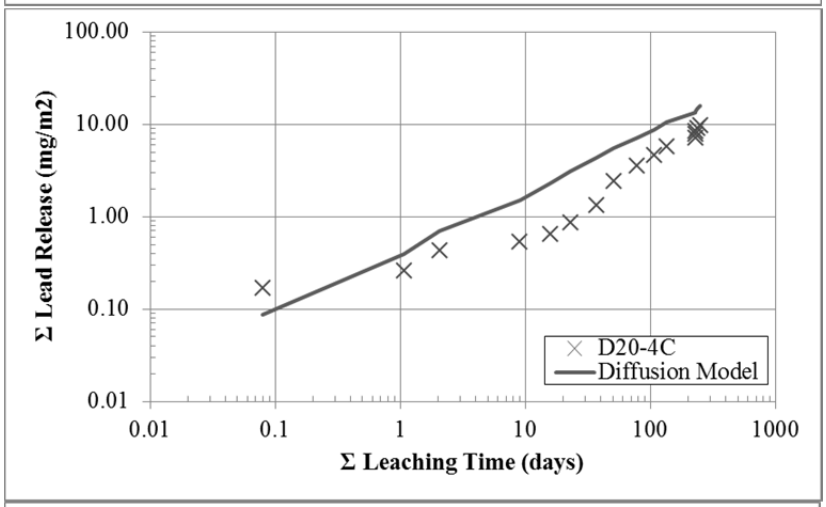
100.00
10.00
1.00
0.10
0.01
Σ Lead Release (mg/m2)
0.01
0.1
1
10
100
1000
Σ Leaching Time (days)
D20-4C
Diffusion Model

e)

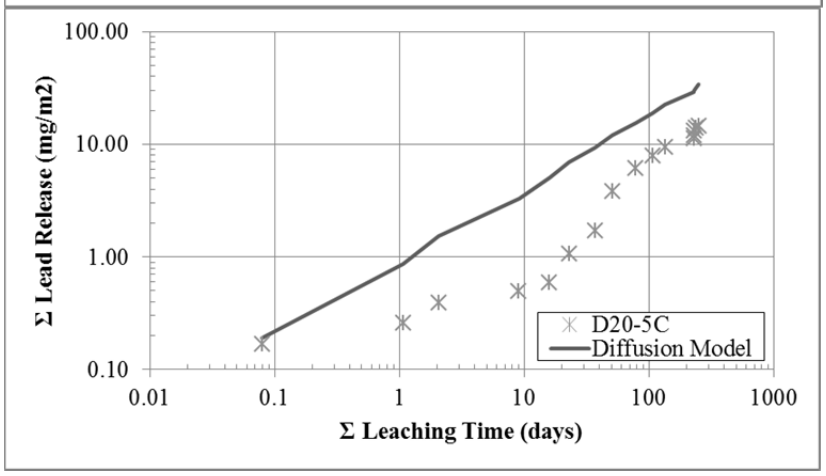
100.00
10.00
1.00
0.10
Σ Lead Release (mg/m2)
0.01
0.1
1
10
100
1000
Σ Leaching Time (days)
D20-5C
Diffusion Model

f)

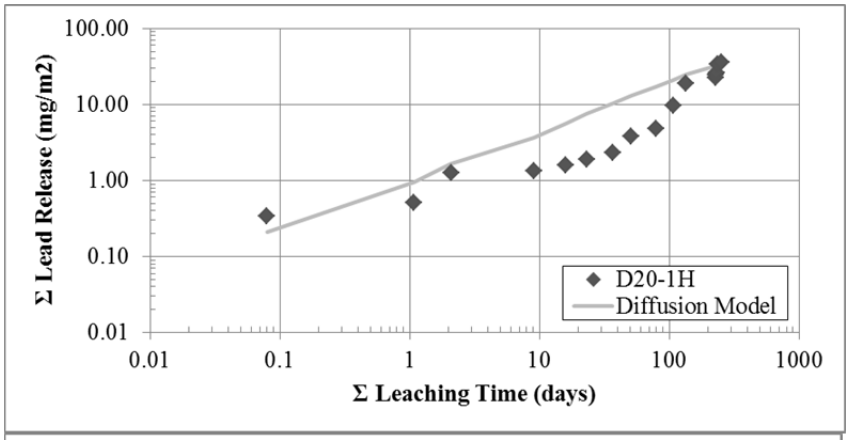
100.00
10.00
1.00
0.10
0.01
Σ Lead Release (mg/m2)
0.01
0.1
1
10
100
1000
Σ Leaching Time (days)
D20-1H
Diffusion Model

g)

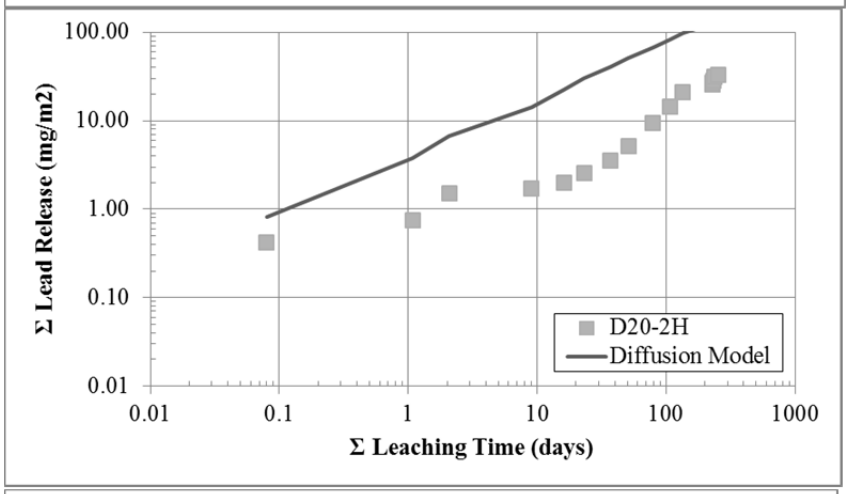
100.00
10.00
1.00
0.10
0.01
Σ Lead Release (mg/m2)
0.01
0.1
1
10
100
1000
Σ Leaching Time (days)
D20-2H
Diffusion Model

h)

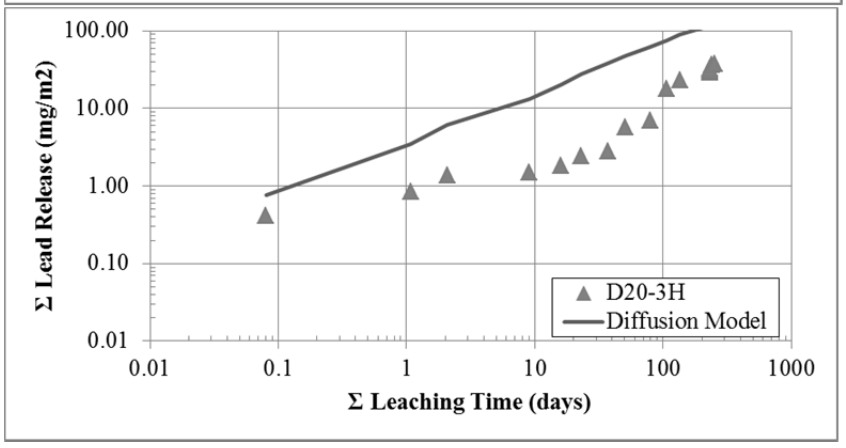
100.00
10.00
1.00
0.10
0.01
Σ Lead Release (mg/m2)
0.01
0.1
1
10
100
1000
Σ Leaching Time (days)
D20-3H
Diffusion Model

i)

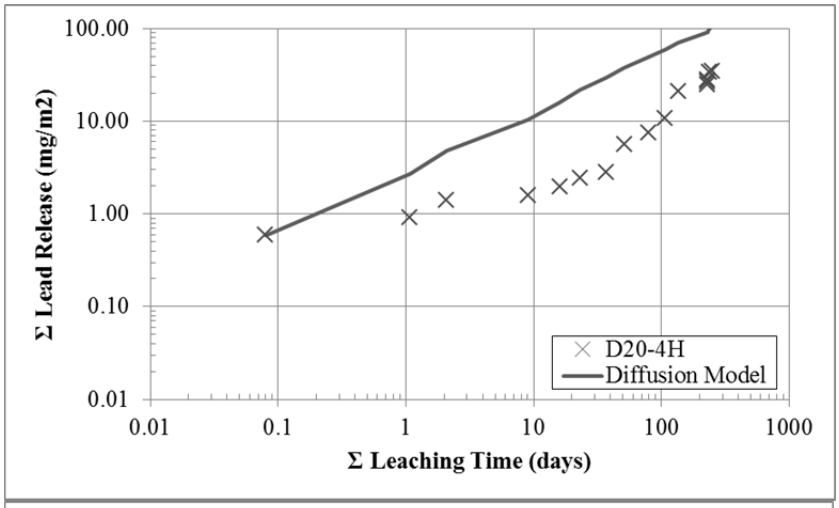

j)

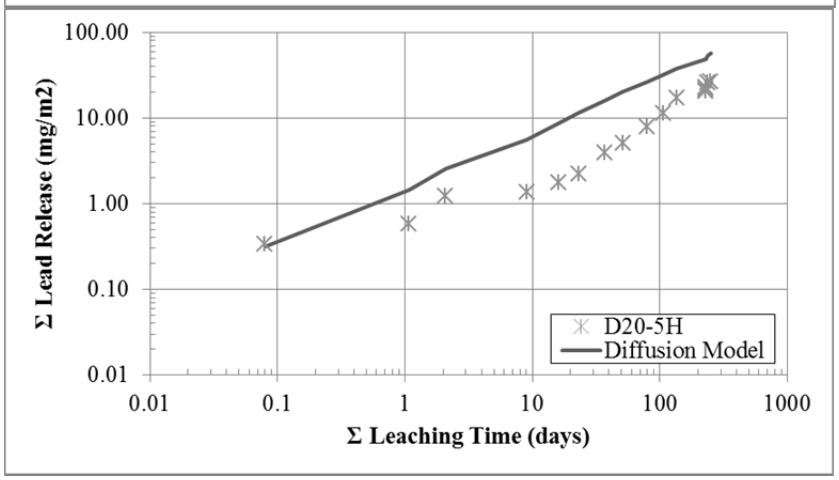

Figure C-26 - 20% CRT Lead Diffusion specimens. (A-E: Cold, F-J: Hot environment)

a)

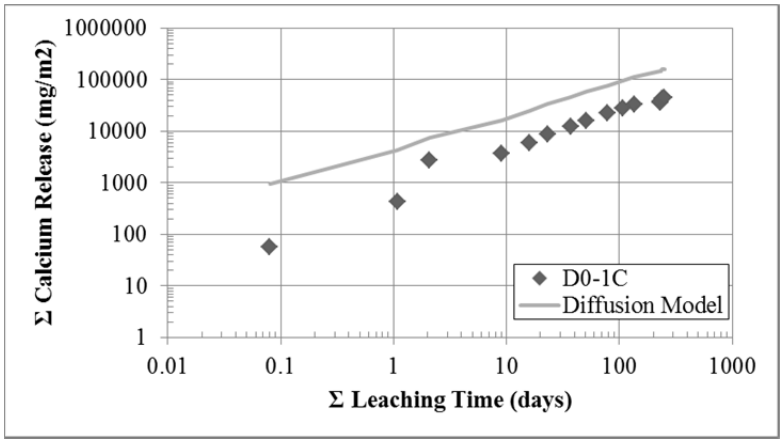

b)

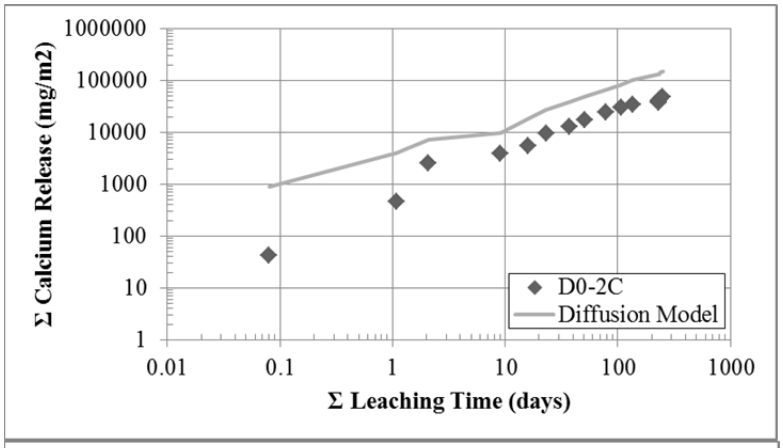
Σ Calcium Release (mg/m2)
1000000
100000
10000
1000
100
10
1
0.01
0.1
1
10
100
1000
Σ Leaching Time (days)
D0-2C
Diffusion Model

c)

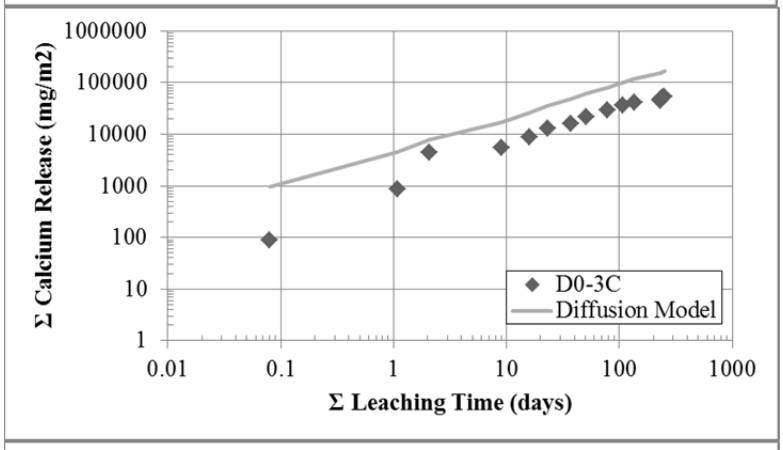
Σ Calcium Release (mg/m2)
1000000
100000
10000
1000
100
10
1
0.01
0.1
1
10
100
1000
Σ Leaching Time (days)
D0-3C
Diffusion Model

d)

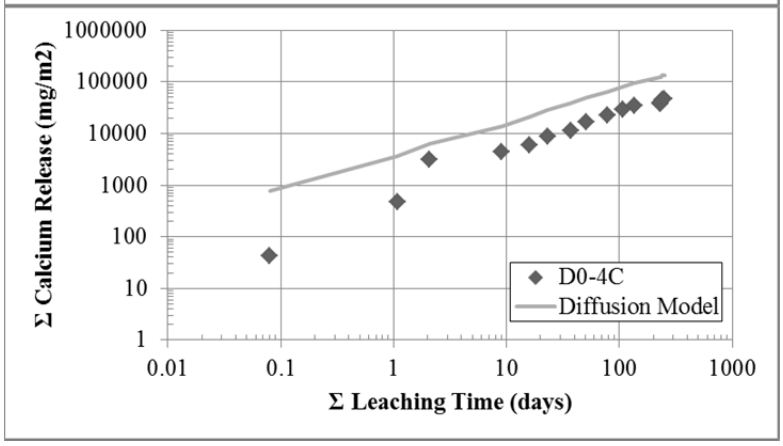
Σ Calcium Release (mg/m2)
1000000
100000
10000
1000
100
10
1
0.01
0.1
1
10
100
1000
Σ Leaching Time (days)
D0-4C
Diffusion Model

e)

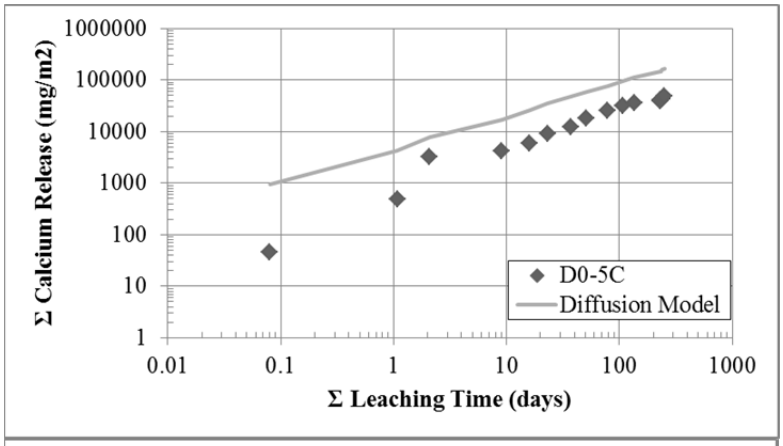
1000000
100000
10000
1000
100
10
1
0.01
0.1
1
10
100
1000
Σ Calcium Release (mg/m2)
Σ Leaching Time (days)
D0-5C
Diffusion Model

f)

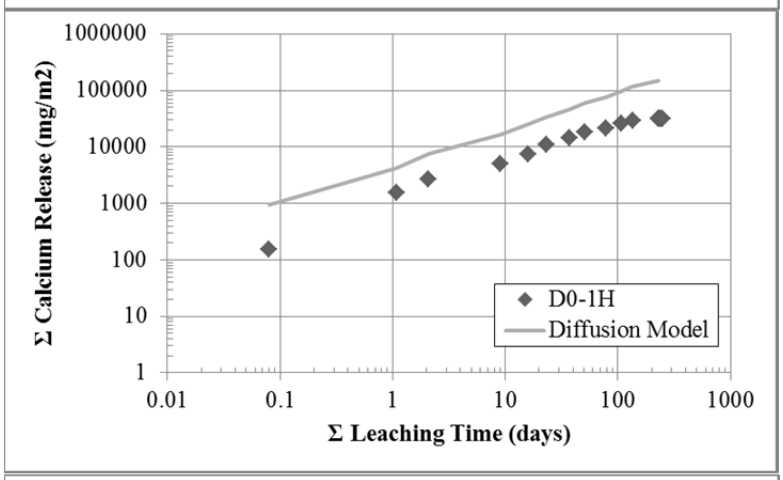
1000000
100000
10000
1000
100
10
1
0.01
0.1
1
10
100
1000
Σ Calcium Release (mg/m2)
Σ Leaching Time (days)
D0-1H
Diffusion Model

g)

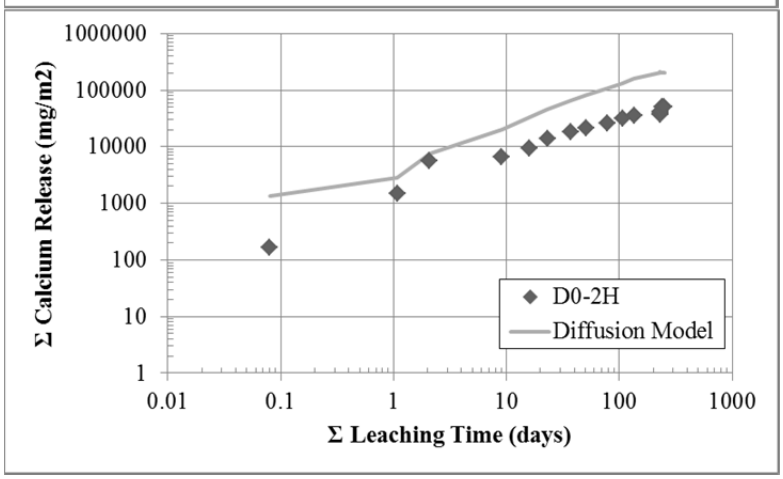
1000000
100000
10000
1000
100
10
1
0.01
0.1
1
10
100
1000
Σ Calcium Release (mg/m2)
Σ Leaching Time (days)
D0-2H
Diffusion Model

h)

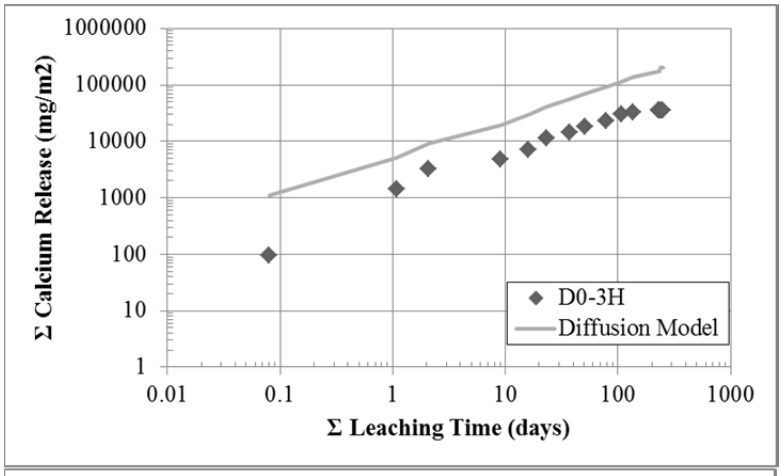

i)

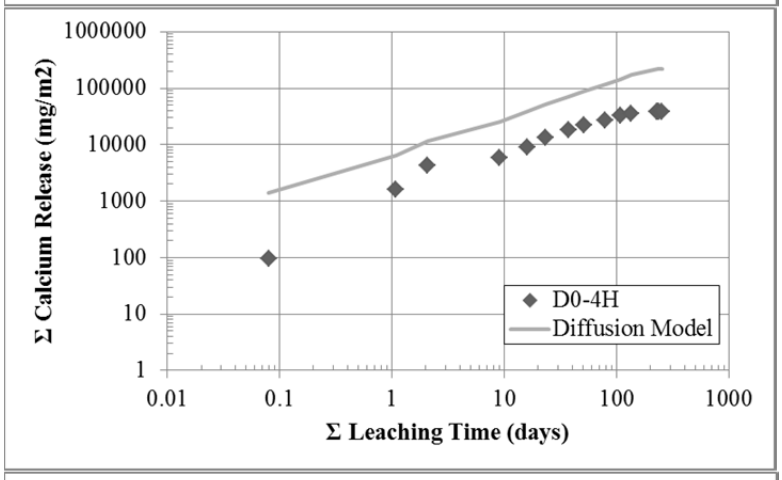

j)

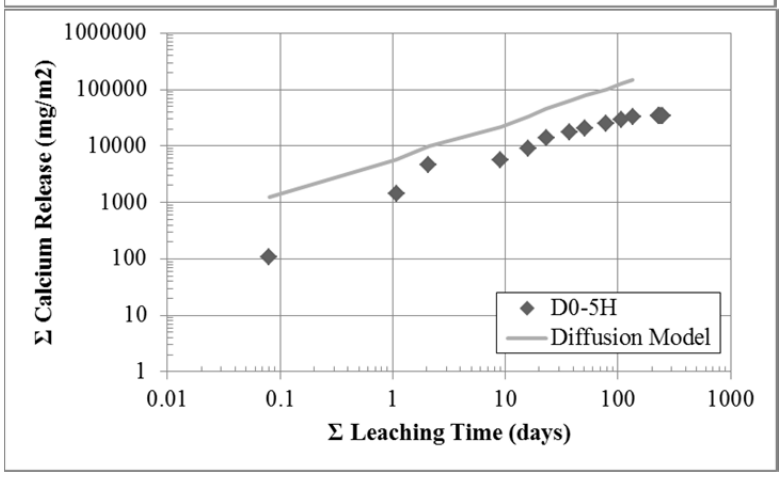

Figure C-27 - 0% CRT Calcium Diffusion specimens. (A-E: Cold, F-J: Hot environment)

a)

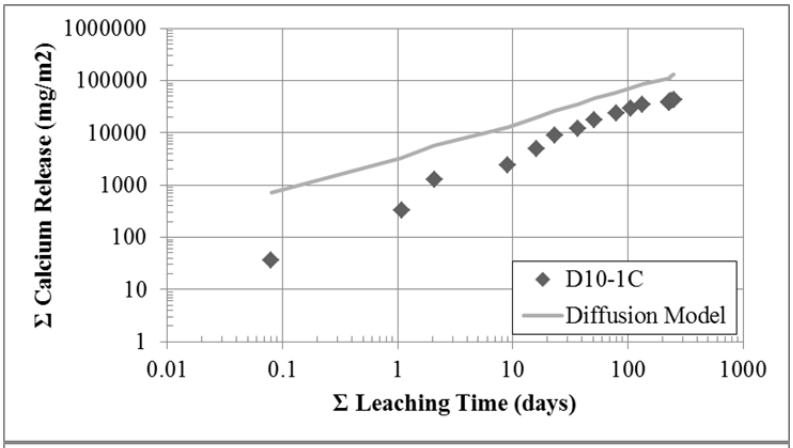
Σ Calcium Release (mg/m2)
1000000
100000
10000
1000
100
10
1
0.01
0.1
1
10
100
1000
Σ Leaching Time (days)
D10-1C
Diffusion Model

b)

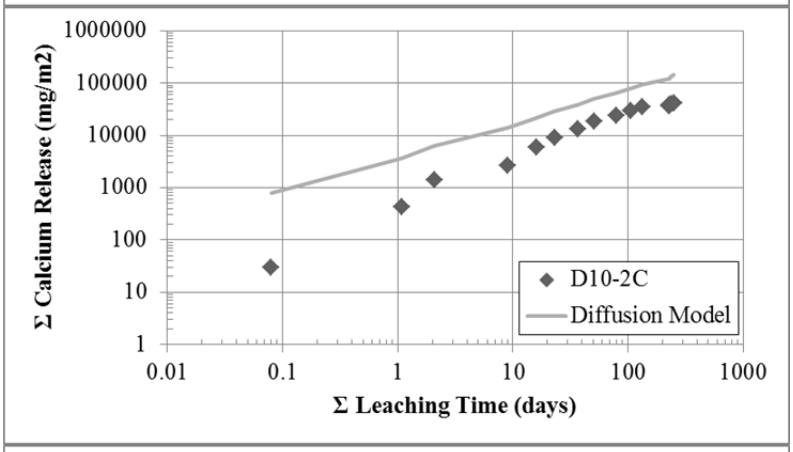
Σ Calcium Release (mg/m2)
1000000
100000
10000
1000
100
10
1
0.01
0.1
1
10
100
1000
Σ Leaching Time (days)
D10-2C
Diffusion Model

c)

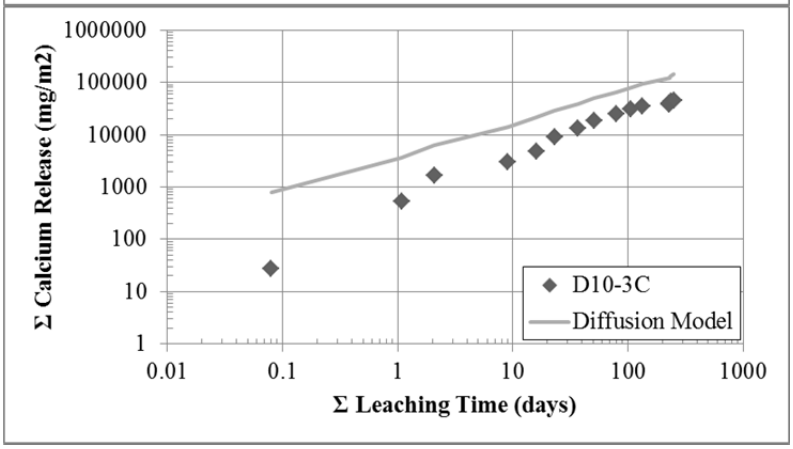
Σ Calcium Release (mg/m2)
1000000
100000
10000
1000
100
10
1
0.01
0.1
1
10
100
1000
Σ Leaching Time (days)
D10-3C
Diffusion Model

d)

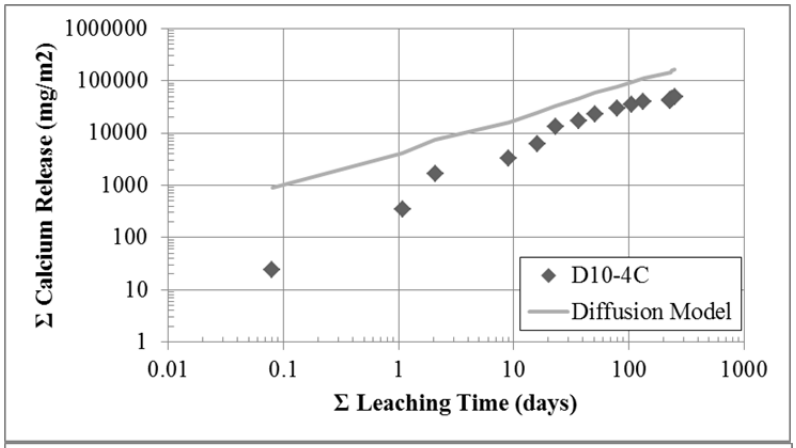
Σ Calcium Release (mg/m2)
1000000
100000
10000
1000
100
10
1
0.01
0.1
1
10
100
1000
Σ Leaching Time (days)
D10-4C
Diffusion Model

e)

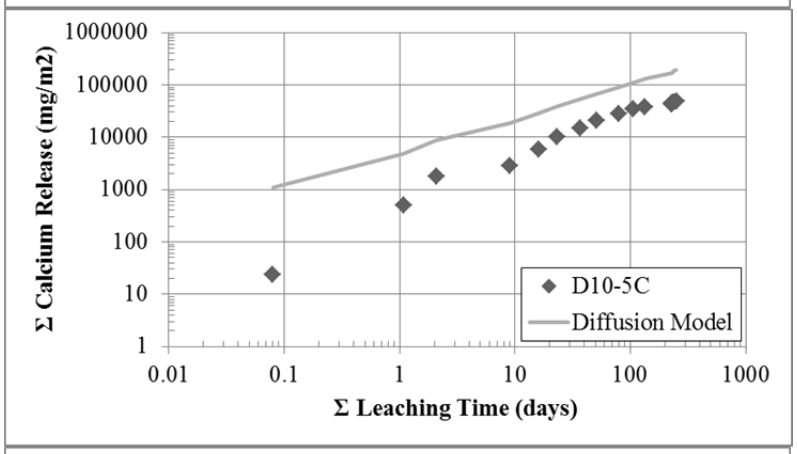
Σ Calcium Release (mg/m2)
1000000
100000
10000
1000
100
10
1
0.01
0.1
1
10
100
1000
Σ Leaching Time (days)
D10-5C
Diffusion Model

f)

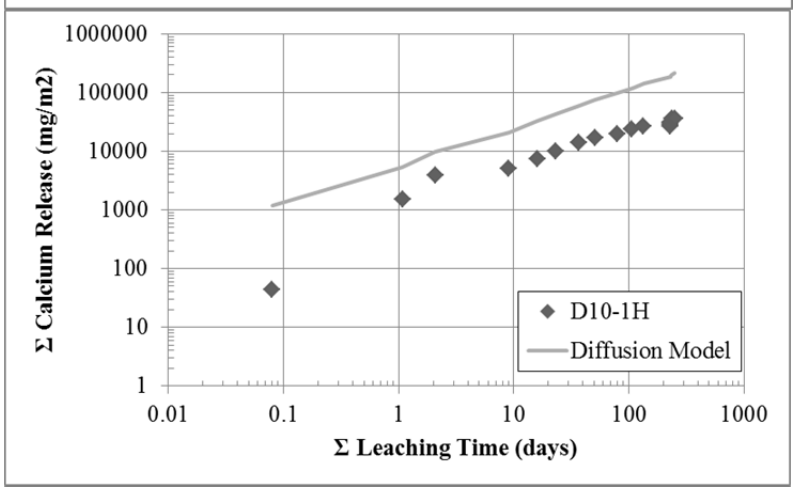
Σ Calcium Release (mg/m2)
1000000
100000
10000
1000
100
10
1
0.01
0.1
1
10
100
1000
Σ Leaching Time (days)
D10-1H
Diffusion Model

g)

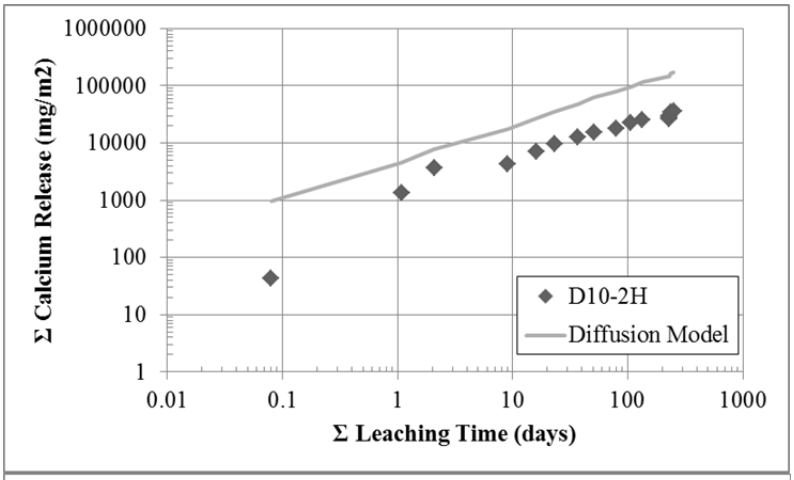
1000000
100000
10000
1000
100
10
1
Σ Calcium Release (mg/m2)
0.01
0.1
1
10
100
1000
Σ Leaching Time (days)
D10-2H
Diffusion Model

h)

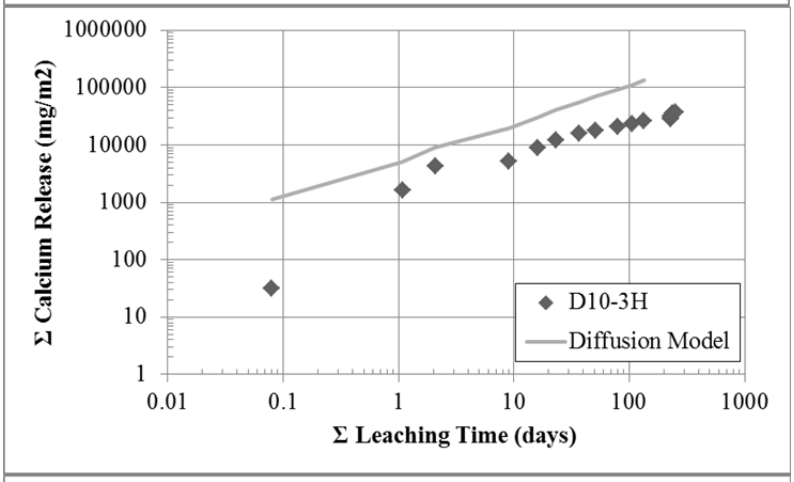
1000000
100000
10000
1000
100
10
1
Σ Calcium Release (mg/m2)
0.01
0.1
1
10
100
1000
Σ Leaching Time (days)
D10-3H
Diffusion Model

i)

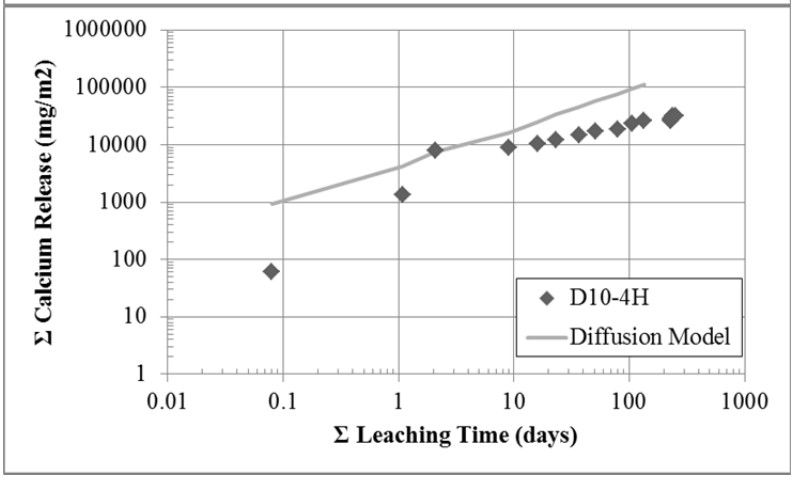
1000000
100000
10000
1000
100
10
1
Σ Calcium Release (mg/m2)
0.01
0.1
1
10
100
1000
Σ Leaching Time (days)
D10-4H
Diffusion Model

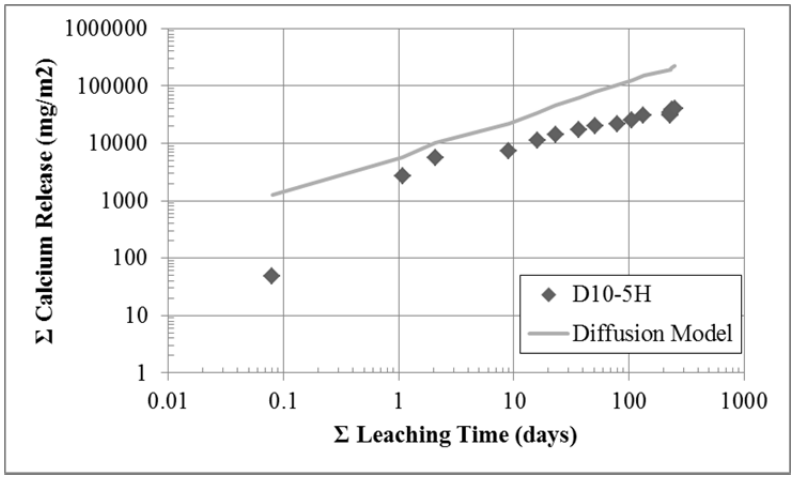

j)

Figure C-28 - 10% CRT Calcium Diffusion specimens. (A-E: Cold, F-J: Hot environment)

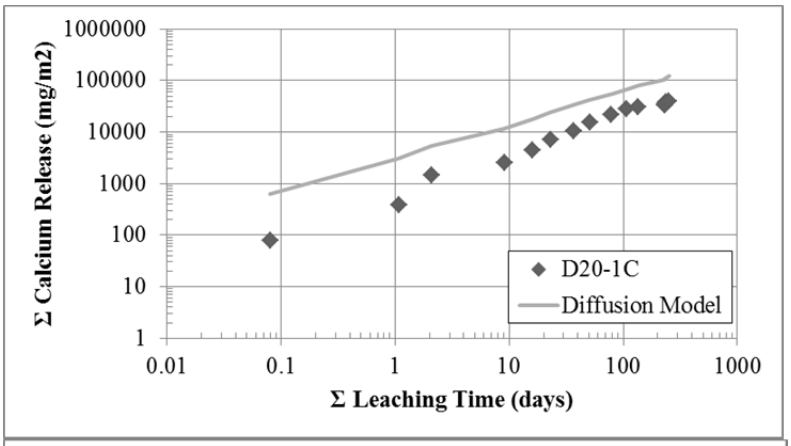

a)

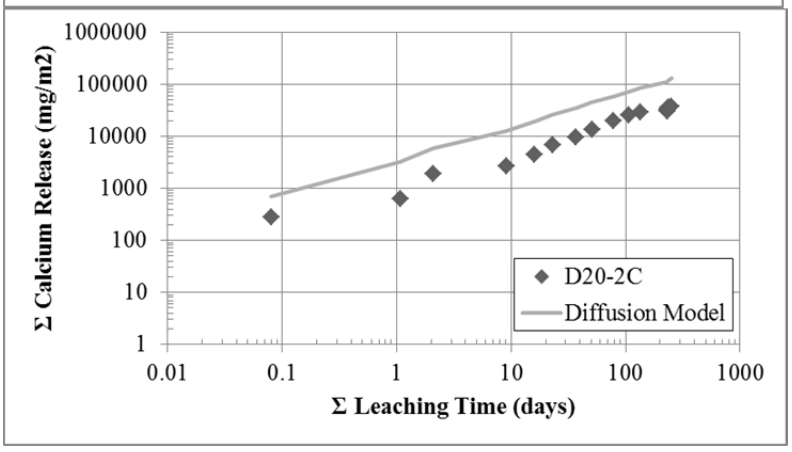

b)

c)

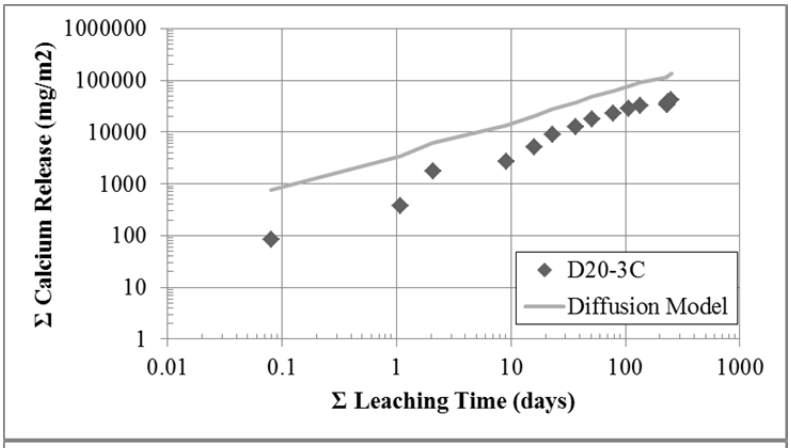
Σ Calcium Release (mg/m2)
1000000
100000
10000
1000
100
10
1
0.01
0.1
1
10
100
1000
Σ Leaching Time (days)
D20-3C
Diffusion Model

d)

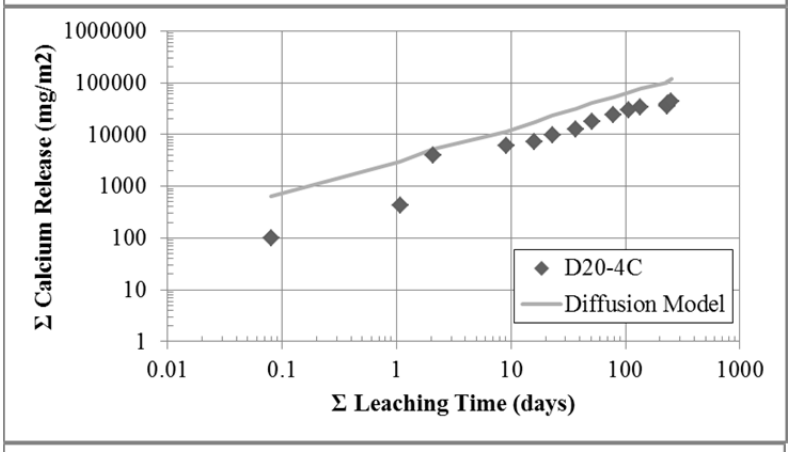
Σ Calcium Release (mg/m2)
1000000
100000
10000
1000
100
10
1
0.01
0.1
1
10
100
1000
Σ Leaching Time (days)
D20-4C
Diffusion Model

e)

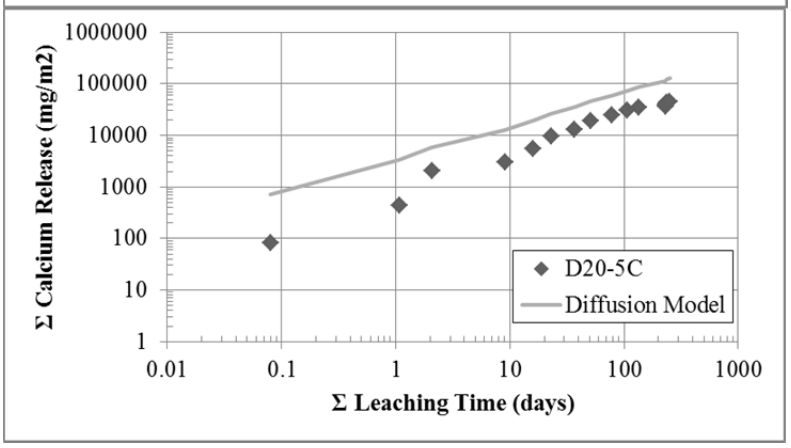
Σ Calcium Release (mg/m2)
1000000
100000
10000
1000
100
10
1
0.01
0.1
1
10
100
1000
Σ Leaching Time (days)
D20-5C
Diffusion Model

f)

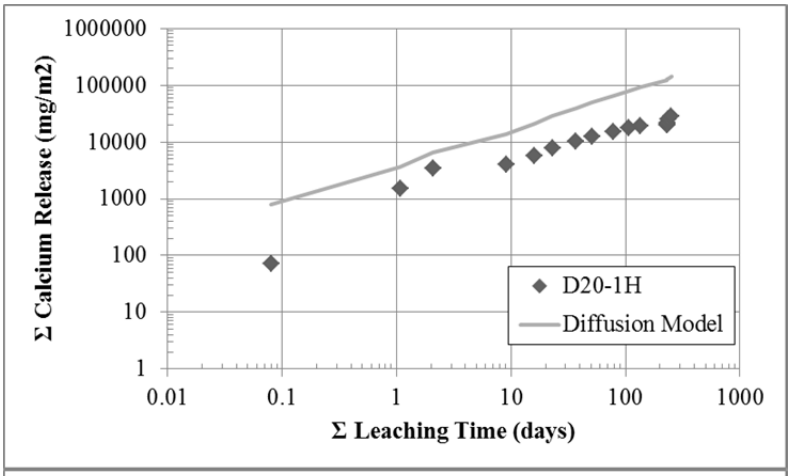
1000000
100000
10000
1000
100
10
1
Σ Calcium Release (mg/m2)
0.01
0.1
1
10
100
1000
Σ Leaching Time (days)
D20-1H
Diffusion Model

g)

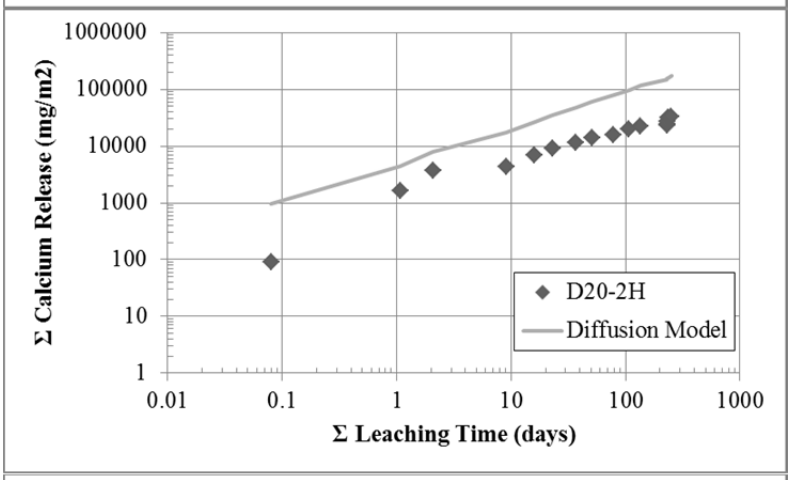
1000000
100000
10000
1000
100
10
1
Σ Calcium Release (mg/m2)
0.01
0.1
1
10
100
1000
Σ Leaching Time (days)
D20-2H
Diffusion Model

h)

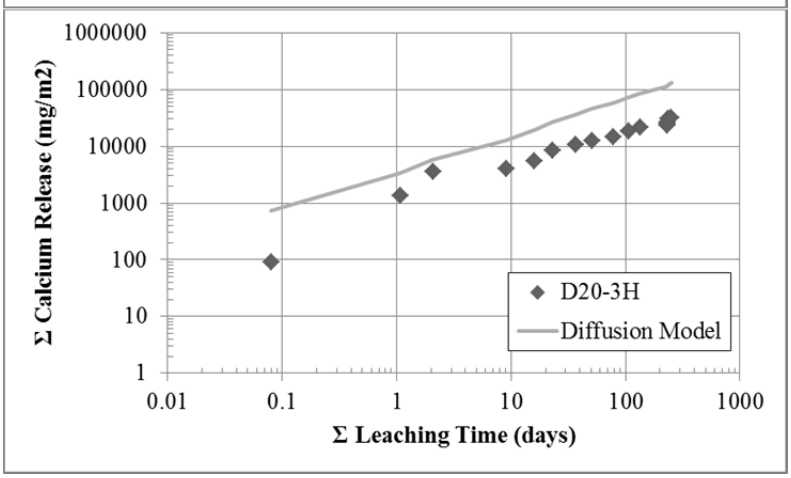
1000000
100000
10000
1000
100
10
1
Σ Calcium Release (mg/m2)
0.01
0.1
1
10
100
1000
Σ Leaching Time (days)
D20-3H
Diffusion Model

i)

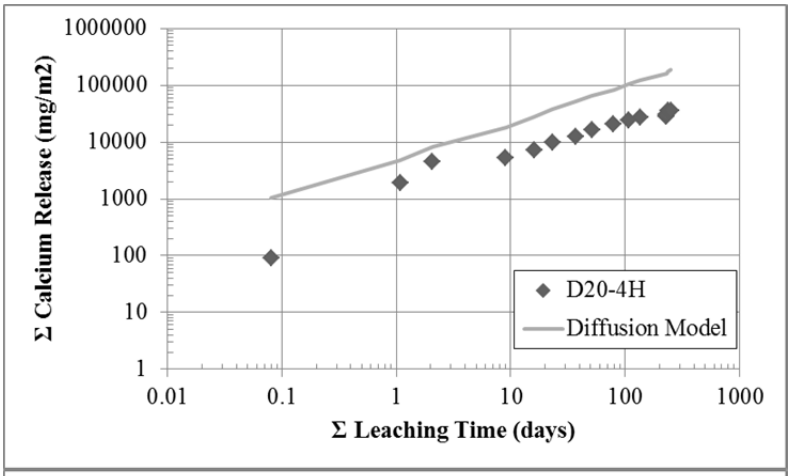

j)

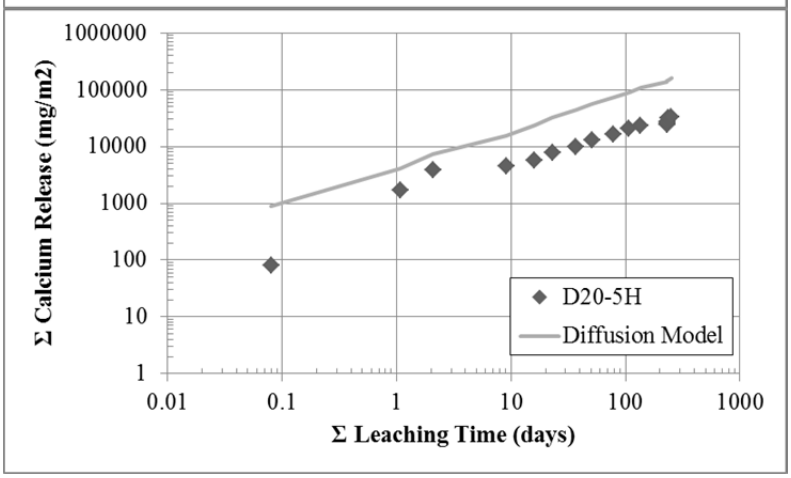

Figure C-29 - 20% CRT Calcium Diffusion specimens. (A-E: Cold, F-J: Hot environment)

Figure C-30 - Discoloration from Diffusion samples. Lighter samples were exposed to the hot environment

Figure C-31 - Residue left over by diffusion specimen

Table C-3 - Loss in mass and modulus of elasticity for control specimens

Specimen ID	Mass Retained (%)	Modulus of Elasticity Loss (%)
0-1-C	78.41%	94.20%
0-2-C	71.30%	93.91%
0-3-C	93.30%	95.22%
0-4-C	69.06%	92.77%
0-5-C	93.16%	96.70%
0-2-H	84.95%	90.24%

Table C-4 - Loss of mass and modulus of elasticity for 10% CRT-Concrete

Specimen ID	Mass Retained (%)	Modulus of Elasticity Loss (%)
10-1-C	91.39%	95.21%
10-2-C	93.96%	95.24%
10-3-C	92.82%	95.32%
10-4-C	93.64%	96.04%
10-5-C	85.07%	94.28%
10-1-H	75.46%	90.18%
10-2-H	81.97%	91.39%
10-3-H	82.17%	89.01%
10-4-H	90.58%	96.02%
10-5-H	82.46%	86.41%

Table C-5 - Loss of mass and modulus of elasticity for 20% CRT-Concrete

Specimen ID	Mass Retained (%)	Modulus of Elasticity Loss (%)
20-1-C	80.03%	95.66%
20-2-C	84.15%	96.04%
20-3-C	65.25%	95.70%
20-4-C	92.46%	96.25%
20-5-C	77.78%	94.77%
20-1-H	93.91%	96.96%
20-2-H	65.38%	89.76%
20-3-H	89.15%	93.17%
20-4-H	82.48%	92.73%
20-5-H	86.37%	93.05%

Table C-6 - Percent change in Lead flux versus Mass loss for 10% CRT Specimens

Specimen ID	Mass Retained	Percent Change in Lead Flux (%)			
		0.08 Days	1 Day	7 Days	14 Days
D10-2C	93.96%	172.7	718.2	81.8	-39.4
D10-4C	93.64%	354.5	354.5	316.7	15.4
D10-3C	92.82%	172.7	263.6	172.7	-23.1
D10-1C	91.39%	0.0	809.1	87.5	-66.7
D10-5C	85.07%	263.6	354.5	81.8	3.4
D10-4H	90.58%	266.7	200.0	1062.5	-52.5
D10-5H	82.46%	809.1	75.0	400.0	627.3
D10-3H	82.17%	990.9	445.5	542.9	117.4
D10-2H	81.97%	1900.0	350.0	718.2	100.0
D10-1H	75.46%	445.5	200.0	515.4	127.3

Table C-7 - Percent change in Lead flux versus Mass loss for 20% CRT Specimens

Specimen ID	Mass Retained	Percent Change in Lead Flux (%)			
		0.08 Days	1 Day	7 Days	14 Days
D20-4C	92.46%	250.0	627.3	-42.9	130.8
D20-2C	84.15%	300.0	718.2	-19.6	81.8
D20-1C	80.03%	60.0	627.3	-54.1	7.1
D20-5C	77.78%	250.0	1172.7	-1.8	108.3
D20-3C	65.25%	445.5	1081.8	-42.9	114.3
D20-1H	93.91%	400.0	700.0	54.0	900.0
D20-3H	89.15%	400.0	340.0	-14.7	275.0
D20-5H	86.37%	225.0	300.0	-23.1	130.8
D20-4H	82.48%	200.0	425.0	57.4	172.7
D20-2H	65.38%	220.0	300.0	-43.2	159.3

Table C-8 - Percent change in calcium flux versus Mass loss for control Specimens

Specimen ID	Mass Retained	Percent Change in Calcium Flux (%)			
		0.08 Days	1 Day	7 Days	14 Days
D0-3C	93.30%	229.0	16.9	-83.4	65.8
D0-5C	93.16%	527.8	53.2	-85.0	136.4
D0-1C	78.41%	197.0	258.7	-67.7	71.3
D0-2C	71.30%	986.0	249.2	-66.0	11.6
D0-4C	69.06%	1180.4	258.0	-70.1	1.0
D0-2H	84.95%	653.8	144.9	-72.2	-21.9

Table C-9 - Percent change in calcium flux versus Mass loss for 10% CRT Specimens

Specimen ID	Mass Retained	Percent Change in Calcium Flux (%)			
		0.08 Days	1 Day	7 Days	14 Days
D10-2C	93.96%	1136.1	154.8	-61.7	-52.4
D10-4C	93.64%	1417.2	300.5	-69.4	-26.3
D10-3C	92.82%	1218.2	216.7	-64.7	-46.7
D10-1C	91.39%	1076.7	285.7	-58.5	-30.0
D10-5C	85.07%	2025.0	165.7	-70.6	10.8
D10-4H	90.58%	805.5	10.0	-92.8	-42.5
D10-5H	82.46%	2537.9	-4.5	-80.5	-68.0
D10-3H	82.17%	3794.7	62.8	-77.0	-41.7
D10-2H	81.97%	2468.6	91.4	-72.7	-35.9
D10-1H	75.46%	2630.8	113.6	-73.6	-56.5

Table C-10 - Percent change in calcium flux versus Mass loss for 20% CRT Specimens

Specimen ID	Mass Retained	Percent Change in Calcium Flux (%)			
		0.08 Days	1 Day	7 Days	14 Days
D20-4C	92.46%	435.5	446.6	26.4	1.4
D20-2C	84.15%	166.8	459.7	234.1	-38.5
D20-1C	80.03%	579.6	502.7	131.9	-64.6
D20-5C	77.78%	1087.5	343.6	298.3	-72.1
D20-3C	65.25%	583.7	475.1	227.3	-20.1
D20-1H	93.91%	833.3	-20.8	594.6	28.6
D20-3H	89.15%	1422.9	50.0	775.4	-63.9
D20-5H	86.37%	1100.0	23.2	626.5	-47.5
D20-4H	82.48%	862.6	6.9	487.3	-67.1
D20-2H	65.38%	1761.1	58.2	600.5	-62.2